

Dissertation

**Development of Methods for the Evaluation of
Continuous and Non-Continuous Industrial
Processes and Cost-Efficient Thermal Energy
Storage Integration**

ausgeführt zum Zwecke der Erlangung des akademischen Grades eines
Doktors der technischen Wissenschaften (Dr. techn.)

eingereicht an der Technischen Universität Wien, Fakultät für Maschinenwesen
und Betriebswissenschaften

von

Dipl.-Ing. Anton BECK

Matr.Nr.: 0826349
Haidmannsgasse 10/29
A-1150 Wien

unter der Leitung von

Univ.Prof. Dipl.-Ing. Dr. techn. René Hofmann
Institut für Energietechnik und Thermodynamik, E302

begutachtet von

Ao. Univ.Prof. Dipl.-Ing. Dr.techn.
Heimo WALTER
Technische Universität Wien
Institut für Energietechnik und
Thermodynamik

Univ.Prof. Univ.Prof. Dipl.-Ing.
Dr.techn.
Anton FRIEDL
Technische Universität Wien
Institut für Verfahrenstechnik,
Umwelttechnik und technische
Biowissenschaften

Eidesstattliche Erklärung

Ich erkläre an Eides statt, dass die vorliegende Arbeit nach den anerkannten Grundsätzen für wissenschaftliche Abhandlungen von mir selbstständig erstellt wurde. Alle verwendeten Hilfsmittel, insbesondere die zugrunde gelegte Literatur, sind in dieser Arbeit genannt und aufgelistet. Die aus den Quellen wörtlich entnommenen Stellen sind als solche kenntlich gemacht.

Das Thema dieser Arbeit wurde von mir bisher weder im In- noch Ausland einer Beurteilerin/einem Beurteiler zur Begutachtung in irgendeiner Form als Prüfungsarbeit vorgelegt. Diese Arbeit stimmt mit der von den Begutachterinnen/Begutachtern beurteilten Arbeit überein.

Wien, am 23. März, 2019

.....
(Anton Beck)

Kurzfassung

Energieeffizienz in industriellen Prozessen spielt eine große Rolle bei der Reduktion von Treibhausgasemissionen. In der Vergangenheit wurden Methoden und Werkzeuge entwickelt, die es ermöglichen Potentiale zur Wärmerückgewinnung zu identifizieren und die zur Entscheidungshilfe für Investitionen in Wärmerückgewinnungsequipment herangezogen werden können. Wärmerückgewinnung verringert den Gesamtenergiebedarf und damit den Verbrauch fossiler Brennstoffe, die hauptsächlich als Primärenergieträger in der Industrie eingesetzt werden.

Jedoch wurde erst in den letzten Jahren mehr Aufmerksamkeit auf die Wärmerückgewinnung in diskontinuierlichen Prozessen und Batchprozessen gerichtet. Diese Prozesse wurden vernachlässigt, da angenommen wurde, dass sie aufgrund eines geringeren Energiebedarfs niedrigere Einsparpotentiale aufweisen. Dies gilt jedoch nicht für alle diskontinuierlichen Prozesse und Batchprozesse. Beispielsweise im Lebensmittelbereich und insbesondere in Brauereien und Molkereibetrieben besteht ein hoher Wärmebedarf.

Diskontinuierliche Prozesse und Batchprozesse bieten oft Potentiale für die Integration von thermischen Energiespeichern zur zeitlichen Entkopplung von Wärmequellen und Wärmesenken und damit für eine erhöhte Wärmerückgewinnung. Im Rahmen der vorliegenden Arbeit wurde ein Framework für Prozessintegration entwickelt, mit dem thermische Energiespeicher in diskontinuierliche Prozesse und Batchprozesse integriert werden können. Das Framework basiert auf einer Mixed-Integer Nonlinear Programming Superstructure-Formulierung für die Synthese von Wärmetauschernetzwerken, die für thermische Energiespeicher erweitert wurde. Diese Formulierung ist jedoch selbst für kleinere Probleme mit wenigen Prozessströmen und Zeitintervallen schwer zu lösen. Um diesen Nachteil zu überwinden, wurde ein Linearisierungsverfahren vorgestellt, das alle nichtlinearen Terme in der Superstructure-Formulierung eliminiert. Die Superstructure kann anschließend wesentlich schneller gelöst werden. Außerdem wurden Maßnahmen vorgestellt, die den Lösungsraum der Formulierung einschränken und so zu einer weiteren Reduktion der Rechenzeit führen. Vereinfachende Modellannahmen und Problemreduktionen wurden ebenfalls vorgestellt, die zur Lösung

größerer Probleme von industriellem Maßstab erforderlich sind.

In die Wärmetauschernetzwerke können mehrere unterschiedliche Arten von thermischen Energiespeichern integriert werden. Die zwei Haupttypen sind Speicher mit variabler Masse und fixer Temperatur, wie Mehrtankssysteme oder Schichtspeicher, und Speicher mit fixer Masse und variabler Temperatur, wie Latentwärmespeicher, Wirbelschichtregeneratoren, Druckwasserspeicher und Feststoffspeicher im Allgemeinen.

Außerdem wurde ein zweistufiges Verfahren vorgestellt, das die Integration von Speichern mit fixer Masse und variabler Temperatur vereinfacht. In der ersten Stufe wird ein Mixed-Integer Nonlinear Programming Modell basierend auf Composite Curves zur Identifikation optimaler Speichergrößen gelöst. In der zweiten Stufe wird die Superstructure-Formulierung mit den im ersten Schritt fixierten Speichergrößen für die Wärmetauschernetzwerksynthese gelöst.

Die Wirksamkeit der vorgestellten Methoden wurden anhand verschiedener Fallbeispiele aus der Literatur demonstriert. Zudem wurde anhand eines realen Molkereibetriebs gezeigt, dass mit dem vorgestellten Framework Probleme von industriellem Maßstab gelöst werden können.

Abstract

Energy efficiency in industrial processes plays a major role for the mitigation of greenhouse gas emissions. In the past methods and tools have been developed that allow to identify potentials for heat recovery and for decision support when it comes to investments in heat recovery equipment. Heat recovery reduces the overall energy demand and thus decreases consumption of fossil fuel which are mainly used as primary energy sources in industry.

However, only in recent years more attention has been directed towards heat recovery in non-continuous and batch processes. These processes were somewhat neglected as they were believed to have lower saving potentials due to lower energy demand which is not true for all non-continuous and batch processes. For example the food sector, especially brewing and dairy plants, has high heat demands.

Non-continuous and batch processes often yield potentials for the integration of thermal energy storages for temporal decoupling of heat sources and heat sinks and thus for increasing heat recovery. Within the present thesis a framework for process integration was developed with the ability to integrate thermal energy storages into non-continuous and batch processes. The framework is built around a Mixed-Integer Nonlinear Programming superstructure formulation for heat exchanger network synthesis that is extended for thermal energy storages. This formulation, however, is hard to solve even for relatively small problems with only a few process streams and time intervals. To overcome this drawback, a linearization procedure was presented that eliminates all nonlinear terms in the superstructure formulation which can then be solved significantly faster. Also, measures were presented that tighten the formulation and yield further reductions in computational time. Simplifications such as model assumptions and problem reductions are also presented that are necessary to solve large industry-scale problems.

Several different types of thermal energy storages can be integrated into the heat exchanger networks. The two main types are storages with variable mass and fixed temperature such as multi-tank systems or stratified tanks, and fixed mass

and variable temperature storages such as latent heat thermal energy storages, fluidized bed regenerators, pressurized water storages or solid matter storages in general.

Also, in order to simplify the integration of fixed mass and variable temperature storages a two-step procedure was proposed. The first step is a novel Mixed-Integer Nonlinear Programming formulation for storage sizing that is based on Composite Curves. The second step is a superstructure formulation for heat exchanger networks synthesis using the fixed storage sizes obtained in the first step.

The proposed features of the framework were demonstrated using various example cases from literature. Also, a real dairy plant was used to demonstrate capabilities for solving large-scale problems.

Preface/Acknowledgements

The present thesis was conducted at the Austrian Institute of Technology GmbH (AIT) in the research field Sustainable Thermal Energy Systems from November 2015 to October 2018 under supervision of Univ. Prof. Dipl.-Ing. Dr.techn. René Hofmann. The thesis and the related publications were initiated and realized by means of the endowed professorship through the cooperation between Technische Universität Wien (TU Wien) and AIT in the research group Industrial Energy Systems.

I would like to thank all my colleagues both at AIT and TU Wien who contributed ideas and thoughts. Special thanks goes to Sabrina who always had an open ear for problems but was also available for productive discussions.

I would also like to thank my supervisor Univ. Prof. Dipl.-Ing. Dr.techn. René Hofmann who did a great job promoting our work and was important as a guide both technical and organizational.

Last but not least, I would like to thank my family and my girlfriend for moral support throughout my studies. It wouldn't have been as enjoyable without you.

List of Figures

1.1	Projection of energy consumption, share of renewable energy and GHG emissions in the EU, [25]	2
1.2	Projected worldwide primary energy consumption by sources, [90]	3
1.3	Technology readiness levels for storage technologies, adapted from [54]	5
2.1	Composite Curves and Grand Composite Curves	8
2.2	SYNHEAT superstructure for two hot streams (H1 and H2), two cold streams (C1 and C2) and two temperature stages	13
2.3	Classification of TES	17
3.1	Structure of the proposed framework: a multi-period superstructure formulation, complexity reduction and storage integration . .	25
3.2	Extended superstructure for storage integration for two hot streams, two cold streams and two temperature stages	29
3.3	Different thermal energy storages in the framework	31
3.4	Modelled characteristics of sensible FMVT storages (left) and LHTS (right)	35
3.5	Discrete temperature and energy values that characterize LHTS systems	36
3.6	Modified big-M constraints used for modelling of the LHTS characteristics	38
3.7	Identification of the model parameters T_s , T_h and T_l	41
3.8	Simulation results compared with measurement data and least squares fit	42

3.9	From left to right: CCs, GCCs, mGCCs	43
3.10	mGCCs for a small example with two operating periods and a solution for storage temperatures and heat loads; feasible range for temperature and heat loads is marked in grey	44

List of Tables

3.1	Model parameter comparison for LHTS and sensible FMVT storage systems; X... required, (X)... either solid or liquid properties required	33
3.2	Coefficients for piecewise linear functions	37
3.3	Storage data for LHTS storage system [98]	40
3.4	Weighted specific heat capacities for example case	40
3.5	Fitted storage parameters for the LHTS example	42

Nomenclature

Acronyms

AIT	Austrian Institute of Technology
CC	Composite Curves
CHP	Combined Heat and Power
EU	European Union
FMVT	Fixed Mass and Variable Temperature
GCC	Grand Composite Curves
GHG	Greenhouse Gas
HEN	Heat Exchanger Network
HENS	Heat Exchanger Network Synthesis
HEX	Heat Exchanger
HTF	Heat Transfer Fluid
ISC	Intermediate Storage Cycle
LHTS	Latent Heat Thermal Energy Storage
LP	Linear Programming
mGCC	modified Grand Composite Curves
MILP	Mixed-Integer Linear Programming
MINLP	Mixed-Integer Nonlinear Programming
NLP	Nonlinear Programming

PCM Phase Change Material
PDM Pinch Design Method
SCC Storage Composite Curves
SOCO Storage Optimisation Concepts
TAC Total Annual Costs
TAM Time Average Method
TES Thermal Energy Storage
TSM Time Slice Method
TU Wien Technische Universität Wien
VMFT Variable Mass and Fixed Temperature

Greek Symbols

Γ big-M coefficients
 Ω place holder for storage temperatures ($^{\circ}\text{C}$)
 Φ abbreviation coefficients
 τ time interval duration (s)

Roman Symbols

ΔT temperature difference ($^{\circ}\text{C}$)
 \dot{m} mass flow (kg/s)
 \dot{Q} heat flow (kW)
 CP set of cold process streams
 HP set of hot process streams
 $LMTD$ logarithmic mean temperature difference ($^{\circ}\text{C}$)
 NOK number of temperature stages
 NOP number of time intervals
 A heat exchanger area (m^2)

c_p	specific heat capacity (kJ/kg K)
$c_{p,h}$	lumped specific heat capacity during phase change (kJ/kg K)
$c_{p,l}$	lumped specific heat capacity of the liquid phase (kJ/kg K)
$c_{p,s}$	lumped specific heat capacity of the solid phase (kJ/kg K)
h	phase change enthalpy (kJ/kg)
L	number of heat recovery loops
M	big-M coefficients
m	mass (kg)
N	total number of process streams and utilities
Q	energy (kWh)
q	specific energy (kJ/kg)
q_0	specific storage energy at T_{min} (kJ/kg)
q_1	specific storage energy at $T_{melt} - T_{var}/2$ (kJ/kg)
q_2	specific storage energy at $T_{melt} + T_{var}/2$ (kJ/kg)
q_3	specific storage energy at T_{max} (kJ/kg)
q_{shift}	specific initial storage energy (kJ/kg)
s	number of separate components
T	temperature (°C)
T_h	auxiliary temperature for PCM during phase change (°C)
T_l	auxiliary temperature for PCM in liquid state (°C)
T_m	mean temperature (°C)
T_s	auxiliary temperature for PCM in solid state (°C)
T_{melt}	PCM melting temperature (°C)
T_{var}	PCM temperature range of phase change (°C)
U	overall heat transfer coefficient (kW/m ² K)

u	number of heat exchanger units
U_h	overall heat transfer coefficient during phase change (kW/m ² K)
U_l	overall heat transfer coefficient of the liquid phase (kW/m ² K)
U_s	overall heat transfer coefficient of the solid phase (kW/m ² K)
X	admissible values
x	continuous variables
Y	admissible integer values
y	integer variables
z	binary variables for existence of heat exchangers
z^{switch}	binary variables representing storage charging state
z_h	binary variables for phase change
z_l	binary variables for liquid phase
z_s	binary variables for solid phase

Subscripts

h	phase change
i	hot stream
j	cold stream
k	temperature stage
l	liquid phase
max	maximum value
min	minimum value
s	solid phase
t	time interval

Superscripts

c	cold
---	------

NOMENCLATURE

NOMENCLATURE

h hot

HTF Heat Transfer Fluid

in inlet

ISC Intermediate Storage Cycle

out outlet

STO Storage

Contents

1	Background and Motivation	1
1.1	Industry and its Impact on Climate	1
1.2	Potentials for Energy Efficiency Measures	2
1.3	Thermal Energy Storages in Industry	4
2	Process Integration	6
2.1	Pinch Analysis	7
2.2	Mathematical Programming	11
2.3	Process Integration in Batch-Processes	14
2.4	Integration of Thermal Energy Storages	16
2.4.1	Storage Types	17
2.4.2	Integration Approaches	18
2.5	Synthesis of the State-of-the-Art & Problem Statement	21
2.6	Related Publications	23
3	Process Integration Framework	25
3.1	Input Data	27
3.1.1	Thermodynamic Parameters	28
3.1.2	Cost Coefficients	28
3.1.3	Optimization Parameters	28
3.1.4	Model Parameters	29

3.2	Extended Superstructure Formulation	29
3.3	Storage Models	31
3.3.1	Storages with Variable Mass and Fixed Temperature . . .	32
3.3.2	Storages with Fixed Mass and Variable Temperature . . .	32
3.3.3	Identification of Model Parameters	39
3.4	Storage Sizing	43
3.5	Targeting	44
3.5.1	Energy Targets	44
3.5.2	Area Targets	45
3.5.3	Target for Minimum Number of HEX Units	45
3.6	Linearization	45
3.7	Tighter Constraints	46
3.8	Simplifications	47
3.8.1	Single HEX per Stream Pair	47
3.8.2	Sequential Storage Integration	48
3.8.3	Reduction of Process Streams	48
3.8.4	Reduction of the Number of Binary Variables	49
3.9	Post-Processing	49
4	Conclusion	50
5	Papers	52
5.1	Paper 1	53
5.2	Paper 2	64
5.3	Paper 3	74
5.4	Paper 4	86
5.5	Paper 5	93
5.6	Paper 6	111

Chapter 1

Background and Motivation

1.1 Industry and its Impact on Climate

Most of the scientific community agrees that anthropogenic greenhouse gas (GHG) emissions play a key role in global warming. According to Eurostat [26], the energy sector was accountable for 78% of the European Union's (EU) GHG emissions in 2015. The industrial sector consumes a considerable amount of energy, according to Olsen et al. [21] in many countries it is 20% or more of the total energy use, and contributes about 37% of total GHG emissions as stated in an assessment by Worrell et al. [92]. Therefore, improving industrial energy efficiency is one of the most important ways to reduce the threat of increased global warming. In order to tackle the problem of global warming, the EU set 20-20-20 environmental targets for the reduction of energy consumption and CO₂ emissions, for the increase of renewable energy. The 2020 energy goals are a 20% (or even 30%) reduction in CO₂ emissions and a 20% increase in energy efficiency compared to 1990 and a share of renewable energy sources of 20% (EU's 2020 climate & energy package). Figure 1.1 shows the status of 2016 on these goals. By 2030 and 2050 the EU's goals are to achieve CO₂-reductions of 40% and 80% compared to the 1990's emissions level respectively, which are necessary to tackle the issue of climate change (EU's 2050 low-carbon economy). Significant energy savings are necessary for reaching these ambitious goals. According to Bergamini et al. [9] these goals can be met by

- shifting to renewable energy sources,
- decreasing the energy intensity of human activities, and
- improving the efficiency of energy conversion processes.

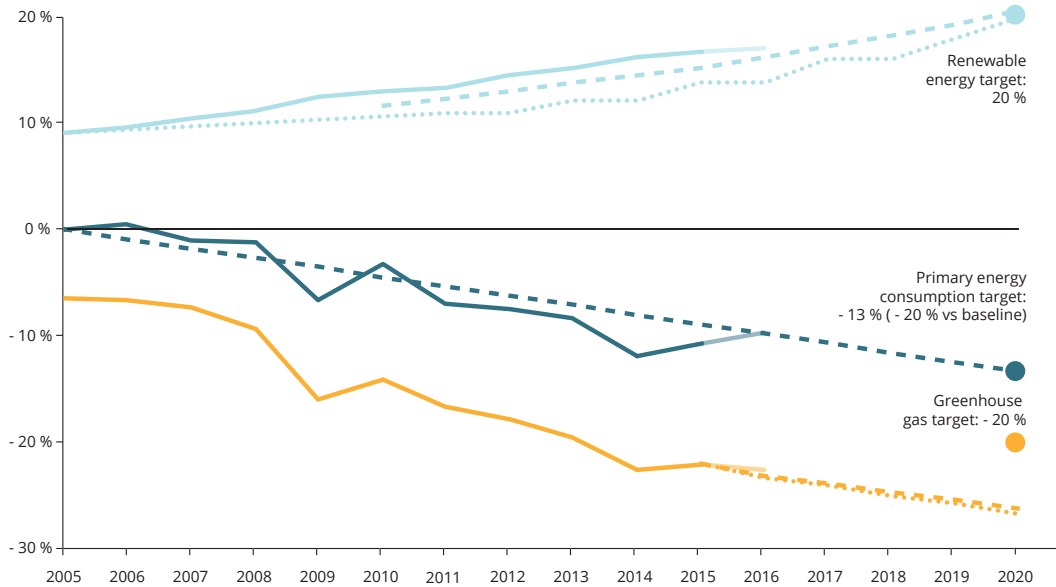


Figure 1.1: Projection of energy consumption, share of renewable energy and GHG emissions in the EU, [25]

Although the EU proposed these goals to decrease energy consumption, worldwide industrial energy use is projected to increase over the coming 50 years even from the most "techno-optimistic" perspective, according to Gielen and Taylor [35]. Also, the BP Statistical Review of World Energy 2018 [14] declared that the worldwide primary energy consumption grew by 2.2% in 2017 which was the largest increase (in percentage terms) since 2013. Figure 1.2 shows the projected consumption of primary energy until 2040 which indicates a steady increase for all the different energy sources except for coal which remains at the level of 2015. When considering the environmental effect due to the growing energy consumption the aim needs to be to decrease the global energy demand, either by increasing the efficiency of current energy production or by increased exploitation of sustainable energy sources, as stated by Klemes et al. [53].

1.2 Potentials for Energy Efficiency Measures

The industry is one of the most energy consuming sectors worldwide. Recovery of industrial excess heat and its reuse could decrease both CO₂ emissions and energy costs, which would lead to more efficient and more competitive industrial activities. Eichhammer et al. [23] highlighted that energy saving potentials in industry and the tertiary sector comprise highly economical measures with

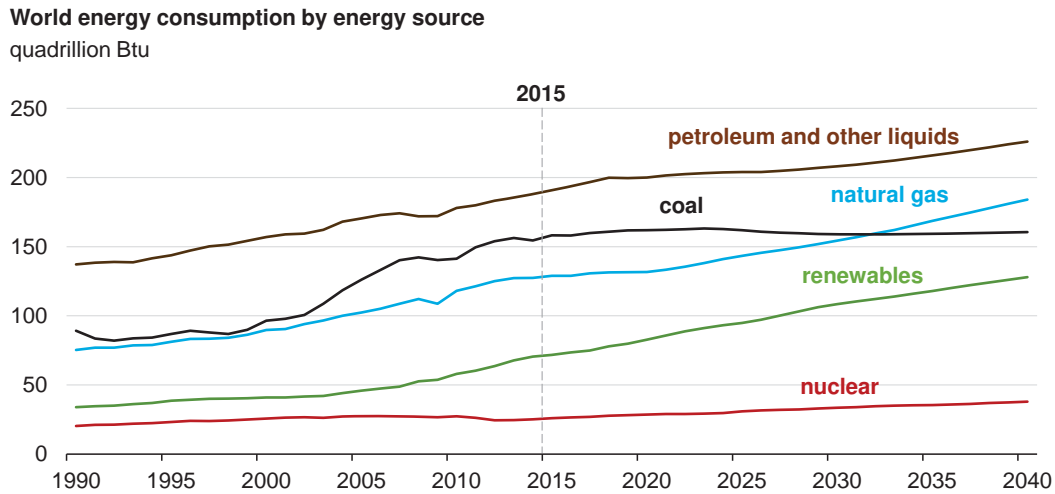


Figure 1.2: Projected worldwide primary energy consumption by sources, [90]

short payback times, as was shown in several studies [13, 80, 44]. However, research demonstrates that the normal outcome of any industrial energy program is that only about 40-50% of the proposed measures are implemented [85]. This means that half of the technical potential for improved energy efficiency is left unexploited, even though the benefits of implementing energy efficiency measures go beyond monetary savings. According to Miro et al. [72] one of main reasons for the underusage of industrial excess heat is due to technological and financial barriers. However, according to the International Energy Agency IEA study [42] on multiple benefits, the monetary value of those benefits from excess heat usage can exceed the pure energy conservation effects by 250%.

Potentials for increased energy efficiency in industry can be exploited by internal or external usage of excess heat sources. These sources include hot combustion gases discharged to the atmosphere, heated products exiting industrial processes, but also heat discharged through cooling utilities such as cooling water. While some heat losses from industrial processes are inevitable, industries can reduce these losses by improving equipment efficiency or installing heat recovery equipment such as heat exchangers (HEX), heat pumps or power cycles for the electrification of excess heat. Internal heat reuse reduces the energy demand of the respective plant and thus the operating costs. However, direct reuse of excess heat by means of HEX or heat pumps is only possible if the heat sources and heat sinks co-exist. This is true for continuous processes but might not be the case for batch operation.

According to a review paper by Fernandez et al. [27] the implementation of batch processes has increased over the last few decades as they have several

advantages compared to continuous processes. While continuous processes are designed to serve basically one major purpose, batch processes typically consist of more general-purpose equipment, which makes such plants far more flexible. They are essential to produce high-value products in the fields of agrochemicals, pharmaceuticals, foods and chemicals [16, 15, 70]. In the past, batch industries could tolerate high energy inefficiencies due to the high value of final products. Also, energy savings in batch plants were neglected because of low energy costs, however energy intensive batch processes such as breweries and dairy plants show significant energy use and thus implementation of efficiency measures is often worthwhile. In the simplest form, the aim of heat integration is to establish matches between streams that require cooling and those that require heating in order to minimize the use of external utilities (cooling water and steam). Potentials for heat integration are likely to be higher in batch processes because of the lack of implemented heat recovery measures. However, due to the fact that heat sinks and heat sources vary in time and thus might not co-exist, the need for thermal energy storages (TES) arises in order to exploit all heat recovery potentials.

1.3 Thermal Energy Storages in Industry

In a literature review by Miro et al. [72] they described TES as a powerful thermal management tool that allows the temporary match of energy supply and energy demand. In their review paper they identified more than 50 cases of industrial TES application. On-site heat recovery and reuse of industrial excess heat was identified in the following activities: energy-intensive manufacturing industry (basic metals, non-metallic minerals, chemicals, paper, and food), vehicle engines, power plants and incineration plants. Among the energy-intensive manufacturing sub-sectors, they identified the basic metals sub-sector as the one which has drawn most attention and the only one with pilot plant scale studies. In their study, they state that water (or steam) storage tanks have been the most used on-site TES systems while power generation as well as space heating and cooling have been the most recurrent applications.

The savings obtained as a result of the implementation of TES systems have been mainly reported from the point of view of economics and environmental parameters, such as CO₂ mitigation and reduction of fuel consumption. Miro et al. [72] stated that there is a lack of studies in literature which may be due to the low maturity level of several TES systems (Figure 1.3) and due to financial barriers. Regarding to the technology maturity, and according to the IEA Energy Storage Roadmap [3], only residential hot water heaters with storage, underground TES, cold water storage and pit TES are the thermal

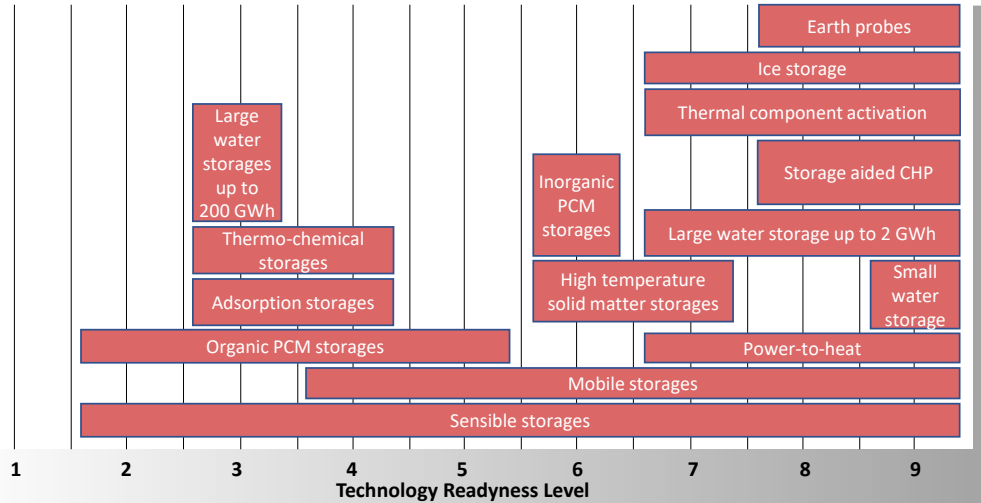


Figure 1.3: Technology readiness levels for storage technologies, adapted from [54]

storage technologies at a commercial maturity level. The rest are still in early or middle stage of development and will require further attention before their potential can be fully realized.

According to a report on storage systems conducted in Austria [54] the economic feasibility of medium to large storage for temperatures from 40 to 130 °C in businesses is already given today. There is a high potential for implementation for heat load management in companies, e.g. for excess heat utilization and increased process efficiency. In the report, it was stated that in the long-term new storage materials such as phase change material (PCM) and thermo-chemical material might gain importance. Also, long-term strategies will increasingly consider energy efficiency in industrial processes and the expansion of renewable energy will increase the importance of storage for heat load management in high-temperature processes.

According to Miro et al. [72], industrial activities have a huge potential for recovery of excess heat. In spite of this potential, industrial excess heat is currently underutilized. Even though, the reuse of recovered excess heat leads to energy savings and thus to mitigation of CO₂ emissions and to economic benefits.

Chapter 2

Process Integration

One of the most promising techniques to increase energy efficiency in industries is Process Integration. Gundersen stated in an IEA Tutorial on Process Integration [37] that the term Process Integration emerged in the 80's and has been extensively used in the 90's to describe certain system-oriented activities related primarily to process design. Since 1993 the IEA defines Process Integration as

systematic and general methods for designing integrated production systems, ranging from individual processes to total sites, with special emphasis on the efficient use of energy and reducing environmental effects.

However, Process Integration is not only focused on energy efficiency but also considers water management and improvement of mass flows and is used during the design and retrofit of industrial processes in order to obtain an optimal use of resources. Heat Integration is an essential aspect of all industrial processes due to its ability to reduce the amount of hot and cold utilities consumed and, consequently, to reduce operating costs.

Process Integration methods use heuristics (insight) about design and economy, thermodynamics and optimization techniques. There is significant overlap between the various methods and, according to Gundersen [37], the trend today is strongly towards methods using all three features mentioned above. Gundersen [37] emphasises that the large number of structural alternatives in Process Integration can be significantly reduced by the use of insight, heuristics and thermodynamics, and that the remaining problem and its multiple economic trade-offs can then be tackled with optimization techniques. Optimization techniques can be divided into deterministic (Mathematical Programming) and non-deterministic methods (stochastic search methods such as Simulated Annealing,

Genetic Algorithms [68, 67] or a combination of both [69, 96], Tabu Search [58] and others [95, 41]).

One of the main problems in Process Integration is the synthesis of efficient heat exchanger networks (HENs) for heat recovery in industrial processes. In the last 50 years a significant amount of research work has been presented that addresses the heat exchanger network synthesis (HENS) problem as shown in the review papers [36, 34, 59, 46, 45]. The basic HENS problem was stated by Furman and Sahinidis [34] as follows:

Given a set of hot process streams, which should be cooled from its supply temperature to its target temperature; a set of cold process streams, which should be heated from its supply temperature to its target temperature; the heat capacities and flow rates of the hot and cold process streams; the utilities available (e.g., hot utilities and cold utilities) and their corresponding temperature and costs; develop a heat exchanger network with the minimum annualized investment and annual operating costs, i.e. minimum Total Annual Cost (TAC).

Methods for HENS are commonly classified as **sequential** and **simultaneous** approaches. Sequential synthesis approaches decompose the problem into sub-problems, whereas simultaneous synthesis approaches directly synthesise the HEN without decomposition of the problem. Simultaneous approaches primarily rely on different Mathematical Programming techniques.

Identification of heating and cooling requirements in the process is the basis for HENS. The necessary data for each process stream is the following:

- \dot{m} ... mass flow rate (kg/s, tons/h, etc.)
- c_p ... specific heat capacity (kJ/kg K)
- T^{in} ... supply temperature (K)
- T^{out} ... target temperature (K)

This stream data is used by all Heat Integration techniques presented in the following chapters, and must be available to conduct Heat Integration studies.

2.1 Pinch Analysis

Probably the most important concept in the field of Process Integration is Pinch Analysis. The Pinch Point is the thermodynamic bottleneck for heat recovery in

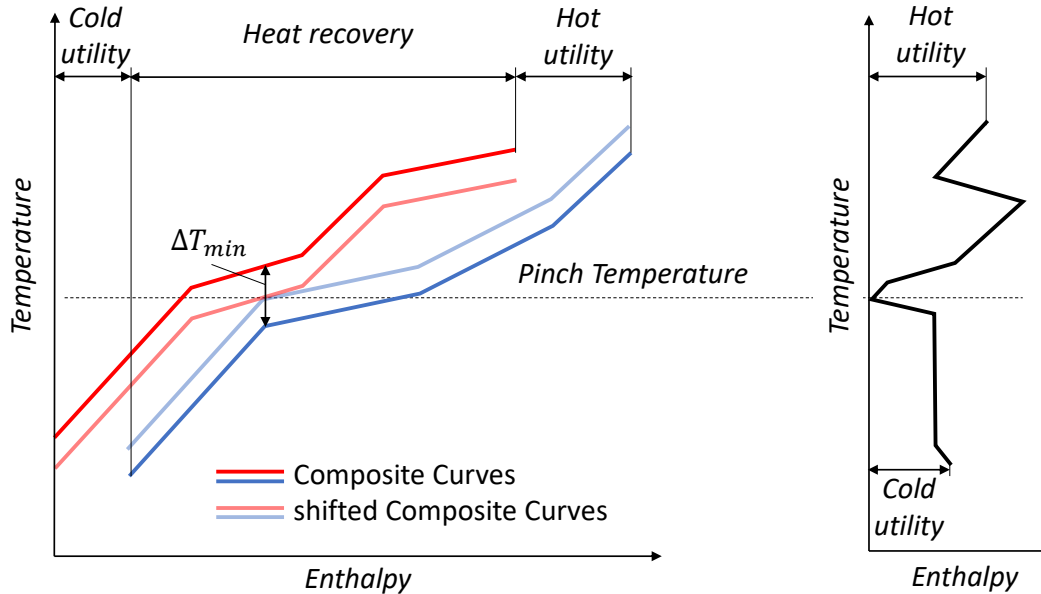


Figure 2.1: Composite Curves and Grand Composite Curves

thermal energy systems. The concept was independently discovered by Hohmann [40], Umeda et al. [88, 89] and Linnhoff et al. [65, 64]. Pinch Analysis is a tool that provides critical information on heat recovery potentials on a total plant or even site level.

The calculation of estimates for key performance indicators for a process is called Targeting and the obtained estimates are called targets. It is possible to obtain targets representing an upper bound on system performance and/or a lower bound on the system cost as mentioned by Klemes et al. [53].

The concept of the Composite Curves (CCs) (Figure 2.1, left) is a graphical representation of the cold and hot process streams in an industrial process. They show the theoretical maximum for energy recovery and the minimum hot and cold utility requirements for a given minimum approach temperature difference (ΔT_{min}). The CCs are constructed in temperature-enthalpy diagrams, where hot and cold streams are matched in terms of temperature. For HENS, maximum energy recovery targets can be established and most of the HENS achieving them also have reasonable costs. However, as stated by Klemes et al. [53], these costs are hardly ever the global minimum.

The Grand Composite Curve (GCC) is a modification of the CCs which is obtained by plotting the horizontal difference between the shifted hot and cold CCs. Shifted CCs are the result of shifting the CCs toward each other by $\Delta T_{min}/2$ so that the curves touch each other at the Pinch Point. The GCC shows how

much heating (above the Pinch Point) and cooling (below the Pinch Point) can be introduced to the system at a certain temperature level. An example for the GCC is shown in Figure 2.1 on the right side.

While graphical diagrams such as the CCs are excellent tools for understanding the overall energy situation, minimum energy consumption and the heat recovery pinch are more often obtained by numerical procedures, as stated by Gundersen [37]. Typically, these procedures are based on the Heat Cascade where the temperature scale is divided into intervals. Each supply and target temperature of the process streams starts a new interval. This is done in a similar way as the CCs are constructed.

Besides methods for energy Targeting, also targets for the minimum number of HEX units and for minimum total HEX areas were developed. Hohmann [40] stated in his thesis that the minimum number of units u_{min} including utility HEX can be calculated by

$$u_{min} = N - 1 \quad (2.1)$$

where N is the total number of streams and utilities. According to Linnhoff et al. [66] the same result can be obtained when applying Euler's theorem to HENs, which states that:

$$u = N + L - s \quad (2.2)$$

where u is the number of units (including heaters and coolers), L is the number of heat recovery loops and s is the number of separate components. Usually extra units are avoided in the design and thus $L = 0$. Also, in general, there will be no subset equality in the data set and hence $s = 1$. Which leads to the Targeting equation Eq. (2.1).

Townsend and Linnhoff [86] developed the so-called bath formula to calculate the minimum total heat transfer area. In order to maximize driving temperature differences, only vertical heat transfer is allowed. The CCs are divided into enthalpy intervals whenever there is a change of slope in either hot or cold CC. All hot streams in a certain interval are allowed to match with all cold streams in the same interval. The resulting network would consist of a very large number of HEX, stream splits and mixers. However, assuming equal heat transfer coefficients the network would in theory yield the lowest possible total HEX areas. The important implication is, that for unequal heat transfer coefficients this is not necessarily the case. In order to minimize the total area, not the driving temperature differences needs to be optimally distributed but the product of heat transfer coefficient and temperature differences. This means that vertical heat transfer will not always minimize total heat transfer area. For this reason, more advanced Targeting procedures such as the minimum area target proposed by Ahmad et al. [4] were proposed that account for different heat transfer coefficients.

For the evaluation of expected TAC Supertargeting was developed by Linnhoff and Ahmad [60, 61]. Supertargeting is a procedure for obtaining simultaneously targets for heat recovery and heat transfer area of a HEN, ultimately producing also a cost target. The procedure involves evaluation of these targets for various values of ΔT_{min} .

Design of HENs for heat recovery in industrial processes can be carried out using the classical Pinch Design Method (PDM) [63]. Simple design guidelines and rules allow engineers to develop HENs that are near-optimal from a cost perspective. However, according to Klemes et al. [53] there are important limitations with the PDM. Some of them are:

- It is a sequential design procedure thus providing no guarantee on optimality for the complete design.
- The multiple trade-offs involved in HENS are very difficult to balance or optimize by manual procedures.
- In cases with considerable differences in heat transfer coefficients, the matching of hot and cold streams becomes much more difficult since non-vertical heat transfer can be favourable.
- The strict Pinch Decomposition, that is splitting the problem into two subproblems above the pinch and below the pinch, often prevents the engineer from identifying networks with reduced cost and reduced complexity (fewer units and fewer stream splits).
- PDM and Pinch Analysis in general are unable to properly address heat recovery situations where there are restrictions in the matching between hot and cold streams. This applies to cases with forbidden matches (due to safety, integrity, operability, product purity, etc.) as well as required (for start-up) and restricted matches.

It is the limitations explained in the bulleted list above that have motivated the use of advanced methods to design HENs. New heuristic approaches have addressed the issue of unequal heat transfer coefficients. Rev and Fonyo [78] introduced the Diverse Pinch Concept and the corresponding curves which can be determined after shifting the streams over their whole temperature range according to their individual contributions to ΔT_{min} . They claim that Supertargeting based on Diverse Pinch CCs is much more realistic than that based on uniform (conventional) pinch CCs. Similarly, ΔT_{min} contribution is considered in a study by Bakar et al. [7].

Simultaneous optimization approaches proved to have considerably better capabilities of handling the complex trade-offs in the network design problem and

that they allow to easily consider issues such as forbidden matches. However, the major limitation with these methods is numerical problems related to non-convexity (local optima) and computational complexity (combinatorial explosion). To overcome this limitation, Jiang et al. [48] proposed a combined design approach based on Diverse Pinch Point and Mathematical Programming for the optimal synthesis of HENs, which is suitable for cases with streams of different heat transfer coefficients.

2.2 Mathematical Programming

Methodologies for design of HENs based on Pinch Analysis and the PDM have obvious limitations as mentioned in Section 2.1. Klemes et al. [53] pointed out that despite the fact that Pinch Analysis and the PDM are firmly based on thermodynamics, there is also considerable use of heuristics. As soon as restrictions such as forbidden, required or restricted matches are introduced, other methods are required for Energy Targeting. Mathematical Programming is often used to overcome these problems due to its modelling flexibility.

In his book about Mixed-Integer Nonlinear Programming (MINLP) Floudas [29] described a mathematical model of a system as a set of mathematical relationships (e.g., equalities, inequalities, logical conditions) which represent an abstraction of the real world system under consideration and an optimization problem as a mathematical model which contains one or multiple performance criteria. The performance criterion is described in the form of an objective function, which can be the minimization of cost or the maximization of profit or yield of a process for instance. A well defined optimization problem features a number of variables greater than the number of equality constraints, which implies that there exist certain degrees of freedom. The structure of such nonlinear and mixed-integer optimization models takes the form

$$\begin{aligned}
 \min_{\mathbf{x}, \mathbf{y}} \quad & f(\mathbf{x}, \mathbf{y}) \\
 \text{s.t.} \quad & \mathbf{h}(\mathbf{x}, \mathbf{y}) = \mathbf{0} \\
 & \mathbf{g}(\mathbf{x}, \mathbf{y}) \leq \mathbf{0} \\
 & \mathbf{x} \in \mathbf{X} \subseteq \mathbb{R}^n \\
 & \mathbf{y} \in \mathbf{Y} \text{ integer}
 \end{aligned} \tag{2.3}$$

where \mathbf{x} is a vector of n continuous variables, \mathbf{y} is a vector of integer variables, $\mathbf{h}(\mathbf{x}, \mathbf{y}) = \mathbf{0}$ are equality constraints, $\mathbf{g}(\mathbf{x}, \mathbf{y}) \leq \mathbf{0}$ are inequality constraints, and $f(\mathbf{x}, \mathbf{y})$ is the objective function. Mixed-integer nonlinear optimization problems of the form of Eq. (2.3) are encountered in various applications in all branches

of engineering, applied mathematics, and operations research.

For Process Integration using Mathematical Programming often so called superstructures are used, which contain all possible network structures following certain restrictions. According to Klemes et al. [53], the first really successful Mathematical Programming superstructure for HENS was the superstructure proposed by Floudas et al. [28]. They proposed a sequential approach consisting of the following steps:

1. Minimum utility requirements as a Linear Programming (LP) problem using the transshipment model.
2. Minimum number of units as a Mixed-Integer Linear Programming (MILP) problem, also using the transshipment model.
3. Network generation and optimization as a Nonlinear Programming (NLP) problem minimizing total cost.

To overcome the limitations of the sequential approach, MINLP superstructure models were formulated that were able to consider the trade-offs between operating costs and investment costs simultaneously. The most commonly used of these superstructures is the stage-wise model proposed by Yee and Grossmann [94] which is shown in Figure 2.2. The main limitations of this superstructure are the isothermal mixing assumption for split streams, and the fact that only one HEX can be placed on each stream branch. The first assumption makes the model linear except for the objective function. The second assumption is related to the layout of the superstructure and the use of binary variables representing HEXs. Another superstructure was proposed by Ciric and Floudas [19] which allows for feedback streams and includes mass balance equations to allow for non-isothermal mixing of split streams. Relations accounting for HEX areas and mass balances used in this superstructure are nonconvex, which means there is a tendency to end up in locally optimal solutions.

Binary variables necessary to account for the different HEN structures cause a combinatorial explosion and prohibitive computational times for large industrial problems. Furman and Sahinidis [33] proved the HENS problem to be even NP-hard. Even though all superstructures including the stage-wise superstructure by Yee and Grossmann [94] scale very poorly with problem size, the latter was extended by Sorsak et al. [82] to incorporate alternative HEX types. The selection of the types is modeled by disjunctions based on operating limitations and the required heat transfer area. Since different types of HEXs involve different design geometries, which influences the inlet and outlet temperatures of HEXs, additional constraints are specified to provide a feasible temperature

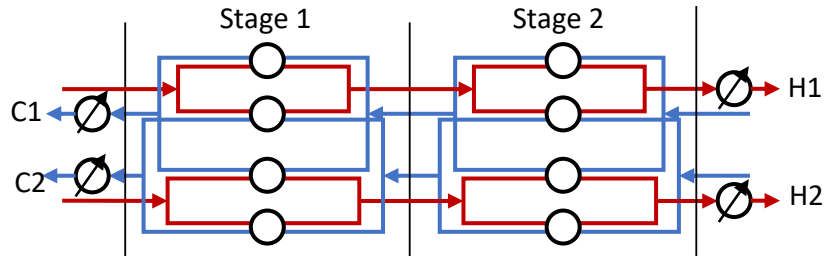


Figure 2.2: SYNHEAT superstructure for two hot streams (H1 and H2), two cold streams (C1 and C2) and two temperature stages

distribution in the HEN. Sorsak et al. [82] claimed that the consideration of different HEX types drastically increases the combinatorial complexity and thus the computation effort necessary to solve the problem.

Because of the difficulty and complexity of the HENS problem a lot of effort was directed towards improved solution algorithms and model reformulations to push the limits of HENS towards industry-scale problems. One way to improve solution speed is to apply model reformulations that tighten the formulations. Tightening in this case means that the solution space of the subproblems solved in MILP and MINLP problems is reduced without reduction of the feasible solution space of the master problem. Anantharaman et al. [5] studied different approaches for improving the solution performance for the MILP transshipment model. Several ideas for model modification and reformulation were investigated, including decreasing the upper bounds, adding integer cuts and reformulating the original model. Similarly, Chen et al. [18] investigated the effect of tightening measures and different other approaches on computation time for the MILP transshipment model for HENS.

But also solution algorithms have been developed for global optimization of HENS and to increase the problem complexity that can be handled. Chen et al. [18] also proposed strategies for improving the efficiency of the branch and bound method and approximation approaches for finding good approximate solutions in relatively short times. A hybrid branch and bound/outer-approximation global optimization algorithm for the synthesis of HENs has been presented by Zamora and Grossmann [97]. They proposed a convex MINLP model, that incorporates two new sets of convex underestimators for the area of HEXs which provides bounds for the global minimum of the TAC of HENs. Although arithmetic mean temperature differences have been used as driving forces in their model, the results obtained with the proposed algorithm provide a valid lower bound to the TAC for the case using logarithmic mean temperature differences as driving

forces. Another approach for obtaining globally optimal solutions to the HENS problems was presented by Bogataj et al. [11] which relies on a concept of a stage-wise superstructure augmented by an aggregated substructure. This concept reduces the number of nonconvex terms. A set of piecewise linear and convex nonlinear underestimators are incorporated in the formulation of the convex MINLP, which is solved by the proposed solution strategy based on a modified outer-approximation/equality relaxation algorithm.

Other authors reduced the HENS problem using different simplifications and decomposition methods. Zhang et al. [99] proposed a process stream arrangement strategy to reduce the search region for the optimal stream match and a stage-wise chessboard model, which is a superstructure with restricted match sequence, to expand the new feasible search region and to avoid missing optimal matches other than those proposed in the arrangement strategy. Zhu [102] used block decomposition and heuristics combined with Mathematical Programming and Area Targeting for large-scale HENS. Pouransari and Maréchal [77] used virtual hot and cold process streams to reduce the number of stream connections between subsystems that need to be considered simultaneously. Another reduction method was proposed by Pettersson [76] who presented a sequential Mathematical Programming procedure to simplify the difficult HENS problem by match reduction. The effort directed towards problem reduction for HENS shows the need for simplifications in order to obtain good solutions for large-scale problems but also to obtain these solutions within reasonable computational time. This is not only true for continuous processes but becomes even more important when it comes to time-dependent batch processes.

2.3 Process Integration in Batch-Processes

While the PDM and Mathematical Programming superstructures have been successfully used for continuous processes, different methods are required to identify optimal design for non-continuous and batch processes according to Fernandez et al. [27], because heat recovery is constrained by both temperature and time. Atkins et al. [6] stated that the Time Slice Model (TSM) approach developed by Kemp & Deakin [51, 52] was typically used for the integration of batch processes, but also various Mathematical Programming techniques such as MILP have been applied to improve the integration of batch processes by attempting to optimize the HEN design [32].

A number of different methods exists for identifying minimum energy consumption in batch processes. Many of these methods are inspired by Pinch Analysis originally developed for continuous processes. The Time Average Model (TAM)

[62], for example, neglects time completely and assumes that heating or cooling of a stream takes place in the entire batch period. This target is the minimum energy consumption for cyclic batches with unlimited ideal TES and can be regarded as a rigorous lower bound on energy consumption. Heat exchange between process streams in batch processes can take place in two different ways:

- **Direct heat exchange** using a HEX if the streams exist in the same time period
- **Indirect heat exchange** using a TES system if the streams do not co-exist in time

A more systematic way to consider the time aspect is to use a two-dimensional Heat Cascade [51, 50], where heat can be transferred to lower temperature (direct heat exchange) or a later time interval (indirect heat exchange using storage). Gundersen [37] claimed that using TES adds flexibility to the process, and heat recovery becomes less dependent on a fixed schedule. A method to estimate total HEX area and cost has been proposed by Bolliger et al. [12] in order to solve multi-period problems using pinch techniques. The method includes a technique allowing to estimate a near-optimal $\Delta T_{min}/2$ contribution of all the streams.

Floudas and Grossmann [30] proposed a sequential HENS method using Mathematical Programming which combines a multi-period MILP model based on the transshipment model of Papoulias and Grossmann [74] with the active set strategy to guarantee the desired HEN flexibility. Decomposition of the problem into different stages significantly reduces the size of the problem, but does not rigorously consider the trade-off between area, number of units, and energy. Miranda et al. [71] proposed an approach based on the work of Floudas and Grossmann [30] that generates individual superstructures for each process stream. They included bypass streams from upstream of one device to downstream of another device in the superstructure. Information on the sub-networks of each period is used to reduce the complexity of the NLP model in the third step of the sequential methodology. Kang et al. [49] also proposed a strategy where a representative operating period is identified based on period durations. Then insights from the individual sub-periods are used to simplify the multi-period HENS problem. Zhao et al. [101] proposed a three-step design procedure that decomposes the trade-off problem into several simpler sub-problems. Their procedure allows to use conventional design methods, such as PDM or Mathematical Programming approaches, and heuristic rules developed for the synthesis of HENs in continuous processes to obtain an initial design. Then they used a mathematical model for systematic rematching and heuristic methods to obtain the final design.

Most simultaneous approaches for the synthesis of flexible HENs are based on the stage-wise superstructure representation of Yee and Grossmann [94] (the so-called SYNHEAT model) where isothermal mixing is assumed. The assumptions make the constraint set linear, and hence very attractive and robust on finding solutions using currently available algorithms. Aaltola [2] proposed a model based on SYNHEAT that simultaneously optimizes the multi-period MINLP problem for minimum costs and flexibility, without relying on sequential decomposition. In this model, explicit modeling of by-passes is avoided to simplify the HENS problem. The area of one match is considered to be the mean value of areas in different periods leading to an underestimation of the total area cost and thus TAC. Verheyen and Zhang [100] reformulated the calculation of maximum area through a set of nonlinear inequality constraints in order to avoid the non-differentiability in the objective function. In a work by Isafiade et al. [43] different optimization formulations for the multi-period HENS problem were compared. They proposed a specialized heuristic algorithm that relies on Lagrangean decomposition that exploits the block diagonal structure of the problem. They presented an iterative scheme where feasible solutions are postulated from the Lagrangean decomposition sub-problems, and multipliers are updated through a subgradient method. Despite the high degree of linearity, the model is still nonconvex. Increasing the number of streams and the number of periods increase the number of nonlinearities and nonconvexities. According to Jiang et al. [47], the conventional approach to produce multi-period HEN designs suffers a few drawbacks, that is, the fixed-duration assumption, the area assignment for HEX sizing, and the comprehensive constraints used to satisfy the process requirements of all periods. In their approach one design is created independently for each period instead of solving a single MINLP model for all periods and time-sharing schemes are introduced to reduce the overall capital investment.

2.4 Integration of Thermal Energy Storages

For time dependent processes TES can be used to increase internal reuse of excess heat, as was already mentioned in the previous section. In the following, methods are presented for integration of TES into industrial processes using Process Integration techniques. However, first a short overview of different TES types with potential for industrial application is presented.

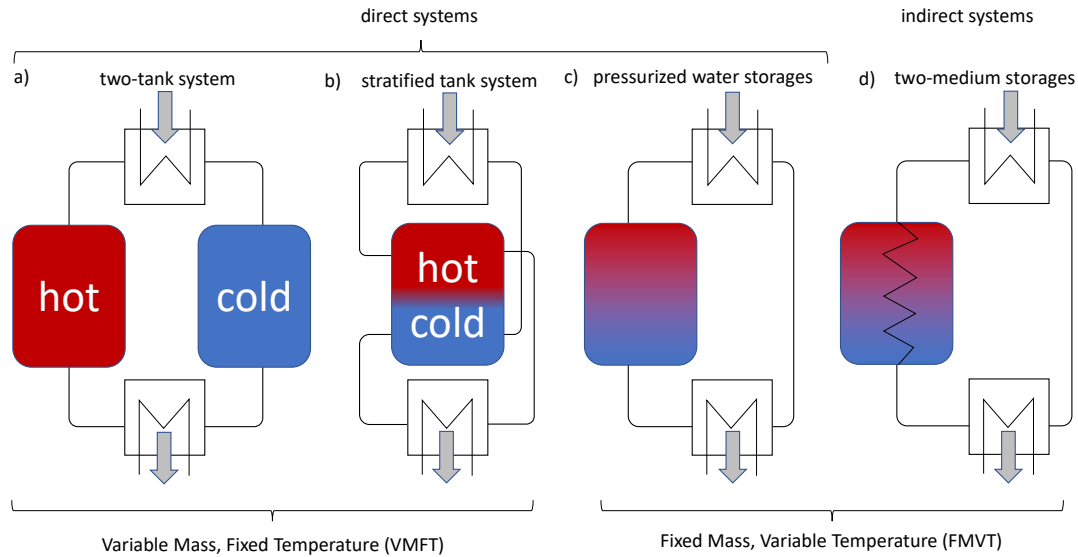


Figure 2.3: Classification of TES

2.4.1 Storage Types

Dos Santos et al. [22] classified storage systems into single (**direct**, Figure 2.3 a)-c)) and two-medium (**indirect**) storages (Figure 2.3 d)). A single medium system usually has two storage tanks, one for hot fluid and the other for cold fluid [38]. During the charging process, fluid from the cold tank is heated and then stored in the hot fluid tank, while during discharging, fluid from the hot fluid tank is pumped out to release heat and afterwards, flows back to the cold fluid tank. The volume occupied by the fluid is at any time equivalent to the volume of one tank. Thus, it is possible to eliminate one tank but as a consequence a stratification, which maintains hot fluid on top of cold fluid, is necessary. The temperature in the tank will therefore vary along the height of the tank creating three regions, a region of higher temperature fluid, a region of lower temperature fluid, and a thermocline. Such stratified tank systems have been utilized at dairy factories in New Zealand with significant energy savings, according to Atkins et al. [6]. Another single material storage system not considered by Dos Santos et al. [22] that uses only a single storage tank and is charged directly is that of pressurized water storage which, for instance, was used by Kulkarni et al. [56] for the integration of solar thermal energy. In this system the storage pressure and also storage temperature increases as the storage is charged, similar to two-medium storages.

Two-medium heat storage systems have a heat transfer fluid (HTF) and a pri-

mary thermal storage material, and typically use only one tank. Depending on the contact and heat transfer interaction between the HTF and the primary energy storage material two types of storage can be distinguished. The first type includes loosely packed solid materials (such as rocks, pebbles of metals, and capsules of PCM, etc.) as a porous bed held in a container and through which the HTF flows and transports energy to or from the solid material. In the second type of two-medium heat storage systems the HTF flows in tubes or pipes that run through thermal storage material, either solid (such as, concrete, wax, sands, salts, etc), or liquid (such as oil, liquid salts, etc). Due to the smaller contact area between the fluid and thermal storage material, the heat transfer between the fluid and the thermal storage material in this case is worse compared to systems with direct contact.

Throughout the present thesis a subdivision of storage types into storages with variable mass and fixed temperature (VMFT) and storages with fixed mass and variable temperature (FMVT) is used. VMFT storages have two or more distinct reservoirs with variable volume of constant temperature. Systems with two or more storage tanks and ideal stratified tanks fall into this category as shown in Figure 2.3. On the other hand, FMVT storages such as latent heat thermal storages (LHTS) or sensible storages using solid materials as storage material consist of only one distinct storage volume that changes temperature while charging or discharging. Even though ideal LHTS do not change temperature during phase change, real LHTS applications do change temperature while being charged and discharged due to inhomogeneous temperature distributions inside the storage vessel and inhomogeneous melting behaviour. This distinction between storage types is especially useful when it comes to Process Integration of TES as they require different modelling approaches.

2.4.2 Integration Approaches

In the past, several Process Integration approaches were presented in the literature for the integration of TES. Vaselenak et al. [1] considered energy efficiency in batch processes by optimizing the heat integration between hot and cold storage tanks using a heuristic approach. For a restricted number of temperature levels, they combined the heuristic approach with MILP. Unfortunately, the problem can only be solved for a limited number of storage tanks and they assumed that heat is available at any time. Time scheduling of operation tasks is also not taken into account. Stoltze et al. [83] proposed a combinatorial method to include TES in the HEN design. The number of storage tanks and their temperature levels are chosen by analyzing the CCs. By choosing only a limited number of storage tanks, the authors stated that the computational

work is not necessarily higher than for the same problem without storage. Also using the CCs resulting from the TAM, Krummenacher and Favrat [55] proposed a heuristic targeting method to identify the minimum number of heat storage units for maximum heat recovery. A methodology that improves upon the work by Krummenacher [55] for the design of TES involving batch processes has been proposed by Olsen et al. [73]. It involves creation of time average based indirect source and sink profiles and calculation and display of assignment zones that are either restricted, extended or dynamically updated. An assumed TSM of the reference schedule is used to allow the calculation of the tank or temperature layer volumes and hence investment costs. The proposed approach was integrated into the Process Integration software PinCH.

Based on the TSM, two different methods for direct and indirect heat integration were proposed by Yang et al. [93] and combined to synthesize HEN by involving TES. They claimed that in previous works of TSM, the stream matching problem between different time intervals is not investigated. Shahane et al. [75] proposed an iterative targeting method for mixed energy integration in batch process systems. The method is based on time-dependent Heat Cascade analysis and accounts for different ΔT_{min} requirements for direct and indirect Heat Integration.

For indirect Heat Integration of batch problems using TES, Chen and Ciou [16] proposed a MINLP formulation. The problem can become soon very complex, since storage tanks are included in the HEN superstructure. According to Atkins et al. [6], integrating non-continuous processes such as a dairy factory is a challenge due to the irregular operation of the several plants on site. They state that direct heat transfer between plants is often impractical and therefore used a recirculating heat recovery loop and a stratified tank also acting as a buffer in case plants go onto a non-productive operating state. Modified source/sink CCs were used to estimate the maximum heat recovery and to determine the optimal temperatures of the stratified tank. They showed that the maximum amount of heat recovery can be increased if the temperature of the HTF in the recirculation loop is varied depending on operating states. Walmsley et al. [91] stated that inter-plant indirect heat integration via a heat recovery loop combined with renewable solar heating might be an economic method for increasing process energy efficiency in large processing sites with a low pinch temperature. They investigated the benefits for storage systems with variable storage temperatures and concluded that solutions could be obtained with more effective distribution of temperature driving forces and an increased average temperature difference between hot and cold storage leading to increased thermal storage density and capacity. Fluch et al. [31] presented a software-tool with the ability to integrate and design storage systems with regards on the HEN. Network synthesis is carried out by means of an algorithm based on Pinch Analysis and

energy criteria.

The storage integration techniques presented in literature mainly focus on direct storage systems using either multiple storage tanks or stratified tank systems (VMFT storages). Indirect storages such as LHTS systems or single tank sensible storages are hardly considered.

2.5 Synthesis of the State-of-the-Art & Problem Statement

It is widely recognized that energy efficiency in industry is one of the main issues when it comes to CO₂ mitigation and that a reduction of GHG emissions is necessary to keep global warming and its negative consequences to a tolerable minimum. Process Integration offers tools to achieve a significant reduction in the use of thermal energy and thus in the consumption of fossil fuels. Well established methods such as Pinch Analysis and Mathematical Programming procedures have been successfully used to improve industrial energy systems. They provide guidelines and decision support for planning of new plants but also for retrofitting of existing ones.

The problem of HENS deals with the energy and cost-efficient combination of process streams. Using HEX hot and cold process streams are connected to reduce the need for external heating and cooling and thus to reduce energy consumption and consequently energy costs. For continuous processes, the PDM and more advanced approaches based on the PDM but also mathematical programming procedures were developed that allow to identify cost-efficient HENS for industry scale problems.

However, as was stated in the extensive review paper by Fernandez et al. [27], heat recovery in non-continuous and batch processes has only recently gained researchers' attention. Batch processes were assumed to only have small energy demand compared to continuous processes, which is not true for energy intensive processes such as brewing or dairy production.

In non-continuous industrial processes time plays a major role and the potential mismatch of surplus and demand of thermal energy makes the HENS problem much more difficult. Only few publications deal with the problem of multi-period and batch HENS compared to HENS for continuous problems.

Despite the potential for heat recovery in non-continuous processes by means of TES, literature reviews show that only few publications about real integration of such storage systems in industry are available. Miro et al. [72] mentioned in their review paper that this might be due to low technology maturity of promising storage systems and also financial barriers.

To overcome financial barriers it is important that TES become cheaper and more efficient. Furthermore, tools are necessary that help to identify cost efficient integration schemes. In fact, there are software tools available that allow for integration of TES into HENS that also consider storage costs.

However, there is still a lack of simultaneous optimization approaches that rig-

ously consider the trade-off between operating costs and investment costs for HEX and storage systems. This might be due to the fact that this makes the already NP-hard HENS problem even more difficult to solve.

Approaches for storage integration found in literature mostly deal either with two-tank storage systems or stratified tanks. Storages using PCM or sensible storages that change temperature when charged and discharged are hardly considered. However, those types of storage systems might either yield cheap alternatives to the two-tank or stratified tank systems or might be applicable for high temperatures. PCM storages might be especially suitable for processes where heat demand and excess heat supply occur in a narrow temperature range. This is often the case for condensing and evaporating streams.

Thus, the main topics addressed in the present thesis can be summarized as follows:

- How can the complex problem of simultaneous HENS for industry-scale multi-period problems be tackled?
- What simplifications and reformulations are needed to solve the problem faster without losing accuracy and feasibility of the solutions?
- How can the problem of simultaneous HENS be extended for storage integration?
- How can storage systems other than two-tank and stratified tank systems be considered for Process Integration?

2.6 Related Publications

The present thesis and the framework described in Section 3 are based on 6 publications. These are listed below in logical order.

- **Paper 1:** A. Beck, R. Hofmann: "A Novel Approach for Linearization of a MINLP Stage-Wise Superstructure Formulation"; *Computers & Chemical Engineering*, 112 (2018), 112; 17 - 26.

This paper presents a method for the linearization of the stage-wise superstructure proposed by Yee and Grossmann [94]. It is demonstrated to yield results comparable to results presented in literature. However, the linearized superstructure formulation can be solved significantly faster compared to the original problem.

- **Paper 2:** A. Beck, R. Hofmann: "How to tighten a commonly used MINLP superstructure formulation for simultaneous heat exchanger network synthesis"; *Computers & Chemical Engineering*, 112 (2018), 112; 48 - 56.

Several tightening measures are proposed that allow to find results for the MINLP superstructure faster. Either new constraints are added to the model or parameters are adjusted in a way that help to reduce the duality gap and to solve the model faster.

- **Paper 3:** A. Beck, R. Hofmann: "Tightening of MINLP Superstructure Relaxation for Faster Solution of Heat Exchanger Network Synthesis Problems"; in "Proceedings of the 12th Conference on Sustainable Development of Energy, Water and Environment Systems", (2017), ISSN: 1847-7178; Paper-Nr. FP-950

Both the linearization approach and a selection of tightening measures are applied to the superstructure. Results for several case studies are compared.

- **Paper 4:** A. Beck, R. Hofmann: "Extensions for Multi-Period MINLP Superstructure Formulation for Integration of Thermal Energy Storages in Industrial Processes"; in: "Proceedings of the 28th European Symposium on Computer Aided Process Engineering", A. Friedl, J. Klemes, S. Radl, P. Varbanov, T. Wallek (Hrg.); Elsevier B.V., Part A (2018), ISBN: 978-0-444-64237-0; 1335 - 1340.

A sequential approach for storage integration is proposed based on the stage-wise superstructure formulation. LHTS, fluidized bed regenerators and two-tank storage systems are integrated into an example process.

- **Paper 5:** A. Beck, R. Hofmann: "A sequential approach for integration of multiple thermal energy storages with fixed mass and variable temperature"; Applied Thermal Engineering, Volume 148, 2019, pp. 278-294, ISSN 1359-4311

A MINLP formulation is proposed that allows for storage sizing for multiple storages simultaneously. Also a pressurized water storage system is presented and integrated into two example cases using the new MINLP formulation for storage sizing and an extended superstructure formulation.

- **Paper 6:** A. Beck, W. Gruber-Glatzl, J. Fluch, R. Hofmann: "Process Integration in a Dairy Factory Considering Thermal Energy Storages - A Comparison of Two Different Approaches"; in "Proceedings of the International Sustainable Energy Conference 2018", (2018), S. 153-161.

The proposed framework is presented and a dairy process is used as a test-case for integration of a two-tank system. Results are compared to results obtained using the software SOCO.

Chapter 3

Process Integration Framework

Within this thesis methods were developed that allow to identify cost-optimized heat recovery networks for continuous large-scale, but also for multi-period and batch problems with the capability for integration of different types of TES.

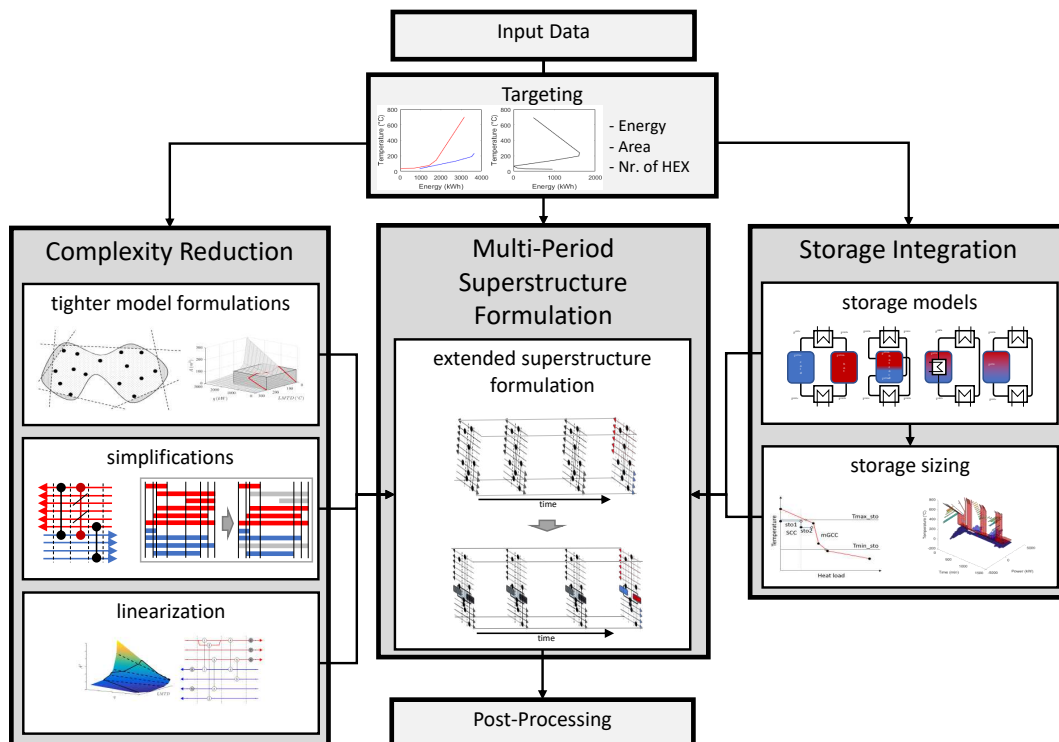


Figure 3.1: Structure of the proposed framework: a multi-period superstructure formulation, complexity reduction and storage integration

All methods were embedded in a Process Integration framework developed in MATLAB that is based on the following three pillars also shown in Figure 3.1:

- An extended **multi-period stage-wise superstructure** MINLP formulation for simultaneous HEN synthesis and storage integration,
- Strategies and methods for **complexity reduction** of the simultaneous HENS problem,
- Models for **storage integration** and methods for storage sizing and parameter fitting of these models

The framework is built in a modular structure that can easily be extended. All of the individual modules shown in Figure 3.1 either define constraints for the Mathematical Programming model or are used to calculate coefficients for these constraints. The basic modules in the framework are:

- **Extended superstructure formulation:** In this module the mathematical model is set up. The extended superstructure is based on a multi-period extension for Yee and Grossmann's [94] stage-wise superstructure formulation for simultaneous HENS (SYNHEAT model). A thorough analysis of the properties of the superstructure was conducted in the course of this thesis and several modifications were introduced that significantly improve the solution time. Depending on whether the linearization module is used, either a nonlinear or linearized version of the superstructure is generated. In the case that also TES should be integrated, the interface between superstructure and storage systems is adjusted accordingly.
- **Storage Models:** In this module, MI(N)LP models for the different storage systems are set up that can be used in both the superstructure and the storage sizing formulation. Mathematical Programming models for FMVT storages such as pressurized water storages, sensible storages using fluidized particles or other solid storage materials and LHTS using PCM as storage material were developed within the thesis. But also models for VMFT systems such as classical stratified tank and multi-tank systems were proposed.
- **Storage Sizing:** Inclusion of optimal storage sizing in the HENS problem increases problem complexity even more compared to synthesis of networks allowing only direct heat recovery using HEX. For this reason, a MINLP model based on modified GCCs is presented that allows to identify close to optimal storage sizes prior to network generation. Using these storage

sizes as fixed parameters within the superstructure formulation significantly simplifies the problem. This way, larger problems can be handled, however, the global optimum of the overall problem might not be obtained.

- **Targeting:** Targets for maximum heat recovery, minimum total HEX areas and number of HEX units are calculated. These targets are used in the post-processing module to evaluate the results obtained with the framework, but are also necessary for linearization and for obtaining tighter model formulations.
- **Linearization:** In this module, coefficients for linear constraints are calculated that are used for replacing the nonlinear terms in the proposed extended superstructure. Furthermore, upper bounds for the individual HEX areas are identified that can be used within the module for model tightening.
- **Model Tightening:** In this module, additional constraints are introduced that tighten the extended MINLP superstructure model. For some tightening constraints results from the targeting and linearization modules are used.
- **Simplifications:** Within this module, the HENS problem can be simplified even more using problem reduction techniques such as intelligent reduction of process streams considered for Process Integration, restriction of the number of HEX for each stream pair or reduction of binary variables used within the model.

In **Paper 6** appended in this thesis, most of the methods included in the framework were used for optimization of the heat recovery network including a two-tank storage system of an industry-scale dairy process.

After a description of the necessary input data, all modules and the methods developed within this thesis are described in more detail in the following chapters.

3.1 Input Data

Depending on which modules within the framework are used for Process Integration, different input data might be necessary, which are described in this section.

3.1.1 Thermodynamic Parameters

As stated in Section 2, inlet and outlet temperature levels of the individual process streams need to be specified, just like for most other heat integration approaches. Also, either heat capacity flow rates or average heat capacity and mass flows need to be supplied. In the case of multi-period problems durations of the individual operating periods and the stream properties mentioned above need to be provided for every period. To account for necessary heat transfer areas in the individual HEX, heat transfer coefficients for process streams, utilities and storage systems need to be specified.

3.1.2 Cost Coefficients

The objective of the proposed optimization problems is to minimize TAC, thus cost data for hot and cold utilities and cost data for heat recovery equipment (HEX, TES) needs to be provided. In contrast to utility costs, which are readily available from contractors and market places for energy, equipment costs are rather difficult to obtain. There are several publications available that present cost functions for certain types of HEX [39, 81], however, comparison of these cost functions shows that they vary by a huge amount and thus are not reliable. An alternative to the cost functions taken from open literature, cost estimation software such as ASPEN Capital Cost Estimator or online resources like the Heat Exchanger Design Handbook [57, 20] can provide suitable cost correlations. But even the selection of the appropriate HEX material might not be straight forward and for individual stream connections different types of HEX might be necessary.

3.1.3 Optimization Parameters

When using the linearization module, the number of approximating planes for the linearization of the nonlinear constraints modelling HEX areas has to be specified. Also, the maximum relative difference for the approximation of the logarithmic mean temperature difference $LMTD$ is required. Furthermore, a reasonable value for ΔT_{min} must be provided for energy targeting and as a lower bound for temperature differences in the superstructure formulation. This value is also necessary for identification of the feasible domain of both $LMTD$ and the heat load \dot{Q} for the linear approximation of HEX areas. Concerning the superstructure formulation, the number of temperature stages NOK needs to be specified. For small-scale problems NOK can be set to the maximum of hot or cold streams. However, for large industry-scale problems NOK needs to be

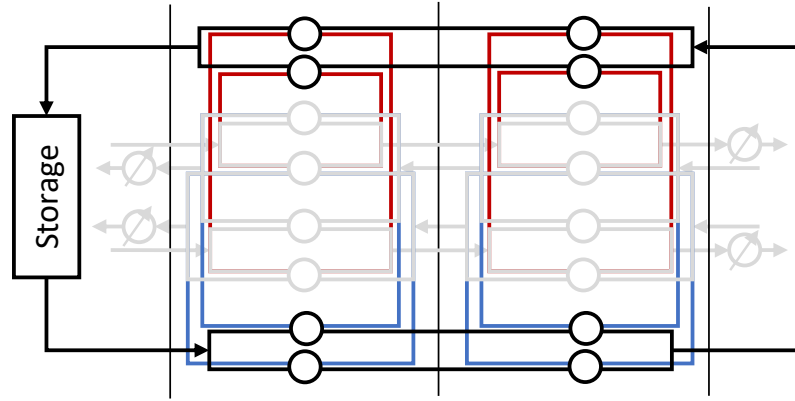


Figure 3.2: Extended superstructure for storage integration for two hot streams, two cold streams and two temperature stages

reduced in order to be able to solve the problem.

3.1.4 Model Parameters

The storage model parameters need to be specified according to the TES systems that should be integrated. Depending on storage material and storage design parameters need to be adjusted. If the model parameters for the simple TES models used within the framework are unknown, regression methods can be used to obtain model parameters from real measurement data. In Section 3.3.3 an example is presented, where model parameters for an LHTS system are obtained.

3.2 Extended Superstructure Formulation

As stated before, the extended superstructure formulation used in the proposed framework is based on the SYNHEAT model by Yee and Grossmann [94]. They proposed a stage-wise superstructure which by now is well-established and was considered by many authors for HENS. Escobar et al. [24] compared the results obtained using this superstructure to the superstructure proposed by Ciric et al. [19] which showed that for the majority of case-studies Yee and Grossmann's superstructure found solutions faster with lower TAC. As mentioned in Section 2.3, modifications of the SYNHEAT model for multi-period HENS were proposed by Aaltola [2] and later by Zhang and Verheyen [100]. In this thesis, a version proposed by Zhang and Verheyen [100] is extended for the integration of TES. The full model of the proposed extended superstructure is presented

in **Paper 5**. For a simple problem consisting of two hot and two cold streams and a single storage system a schematic of this extension is shown in Figure 3.2. Each storage system is connected to the process streams through an intermediate storage cycle (ISC).

The used superstructure of Yee and Grossmann [94] includes several simplifying assumptions that make the model easier to solve:

- External heating or cooling can only take place outside of the temperature stages connecting the individual process streams.
- Streams can only be split within one temperature stage.
- Mixing-temperatures of split-streams need to be equal.

Also, for the extension proposed in this thesis some simplifying assumptions are made:

- Mixing-temperatures for ISC splits are equal.
- Each process stream can be connected to the ISC through only one HEX.
- Cyclic operation is assumed for multi-period processes.
- Storage temperatures are equal at the beginning and the end of each operating cycle.

For the inclusion of storage systems and ISCs in the superstructure, energy balance equations and the objective function need to be altered. In the overall energy balance of process streams but also in energy balances for each temperature stage heat flows to the ISCs need to be considered. Temperature differences, heat loads and HEX areas for HEX connecting process streams and ISCs are modelled similar to the HEX in the basic superstructure to model. The constraints connecting the ISCs to the storage vessels and the storage models themselves are presented in Section 3.3.3.

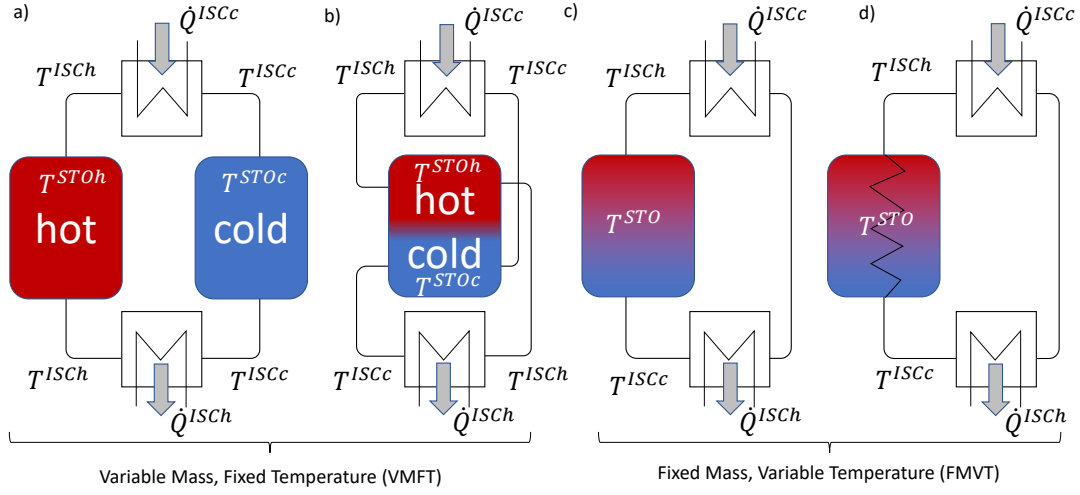


Figure 3.3: Different thermal energy storages in the framework

3.3 Storage Models

The storage models presented in this section can be integrated in both the extended superstructure and the storage sizing formulation presented in Section 3.4. They describe sizes and thermal behaviour of the storages, and the costs for storage material and storage vessels. In order to keep the storage models simple, some assumptions were made:

- Storages are modelled as mass points (uniform temperature distribution in each storage vessel or temperature layer in stratified tanks).
- The storage state is equal at the beginning and the end of the process duration.
- Thermal losses are neglected.

For all storage models, the cumulated energy inside the storage vessels Q^{STO} is calculated using the equality constraints

$$Q_t^{STO} = \sum_{r=1}^t (\dot{Q}_r^{ISCc} - \dot{Q}_r^{ISCh}) \tau_r, \forall t = 1, \dots, NOP. \quad (3.1)$$

In Eq. (3.1) \dot{Q}^{ISCc} is the heat flow from hot process streams to the ISC, similarly, \dot{Q}^{ISCh} is the heat flow from the ISC to the cold process streams. NOP is the number of operating periods and τ is the duration of these operating periods.

In the following, models for FMVT and VMFT storage systems are presented, some of which are also described in **Paper 4** and **Paper 5**. Especially the model for LHTS is presented in more detail in the next section and it is shown how the model parameters can be tuned to fit real storages using measurement data.

3.3.1 Storages with Variable Mass and Fixed Temperature

VMFT storages either consist of at least two distinct reservoirs or of different temperature layers in the case of stratified tanks. In these types of storage systems the storage medium is also the HTF. This means that the cold and hot temperatures of the ISC correspond to the temperatures of the cold and hot storage tanks connected by the ISC, as shown in Figure 3.3 a) and b).

$$T^{ISCc} = T^{STOc}, \quad T^{ISCh} = T^{STOh} \quad (3.2)$$

In this work, this storage type is limited to either two storage tanks or two temperature layers in the case of stratified tank storages. The thermocline in stratified tanks is assumed to be ideal and, thus, no heat flow occurs between the layers.

The temperatures of the hot and cold storages (T^{STOh} and T^{STOc}) are variables that are optimized by the solver. The storage size is modelled by the nonlinear inequality constraint

$$m^{STO} \geq \frac{Q_{max}^{STO} - Q_{min}^{STO}}{(T^{STOh} - T^{STOc})c_p^{STO}}. \quad (3.3)$$

The maximum and minimum stored energy contents Q_{max}^{STO} and Q_{min}^{STO} in Eq. (3.3) are modelled by the following inequality constraints.

$$Q_{max}^{STO} \geq Q_t^{STO}, \quad Q_{min}^{STO} \leq Q_t^{STO}, \quad \forall t = 1, \dots, NOP. \quad (3.4)$$

3.3.2 Storages with Fixed Mass and Variable Temperature

FMVT storages change temperature depending on their state of charge. The models for this type of storage are more complicated than those for VMFT systems. Compared to the single nonlinear equation for VMFT storages that

Table 3.1: Model parameter comparison for LHTS and sensible FMVT storage systems; X... required, (X)... either solid or liquid properties required

Model Coefficients			LHTS	sensible
U_s	heat transfer coefficient (solid)	kW/m ² K	X	(X)
U_h	heat transfer coefficient (latent)	kW/m ² K	X	
U_l	heat transfer coefficient (liquid)	kW/m ² K	X	(X)
T_{var}	melting temperature range	K	X	
m^{STO}	storage mass	kg	X	X
h^{STO}	phase change enthalpy	kJ/kg	X	
$c_{p,s}$	lumped specific heat capacity (solid)	kJ/kgK	X	(X)
$c_{p,h}$	lumped specific heat capacity (latent)	kJ/kgK	X	
$c_{p,l}$	lumped specific heat capacity (liquid)	kJ/kgK	X	(X)

identifies the minimal mass of the storage medium m^{STO} , for FMVT storages *NOP* nonlinear equality constraints are necessary to obtain feasible storage operation.

LHTS ideally work at the melting temperature of the PCM used as storage medium, however, in real operation the temperature cannot be kept constant and the average storage temperature in the storage changes depending on the charging state. For this reason LHTS are modelled as FMVT storages. Sensible storage systems using pressurized water or fluidized beds can also be modelled as FMVT storages.

FMVT storages that are charged and discharged **directly** use the storage medium also for heat transfer and thus do not need an HEX inside the storage unit. Pressurized water storages in a closed-loop operation are an example for this storage type. This means that for storage systems where the HTF corresponds to the storage medium the temperature within the ISC corresponds to the storage temperature.

$$T^{ISCh} = T^{ISCc} = T^{STO} \quad (3.5)$$

FMVT storages that are charged and discharged **indirectly** need to transfer between the HTF and the storage material via HEX. This is the case for LHTS systems, fluidized bed regenerators and other solid matter storage systems opposed to systems like the pressurized water storage presented in **Paper 5**. The parameters necessary for the proposed indirect storage models are presented in Table 3.1. When the storage system is charged, the ISC temperatures need to be higher than the storage temperature in order to obtain positive driving forces for heat transfer.

$$T^{ISCh} \geq T^{ISCc} \geq T^{STO} \quad (3.6)$$

Similarly, while discharging, the ISC temperatures need to be lower than the storage temperature.

$$T^{STO} \geq T^{ISCh} \geq T^{ISCc} \quad (3.7)$$

The necessary heat transfer area A^{STO} for indirect storage systems is modelled using the following inequality constraints

$$A^{STO} \geq \frac{\sum_i \dot{Q}_{it}^{ISCc} + \sum_j \dot{Q}_{jt}^{ISCh}}{U^{STO} LMTD_t^{STO}},$$

$$\forall t = 1, \dots, NOP, i \in HP, j \in CP \quad (3.8)$$

where U^{STO} is the overall heat transfer coefficient between ISC and the storage material and $LMTD^{STO}$ is the logarithmic mean temperature difference between HTF and storage material. HP and CP are the sets of hot and cold process streams.

The temperature differences used to calculate $LMTD_t^{STO}$ inside the storage vessels are modelled using the logical constraints

$$\begin{aligned} \Delta T_t^{STO h1} &\leq T_t^{ISC, in} - T_t^{STO} + \Gamma^{STO}(z_t^{switch}), \\ \Delta T_t^{STO h2} &\leq T_t^{ISC, out} - T_t^{STO} + \Gamma^{STO}(z_t^{switch}), \\ \Delta T_t^{STO c1} &\leq T_t^{STO} - T_t^{ISC, in} + \Gamma^{STO}(1 - z_t^{switch}), \\ \Delta T_t^{STO c2} &\leq T_t^{STO} - T_t^{ISC, out} + \Gamma^{STO}(1 - z_t^{switch}), \end{aligned}$$

$$\forall t = 1, \dots, NOP \quad (3.9)$$

where z_t^{switch} is a binary variable depicting whether the storage is charged or discharged. Here, Γ^{STO} are suitable big-M coefficients. The logarithmic temperature difference inside the storages $LMTD^{STO}$ is modelled using the Chen approximation [17].

$$LMTD_t^{STO} \leq \left(\Delta T_t^{STO h1} \Delta T_t^{STO h2} \frac{\Delta T_t^{STO h1} + \Delta T_t^{STO h2}}{2} \right)^{\frac{1}{3}},$$

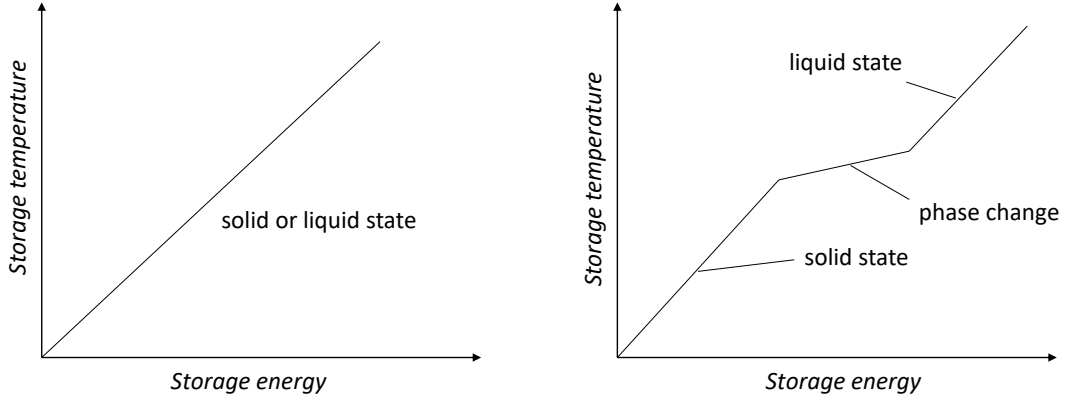


Figure 3.4: Modelled characteristics of sensible FMVT storages (left) and LHTS (right)

$$LMTD_t^{STO} \leq \left(\Delta T_t^{STOc1} \Delta T_t^{STOc2} \frac{\Delta T_t^{STOc1} + \Delta T_t^{STOc2}}{2} \right)^{\frac{1}{3}}, \forall t = 1, \dots, NOP \quad (3.10)$$

Different FMVT storage models are needed to account for the different characteristics of sensible and LHTS systems. In the 1-D models used within the proposed framework these characteristics are modelled as (piecewise) linear functions of temperature and stored energy as shown in Figure 3.4. For LHTS systems a change of temperature is assumed also during phase change which allows to account for both the mushy region of PCMs but also to consider the moving melting or solidification front occurring in real LHTS systems.

For **sensible** storages stored energy and storage temperature are connected through the following nonlinear equality constraints.

$$Q_t^{STO} = T_t^{STO} c_p m^{STO}, \quad \forall t = 1, \dots, NOP \quad (3.11)$$

The mathematical model for **LHTS** systems is presented in detail in the following. Integration of this type of storage was shown in **Paper 4**, however, due to space limitations a detailed description was not possible. Piecewise linear functions are necessary to describe the characteristics of LHTS characteristics. These are modelled using binary variables z_{st}^{STO} , z_{ht}^{STO} and z_{lt}^{STO} that define whether the storage is in solid state s , in phase-change h or in liquid state l . As the storage can only be in one state at once, the sum of the binary variables has to

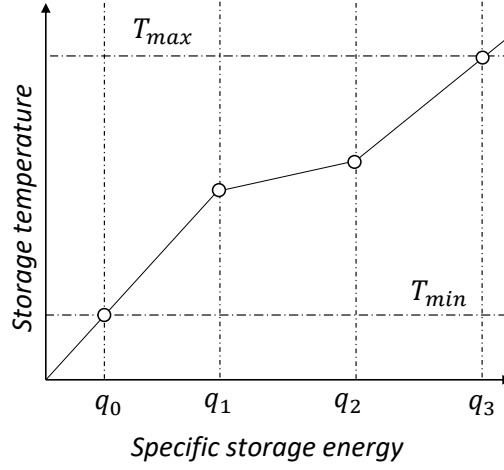


Figure 3.5: Discrete temperature and energy values that characterize LHTS systems

be equal to 1.

$$z_{st}^{STO} + z_{ht}^{STO} + z_{lt}^{STO} = 1, \quad \forall t = 1, \dots, NOP \quad (3.12)$$

Because the storage characteristics change with storage mass, the characteristics are modelled with the specific stored energy q_t^{STO} using the following nonlinear equality constraints.

$$q_t^{STO} = \frac{Q_t^{STO}}{m^{STO}}, \quad \forall t = 1, \dots, NOP \quad (3.13)$$

The specific storage charging state q_t^{STO} can be identified using the lower and upper bounds of the discrete segments. These bounds are shown in Figure 3.5. The feasible specific storage energy range for the solid state is $q_0 \leq q_t^{STO} \leq q_1$. Similarly, the range for the phase change is $q_1 \leq q_t^{STO} \leq q_2$ and for the liquid state $q_2 \leq q_t^{STO} \leq q_3$. Using the binary variables z_{st}^{STO} , z_{ht}^{STO} and z_{lt}^{STO} , the active segment can be identified using the following logical constraints.

$$q_t^{STO} + q_{shift} \leq q_1 z_{st}^{STO} + q_2 z_{ht}^{STO} + q_3 z_{lt}^{STO}, \quad \forall t = 1, \dots, NOP \quad (3.14)$$

$$q_t^{STO} + q_{shift} \geq q_0 z_{st}^{STO} + q_1 z_{ht}^{STO} + q_2 z_{lt}^{STO}, \quad \forall t = 1, \dots, NOP \quad (3.15)$$

Here, q_{shift} is a continuous optimization variable that defines the initial specific

Table 3.2: Coefficients for piecewise linear functions

	solid	phase-change	liquid
Φ_{var}	$1/c_{p,s}$	$1/c_{p,h}$	$1/c_{p,l}$
Φ	0	$(T_{melt} - \frac{T_{var}}{2}) \frac{c_{ph}}{q_1}$	$(T_{melt} + \frac{T_{var}}{2}) \frac{c_{pl}}{q_2}$

energy in the storage. The characteristic relation between storage temperature T_t^{STO} and the specific stored energy q_t^{STO} is modelled using linear inequality constraints and binary variables. To obtain a tight model, the modified big-M formulation by Trespalcios and Grossmann [87] was used.

The linear functions describing the relation for the three different parts are of the form

$$T_t^{STO} = \Phi_{var}(q_t^{STO} + q_{shift}) + \Phi, \quad \forall t = 1, \dots, NOP. \quad (3.16)$$

The corresponding coefficients are presented in Table 3.2. In the mathematical model the piecewise linear characteristics are modelled as

$$T_t^{STO} \leq \Phi_{var,s}(q_t^{STO} + q_{shift}) + \Phi_s, \quad \forall t = 1, \dots, NOP \quad (3.17)$$

$$T_t^{STO} \leq \Phi_{var,h}(q_t^{STO} + q_{shift}) + \Phi_h + M_{hl}^- z_l^{STO}, \quad \forall t = 1, \dots, NOP \quad (3.18)$$

$$T_t^{STO} \leq \Phi_{var,l}(q_t^{STO} + q_{shift}) + \Phi_l + M_{ls}^- z_s^{STO} + M_{lh}^- z_h^{STO}, \quad \forall t = 1, \dots, NOP \quad (3.19)$$

$$T_t^{STO} \geq \Phi_{var,s}(q_t^{STO} + q_{shift}) + \Phi_s - M_{sh}^+ z_h^{STO} - M_{sl}^+ z_l^{STO}, \quad \forall t = 1, \dots, NOP \quad (3.20)$$

$$T_t^{STO} \geq \Phi_{var,h}(q_t^{STO} + q_{shift}) + \Phi_h + M_{hs}^+ z_s^{STO}, \quad \forall t = 1, \dots, NOP \quad (3.21)$$

$$T_t^{STO} \geq \Phi_{var,l}(q_t^{STO} + q_{shift}) + \Phi_l, \quad \forall t = 1, \dots, NOP \quad (3.22)$$

where M are the modified big-M parameters. How they can be calculated is presented in the work by Trespalcios and Grossmann [87]. A graphical representation of these constraints using the tightest possible modified big-M formulation for modelling of the LHTS characteristics is shown in Figure 3.6. Also

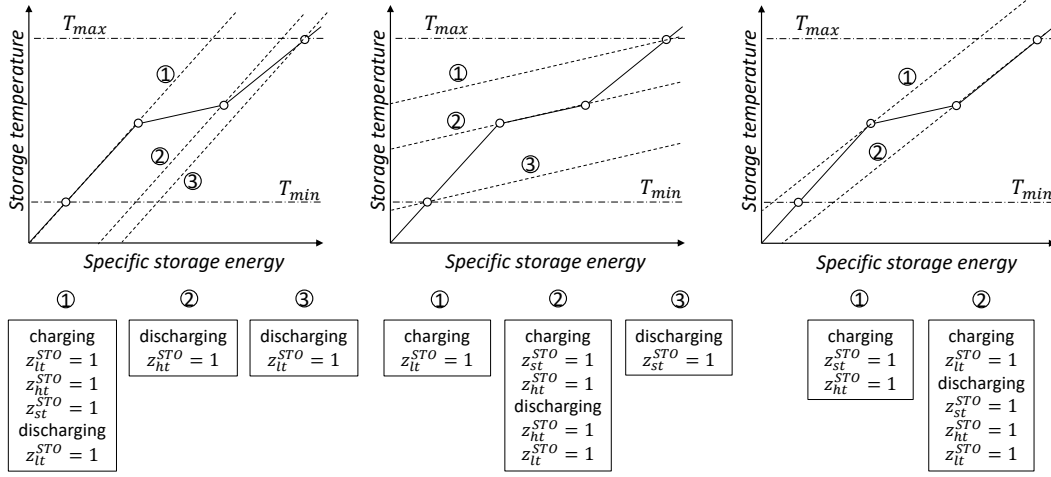


Figure 3.6: Modified big-M constraints used for modelling of the LHTS characteristics

the binary variable values, that are shifting the constraints in combination with the big-M coefficients, are shown in the Figure.

For indirect storage systems heat transfer from the HTF to the storage material is necessary inside the storage vessel. The driving temperature differences ΔT_t^{STO} for heat transfer is modelled using the mean temperature of the in- and outlet temperatures of the ISC.

$$T_{m,t} = \frac{T_t^{ISCh} + T_t^{ISCc}}{2}, \quad \forall t = 1, \dots, NOP \quad (3.23)$$

$$\Delta T_t^{STO} \leq T_{m,t} - T_t^{STO} + (1 - z_t^{switch})\Gamma, \quad \forall t = 1, \dots, NOP \quad (3.24)$$

$$\Delta T_t^{STO} \leq T_t^{STO} - T_{m,t} + z_t^{switch}\Gamma, \quad \forall t = 1, \dots, NOP \quad (3.25)$$

The driving temperature difference ΔT_t^{STO} is necessary for modelling the heat transfer area A^{STO}

$$A^{STO} \geq \frac{\dot{Q}_t^{ISCh} + \dot{Q}_t^{ISCc}}{U^{STO} \Delta T_t^{STO}}, \quad \forall t = 1, \dots, NOP \quad (3.26)$$

where U^{STO} is the overall heat transfer coefficient between HTF and storage material. Different values for U^{STO} in solid, liquid and transition state can be

modelled using the binary variables z_{st}^{STO} , z_{ht}^{STO} and z_{lt}^{STO} . Eq. (3.26) is then replaced by the following constraints.

$$A^{STO} \geq \frac{\dot{Q}_t^{ISCh} + \dot{Q}_t^{ISCc}}{U_s^{STO} \Delta T_t^{STO}} - (1 - z_{st}^{STO})\Gamma^{STO}, \quad \forall t = 1, \dots, NOP \quad (3.27)$$

$$A^{STO} \geq \frac{\dot{Q}_t^{ISCh} + \dot{Q}_t^{ISCc}}{U_h^{STO} \Delta T_t^{STO}} - (1 - z_{ht}^{STO})\Gamma^{STO}, \quad \forall t = 1, \dots, NOP \quad (3.28)$$

$$A^{STO} \geq \frac{\dot{Q}_t^{ISCh} + \dot{Q}_t^{ISCc}}{U_l^{STO} \Delta T_t^{STO}} - (1 - z_{lt}^{STO})\Gamma^{STO}, \quad \forall t = 1, \dots, NOP \quad (3.29)$$

Instead of using Eqs. (3.23), (3.24) and (3.25) to model the driving temperature differences for heat transfer, the logarithmic mean temperature difference could be used. However, this would introduce additional nonlinear constraints and thus would increase problem complexity.

3.3.3 Identification of Model Parameters

In the following, an example is presented that shows how the parameters of a real storage system can be tuned using measurement data. The storage model used for demonstration is the LHTS system presented previously. The unknown parameters are the temperature range T_{var} over which melting and solidification takes place and the overall heat transfer coefficient U from HTF to the storage material. The storage parameters presented in Table 3.3 and the experimental measurement data used for parameter fitting were presented by Zauner et al. [98].

Because the sensible heat capacities of steel (structure, pipes) and aluminium (fins) do not occur explicitly in the mathematical model, the lumped parameters $c_{p,s}$, $c_{p,h}$ and $c_{p,l}$ are introduced considering all heat capacities of the real TES. The lumped parameters $c_{p,s}$ and $c_{p,l}$ are calculated by

$$c_{p,s} = \frac{m^{steel} c_p^{steel} + m^{alu} c_p^{alu} + m^{PCM} c_{p,s}^{PCM}}{m^{PCM}}, \quad (3.30)$$

$$c_{p,l} = \frac{m^{steel} c_p^{steel} + m^{alu} c_p^{alu} + m^{PCM} c_{p,l}^{PCM}}{m^{PCM}}, \quad (3.31)$$

which leads to the values presented in Table 3.4. The lumped parameter for specific heat capacity during phase change $c_{p,h}$ changes with the tuning parameter

Table 3.3: Storage data for LHTS storage system [98]

Storage Vessel			
m^{steel}	mass of steel components	259.3	kg
m^{alu}	mass of aluminium components	18.3	kg
c_p^{steel}	spec. heat capacity of steel	0.45	kJ/kgK
c_p^{alu}	spec. heat capacity of aluminium	0.85	kJ/kgK
A	heat transfer area	72.7	m ²
PCM			
m^{PCM}	mass of PCM	170	kg
$c_{p,s}^{PCM}$	spec. heat capacity of solid PCM	2	kJ/kgK
$c_{p,l}^{PCM}$	spec. heat capacity of liquid PCM	2.5	kJ/kgK
h_{melt}	spec. melting enthalpy	240	kJ/kg
T_{melt}	melting temperature	120	°C
Thermal Oil			
c_p^{oil}	spec. heat capacity of thermal oil	2	kJ/kgK

Table 3.4: Weighted specific heat capacities for example case

$c_{p,s}$	spec. heat capacity of solid PCM	2.78	kJ/kgK
$c_{p,l}$	spec. heat capacity of liquid PCM	3.28	kJ/kgK

T_{var} and thus has to be calculated for every iteration during parameter fitting. The specific heat capacity of the PCM during phase-change is calculated by

$$c_{p,h}^{PCM} = \frac{h_{melt}}{T_{var}}. \quad (3.32)$$

With $c_{p,h}^{PCM}$ the lumped parameter $c_{p,h}$ is then obtained by

$$c_{p,h} = \frac{m^{steel} c_p^{steel} + m^{alu} c_p^{alu} + m^{PCM} c_{p,h}^{PCM}}{m^{PCM}}. \quad (3.33)$$

The governing equations describing the LHTS system are

- the energy balance for the HTF

$$\dot{Q}^{STO} = (T^{HTF,in} - T^{HTF,out}) \dot{m}^{oil} c_p^{oil}, \quad (3.34)$$

- the equations describing the energy content inside the storage, which is a

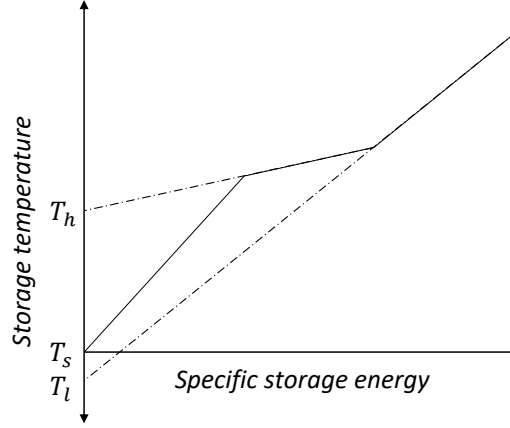


Figure 3.7: Identification of the model parameters T_s , T_h and T_l

piecewise function depending on the storage charging state

$$Q^{STO} = \begin{cases} (T^{STO} - T_s)m^{STO}c_{p,s} & \text{if } T^{STO} \leq T_{melt} - T_{var}/2 \\ (T^{STO} - T_h)m^{STO}c_{p,h} & \text{if } T_{melt} - T_{var}/2 \leq T^{STO} \leq T_{melt} + T_{var}/2 \\ (T^{STO} - T_l)m^{STO}c_{p,l} & \text{if } T_{melt} + T_{var}/2 \leq T^{STO} \end{cases} \quad (3.35)$$

- and the equation describing the heat transfer between the HTF and the storage material

$$\dot{Q}^{STO} = UA\Delta T = UA \left(\frac{T^{HTF,in} + T^{HTF,out}}{2} - T^{STO} \right). \quad (3.36)$$

Here, for ΔT the temperature difference according to Eqs. (3.23), (3.24) and (3.25) was used instead of the logarithmic mean temperature difference. This way, a piecewise differential equation describing the storage behaviour can be derived in the explicit form

$$\dot{Q}^{STO} + Q^{STO}\Phi_1 = \Phi_2 \quad (3.37)$$

with the parameters Φ_1 and Φ_2

$$\Phi_1 = \frac{UA}{m^{STO}c_p \left(1 + \frac{UA}{2\dot{m}^{oil}c_p^{oil}}\right)}, \quad \Phi_2 = \frac{UA(T^{HTF,in} - \Omega)}{1 + \frac{UA}{2\dot{m}^{oil}c_p^{oil}}} \quad (3.38)$$

Table 3.5: Fitted storage parameters for the LHTS example

U	heat transfer coefficient	0.0135	kW/m ² K
T_{var}	temperature range of melting	25	K
$c_{p,h}$	spec. heat capacity PCM latent	10.38	kJ/kgK

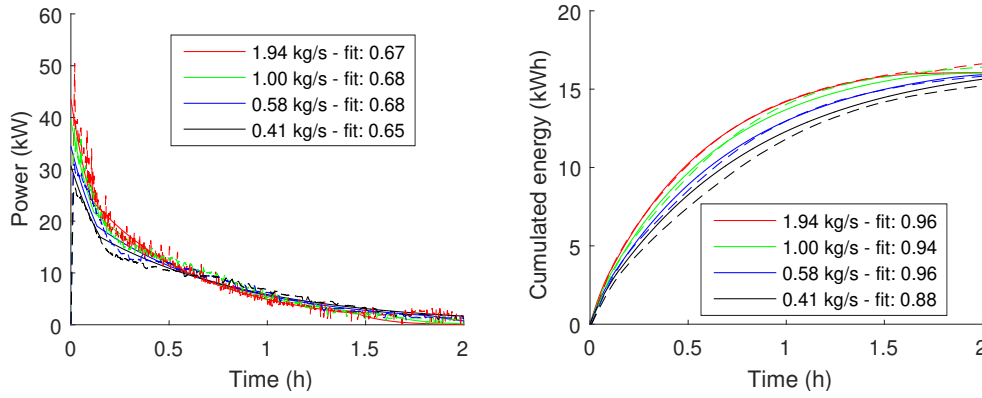


Figure 3.8: Simulation results compared with measurement data and least squares fit

where c_p and Ω also depend on the charging state of the storage.

$$c_p = \begin{cases} c_{p,s} & \text{if } T^{STO} \leq T_{melt} - T_{var}/2 \\ c_{p,h} & \text{if } T_{melt} - T_{var}/2 \leq T^{STO} \leq T_{melt} + T_{var}/2 \\ c_{p,l} & \text{if } T_{melt} + T_{var}/2 \leq T^{STO} \end{cases} \quad (3.39)$$

$$\Omega = \begin{cases} T_s & \text{if } T^{STO} \leq T_{melt} - T_{var}/2 \\ T_h & \text{if } T_{melt} - T_{var}/2 \leq T^{STO} \leq T_{melt} + T_{var}/2 \\ T_l & \text{if } T_{melt} + T_{var}/2 \leq T^{STO} \end{cases} \quad (3.40)$$

In the presented example, the piecewise differential equation Eq. (3.37) was solved for various manually selected parameter values and a least squares fit for the measurement data was calculated. The identified values with the best fit are presented in Table 3.5. A reason for the low fitting value is the noise in the measurement data. Alternatively, the selection of parameter values could be done using optimization techniques such as genetic algorithms.

3.4 Storage Sizing

The storage sizing module includes a novel MINLP model for storage sizing. The storage sizes obtained using this model can then be used within the extended superstructure as fixed parameters. This simplifies the problem of HENS including FMVT storages significantly.

The proposed model for storage sizing is based on modified GCCs (mGCCs) which are similar to the shifted GCC proposed by Bandyopadhyay et al. [8] for total-site integration. Within the MINLP model the mGCCs are formulated as piecewise linear functions and are used as upper bounds for storage heat loads.

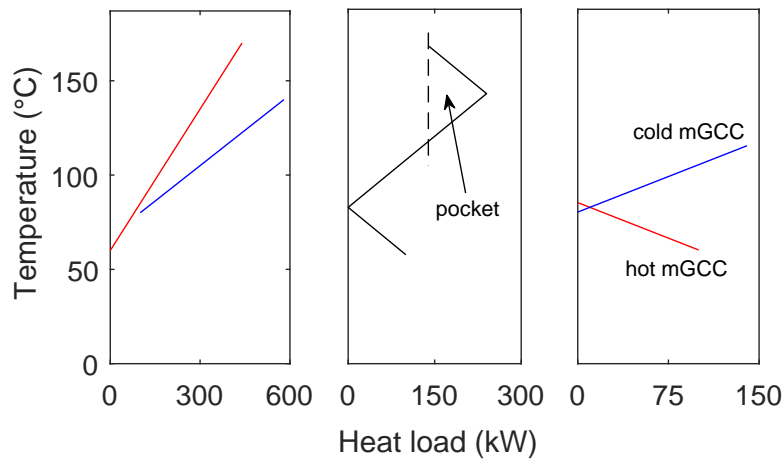


Figure 3.9: From left to right: CCs, GCCs, mGCCs

The objective of the MINLP formulation for storage sizing is to minimize TAC considering the trade-off between storage costs and costs for residual utilities. No individual HEX are considered which makes the problem relatively easy to solve.

In order to obtain mGCCs, first, GCCs are constructed according to Section 2.1. The so called heat recovery pockets are removed and the GCC is split at the pinch point. Finally, the mGCCs are obtained by shifting the split curves back by $\Delta T_{min}/2$. The mGCCs are calculated for every operating period which are modelled as piecewise linear constraints for storage temperatures and heat loads within the MINLP formulation.

To illustrate this idea, a graphical representation of the solution for a simple example with two operating periods is presented in Figure 3.10 which was obtained using the global optimization solver BARON 16.5.16 [84, 79]. The grey areas defined by the mGCCs and the upper and lower bounds for storage tem-

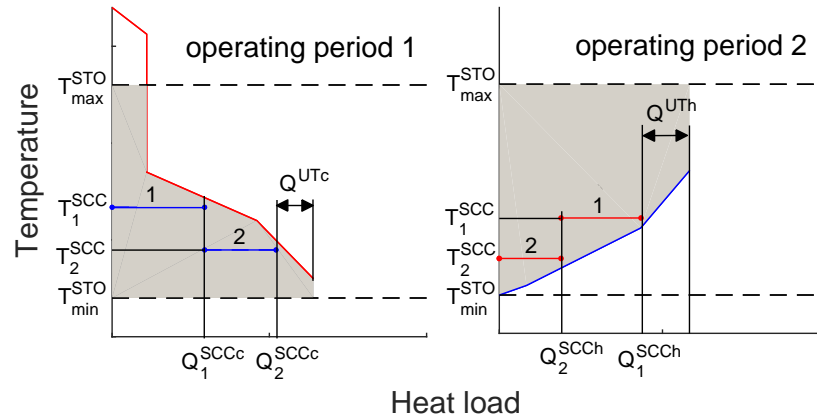


Figure 3.10: mGCCs for a small example with two operating periods and a solution for storage temperatures and heat loads; feasible range for temperature and heat loads is marked in grey

peratures show the feasible temperature range and the corresponding feasible storage charging and discharging heat loads. The numbered lines in this Figure represent storage temperatures after the respective operating periods and the corresponding heat loads. These lines can be interpreted as Storage Composite Curves as they are constructed the same way as standard CCs. In this small example, both storage 1 and 2 are charged during operating period 1 and storage 1 has the higher end-temperature. This means that the mGCC yields an upper bound for the heat load of storage 1 and an upper bound for the cumulated energy of storage 1 and storage 2. Both storages are discharged during operating period 2. Here, the mGCC yields an upper bound for the heat load of storage 2 with the lowest end-temperature and an upper bound for the cumulated heat loads for storages 1 and 2. A detailed description of the MINLP formulation for storage sizing is presented in **Paper 5**.

3.5 Targeting

3.5.1 Energy Targets

The calculation of targets is optional. However, knowledge of the theoretical maximum energy recovery for a given ΔT_{min} provides insights on the energy recovery potentials. Furthermore, energy targets are necessary for the linearization procedure proposed in **Paper 1** and for the proposed additional constraints for tightening of the superstructure formulation (**Paper 2** and **Paper 3**). In

the targeting module not only energy targets are calculated, but also maximum energy recovery for each individual stream match and for all possible stream combinations are obtained. These targets yield rigorous upper bounds for heat recovery for each combination of stream matches.

Calculation of energy targets using the TAM yields potentials for the integration of TES and a rigorous upper bound for total heat recovery. These TAM targets also provide insights, that can be used to specify the temperature range in which placement of TES is worthwhile.

3.5.2 Area Targets

Area targeting yields a lower bound for the total HEX area required to obtain a certain degree of heat recovery. Approaches for the calculation of area targets have been proposed that assume constant heat transfer coefficients, but also allowing for non-uniform heat transfer coefficients and criss crossing. These area targets can be used to tighten the MINLP formulation. In the proposed framework, area targets are calculated using the smallest of all overall heat transfer coefficients in the system. This way, no feasible solutions are excluded from the solution space of the HENS problem.

3.5.3 Target for Minimum Number of HEX Units

In literature several mathematical programming formulations have been proposed to find the minimum number of HEX units necessary to reach maximum energy recovery within the HEN. In the proposed framework, the target for minimum number of HEX units is calculated using a modified version of the SYNHEAT model, which neglects HEX areas and can thus be solved as a MILP model. The target is calculated for each individual operating period and can then be used within the tightening module to obtain rigorous lower bounds for the total number of HEX units.

3.6 Linearization

As stated before, the stage-wise MINLP superstructure proposed by Yee and Grossmann [94] is nonlinear and nonconvex which makes it very hard to solve for medium to large-scale problems. Additionally, most MINLP solvers require a feasible initial guess and thus a proper initialization procedure is necessary. For this reason, an approach for the linearization of the stage-wise superstructure

was proposed. The linearized superstructure can be solved to global optimality without the need for an initial guess. With state-of-the-art solvers for MILP problems such as Gurobi or CPLEX the linearized superstructure can be solved significantly faster compared to the original version.

The only nonlinear terms in the stage-wise MINLP superstructure are those used to model logarithmic mean temperature differences *LMTD* and the required HEX areas. Because *LMTD* is a convex function in the sense of the optimization problem, it can be approximated by linear inequality constraints to any degree. Therefore, a maximum allowable relative difference between approximation and original function is specified and an inner approximation is carried out leading to an underestimation of real temperature differences. For the approximation of HEX areas information on maximum transferable energy and maximum temperature differences is used to identify the feasible domain in which HEX areas have physically feasible values. In a nonlinear optimization step a least square fit for the convex approximation of the function is carried out for a predefined number of linear inequality constraints. The approximation procedure used in the linearization module is presented in detail in **Paper 1**. In **Paper 1** and **Paper 3** results are presented that compare the solutions for the linearized and the original superstructure formulation.

3.7 Tighter Constraints

Besides linearization of nonlinear terms also reformulations can be introduced that tighten the model. This means that the problem relaxation and thus the LP-subproblems yield higher objective values. This way, branches can be excluded from the MILP search tree faster and the solution speed can potentially be increased. Similarly, for nonlinear terms tight initial variable bounds are introduced that reduce the domain for outer approximations and thus, again, yield higher objective values of the subproblems. It needs to be mentioned that these tightening measures do not reduce the feasible solution space for the main problem. In the case of the superstructure used in the framework, tightening of the model can be achieved in three different ways:

1. Identification of the smallest possible feasible big-M parameters for the logical constraints in the superstructure model
2. Identification of the smallest feasible upper bounds and largest feasible lower bounds on variables involved in nonlinear terms
3. Introduction of additional constraints based on physical and thermodynamic insights

In **Paper 2** and **Paper 3**, the proposed tightening measures are described in detail and results are presented for comparison of the original and tightened versions of the superstructure formulation.

3.8 Simplifications

Due to the combinatorial nature of the multi-period HENS problem only few operating periods (depending on the number of process streams and used temperature stages) can be considered. The complexity of these type of problems increases exponentially. In order to find good solutions within reasonable time the solution space and the combinatorial complexity can be narrowed by making reasonable simplifying assumptions. All of the simplifications presented in the following were applied for HENS in the case-study presented in **Paper 6** but were not described in detail.

3.8.1 Single HEX per Stream Pair

One way to reduce the problem is to allow only one HEX per stream pair, as was proposed by Björk and Nordman [10] for solving large-scale HEN retrofit problems. This tightens the formulation and reduces the number of necessary constraints. This simplification is especially useful for superstructures with many temperature stages. A drastic reduction of nonlinear constraints or, in the case of the linearized superstructure, sets of linear inequality constraints can be obtained. The number of nonlinear equations is reduced by the factor of temperature stages NOK .

$$\text{number of equations}_{new} = \frac{\text{number of equations}_{old}}{NOK} \quad (3.41)$$

For this simplification, additional constraints are necessary to limit the sum of all binary variables z_{ijk} for one pair of hot i and cold j streams in temperature stages k .

$$\sum_k z_{ijk} \leq 1. \quad (3.42)$$

Also, some model constraints need to be slightly altered. In the original formulation temperature differences are calculated for each temperature stage. Using

this simplification, for each stream pair only the two variables for temperature differences $\Delta T_{ij,1}$ and $\Delta T_{ij,2}$ are necessary.

$$\Delta T_{ij,1} \leq T_{i,k} - T_{j,k} + (1 - z_{ijk})\Gamma \quad (3.43)$$

$$\Delta T_{ij,2} \leq T_{i,k+1} - T_{j,k+1} + (1 - z_{ijk})\Gamma \quad (3.44)$$

Here, the big-M parameter Γ needs to be sufficiently large so that the feasible solution space is not reduced. The logarithmic mean temperature difference $LMTD_{ij}$ is modelled using a single nonlinear constraint for each stream pair

$$LMTD_{ij} \leq \left(\Delta T_{ij,1} \Delta T_{ij,2} \left(\frac{\Delta T_{ij,1} + \Delta T_{ij,2}}{2} \right) \right)^{\frac{1}{3}}. \quad (3.45)$$

Also, for modelling the HEX area, only a single equation is needed.

$$A_{ij} \leq \frac{\sum_k q_{ijk}}{U_{ij} LMTD_{ij}} \quad (3.46)$$

3.8.2 Sequential Storage Integration

Another way to reduce the problem complexity is by decomposing the simultaneous HENS including storages. First, the optimal HEN is calculated without consideration of TES. Then, storages are introduced but the binary variables for the existing of HEX connecting process streams are fixed. This way, only binary variables for HEX connecting process streams to the ISCs need to be considered, which simplifies the problem significantly.

3.8.3 Reduction of Process Streams

A very simple, yet effective way to reduce problem complexity is by neglecting process streams for a first solution. In a reduction step all process streams are neglected that have an energy contribution that is below a certain threshold or below a certain fraction of the total energy in the system. For the problem with reduced process streams an optimal solution can be found faster as the combinatorial complexity of the problem is decreased. To obtain a feasible solution for the original problem, the full superstructure model considering all process streams is solved again, but with binary variables connecting process streams fixed to the values obtained from the solution for the reduced problem.

3.8.4 Reduction of the Number of Binary Variables

In the introduction of this section, it was mentioned that the combinatorial complexity of the simultaneous HENS problem not only scales exponentially with the number of process streams but also with the number of operating periods. This, however, is only the case if binary variables are used in every individual operating period depicting whether a HEX is bypassed or not. This also means that a HEX can be bypassed in periods where streams do not have feasible driving temperature differences. For processes where this is not necessary, a single binary variable depicting the existence of the respective HEX is sufficient. With this assumption, the exponential increase in combinatorial complexity for increasing numbers of operating periods can be avoided. However, for HEX connecting process streams to FMVT storage systems, this reduction is likely to exclude optimal solutions because of the temperature changes in the storage vessels.

3.9 Post-Processing

Finally, the post-processing module of the framework allows to visualize the results obtained using the proposed Process Integration framework. It is possible to plot HENs in grid-diagrams, to compare the heat recovery obtained to the energy targets calculated in the targeting module, to analyse storage behaviour and to analyse costs for the solution. Also, payback-times for the economic assessment of the proposed solutions can be calculated.

Chapter 4

Conclusion

This thesis contributes to the scientific topic of cost-optimal HENS for multi-period problems including integration of TES. A framework was presented which is based on an extended superstructure formulation for simultaneous HENS. The methods included in the framework were published in three SCI rated journal contributions and three peer reviewed conference contributions.

The framework is module based and the use of most modules is optional. It includes a linearization module that replaces all nonlinearities with convex linear inequality constraints. The proposed linearization approach showed to yield results comparable to literature within acceptable computational time without the use of specialized solution algorithms. The tightening module adds linear constraints to the model tightening the LP relaxation of the sub-problems involved in the solution process. Tight variable bounds that reduce the domain for the approximation for the nonlinear expressions are introduced based on insights from the linearization module. Both linearization and tightening measures help the solvers to find solutions to the simultaneous HENS problem significantly faster which was demonstrated using several case studies from literature. Especially for more complex multi-period problems these improved solution strategies are necessary to solve industry-scale problems in acceptable computational time. Moreover, using the linearization strategy, no initialization procedure is necessary for solving the superstructure formulation.

For multi-period problems, the storage module can be used to simultaneously integrate various types of TES which was demonstrated by means of a simple test case. The stage-wise superstructure is extended so that process streams can exchange heat with intermediate storage cycles connected to the storages. The proposed formulation has the flexibility to be used with VMFT storage tanks such as multi-tank systems or stratified tank systems but also the integration of

CONCLUSION

FMVT storage systems such as LHST can be carried out. The latter have hardly been considered with Process Integration techniques, even though these types of storages potentially yield cost efficient heat recovery solutions for processes with heat sinks and sources in a narrow temperature range.

Because the simultaneous HENS problem including TES is very difficult to solve, a sequential procedure was proposed. In a first step, the storage sizes are obtained using a novel MINLP formulation that uses insights from Pinch Analysis to simplify the problem. HEX are neglected in this step which reduces the combinatorial complexity of the problem significantly. In the second step the extended superstructure is used with fixed storage sizes. The procedure was demonstrated by means of integration of pressurized water storages into two example cases.

Finally, an industry-scale problem was solved to demonstrate the effectiveness of the framework. A two-tank hot water storage system was integrated into a multi-period dairy process with 36 process streams. Problem reduction techniques presented in this work were used to handle the complexity of the problem. A comparison with the Process Integration tool SOCO showed that the proposed framework yields more cost-efficient solutions for storage integration compared to SOCO's heuristic approach. However, the study motivates the use of heuristics for either problem reduction or for initialization as it might further improve solution speed and thus makes the framework more practical.

Chapter 5

Papers

5.1 Paper 1

Full paper journal contribution in
Computers and Chemical Engineering
(2017 Impact Factor: 3.113)



Contents lists available at ScienceDirect

Computers and Chemical Engineering

journal homepage: www.elsevier.com/locate/compchemeng

A Novel Approach for Linearization of a MINLP Stage-Wise Superstructure Formulation

Anton Beck^a, René Hofmann^{a,b,*}^aAIT Austrian Institute of Technology GmbH, Energy Department, Sustainable Thermal Energy Systems, Giefinggasse 2, Wien, 1210, Austria^bInstitute for Energy Systems and Thermodynamics, Vienna University of Technology, Getreidemarkt 9/BA, Wien, 1060, Austria

ARTICLE INFO

Article history:

Received 3 October 2017

Revised 17 January 2018

Accepted 18 January 2018

Available online 31 January 2018

Keywords:

Mathematical programming

Heat integration

Linearization

Heat exchanger network synthesis

ABSTRACT

Mathematical programming using superstructure formulations has been used for cost efficient heat exchanger network synthesis (HENS) for about three decades now and significant improvements have been achieved since then. One major problem is the combinatorial nature of the underlying superstructure formulations which means that the mathematical complexity of the HENS problem scales exponentially with problem size. In this paper a novel approach using convex linear approximations is presented for simultaneous HENS. The linearization is carried out prior to optimization and the original Mixed Integer Non-Linear Programming (MINLP) problem is reformulated into a Mixed Integer Linear Programming (MILP) problem. For the linearized problem a global optimum can be obtained much faster compared to the original MINLP formulation. For all presented case-studies feasible solutions could be obtained, which compare well with results from other authors.

© 2018 Elsevier Ltd. All rights reserved.

1. Introduction

1.1. Mathematical programming in HENS

In the early 1980s sequential mathematical optimization procedures were developed to obtain minimum energy costs (linear programming (LP) transshipment model), the minimum number of heat exchangers (mixed integer linear programming (MILP) transshipment model (Papoulias and Grossmann, 1983)) and cost efficient HENS using a nonlinear programming (NLP) superstructure (Floudas et al., 1986). In the early 1990s simultaneous approaches for the design of cost optimal HENS were developed as the sequential approaches can lead to suboptimal network structures. Yee and Grossmann (1990) proposed a stage-wise superstructure (SWS) MINLP formulation that considers the trade-off between investment costs for heat exchangers and energy costs simultaneously. The mixing of split streams is assumed to be isothermal. This simplification was overcome by Ciric and Floudas (1991) who used mass balances according to the NLP model by Floudas et al. (1986) to account for non-isothermal mixing. Both superstructure formulations allow heating and cool-

ing only at the hot and cold end of the process streams, respectively. Escobar and Trierweiler (2013) gave an overview over heat exchanger network synthesis (HENS) procedures published in literature and evaluated them using five different benchmark cases. They also gave an overview over state-of-the-art solvers and their performance on the presented test-cases. Their work showed that for HENS problems, the superstructure formulation by Yee and Grossmann (1990) performed better in terms of computation time and total annual costs (TAC) for most test cases. Despite the assumption of isothermal mixing, the superstructure formulation proposed by Yee and Grossmann (1990) is still nonlinear and non-convex and thus it is difficult to find the global optimum. Bogataj and Kravanja (2012) proposed a strategy for global optimization of the superstructure formulation by introducing an aggregated substructure. Their idea was to use piecewise linear and nonlinear under-estimators of the non-convex terms to provide a lower bound for the problem in order to reduce the relative gap between upper and lower bounds. Mistry and Misener (2016) proposed an iterative linearization scheme for the non-convex terms allowing to solve the original MINLP problem as a MILP and to global optimality. Alternatively, authors used genetic algorithms and simulated annealing to solve the simultaneous HENS problem (Luo et al., 2009; Ma et al., 2008; Yu et al., 2000). Despite all improvements and recent developments, the simultaneous HENS synthesis problem still remains complex and hard to solve. In this

* Corresponding author.

E-mail address: rene.hofmann@tuwien.ac.at (R. Hofmann).URL: <http://www.tuwien.ac.at> (R. Hofmann)<https://doi.org/10.1016/j.compchemeng.2018.01.010>

0098-1354/© 2018 Elsevier Ltd. All rights reserved.

Nomenclature*Acronyms*

HEN	heat exchanger network
HENS	heat exchanger network synthesis
HEX	heat exchanger
LP	linear programming
MILP	mixed integer linear programming
MINLP	mixed integer non-linear programming
NLP	non-linear programming
SWS	stage-wise superstructure

Parameters

α	coefficients for linear approximation of A
β	cost exponent (-)
ΔT_{min}	minimum approach temperature ($^{\circ}\text{C}$)
$\Delta_{rel, max}$	maximum relative difference (-)
ϵ	arbitrarily small positive real number
Γ	upper bound for temperature difference ($^{\circ}\text{C}$)
λ	coefficients for linear approximation of $LMTD$
Ω	upper bound for heat exchange (kW)
Φ	big-M coefficient
c	cost coefficient for variable heat exchanger costs ($\text{€ m}^{-2\beta}$)
$C, C1, C2$	constants
c_f	step-fixed cost coefficient (€)
c_{cu}	cost coefficient for cold utility (€ kWh^{-1})
c_{hu}	cost coefficient for hot utility (€ kWh^{-1})
F	flow capacity of process streams (kW/K)
I	number of data points
M	number of linear equations for approximation of $LMTD$
N	number of linear equations for approximation of A
NOK	number of stages
U	heat transfer coefficient ($\text{kW/m}^2\cdot\text{K}$)

Subscripts

cu	cold utility
hu	hot utility
i	hot stream
j	cold stream
k	temperature stage
m	index of linear equation for the approximation of $LMTD$
max	maximum value
min	minimum value
n	index of linear equation for the approximation of A
p	index of data point

Superscripts

cold	heat exchanger cold side
hot	heat exchanger hot side
in	inlet
out	outlet
p	coordinate of data point \vec{p}
s	symmetric

Variables

ΔT	temperature difference ($^{\circ}\text{C}$)
Δ_{rel}	relative difference (-)
\hat{A}	heat exchanger area (m^2)
$LMTD$	logarithmic mean temperature difference ($^{\circ}\text{C}$)
TAC	total annualized costs
\hat{A}	approximate reduced heat exchanger area ($\text{m}^{2\beta}$)
\vec{n}	normal vector ($^{\circ}\text{C}$)

\vec{p}	data point for approximation of $LMTD$ ($^{\circ}\text{C}$)
\vec{x}	point vector ($^{\circ}\text{C}$)
\widetilde{LMTD}	approximate logarithmic mean temperature difference ($^{\circ}\text{C}$)
A	reduced heat exchanger area ($\text{m}^{2\beta}$)
$D1, D2$	minor determinants
H	Hessian matrix
q	heat flow (kW)
T	temperature ($^{\circ}\text{C}$)
z	binary variable for existence of HEX (-)

paper a novel approach for the simplification of the the classical SWS formulation by Yee and Grossmann (1990) is proposed. All nonlinear terms within this formulation are linearized and the original MINLP superstructure is approximated by a MILP model.

1.2. Benefits of the proposed linearization

Linear approximation of the original problem has the following advantages:

- No initialization procedure needed as MILP problems do not depend on an initial guess.
- MILPs solve to global optimality.
- If the reformulated MILP model is a good representation of the original MINLP potentially better HENs can be found than by local MINLP solvers as the MILP solvers do not get stuck in local minima.
- The linear problem is easier to solve leading to lower computation times.

2. Linearization**Stage-wise superstructure formulation (Yee and Grossmann, 1990)**

$$\min TAC = \underbrace{\sum_i c_{cu} q_{cui} + \sum_j c_{hu} q_{huj}}_{\text{energy costs}} + \underbrace{\sum_i \sum_j \sum_k c_f z_{ijk} + \sum_i c_f z_{cui} + \sum_j c_f z_{huj}}_{\text{step-fixed investment costs}} + \underbrace{\sum_i \sum_j \sum_k c \left(\frac{q_{ijk}}{U_{ij} LMTD_{ijk}} \right)^{\beta}}_{A_{ijk}} + \underbrace{\sum_i c \left(\frac{q_{cui}}{U_{cui} LMTD_{cui}} \right)^{\beta}}_{A_{cui}} + \underbrace{\sum_j c \left(\frac{q_{huj}}{U_{huj} LMTD_{huj}} \right)^{\beta}}_{A_{huj}}$$

variable investment costs
subject to

$$\left. \begin{aligned} \sum_j \sum_k q_{ijk} + q_{cui} &= F_i (T_i^{in} - T_i^{out}), i \in HP \\ \sum_i \sum_k q_{ijk} + q_{huj} &= F_j (T_j^{out} - T_j^{in}), j \in CP \end{aligned} \right\} \text{stream-wise energy balance}$$

$$\left. \begin{aligned} \sum_i q_{ijk} &= F_i (T_{ik} - T_{i,k+1}), i \in HP \\ \sum_j q_{ijk} &= F_j (T_{jk} - T_{j,k+1}), j \in CP \end{aligned} \right\} \text{energy balance for each stage}$$

$$T_{i,k=1} = T_i^{in}, T_{j,k=NOK} = T_j^{in} \quad \text{assignment of inlet temperatures}$$

$$\left. \begin{aligned} T_{ik} &\geq T_{i,k+1}, T_{jk} \geq T_{j,k+1} \\ T_{i,k=NOK+1} &\geq T_i^{out}, T_{j,k=1} \geq T_j^{out} \end{aligned} \right\} \text{monotonic decrease in Temperature}$$

$$\left. \begin{aligned} q_{cui} &= F_i (T_{i,k=NOK+1} - T_i^{out}) \\ q_{huj} &= F_j (T_j^{out} - T_{j,k=1}) \end{aligned} \right\} \text{utility heat loads}$$

$$\Delta T_{ijk} \geq \Delta T_{min}, \Delta T_{cui} \geq \Delta T_{min}, \Delta T_{huj} \geq \Delta T_{min} \quad \text{lower bounds for temperature differences}$$

$$q_{ijk} \leq \Omega z_{ijk}, q_{cui} \leq \Omega z_{cui}, q_{huj} \leq \Omega z_{huj} \quad \text{upper bounds for heat loads}$$

$$\left. \begin{aligned} \Delta T_{ijk} &\leq T_{ik} - T_{jk} + \Gamma(1 - z_{ijk}) \\ \Delta T_{i,j,k+1} &\leq T_{i,k+1} - T_{j,k+1} + \Gamma(1 - z_{ijk}) \\ \Delta T_{cui1} &\leq T_{i,k=NOK} - T_{cui}^{out} + \Gamma(1 - z_{cui}) \\ \Delta T_{cui2} &\leq T_{i}^{out} - T_{cui}^{in} + \Gamma(1 - z_{cui}) \\ \Delta T_{huj1} &\leq T_{hu}^{out} - T_{j,k=1} + \Gamma(1 - z_{huj}) \\ \Delta T_{huj2} &\leq T_{hu}^{in} - T_{j}^{out} + \Gamma(1 - z_{huj}) \end{aligned} \right\} \text{upper bounds temperature differences}$$

$$LMTD_{ijk} = \frac{\Delta T_{ijk} - \Delta T_{i,j,k+1}}{\ln \frac{\Delta T_{ijk}}{\Delta T_{i,j,k+1}}} \quad \text{definition of LMTD for process-process HEX} \quad (1)$$

$$\left. \begin{aligned} LMTD_{cui} &= \frac{\Delta T_{cui1} - \Delta T_{cui2}}{\ln \frac{\Delta T_{cui1}}{\Delta T_{cui2}}} \\ LMTD_{huj} &= \frac{\Delta T_{huj1} - \Delta T_{huj2}}{\ln \frac{\Delta T_{huj1}}{\Delta T_{huj2}}} \end{aligned} \right\} \text{definition of LMTD for utility HEX}$$

$$T_i^{out} \leq T_{ik} \leq T_i^{in}, T_j^{in} \leq T_{jk} \leq T_j^{out} \quad \text{upper temperature bounds}$$

$$q_{ijk}, q_{cui}, q_{huj} \geq 0 \quad \text{non-negativity constraints}$$

$$z_{ijk}, z_{cui}, z_{huj} \in \{0, 1\} \quad \text{integrality constraints}$$

The approach presented in the following aims at the convexification of the heat exchanger area calculations within the MINLP superstructure presented by Yee and Grossmann (1990) (Eq. (1)) by replacing the nonlinear terms with linear inequality constraints. In the following the indices that determine the stream match (*ij*) and the stage (*k*) are dropped and ΔT_1 and ΔT_2 are used instead of ΔT_{ijk} and $\Delta T_{i,j,k+1}$ for simplicity. The equation for LMTD

$$LMTD = \frac{\Delta T_1 - \Delta T_2}{\ln \frac{\Delta T_1}{\Delta T_2}} \quad (2)$$

is replaced by the set of linear inequality constraints

$$\widetilde{LMTD} \leq LMTD_m = \Delta T_1 \lambda_{1m} + \Delta T_2 \lambda_{2m} + \lambda_{3m}, \quad (3)$$

where $1 \leq m \leq M$, $m, M \in \mathbb{N}$ and λ_{1m} , λ_{2m} and λ_{3m} are coefficients. Similarly, the equation for the reduced heat exchanger area *A*

$$A = \hat{A}^\beta = \left(\frac{q}{U LMTD} \right)^\beta, \quad (4)$$

which is the heat exchanger area \hat{A} reduced by the cost exponent β ($\beta \leq 1$), is approximated by the set of inequality constraints

$$\tilde{A} \geq A_n = q \alpha_{1n} + \widetilde{LMTD} \alpha_{2n} + \alpha_{3n} \quad (5)$$

with the coefficients α_{1n} , α_{2n} and α_{3n} where $1 \leq n \leq N$, and $n, N \in \mathbb{N}$.

2.1. Logarithmic mean temperature difference

Mistry and Misener (2016) proved in their paper that LMTD is concave and thus its mirror image $-LMTD$ is a convex function. Therefore, $-LMTD$ can be approximated by linear inequality constraints to any degree (Eq. (6)).

$$\begin{aligned} LMTD &= f(\Delta T_1, \Delta T_2), \quad \Delta T_1, \Delta T_2 \in \mathbb{R}^+, \\ \text{s.t. } \forall \epsilon > 0, \exists M \in \mathbb{N}, f_1, \dots, f_M &: \text{linear} \\ \| \min(f_1, \dots, f_M) - f \|_{L_2} &< \epsilon \end{aligned} \quad (6)$$

In Eq. (6) L_2 means the integral of the squared difference of the functions $\min(f_1, \dots, f_M)$ and f . The accuracy of that approximation depends on the number of linear inequalities resulting in a trade-off between smaller problem size (i.e. less inequality constraints) and the resulting error. Here, LMTD is linearized by a lower linear approximation, which yields underestimations for LMTD.

Before the linearization is performed a reasonable upper bound $\Delta_{rel, max}$ for the relative difference Δ_{rel} is set (Eq. (7)). The lower bound for Δ_{rel} is set to 0.

$$\begin{aligned} \Delta_{rel} &= \frac{LMTD(\Delta T_1, \Delta T_2) - \widetilde{LMTD}(\Delta T_1, \Delta T_2)}{LMTD(\Delta T_1, \Delta T_2)} \\ 0 &\leq \Delta_{rel} \leq \Delta_{rel, max} \\ \forall \Delta T_1, \Delta T_2 &\geq \Delta T_{min} \end{aligned} \quad (7)$$

With $\Delta T_1 = \Delta T_2 C$, LMTD($\Delta T_1, \Delta T_2$) becomes the 1-dimensional function LMTD(ΔT_2). Analysis of the derivative of this function shows that its slope is constant for any $C \in (0, \infty)$ (Eq. (8)).

$$\frac{d LMTD(\Delta T_2)}{d \Delta T_2} = \frac{C - 1}{\ln C} = \text{const.} \quad (8)$$

For $\Delta T_2 = 0$ it follows that

$$LMTD(\Delta T_2) = \frac{0}{\ln C} = 0, \quad \Delta T_2 = 0. \quad (9)$$

From Eq. (8) and Eq. (9) it can be concluded that the relative difference Δ_{rel} (Eq. (7)) is constant for any linear function *f*

$$f(\Delta T_1 = \Delta T_2 C, \Delta T_2) = k_1 \Delta T_2 C + k_2 \Delta T_2 = k_3 \Delta T_2 \quad (10)$$

going through the point $\vec{p}_0 = (0, 0, 0)$ (Eq. (11)).

$$\Delta_{rel} = \frac{\frac{\Delta T_2(C-1)}{\ln C} - \Delta T_2 k_3}{\frac{\Delta T_2(C-1)}{\ln C}} = 1 - \frac{\ln C k_3}{C - 1} = \text{const.} \quad (11)$$

Because of

$$LMTD(C \Delta T_1, C \Delta T_2) = \frac{C \Delta T_1 - C \Delta T_2}{\ln \left(\frac{C \Delta T_1}{C \Delta T_2} \right)} = C LMTD(\Delta T_1, \Delta T_2) \quad (12)$$

where $C \neq 0$ it can be concluded that the linear equation defined by \vec{p}_0 and any two points \vec{p}_1 and \vec{p}_2

$$\vec{p}_0 = \begin{pmatrix} 0 \\ 0 \\ 0 \end{pmatrix}, \quad \vec{p}_1 = \begin{pmatrix} \Delta T_{1,1} \\ \Delta T_{2,1} \\ \frac{\Delta T_{1,1} - \Delta T_{2,1}}{\ln \left(\frac{\Delta T_{1,1}}{\Delta T_{2,1}} \right)} \end{pmatrix}, \quad \vec{p}_2 = \begin{pmatrix} \Delta T_{1,2} \\ \Delta T_{2,2} \\ \frac{\Delta T_{1,2} - \Delta T_{2,2}}{\ln \left(\frac{\Delta T_{1,2}}{\Delta T_{2,2}} \right)} \end{pmatrix} \quad (13)$$

is equivalent to the linear equation defined by \vec{p}_0 , \vec{p}_1^* and \vec{p}_2^* where $\vec{p}_1^* = C_1 \vec{p}_1$ and $\vec{p}_2^* = C_2 \vec{p}_2$. This can be shown by the definition of the point-normal plane equation. The normal vector \vec{n} defined by the points \vec{p}_0 , \vec{p}_1 and \vec{p}_2

$$\vec{n} = \begin{pmatrix} \Delta T_{1,1} \frac{\Delta T_{1,2} - \Delta T_{2,2}}{\ln \left(\frac{\Delta T_{1,2}}{\Delta T_{2,2}} \right)} - \Delta T_{1,2} \frac{\Delta T_{1,1} - \Delta T_{2,1}}{\ln \left(\frac{\Delta T_{1,1}}{\Delta T_{2,1}} \right)} \\ -\Delta T_{2,1} \frac{\Delta T_{1,2} - \Delta T_{2,2}}{\ln \left(\frac{\Delta T_{1,2}}{\Delta T_{2,2}} \right)} + \Delta T_{2,2} \frac{\Delta T_{1,1} - \Delta T_{2,1}}{\ln \left(\frac{\Delta T_{1,1}}{\Delta T_{2,1}} \right)} \\ \Delta T_{1,1} \Delta T_{2,2} - \Delta T_{1,2} \Delta T_{2,1} \end{pmatrix}, \quad (14)$$

and the normal vector \vec{n}^* defined by the points \vec{p}_0 , \vec{p}_1^* and \vec{p}_2^*

$$\vec{n}^* = \begin{pmatrix} C_1 \Delta T_{1,1} \frac{C_2 \Delta T_{1,2} - C_2 \Delta T_{2,2}}{\ln \left(\frac{C_2 \Delta T_{1,2}}{C_2 \Delta T_{2,2}} \right)} - C_2 \Delta T_{1,2} \frac{C_1 \Delta T_{1,1} - C_1 \Delta T_{2,1}}{\ln \left(\frac{C_1 \Delta T_{1,1}}{C_1 \Delta T_{2,1}} \right)} \\ -C_1 \Delta T_{2,1} \frac{C_2 \Delta T_{1,2} - C_2 \Delta T_{2,2}}{\ln \left(\frac{C_2 \Delta T_{1,2}}{C_2 \Delta T_{2,2}} \right)} + C_2 \Delta T_{2,2} \frac{C_1 \Delta T_{1,1} - C_1 \Delta T_{2,1}}{\ln \left(\frac{C_1 \Delta T_{1,1}}{C_1 \Delta T_{2,1}} \right)} \\ C_1 C_2 \Delta T_{1,1} \Delta T_{2,2} - C_1 C_2 \Delta T_{1,2} \Delta T_{2,1} \end{pmatrix} \quad (15)$$

$$\vec{n}^* = C_1 C_2 \vec{n}, \quad C_1, C_2 \in (0, \infty) \quad (16)$$

define the same plane going through point \vec{p}_0

$$\vec{n} \cdot (\vec{p}_0 - \vec{x}) = 0 \quad \equiv \quad \vec{n}^* \cdot (\vec{p}_0 - \vec{x}) = 0. \quad (17)$$

This is shown in Fig. 1. The objective now is to find the least number of equations *M* defined by *M* + 2 data points (the point \vec{p}_0 plus *M* + 1 additional points) that satisfy Eq. (7). The result from

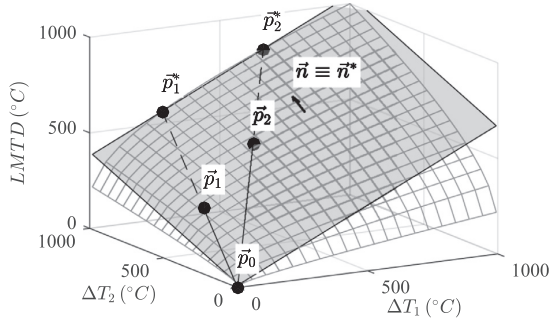


Fig. 1. Equivalence of planes defined by $\vec{p}_0, \vec{p}_1, \vec{p}_2$ and $\vec{p}_0, \vec{p}_1, \vec{p}_2$.

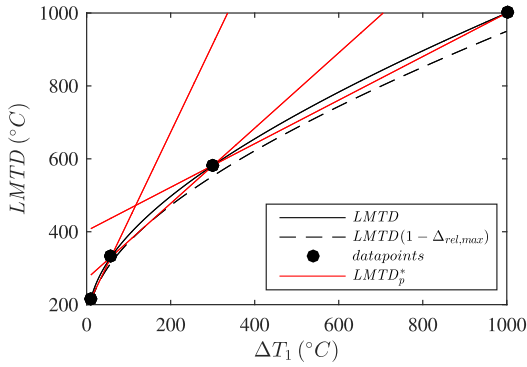


Fig. 2. Data points and linear constraints, $\Delta T_2 = \Delta T_{max} = 1000^\circ\text{C}$, $\Delta_{rel,max} = 0.05$.

Eq. (17) shows that it is sufficient to calculate data points in the ΔT_1 - $LMTD$ -plane with $\Delta T_2 = \Delta T_{max}$ where ΔT_{max} can be any real number greater than the maximum possible approach temperature of the underlying heat exchanger network synthesis problem. With a sufficiently large ΔT_{max} it is guaranteed that for any feasible values of ΔT_1 and ΔT_2 , the bounds for Δ_{rel} are satisfied as they lie within the approximated space. The data points used to obtain these M linear equations are found using a numerical procedure. Starting with the first data point \vec{p}_1

$$\vec{p}_1 = (\Delta T_{min}, \Delta T_{max}, LMTD(\Delta T_{min}, \Delta T_{max})). \quad (18)$$

additional data points in the ΔT_1 - $LMTD$ -plane are calculated that fulfill the requirement

$$\frac{LMTD(\Delta T_1, \Delta T_{max}) - LMTD_p^*(\Delta T_1)}{LMTD(\Delta T_1, \Delta T_{max})} \leq \Delta_{rel,max} \quad \forall \Delta T_1 > 0 \quad (19)$$

until the total domain of ΔT_1 is covered. $LMTD_p^*(\Delta T_1)$ is the linear function connecting the data points \vec{p}_p and \vec{p}_{p-1} . The last data point $\vec{p}_{p=P}$ is then set to be $(\Delta T_{max}, \Delta T_{max}, \Delta T_{max})$ (Fig. 2).

Because $LMTD$ is symmetric

$$LMTD(\Delta T_1, \Delta T_2) = LMTD(\Delta T_2, \Delta T_1) \quad (20)$$

the ΔT_1 - and ΔT_2 -coordinates of the calculated data points \vec{p}_p , $p = 1, \dots, P-1$ can be swapped ($\vec{p}_p \rightarrow \vec{p}_p^*$) to obtain the data points for the ΔT_2 - $LMTD$ -plane. With the point $\vec{p}_0 = (0, 0, 0)$ the final set consists of $2P = M + 2$ data points. Now each plane equation $LMTD_m$ (Eq. (3)) is constructed from the three data points \vec{p}_0 , \vec{p}_m and \vec{p}_{m+1} .

2.2. Reduced heat exchanger area

Within the reformulated mathematical model the reduced area is used instead of the real HEX area to eliminate all nonlinearities

involving the heat exchanger area at once. The reduced heat exchanger area A corresponds to the function

$$f(x, y) = \left(\frac{x}{y}\right)^\beta, \quad 0 < \beta \leq 1 \quad (21)$$

which will be discussed in the following due to its simpler form. The Hessian H of f , which is a symmetric 2×2 matrix, is

$$H = \begin{pmatrix} \beta(\beta-1)\frac{x^{\beta-2}}{y^\beta} & -\beta^2\frac{x^{\beta-1}}{y^{\beta+1}} \\ -\beta^2\frac{x^{\beta-1}}{y^{\beta+1}} & \beta(\beta+1)\frac{x^\beta}{y^{\beta+2}} \end{pmatrix}. \quad (22)$$

Its minor determinants $D1$ and $D2$ are

$$D1 = \beta(\beta-1)\frac{x^{\beta-2}}{y^\beta} \leq 0, \quad D2 = -\beta^2\frac{x^{2\beta-2}}{y^{2\beta+2}} < 0, \quad \forall x \in \mathbb{R}_0^+, y \in \mathbb{R}^+ \quad (23)$$

which shows that H is an indefinite matrix and thus f is neither convex nor concave for all $\beta \in (0, 1]$. This means that for any finite interval in x the linear approximation of f cannot be exact.

2.2.1. Approximation domain

For the underlying HEN synthesis problem it is reasonable to reduce the approximation domain to the physically feasible range for the transferred heat flow q and the logarithmic mean temperature difference $LMTD$. The feasible range of q and $LMTD$ respectively can be identified by analysis of the stream-wise heat transfer and the temperature range it can take place in.

- For the identification of the maximum transferable heat flow q_{max} of a certain stream match the Problem Table-Algorithm proposed by Linnhoff and Flower (1978) can be used.
- The lower bound for q is zero as the heat flow cannot be negative. Here, the assumption is made that for heat exchangers it is not cost efficient if they transfer only a small fraction of the maximum possible heat between two streams as the costs per unit of recovered energy increase to an economically infeasibly extent. Thus, the lower bound of the interval of $q \in [q_{min}, q_{max}]$ over which the function for the calculation of the reduced heat exchanger area A is approximated is set to $q_{min} > 0$. This yields better approximations within the approximation interval but results in worse approximations for the interval $0 \leq q < q_{min}$. It is important to note that this does not imply that stream matches with a heat flow $q < q_{min}$ are prohibited within the optimization model, but the costs for the heat exchangers connecting these streams are increasingly overestimated as the transferred heat q approaches zero, thus making it unlikely for the optimizer to choose them.
- The physically feasible space in $LMTD$ is bounded by $LMTD_{max}(q)$ and $LMTD_{min}(q)$. $LMTD_{max}$ is defined by

$$LMTD_{max} = \frac{\Delta T_{max}^{hot} - \Delta T_{max}^{cold}}{\ln\left(\frac{\Delta T_{max}^{hot}}{\Delta T_{max}^{cold}}\right)} \quad (24)$$

where ΔT_{max}^{hot} and ΔT_{max}^{cold} are the maximum temperature approaches on the hot and the cold side of the heat exchanger (Eq. (25) and Eq. (26)).

$$\Delta T_{max}^{hot}(q) = T_i^{in} - T_j^{in} - \frac{q}{F_j} \quad (25)$$

$$\Delta T_{max}^{cold}(q) = T_i^{in} - T_j^{in} - \frac{q}{F_i} \quad (26)$$

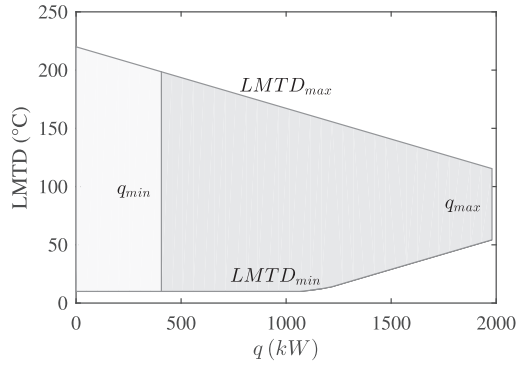


Fig. 3. Example for the feasible solution space of $LMTD$ and q (total grey area) and the space used for approximation (dark grey area). Hot stream: $T^m = 270^\circ\text{C}$, $T^{out} = 160^\circ\text{C}$, $F = 18\text{kW/K}$; Cold stream: $T^m = 50^\circ\text{C}$, $T^{out} = 210^\circ\text{C}$, $F = 20\text{kW/K}$.

- Depending on the process streams, $LMTD_{min}$ is a function or piecewise function

$$LMTD_{min} = \frac{\Delta T_{min}^{hot} - \Delta T_{min}^{cold}}{\ln\left(\frac{\Delta T_{min}^{hot}}{\Delta T_{min}^{cold}}\right)} \quad (27)$$

which is obtained by solving the linear problems (LP, Eq. (28)) I, II and III.

$$\text{I,II: } \max q, \quad \text{III: } \min \Delta T^{hot} + \Delta T^{cold}$$

subject to

$$\text{I,II,III: } \begin{cases} q \leq q_{max} \\ q \leq (T_i^{hot} - T_i^{cold})F_i, \quad q \leq (T_j^{hot} - T_j^{cold})F_j \\ T_i^{hot} \leq T_i^{in}, \quad T_i^{cold} \geq T_i^{out}, \quad T_i^{hot} > T_i^{cold} \\ T_j^{hot} \leq T_j^{out}, \quad T_j^{cold} \geq T_j^{in}, \quad T_j^{hot} > T_j^{cold} \\ \Delta T^{hot} = T_i^{hot} - T_j^{hot}, \quad \Delta T^{cold} = T_i^{cold} - T_j^{cold} \\ \Delta T^{hot}, \Delta T^{cold} \geq \Delta T_{min} \end{cases}$$

$$\text{I: } \Delta T^{hot}, \Delta T^{cold} = \Delta T_{min}$$

$$\text{II: } \begin{cases} \Delta T^{hot} = \Delta T_{min}, & \text{if } F_j \leq F_i \\ \Delta T^{cold} = \Delta T_{min}, & \text{if } F_j \geq F_i \end{cases}$$

$$\text{III: } q = q_{max} \quad (28)$$

In these LPs $T_{i,j}^{in}$, $T_{i,j}^{out}$ and $F_{i,j}$ are the stream parameters. It needs to be stated that the LPs I and II might not be solvable because either ΔT^{hot} , ΔT^{cold} or both cannot have values as low as ΔT_{min} . This is the case if the outlet temperature of the cold stream is lower than the outlet temperature of the hot stream minus ΔT_{min} . In that case only LP III needs to be solved to obtain $\Delta T_{min}^{hot}(q)$ and $\Delta T_{min}^{cold}(q)$, which in that case both are linear (not piecewise-linear) functions.

In Fig. 3 the obtained solution space is shown for two example streams.

2.2.2. Approximation of the reduced process heat exchanger areas

The approximation is carried out in a three-step procedure.

- The reduced feasible solution space is discretised into a set of data points and split into N regions.
- For each of the N regions defined by their sets of data points, the reduced heat exchanger area is then approximated by a linear least squares regression.

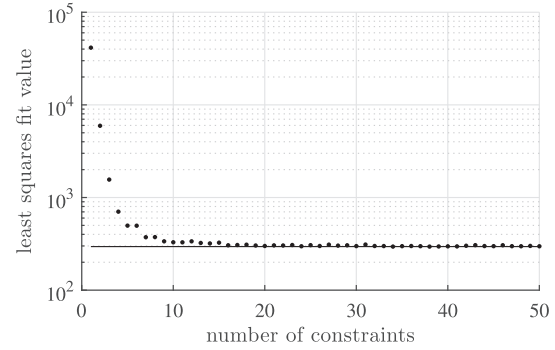


Fig. 4. Influence of the number of constraints on least squares fit.

- The N planes obtained in step 2 are then used to initialize a nonlinear optimization step that solves

$$\min \sum_i (\max(A_1, \dots, A_N) - A)^2, \quad i = 1, \dots, I \quad (29)$$

which is a least squares optimization of the coefficients of A_n where I is the number of discrete data points used for the numerical optimization and A_n are the linear equations (Eq. (5)) for the linear approximation of A .

The number of linear inequality constraints used for the approximation affects the accuracy of the approximation. This is shown in Fig. 4 for the same example streams as in Fig. 3. It can be seen that the least squares fit converges to a finite positive value (black line) as the number of planes is increased because A cannot be approximated exactly by linear inequality constraints.

2.2.3. Approximation of the reduced utility heat exchanger areas

The approximation for the reduced utility heat exchanger areas A_{cui} and A_{huj} is much easier. With fixed inlet and outlet temperatures of the utility streams, a direct connection of the transferred heat q and the reduced heat exchanger areas can be found. The temperature differences on the hot and cold side of the cold utility exchangers are calculated by

$$\Delta T_{cui}^{cold} = T_i^{out} - T_{cu}^{in} \quad (30)$$

$$\Delta T_{cui}^{hot} = T_i^{out} + \frac{q_{cui}}{F_i} - T_{cu}^{out} \quad (31)$$

and thus the logarithmic mean temperature difference becomes

$$LMTD_{cui} = \frac{\Delta T_{cui}^{hot} - \Delta T_{cui}^{cold}}{\ln \frac{\Delta T_{cui}^{hot}}{\Delta T_{cui}^{cold}}} = \frac{\frac{q_{cui}}{F_i} - T_{cu}^{out} + T_{cu}^{in}}{\ln(T_i^{out} + \frac{q_{cui}}{F_i} - T_{cu}^{out}) - \ln(T_i^{out} - T_{cu}^{in})} \quad (32)$$

The equations for the reduced heat exchanger area for cold utilities A_{cui} can be written as

$$A_{cui}(q_{cui}) = \left(\frac{q_{cui} (\ln(T_i^{out} + \frac{q_{cui}}{F_i} - T_{cu}^{out}) - \ln(T_i^{out} - T_{cu}^{in}))}{U_{cui} (\frac{q_{cui}}{F_i} - T_{cu}^{out} + T_{cu}^{in})} \right)^\beta \quad (33)$$

Similarly, the reduced area for the hot utility exchangers A_{huj} becomes

$$A_{huj}(q_{huj}) = \left(\frac{q_{huj} (\ln(T_{hu}^{in} - T_j^{out}) - \ln(T_{hu}^{out} - T_j^{out} + \frac{q_{huj}}{F_j}))}{U_{huj} (T_{hu}^{in} - T_{hu}^{out} - \frac{q_{huj}}{F_j})} \right)^\beta \quad (34)$$

The approximation for this functions is performed by a linear least squares regression over the range of $q_{min, cui} \leq q_{cui} \leq q_{max, cui}$ and $q_{min, huj} \leq q_{huj} \leq q_{max, huj}$. The maximum values of the heat flows $q_{max, cui}$ and $q_{max, huj}$ are simply the total heat flow of the respective process streams. The lower bounds for the approximation $q_{min, cui}$ and $q_{min, huj}$ are chosen the same way as described in Section 2.2.1. One single inequality constraint for each potential utility exchanger match is obtained by the linear least squares regression.

$$\tilde{A}_{cui} \geq q_{cui}\alpha_{1,cui} + \alpha_{2,cui} \quad (35)$$

$$\tilde{A}_{huj} \geq q_{huj}\alpha_{1,huj} + \alpha_{2,huj} \quad (36)$$

2.3. Model Reformulation

The constraints for the calculation of the reduced heat exchanger area obtained by linear least squares regression do not necessarily satisfy that $A(q=0) = 0$. The binary variables z_{ijk} (process to process HEX) and z_{cui}/z_{huj} (utility HEX) are used to activate/deactivate these constraints and thus it is guaranteed that the HEX area can be zero if no heat exchanger exists. This way no new binary variables have to be added to the model. The new inequality constraints used within the linearized model are summarized in Eq. (37).

$$\begin{aligned} \tilde{A}_{ijk} &\geq q_{ijk}\alpha_{1n,ijk} + \widetilde{LMTD}_{ijk}\alpha_{2n,ijk} \\ &\quad + \alpha_{3n,ijk} - (1 - z_{ijk})\Phi_{n,ijk}, \\ \tilde{A}_{cui} &\geq q_{cui}\alpha_{1,cui} + \alpha_{2,cui} - (1 - z_{cui})\Phi_{cui}, \\ \tilde{A}_{huj} &\geq q_{huj}\alpha_{1,huj} + \alpha_{2,huj} - (1 - z_{huj})\Phi_{huj}, \\ \widetilde{LMTD}_{ijk} &\leq \Delta T_{ijk}\lambda_{1m,ijk} + \Delta T_{i,j,k+1,p}\lambda_{2m,ijk} \end{aligned} \quad (37)$$

For process to process HEX areas, $\Phi_{n,ijk}$ is

$$\Phi_{n,ijk} = \Delta T_{min}\alpha_{2n,ijk} + \alpha_{3n,ijk}. \quad (38)$$

For the reduced utility heat exchanger areas Φ_{cui} and Φ_{huj} are set to

$$\Phi_{cui} = \alpha_{2,cui}, \quad \Phi_{huj} = \alpha_{2,huj}. \quad (39)$$

3. Case-studies and results

In this section, the linearisation approach and the resulting reformulated model described in the last sections is applied to three case-studies with different numbers of hot and cold streams taken from literature. The stream data for each case study is presented in Tables 3, 4, 5, which are presented in the Appendix.

3.1. Solvers

One big advantage of the linear model is that no initial guess has to be provided in order to find the global optimum of the linearised model (MILP). The MILPs were solved using CPLEX 12.6. For comparison the original MINLP formulation was solved using BARON (Sahinidis, 2014; Tawarmalani and Sahinidis, 2005) as it generates multiple starting points itself and thus is not dependent on initial values. Furthermore, BARON is a global solver and should be able to find the global optimum. BARON uses CPLEX as MILP solver and IPOPT (Wächter and Biegler, 2006) to solve the NLP sub-problem. Both CPLEX and BARON are used with their default settings.

3.2. NLP-stage

As the new MILP yields only an approximate solution to the problem a NLP-refinement stage is used to calculate exact heat exchanger areas and heat loads. This NLP stage corresponds to the

Table 1
Problem sizes for case-studies.

CS	variables [binaries]		equations		
	MILP	MINLP	MILP	MINLP	
1	101	89	[12]	333	130
2	1353	1151	[202]	4095	1250
3	4996	4209	[787]	19753	4196

MINLP model with fixed network structure. The network structure is defined by the binary variables obtained from the solution of the MILP and cannot be changed.

3.3. Settings for linearisation

For all case-studies the same settings for the approximations were used. The maximum relative difference $\Delta_{rel,max}$ for the approximation of $LMTD$ was set to 1%. The data points used for the approximation were obtained with $\Delta T_{max} = 1000^\circ\text{C}$ as it guaranteed that for all case-studies the total feasible range of ΔT_1 and ΔT_2 was covered and the approximation had only be done once. The lower limit for the transferred heat q_{min} was set to $0.2q_{max}$.

3.4. Model settings

The superstructure models were set up with two stages ($NOK = 2$) for all case-studies to keep computation time low, although the restriction to two temperature stages might lead to solutions with a lot of stream splits. Values for ΔT_{min} were taken from literature. For the MINLP and NLP models the approximation for $LMTD$ proposed by Chen (1987) was used.

3.5. Case-studies

In this work, three case-studies taken from literature were solved. The first case-study consists of only four streams whereas the second case-study consists of 20 streams and the third case-study can be considered large-scale with 39 process streams.

All of these case-studies were also used by Escobar and Trierweiler (2013) for a case-study comparison. The first case-study is adapted from the work of Gundersen (2013) who used this example for HENS using pinch-methodology. The second was presented by Soršak and Kravanja (2002) who used different types of heat exchangers within HENS and the third case-study was introduced by Bjork et al. (Björk and Nordman, 2005; Björk and Pettersson, 2003) who used the case-study for their approaches for HENS of large-scale problems.

The model sizes for these case-studies in terms of variables and equations are presented in Table 1. It can be seen that the number of equations for the linearization of the problem increase more quickly with problem size than the original MINLP and that the linearized model in general consists of a significantly more equations. Despite the large number of equations within the linearized model it can be solved rather quickly as only linear equations occur.

3.6. Results

All optimization runs were performed on the NEOS server cluster (Czyzyk et al., 1998; Dolan, 2001; Gropp and Moré, 1997). Each optimization problem was run three times. The best solution and lowest computation time is presented in Table 2. The time limit was set to 24 hours and the stopping criteria for relative and absolute duality gap were both set to 10^{-6} .

Table 2
Case-study results, limit = 24 hours.

CS	TAC (€ y ⁻¹)			time (s)		relative gap	
	MILP	NLP	MINLP	MILP	MINLP	MILP	MINLP
1	364,559	366,185	360,745	0.32	3,964	0	0
2	1,342,989	1,306,555	1,309,683	285.79	limit	0	0.45
3	1,959,838	1,985,280	2,100,320	limit	limit	0.67	0.72

3.6.1. Computation time

The linearization approach presented in this paper shows to perform very well in terms of solution time as only the largest case-study could not be solved to optimality within the time limit. BARON was able to close the duality gap for case-study 1 only. For case-study 1 the computation time of the new approach was about 10,000 times lower which is rather significant. A proper comparison of computation times is difficult as BARON was not able to close the duality gap for the other case-studies before the time limit was reached. It needs to be stated that the computation time for the NLP-stage was not considered in this evaluation.

3.6.2. Total annualized costs and number of heat exchangers

Comparing the best solutions from the linearized model after the NLP stage and the rigorous MINLP, the linearized model yields better solutions for the second and third case-study. For case-study 1, which is the smallest of the test-cases, BARON seems to have found the global optimum as the duality gap was closed (gap $\leq 10^{-6}$). BARON found a solution that is about 1.51% better than the solution found using the linearized model. As the solution found by the linearization approach can not be better than the global optimum, it is an expected result that the new approach yields values for TAC equal or worse than the global optimum. The solution found by BARON incorporates only 5 HEX compared to the solution found for the linearized model, which uses 7 HEX units and three stream splits. The number of heat exchanger units within the best solutions obtained by the linearization approach and the original MINLP formulation for the second case-study is 22 and 24, respectively. The obtained TAC for this case-study is slightly better using the linearization approach, as can be seen in Table 2. For case-study 3 a reduction in terms of TAC of about 5.5% could be obtained using the new approach with 48 HEX compared to the solution found by BARON, which uses 45 HEX. Both solutions incorporate a lot of HEX compared to the theoretical minimum number of HEX according to the so-called N-1 rule (Hohmann, 1971), which states that 40 HEX are needed for maximum heat recovery for this case-study. Using more temperature stages k might yield even better networks in terms of TAC with less HEX and stream splits. All HEN (Fig. 5–10) are appended to this paper.

3.6.3. Comparison to literature

Case-study 1 was originally proposed by Gundersen (2013) where they performed HENS using the pinch-method and no TAC was reported. Escobar and Trierweiler (2013) obtained TAC of 366,006.7 € y⁻¹ which is almost identical to the results obtained by the linearization approach used in this paper, which yields to-

tal annual costs of 366,185 € y⁻¹. Using BARON to solve the original MINLP formulation resulted in lower TAC of 360,745 € y⁻¹. Case-study 2 was proposed by Soršak and Kravanja (2002) who obtained a value for TAC of 1,259,900 € y⁻¹. This value was obtained using different heat exchangers with different costs. In this work, the TAC obtained using the new approach is 1,306,555 € y⁻¹. Case-study 3, which is the largest HEN optimized in this work, was proposed by Björk and Pettersson (2003). They found a solution with TAC of about 2,073,000 € y⁻¹ which was later improved by Pettersson (2005) to about 1,998,000 € y⁻¹. In this work a solution of 1,985,280 € y⁻¹ could be obtained which is slightly better.

This shows that the linearization approach presented in this paper yields results that compare well with the best results reported in literature.

4. Summary

The proposed two step approach to find optimal heat exchanger networks in terms of TAC seems to be promising for large HENS problems that cannot be solved to optimality by global MINLP solvers within reasonable computation time. Compared to the original problem the linearized version can be solved to optimality significantly faster without having to provide an initial guess.

Instead of the proposed two step approach where the NLP stage is initialized with the solution obtained by the linearized MINLP formulation, the original MINLP could be initialized with the solution from the linearized model. This way the linearization approach would be used to find a very good initial guess which could be beneficial especially for large HENS problems.

If the proposed linearization approach is used for initialization of local MINLP solvers, a comparison between the proposed linearization approach and initialization procedures from literature might be interesting.

Furthermore, it is desirable to have an estimate of the overall error made by the linear approximation procedure in order to give an indicator on how close to the global optimum the obtained solution might be.

Possibilities to perform direct linearization of the reduced heat exchanger area instead of the separate linearization steps for *LMTD* and the reduced heat exchanger area will also be studied as the direct linearization might yield less constraints with the same accuracy.

Acknowledgement

This paper and the corresponding project were initiated and could be realized by means of the endowed professorship through the cooperation between AIT (Austrian Institute of Technology) and TU Wien (Vienna University of Technology) in the research-field of Industrial Energy Systems.

Appendix

In the Appendix the stream data for all case-studies and the heat exchanger networks obtained by the new linearisation approach and the classic MINLP formulation are presented.

Table 3

Case-study 1 stream data (Gundersen, 2013).

Stream	T^{in} (°C)	T^{out} (°C)	F (kW/K)	h (kW/m ² K)
H1	270	160	18	0.5
H2	220	60	22	0.5
C1	50	210	20	0.5
C2	160	210	50	0.5
HU	250	250	1	1
CU	15	20	1	1

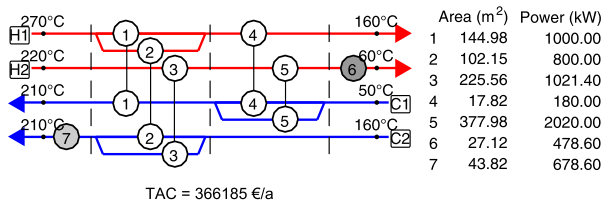
Exchanger capital cost = $4000+500[\text{Area}(\text{m}^2)]^\beta \text{€ y}^{-1}$, $\beta = 0.83$,
 hot utility cost = $200 \text{€ y}^{-1} \text{ kW}^{-1}$, cold utility cost = $20 \text{€ y}^{-1} \text{ kW}^{-1}$, $\Delta T_{\min} = 10^\circ\text{C}$

Table 4

Case-study 2 stream data (Soršak and Kravanja, 2002).

Stream	T^{in} (°C)	T^{out} (°C)	F (kW/K)	h (kW/m ² K)
H1	576	437	23.1	0.06
H2	599	399	15.22	0.06
H3	530	382	15.15	0.06
H4	449	237	14.76	0.06
H5	368	177	10.7	0.06
H6	121	114	149.6	1
H7	202	185	258.2	1
H8	185	113	8.38	1
H9	140	120	59.89	1
H10	69	66	165.79	1
H11	120	68	8.74	1
H12	67	35	7.62	1
H13	1034.5	576	21.3	0.06
C1	123	210	10.61	0.06
C2	20	210	6.65	1.2
C3	156	157	3291	2
C4	20	182	26.63	1.2
C5	182	318	31.19	1.2
C6	318	320	4011.83	2
C7	322	923.78	17.6	0.06
HU	927	927	5	5
CU	9	17	1	1

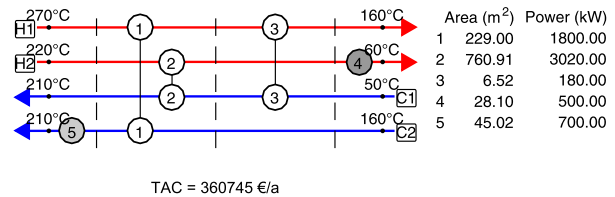
Exchanger capital cost = $4000+500[\text{Area}(\text{m}^2)]^\beta \text{€ y}^{-1}$, $\beta = 0.8$,
 hot utility cost = $250 \text{€ y}^{-1} \text{ kW}^{-1}$, cold utility cost = $25 \text{€ y}^{-1} \text{ kW}^{-1}$, $\Delta T_{\min} = 20^\circ\text{C}$

**Fig. 5.** HEN obtained for case-study 1 using the linearized model.**Table 5**

Case-study 3 stream data (Björk and Pettersson, 2003).

Stream	T^{in} (°C)	T^{out} (°C)	F (kW/K)	h (kW/m ² K)
H1	180	75	30	2
H2	280	120	15	2.5
H3	180	75	30	2
H4	140	45	30	2
H5	220	120	25	1.5
H6	180	55	10	2
H7	170	45	30	2
H8	180	50	30	2
H9	280	90	15	2
H10	180	60	30	2
H11	120	45	30	2
H12	220	120	25	2
H13	180	55	10	2
H14	140	45	20	2
H15	140	60	70	2
H16	220	50	15	2.5
H17	220	60	10	2.5
H18	150	70	20	2
H19	140	80	70	2
H20	220	50	35	2
H21	180	60	10	2
H22	150	45	20	2.5
C1	40	230	20	1.5
C2	120	260	35	1
C3	40	190	35	1.5
C4	50	190	30	2
C5	50	250	60	2
C6	40	150	20	2
C7	40	150	20	2
C8	120	210	35	2.5
C9	40	130	35	2.5
C10	60	120	30	2.5
C11	50	150	10	3
C12	40	130	20	1
C13	120	160	35	1
C14	40	90	35	1.75
C15	50	90	30	1.5
C16	50	150	30	2
C17	30	150	50	2
HU	325	325	1	1
CU	25	40	2	2

Exchanger capital cost = $8000+800[\text{Area}(\text{m}^2)]^\beta \text{€ y}^{-1}$, $\beta = 0.8$,
 hot utility cost = $70 \text{€ y}^{-1} \text{ kW}^{-1}$, cold utility cost = $10 \text{€ y}^{-1} \text{ kW}^{-1}$, $\Delta T_{\min} = 5^\circ\text{C}$

**Fig. 6.** HEN obtained for case-study 1 using the classical MINLP formulation.

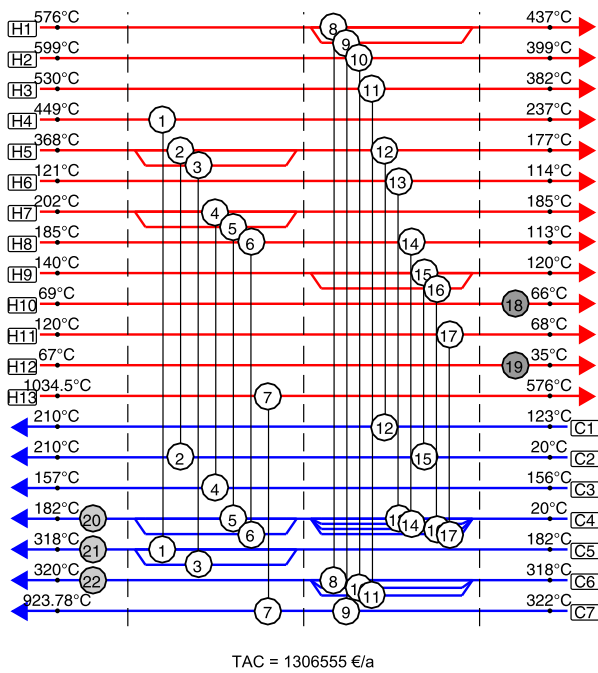


Fig. 7. HEN obtained for case-study 2 using the linearized model.

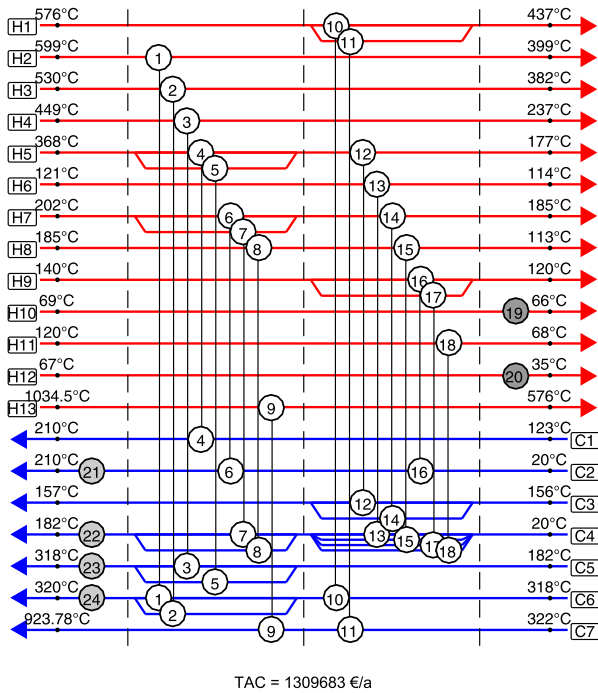


Fig. 8. HEN obtained for case-study 2 using the classical MINLP formulation.

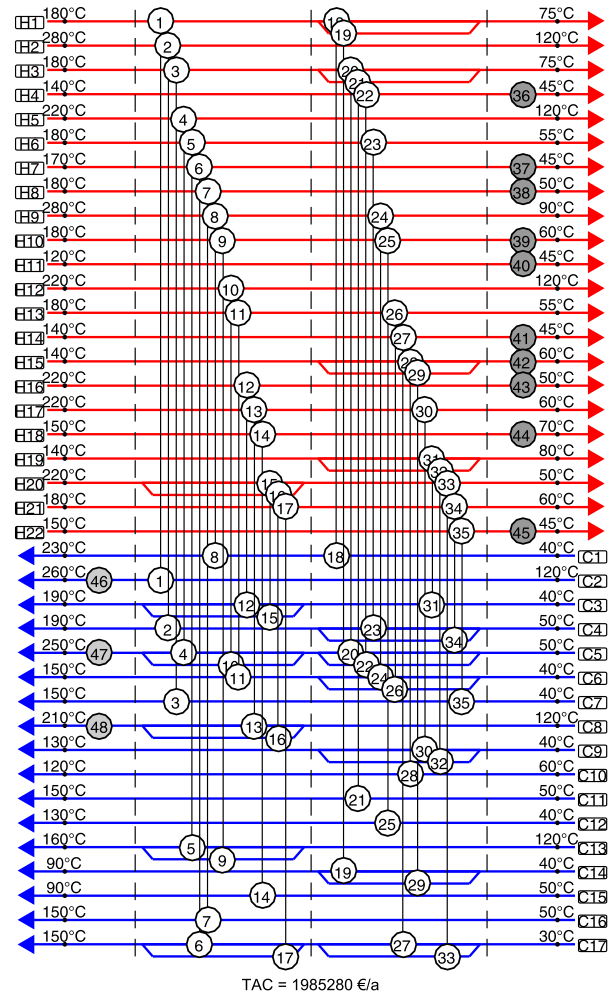


Fig. 9. HEN obtained for case-study 3 using the linearized model.

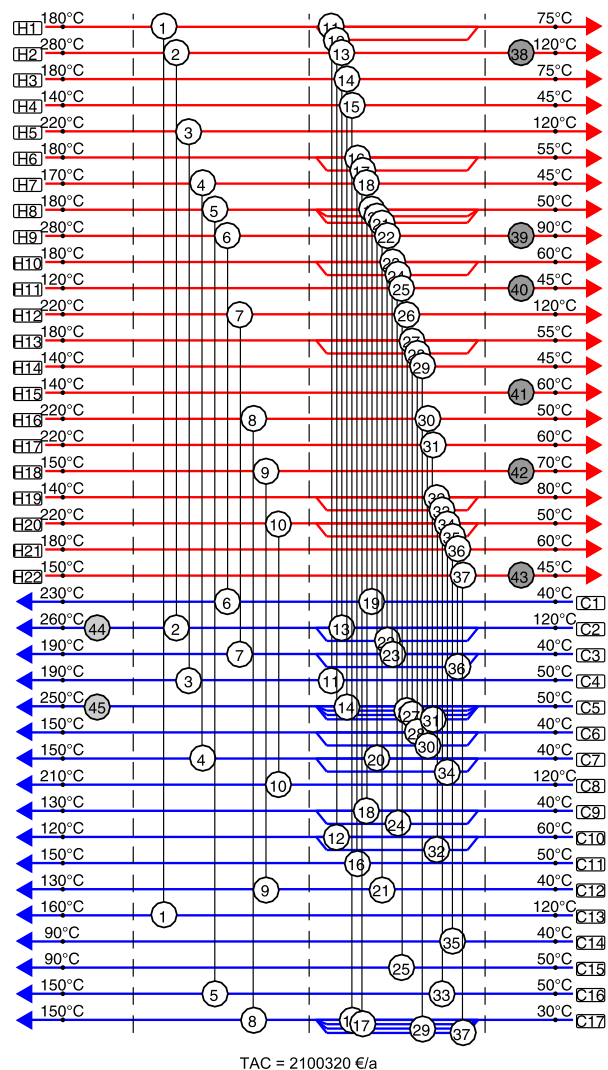


Fig. 10. HEN obtained for case-study 3 using the classical MINLP formulation.

References

- Björk, K.-M., Nordman, R., 2005. Solving large-scale retrofit heat exchanger network synthesis problems with mathematical optimization methods. *Chemical Engineering and Processing: Process Intensification* 44 (8), 869–876. doi:10.1016/j.cep.2004.09.005.
- Björk, K.-M., Pettersson, F., 2003. Optimization of large-scale heat exchanger network synthesis problems. *Modelling and Simulation* 2003, 313–318.
- Bogataj, M., Kravanja, Z., 2012. An alternative strategy for global optimization of heat exchanger networks. *Applied Thermal Engineering* 43, 75–90.
- Chen, J., 1987. Comments on improvements on a replacement for the logarithmic mean. *Chemical Engineering Science* 42 (10), 2488–2489. doi:10.1016/0009-2509(87)80128-8.
- Ciric, A.R., Floudas, C.A., 1991. Heat exchanger network synthesis without decomposition. *Computers & Chemical Engineering* 15 (6), 385–396. doi:10.1016/0098-1354(91)87017-4.
- Czyzyk, J., Mesnier, M.P., Moré, J.J., 1998. The neos server. *IEEE Journal on Computational Science and Engineering* 5 (3), 68–75.
- Dolan, E.D., 2001. The NEOS Server 4.0 Administrative Guide. Technical Memorandum. Mathematics and Computer Science Division, Argonne National Laboratory.
- Escobar, M., Trierweiler, J.O., 2013. Optimal heat exchanger network synthesis: A case study comparison. *Applied Thermal Engineering* 51 (1–2), 801–826.
- Floudas, C.A., Ciric, A.R., Grossmann, I.E., 1986. Automatic synthesis of optimum heat exchanger network configurations. *AIChE Journal* 32 (2), 276–290. doi:10.1002/aic.690320215.
- Gropp, W., Moré, J.J., 1997. Optimization environments and the neos server. In: Buhman, M.D., Iserles, A. (Eds.), *Approximation Theory and Optimization*. Cambridge University Press, pp. 167–182.
- Gundersen, T., 2013. Targets and heat exchanger network design. In: Klemes, J.J. (Ed.), *Handbook of Process Integration (PI)*. Woodhead Publishing Ltd., Oxford, pp. 129–167.
- Hohmann, E.C., 1971. *Optimum Networks for Heat Exchangers*. PhD Thesis, University of Southern California, USA.
- Linnhoff, B., Flower, J.R., 1978. Synthesis of heat exchanger networks: ii. evolutionary generation of networks with various criteria of optimality. *AIChE Journal* 24 (4), 642–654. doi:10.1002/aic.690240412.
- Luo, X., Wen, Q.-Y., Fieg, G., 2009. A hybrid genetic algorithm for synthesis of heat exchanger networks. *Computers & Chemical Engineering* 33 (6), 1169–1181. doi:10.1016/j.compchemeng.2008.12.003.
- Ma, X., Yao, P., Luo, X., Roetzel, W., 2008. Synthesis of multi-stream heat exchanger network for multi-period operation with genetic/simulated annealing algorithms. *Applied Thermal Engineering* 28 (8–9), 809–823.
- Mistry, M., Misener, R., 2016. Optimising heat exchanger network synthesis using convexity properties of the logarithmic mean temperature difference. *Computers & Chemical Engineering* 94, 1–17. doi:10.1016/j.compchemeng.2016.07.001.
- Papoulias, S.A., Grossmann, I.E., 1983. A structural optimization approach in process synthesis—ii. *Computers & Chemical Engineering* 7 (6), 707–721. doi:10.1016/0098-1354(83)85023-6.
- Pettersson, F., 2005. Synthesis of large-scale heat exchanger networks using a sequential match reduction approach. *Computers and Chemical Engineering* 29, 993–1007.
- Sahinidis, N. V., 2014. *BARON 14.3.1: Global Optimization of Mixed-Integer Nonlinear Programs*. User's Manual.
- Soršak, A., Kravanja, Z., 2002. Simultaneous minlp synthesis of heat exchanger networks comprising different exchanger types. *Computers & Chemical Engineering* 26 (4–5), 599–615. doi:10.1016/S0098-1354(01)00779-7.
- Tawarmalani, M., Sahinidis, N.V., 2005. A polyhedral branch-and-cut approach to global optimization. *Mathematical Programming* 103, 225–249.
- Wächter, A., Biegler, L.T., 2006. On the implementation of an interior-point filter line-search algorithm for large-scale nonlinear programming. *Mathematical Programming* 106 (1), 25–57. doi:10.1007/s10107-004-0559-y.
- Yee, T.F., Grossmann, I.E., 1990. Simultaneous optimization models for heat integration—ii. heat exchanger network synthesis. *Computers & Chemical Engineering* 14 (10), 1165–1184.
- Yu, H., Fang, H., Yao, P., Yuan, Y., 2000. A combined genetic algorithm/simulated annealing algorithm for large scale system energy integration. *Computers & Chemical Engineering* 24 (8), 2023–2035. doi:10.1016/S0098-1354(00)00601-3.

5.2 Paper 2

Full paper journal contribution in
Computers and Chemical Engineering
(2017 Impact Factor: 3.113)



How to tighten a commonly used MINLP superstructure formulation for simultaneous heat exchanger network synthesis

Anton Beck^a, René Hofmann^{a,b,*}

^aAIT Austrian Institute of Technology GmbH, Center for Energy, Sustainable Thermal Energy Systems, Giefinggasse 2, Vienna 1210, Austria

^bTechnische Universität Wien, Institute for Energy Systems and Thermodynamics, Getreidemarkt 9/E302, Vienna 1060, Austria

ARTICLE INFO

Article history:

Received 23 October 2017

Revised 17 January 2018

Accepted 18 January 2018

Available online 3 February 2018

Keywords:

Heat exchanger networks

Tighter formulation

Global optimization

ABSTRACT

MINLP superstructures for heat exchanger network synthesis allow the simultaneous optimization of utility heat loads, the number of heat exchanger units and their area requirements. The algorithms used to solve these nonlinear non-convex optimization problems solve MILP and NLP sub-problems iteratively to find optimal solutions. If these sub-problems are tightened, which means that the solution space is reduced but still includes all feasible integer solutions, the algorithms can potentially go through the solution space faster as branches can be excluded earlier. In this work, tightening measures for a commonly used MINLP stage-wise superstructure formulation are proposed and the impact of tighter variable bounds and additional inequality constraints is investigated using various case-studies taken from literature. It is shown that tighter formulations help the solver to find global optimal solutions and that the duality gap can be reduced significantly if the test cases could not be solved to global optimality.

© 2018 Elsevier Ltd. All rights reserved.

1. Introduction

In the early 90s the first superstructure formulations were proposed that allow simultaneous consideration of the number of heat exchangers, their respective heat exchanger area requirements and costs for utilities (Ciric and Floudas, 1991; Yee and Grossmann, 1990). As the simultaneous heat exchanger network synthesis (HENS) problem belongs to the class of NP-hard problems (Furman and Sahinidis, 2001) global optimal solutions are hard to find even for small problems and state of the art solvers available (Yerramsetty and Murty, 2008). Specialized algorithms for the solution of simultaneous HENS problems have been proposed that exploit problem specific properties to push the limits of problem size for which global optima can be obtained. Zamora and Grossmann (1998) presented an outer approximation branch and bound algorithm that uses convex underrelaxations to solve the non-convex Mixed Integer Nonlinear Programming (MINLP) superstructure proposed by Yee and Grossmann (1990) to global optimality with the restriction that no stream splits are allowed. Björk and Westerlund (2002) presented a global optimization procedure for the same superstructure formulation that allows for stream splits

and non-isothermal mixing by convexifying signomial terms and creating convex subproblems. Bergamini et al. (2007) developed a methodology for global optimization based on outer approximation methods which uses physical insights to reduce the number of physically feasible network structures. Bogataj and Kravanja (2012) proposed an approach for obtaining globally optimal solutions to the HENS problems which uses an aggregated substructure to reduce the number of nonconvex terms, which need to be convexified in order to derive a convex underestimating problem. They stated that it might be helpful to add logical constraints that reduce the combinatorial complexity especially for larger HENS problems.

Tightening of the relaxed sub-problems that need to be solved by global optimization algorithms potentially helps to exclude infeasible branches or branches that yield no improvement on the current objective value from the search space more quickly. Additional constraints derived from physical insights that tighten the problem were used by Bergamini et al. (2007). They incorporated linear inequality constraints that form a lower bound for the total heat exchanger area, stream-wise heat exchanger areas and total number of heat exchanger units in their global optimization methodology. Anantharaman et al. (2010) used physically feasible upper bounds for the maximum transferable heat of individual stream pairs and derived lower bounds for stream-wise heat exchanger matches to tighten a Mixed Integer Linear Programming (MILP) transshipment model for the identification of the overall minimum number of heat exchangers.

* Corresponding author at: Technische Universität Wien, Institute for Energy Systems and Thermodynamics, Getreidemarkt 9/E302, Vienna 1060, Austria.

E-mail addresses: rene.hofmann@tuwien.ac.at, rene.hofmann@ait.ac.at (R. Hofmann).

URL: <http://www.tuwien.ac.at> (R. Hofmann)

<https://doi.org/10.1016/j.compchemeng.2018.01.011>

0098-1354/© 2018 Elsevier Ltd. All rights reserved.

Nomenclature

Acronyms

CS	Case-study
HENS	Heat exchanger network synthesis
LP	Linear programming
MILP	Mixed integer linear programming
MINLP	Mixed integer nonlinear programming
NLP	Nonlinear programming

Parameters

β	Cost exponent (-)
ΔT_{min}	Minimum approach temperature (°C)
Γ	Upper bound for temperature difference (°C)
Ω	Upper bound for heat exchange (kW)
c_{area}	Cost coefficient for heat exchanger area (€ m ⁻²)
F	Flow capacity of process streams (kW/K)
NOK	Number of stages
U	Heat transfer coefficient (kW/m ² K)

Subscripts

cu	Cold utility
hu	Hot utility
i	Hot stream
j	Cold stream
k	Temperature stage
LB	Lower bound
max	Maximum value
min	Minimum value
rec	Heat recovery
UB	Upper bound

Superscripts

cold	Cold side of heat exchanger
hot	Hot side of heat exchanger
in	Inlet
out	Outlet

Variables

ΔT	Temperature difference (°C)
$LMTD$	Logarithmic mean temperature difference (°C)
TAC	Total annual costs (€)
A	Heat exchanger area (m ²)
c_{area}	Annualized costs for heat exchanger area (€)
q	Heat flow (kW)
T	Temperature (°C)
z	Binary variable for existence of heat exchanger (-)

Finding tight bounds for the domains of linear and nonlinear expressions is also a common subproblem in global optimization strategies. Puranik and Sahinidis (2017) reviewed techniques for domain reduction and proposed that future work on domain reduction should also focus on typical engineering problems such as network design.

The scope of this work is to present modifications to the commonly used MINLP stage-wise superstructure formulation proposed by Yee and Grossmann (1990) that tighten the problem and thus reduce the complexity of the simultaneous HENS problem. The individual terms and equations of the superstructure formulation are analysed and modifications are presented that tighten both variable bounds and model constraints. Also, additional constraints are introduced that further tighten the linear relaxation. The presented modifications are then tested with various case-studies and the impact of these modifications is analysed. All of the proposed tightening measures are introduced to the MINLP

model prior to optimization and thus are independent of the solvers used.

The application of tightening measures should potentially result in lower computation time for global optimal solutions. On the other side, global optimal solutions can potentially be found for larger problems which pushes the limits for industrial applications.

2. Tightening of linear relaxation

In the following, methods are proposed that allow to find feasible tight variable bounds and tighter constraints for the stage-wise superstructure model proposed by Yee and Grossmann (1990). Also, additional inequality constraints are introduced that further tighten the sub-problems involved in global optimization procedures. The original model formulation is stated in the appendix.

2.1. Variable bounds

Within the NLP relaxation tight initial bounds on the variables involved in the nonlinear expressions reduce the domain in which these expressions are defined. Especially for non-convex terms this is beneficial as the convex relaxations then yield better approximations to these nonlinearities. Three sets of nonlinear terms occur within the superstructure formulation. All of them are involved in the calculation of the costs for the heat exchanger areas c_{area}

$$c_{area} = \sum_i \sum_j \sum_k c_{area} A_{ijk}^{\beta} \quad (1)$$

where c_{area} is the cost coefficient for heat exchanger area and β is the cost exponent. The heat exchanger area A_{ijk} is calculated by

$$A_{ijk} \geq \frac{q_{ijk}}{U_{ij} LMTD_{ijk}} \quad (2)$$

where U_{ij} is the heat transfer coefficient and $LMTD_{ijk}$ is the logarithmic mean temperature difference calculated by

$$LMTD_{ijk} \leq \left(\Delta T_{ijk} \Delta T_{ijk+1} \frac{\Delta T_{ijk} + \Delta T_{ijk+1}}{2} \right)^{1/3} \quad (3)$$

which is a convex function in the sense of the underlying optimization problem. Here, the Chen-approximation (Chen, 1987) is used that eliminates the singularity involved in the equation for $LMTD$ that occurs at equal temperature differences at the hot and cold sides of the heat exchangers.

Lower bounds for the involved variables ΔT_{ijk} , $LMTD_{ijk}$, q_{ijk} and A_{ijk} need to be set to guarantee physical feasibility. The lower bounds for ΔT_{ijk} and $LMTD_{ijk}$ are usually set to ΔT_{min} . Tighter variable bounds can potentially be obtained if Eq. (4) is used instead.

$$\Delta T_{ijk, LB}, LMTD_{ijk, LB} = \max\{T_i^{out} - T_j^{out}, \Delta T_{min}\}. \quad (4)$$

Most solvers are able to set feasible upper variable bounds themselves as they are not needed for physical feasibility. Upper limits for ΔT_{ijk} , $LMTD_{ijk}$ and q_{ijk} are provided through the model equations. However, providing low upper variable bounds that do not reduce the feasible solution space can help the solver.

The upper bound for q_{ijk} ($q_{ijk, UB}$) is obtained by calculating the maximum transferable heat between each hot stream i and cold stream j . This can be done by performing pinch analysis on each stream pair, i.e. calculating the overlap of the stream pair in the Q-T diagram at the minimum approach temperature ΔT_{min} as demonstrated in Fig. 1. This can be done using the Problem-Table-Algorithm proposed by Linnhoff and Flower (1978). The same upper bounds were also used by Anantharaman et al. (2010) in their sequential approach to the minimum number of heat exchangers problem. The upper bounds for ΔT_{ijk} and for $LMTD_{ijk}$ are simply

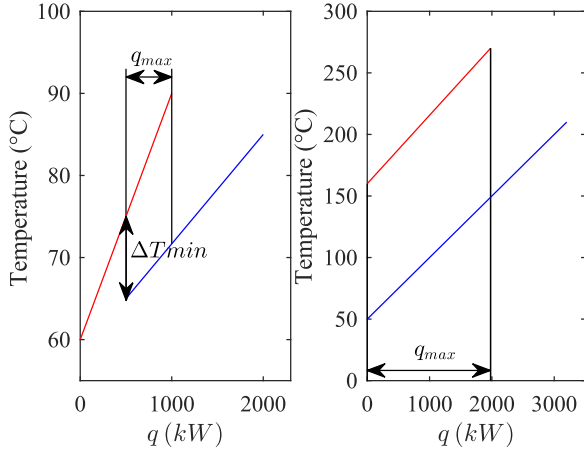


Fig. 1. Calculation of q_{max} using pinch analysis.

the temperature difference between the inlet temperature of the hot stream i and the inlet temperature of cold stream j for all stages k . If the difference is lower than ΔT_{min} the upper bound is set to ΔT_{min} (Eq. (5)).

$$\Delta T_{ijk,UB}, LMTD_{ijk,UB} = \max\{T_i^{in} - T_j^{in}, \Delta T_{min}\}. \quad (5)$$

For the identification of the lowest feasible upper bound for A_{ijk} the potentially piecewise function $LMTD_{ijk, min}(q_{ijk})$ needs to be known. $LMTD_{ijk, min}$ is the lowest possible logarithmic mean temperature as a function of the transferred heat q_{ijk} and can be obtained by solving the linear problems I, II and III (Eq. (6)) that yield the minimum values for the temperature differences ΔT^{hot} and ΔT^{cold} as a function of the transferred heat q_{ijk} . The superscripts *hot* and *cold* represent the hot and cold side of the heat exchanger.

$$\begin{aligned} \text{I,II} : & \max q \\ \text{III} : & \min \Delta T^{hot} + \Delta T^{cold} \\ & \text{subject to} \\ & q \leq q_{max} \\ & q \leq (T_i^{hot} - T_i^{cold})F_i, \quad q \leq (T_j^{hot} - T_j^{cold})F_j \\ & T_i^{hot} \leq T_i^{in}, \quad T_i^{cold} \geq T_i^{out}, \quad T_i^{hot} > T_i^{cold} \\ & T_j^{hot} \leq T_j^{out}, \quad T_j^{cold} \geq T_j^{in}, \quad T_j^{hot} > T_j^{cold} \\ & \Delta T^{hot} = T_i^{hot} - T_j^{hot}, \quad \Delta T^{cold} = T_i^{cold} - T_j^{cold} \\ & \Delta T^{hot}, \Delta T^{cold} \geq \Delta T_{min} \\ \text{I} : & \Delta T^{hot}, \Delta T^{cold} = \Delta T_{min} \\ \text{II} : & \begin{cases} \Delta T^{hot} = \Delta T_{min}, & \text{if } F_j \leq F_i \\ \Delta T^{cold} = \Delta T_{min}, & \text{if } F_j \geq F_i \end{cases} \\ \text{III} : & q = q_{max} \end{aligned} \quad (6)$$

The lowest possible upper bound for A_{ijk} is then found by solving

$$\max_{q_{ijk}} A_{ijk,max} = \frac{q_{ijk}}{U_{ij}LMTD_{ijk,min}(q_{ijk})} \quad (7)$$

$$\text{s.t.} \quad 0 \leq q_{ijk} \leq q_{ijk,UB}.$$

In Fig. 2 the tightest possible bounds that do not reduce the physically feasible solutions are shown for two example streams.

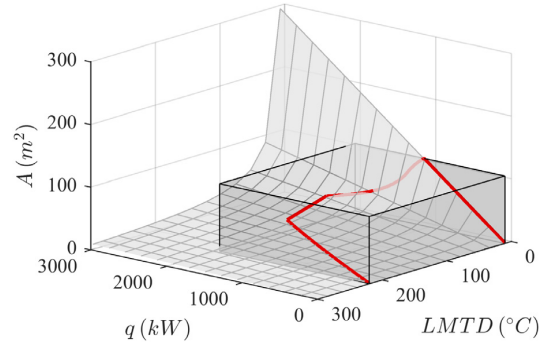


Fig. 2. Reduced domain for heat exchanger area.

The area marked with red outlines is the physically feasible solution space. This space is bounded by the upper and lower variable bounds for q , $LMTD$ and A which are represented by the grey cuboid that circumscribes the physically feasible solutions space.

2.2. Model constraints

In the model, two different sets of logical constraints involving binary variables are used that allow for physically feasible solutions of the combinatorial problem.

- The logical constraints that limit the transferred heat q_{ijk} between hot stream i and cold stream j in temperature stage k are stated as

$$q_{ijk} \leq \Omega_{ij}z_{ijk}. \quad (8)$$

These constraints are used to force q_{ijk} to zero if no heat exchanger exists ($z_{ijk} = 0$). Ω_{ij} is a parameter that keeps the transferred heat q_{ijk} in bounds and is usually set to

$$\Omega_{ij} = \min\{F_i(T_i^{in} - T_i^{out}), F_j(T_j^{out} - T_j^{in})\} \quad (9)$$

which is the minimum of the total heat flows of the hot stream i and the cold stream j . However, the lowest feasible value for Ω_{ij} is equal to the upper variable bound for q_{ijk} and thus is set to

$$\Omega_{ij} = q_{ijk,UB}. \quad (10)$$

- To ensure that the variables representing the temperature differences ΔT_{ijk} and ΔT_{ijk+1} do not become negative even in the case where the cold stream j is hotter than the hot stream i in stage k and thus no feasible heat transfer from the hot stream to the cold stream is possible the inequality constraints

$$\Delta T_{ijk} \leq T_{ik} - T_{jk} + \Gamma_{ij}(1 - z_{ijk}), \quad (11)$$

$$\Delta T_{ijk+1} \leq T_{i,k+1} - T_{j,k+1} + \Gamma_{ij}(1 - z_{ijk}) \quad (12)$$

are used. Γ_{ij} is a sufficiently large positive real number so that ΔT_{ijk} is greater than its lower bound in the case that z_{ijk} is zero. Vice versa z_{ijk} is forced to zero if no feasible heat transfer is possible. Γ_{ij} is usually calculated by

$$\Gamma_{ij} = \max\{T_j^{out} - T_i^{out} + \Delta T_{min}, 0\}. \quad (13)$$

The constraints Eqs. (11) and (12) can be tightened if stream temperatures at the hot side in the first ($k = 1$) and the cold side in the last ($k = NOK$) temperature stage are considered. As the inlet temperature of the hot stream corresponds to the inlet temperature into the potential heat exchanger in stage $k = 1$

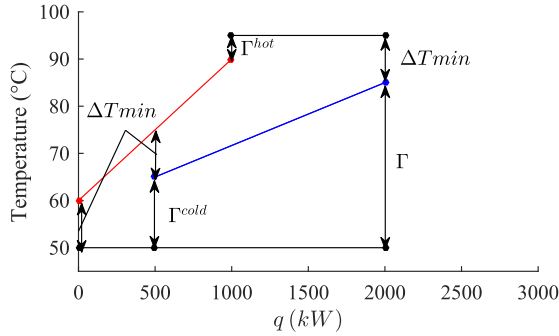


Fig. 3. Lower limits for Γ .

Γ_{ij}^{hot} is the maximum negative temperature difference between hot and cold stream plus ΔT_{min}

$$\Gamma_{ij}^{hot} = \max\{T_j^{out} - T_i^{in} + \Delta T_{min}, 0\} \quad (14)$$

Similarly, as the inlet temperature of the cold stream is known Γ_{ij}^{cold} is

$$\Gamma_{ij}^{cold} = \max\{T_j^{in} - T_i^{out} + \Delta T_{min}, 0\}. \quad (15)$$

In all other cases Γ_{ij} is set according to Eq. (13). A graphical representation of the three Γ values is presented in Fig. 3.

2.3. Constraints for maximum heat recovery

The energy target derived from pinch-analysis is a rigorous upper bound for possible heat recovery q_{rec}^{max} as this target yields the theoretical maximum for heat recovery for a predefined value of ΔT_{min} as stated by Umeda et al. (1979).

$$\sum_i \sum_j \sum_k q_{ijk} \leq q_{rec}^{max} \quad (16)$$

Such upper bounds for heat recovery can also be calculated for every possible process sub-system which can also be obtained by pinch-analysis. For this paper, upper bounds for maximum heat recovery were calculated for sub-systems that consist of all cold streams and an increasing number of hot streams x starting with the hot stream with the lowest inlet temperature. The same was done for sub-systems consisting of all hot streams and an increasing number of cold streams y starting with the cold stream with the highest inlet temperature.

$$\sum_{i=1, \dots, x} \sum_j \sum_k q_{ijk} \leq q_{rec,x}^{max} \quad (17)$$

$$\sum_i \sum_{j=1, \dots, y} \sum_k q_{ijk} \leq q_{rec,y}^{max} \quad (18)$$

Upper bounds for heat recovery were not calculated for all possible sub-systems as the number of these sub-systems increase exponentially with problem size. The upper bounds for the smallest possible sub-systems consisting of only one hot and one cold stream are equivalent to the bounds for pair-wise maximum heat transfer and thus can be implemented directly.

$$\sum_k q_{ijk} \leq q_{ijk,UB} = q_{rec,ij}^{max} \quad (19)$$

2.4. Constraints for the number of heat exchanger units

Lower bounds for the number of heat exchangers z_{min} for recovery of a certain amount of heat can be obtained by solving a reduced version of the stage-wise superstructure MINLP model. In

this model the heat exchanger areas are neglected and thus the MINLP model is reduced to a MILP model which is much easier to solve, although for large problems even the reduced model becomes hard to solve. Using this model the minimum number of heat exchangers is calculated for various discrete values for heat recovery q_{rec} ($0 \leq q_{rec} \leq q_{rec}^{max}$). The lower bound for the number of heat exchangers z_{min} is then set to the minimum of these calculated values. The inequality constraint for the lower bound of the number of heat exchanger units is

$$\sum_i \sum_j \sum_k z_{ijk} + \sum_i z_{cui} + \sum_j z_{huj} \geq z_{min}. \quad (20)$$

Alternatively, a set of inequality constraints can be constructed that form a convex lower approximation of the obtained data points.

The minimum number of heat exchangers for each stream depends on its recovered heat. For each stream the minimum number of heat exchangers can be set to 1 as either all heat is transferred using a utility heat exchanger or a utility heat exchanger and/or one or more process to process heat exchangers.

$$\sum_j \sum_k z_{ijk} + z_{cui} \geq 1, \quad (21)$$

$$\sum_i \sum_k z_{ijk} + z_{huj} \geq 1. \quad (22)$$

In the case that there is no potential process stream that can provide all the cooling or heating needed by the stream in concern, the formulation can be tightened. Even if all the heat is transferred by process to process heat exchangers more than one heat exchanger is needed and the following constraints can be obtained

$$\sum_i \sum_k z_{ijk} + z_{huj} \geq 1 + \frac{\sum_i \sum_k q_{ijk}}{\sum_i \sum_k q_{ijk} + \sum_i q_{cui}}, \quad (23)$$

$$\sum_j \sum_k z_{ijk} + z_{cui} \geq 1 + \frac{\sum_j \sum_k q_{ijk}}{\sum_j \sum_k q_{ijk} + \sum_j q_{huj}}. \quad (24)$$

The constraints for stream-wise minimum heat exchanger units can also be used to tighten the MILP model for identification of the overall minimum number of heat exchanger units. Also the proposed constraints that limit the maximum heat recovery can be implemented in the reduced model.

2.5. Constraints for heat exchanger areas

A lower bound for the total heat exchanger area requirements can be obtained by area targeting of the process. In this work the area targets are calculated using the lowest heat transfer coefficients in the system for process to process heat exchange and for hot and cold utilities respectively. If the heat transfer coefficients differ a lot, more sophisticated targeting algorithms that consider unequal heat transfer coefficients can be used (Ahmad et al., 1990; Saboo et al., 1986). Area targets are calculated for $0 \leq q_{rec} \leq q_{rec}^{max}$. Inequality constraints that function as lower bounds are then derived by calculating a convex outer approximation of these area targets.

$$\sum_i \sum_j \sum_k A_{ijk} + \sum_i A_{cui} + \sum_j A_{huj} \geq a_n q_{rec} + b_n \quad (25)$$

In Eq. (25) a_n and b_n are the coefficients derived from the outer approximations. There is a trade-off between accuracy of that approximation and the number of approximating inequality constraints. Also for sub-systems lower bounds for the heat exchanger area requirements can be calculated. The sub-systems for which lower area bounds were calculated in this paper are the same as were used to bound the maximum transferable heat (Section 2.3).

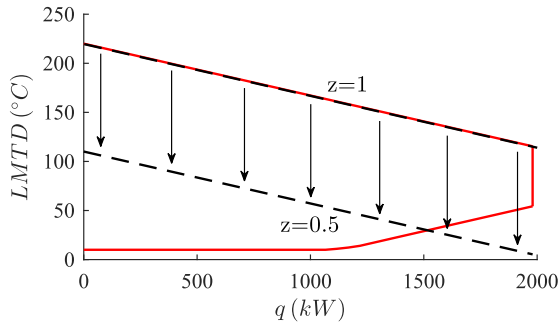


Fig. 4. New linear constraint for $LMTD$ (dashed line) that reduces the domain of $LMTD$ (red outlines) depending on the transferred heat q and the relaxed binary variable z . (For interpretation of the references to colour in this figure legend, the reader is referred to the web version of this article.)

2.6. Constraints for logarithmic mean temperature differences

Within the relaxed problem the upper bound for the transferred heat q_{ijk} scales linearly with z_{ijk} (Eq. (8)). However, the upper limits for ΔT_{ijk} and $\Delta T_{i,j,k+1}$ increase linearly as z_{ijk} decreases if Γ is greater than zero (Eqs. (11) and (12)). This potentially leads to physically infeasibly large temperature differences and thus to smaller heat exchanger areas within the LP relaxed problem. Introducing new constraints that limit $LMTD_{ijk}$ can tighten this formulation. These constraints are derived from the linear outer approximation of the maximum logarithmic mean temperature difference $LMTD_{ijk, \max}(q_{ijk})$ for each potential heat exchanger match.

$$f(q_{ijk}) = LMTD_{ijk, \max}(q_{ijk}) \quad (26)$$

$$c_1 = f'(q_{ijk} = 0) \quad (27)$$

$$c_2 = f(q_{ijk} = 0) - LMTD_{ijk, LB} \quad (28)$$

$$c_3 = LMTD_{ijk, LB} \quad (29)$$

$$LMTD_{ijk} \leq c_1 q_{ijk} + c_2 z_{ijk} + c_3 \quad (30)$$

As an example, the solution space for the heat exchanger area calculation within the relaxed problem is shown in Fig. 4 for $z = 1$ and $z = 0.5$. In this Figure $LMTD_{\max}(q)$ is the upper limit for the physically feasible solution space (red outlines).

3. Case-studies and results

3.1. Case-studies

In order to proof the effectiveness of the presented tightening measures six small case-studies with four to five process streams were solved to global optimality and five larger case-studies with 7 up to 39 process streams were optimized until the time limit of 8 hours was reached. All case-studies were taken from literature and range from small test cases up to industrial size problems. The stream numbers for all case-studies are presented in Table 1.

Case-study 1 was proposed by Zhu (1997) to demonstrate a decomposition approach for HENS. The **second case-study** was proposed by Lin and Miller (2004) who used tabu-search for HENS. **Case-studies 3 and 4** are modified versions of a four stream example proposed by Linnhoff (1994). The modified stream data is presented in Table 2. The **fifth case-study** is taken from

Table 1
Number of hot and cold streams for case-studies.

CS	Process streams			Author
	hot	cold	total	
1	2	2	4	Zhu (1997)
2	2	2	4	Lin and Miller (2004)
3	2	2	4	modified, Linnhoff (1994)
4	3	2	5	modified, Linnhoff (1994)
5	2	2	4	Huo et al. (2012)
6	2	2	4	Gundersen (2013)
7	3	4	7	Isafiade and Short (2016)
8	8	7	15	Björk and Westerlund (2002), Björk and Nordman (2005)
9	6	12	18	Ma et al. (2008)
10	13	7	20	Soršak and Kravanja (2002)
11	22	17	39	Björk and Westerlund (2002), Björk and Nordman (2005)

Table 2
Case-studies 3 and 4 stream data (modifications to Linnhoff, 1994).

Stream	T^{in} (°C)	T^{out} (°C)	F (kW/K)	h (kW/m ² K)
H1	180	40	20	1.5
H2	150	40	40	1.5
H3 ^a	150	80	20	1.5
C1	60	210	30	1.5
C2	30	210	26	1.5
HU	258	258		3
CU	30	40		1.5

Exchanger capital cost = $4000 + 500[\text{Area}(\text{m}^2)]^\beta \text{€ } \text{y}^{-1}$, $\beta = 0.7$, hot utility cost = $200 \text{ € } \text{y}^{-1} \text{ kW}^{-1}$, cold utility cost = $20 \text{ € } \text{y}^{-1} \text{ kW}^{-1}$, $\Delta T_{\text{min}} = 5^\circ\text{C}$

^a Added in case-study 4.

Huo et al. (2012) who performed particle swarm optimization. **Case-study 6** is adapted from the work of Gundersen (2013) who used this example for HENS using pinch-methodology. Björk et al. (Björk and Nordman, 2005; Björk and Westerlund, 2002) presented the **case-studies 8 and 11** for their approaches for HENS of large-scale problems. **Case-study 10** was first presented by Soršak and Kravanja (2002) who used different types of heat exchangers within HENS. The **case-studies 7 and 9** are single-period adaptations from multi-period HENS problems presented by Zhang (2006) and Ma et al. (2008). The stream data for case-study 7 was presented by Isafiade and Short (2016) who proposed a single representative operation period for the multi-period case-study of Zhang (2006).

3.2. Tighter formulations

Three different formulations were used incorporating different measures that tighten the MINLP formulation in addition to the original formulation. These formulations consist of the following tightened bounds and additional constraints:

- **Formulation 1:** original formulation, no additional constraints, no upper bounds set for q , $LMTD$, ΔT and A .
- **Formulation 2:** constraints Eqs. (8), (11) and (12) with adapted coefficients, upper bounds for q , $LMTD$, ΔT and A set according to Section 2.1.
- **Formulation 3:** same as Formulation 2 but with additional constraints for maximum heat recovery (total and stream-wise, Eq. (16)–(18)), minimum number of heat exchanger units (total and stream-wise, Eq. (20)–(23)) and minimum heat exchanger area (total and stream-wise, Eq. (25)).
- **Formulation 4:** same as Formulation 3 but with additional constraints for the logarithmic mean temperature difference (Eq. (30)).

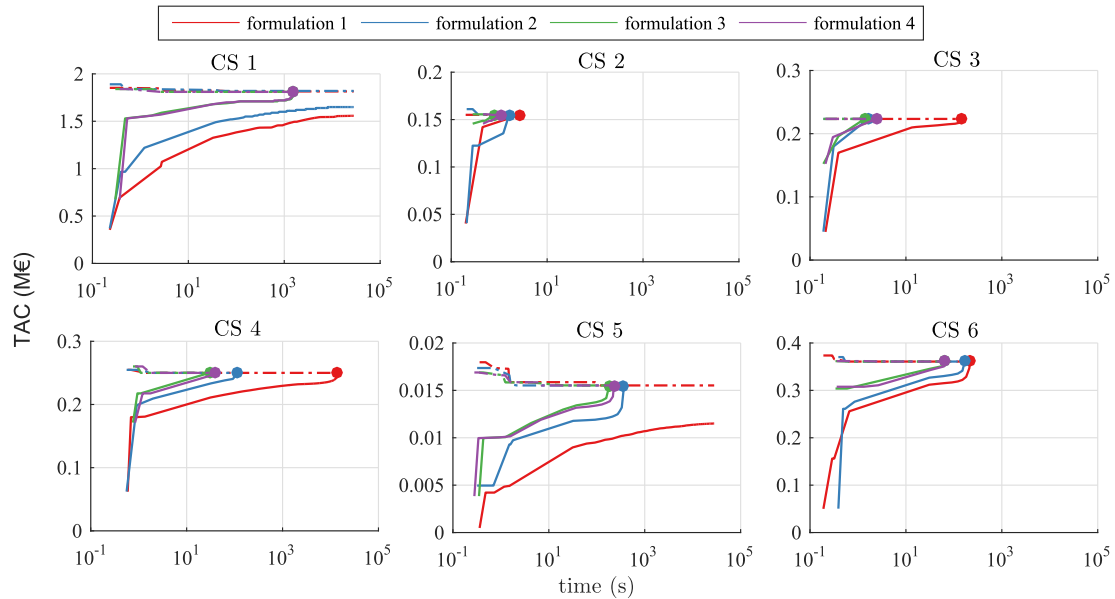


Fig. 5. Bound progression over time for case-studies 1–6 (logarithmic time scale, solid line: lower bound, dash-dotted line: current best objective value).

Table 3

Computation time (s) for global optimization of case-studies 1–6.

CS	Formulation			
	1	2	3	4
1	^a	^a	1,5252.3	1,4739.5
2	2.7	1.6	0.8	1.1
3	145.2	1.6	1.4	2.4
4	13,969.2	117.1	29.7	37.8
5	^a	362.5	182.0	227.8
6	214.7	168.2	66.1	66.1

^a Time limit of 8 h (28,800 s) reached.

All of the small case-studies (CS 1–6) were solved on an Intel Core i7–6700HQ, 8GB RAM running GAMS and BARON (Sahinidis, 2014; Tawarmalani and Sahinidis, 2005) version 16.5.16. The larger case-studies (CS 7–11) were computed on the NEOS server cluster (Czyzyk et al., 1998; Dolan, 2001; Gropp and Moré, 1997) running GAMS and BARON version 17.4.1. CONOPT was used to solve NLP sub-problems and CPLEX was chosen as LP solver. Standard settings were used for the optimization.

3.3. Impact on computation time and bound progression

As a performance indicator, the time needed to find the global optimum was considered. The results for computation time for the small case-studies are presented in Table 3. Fig. 5 shows the progression of the lower bound (theoretical best possible solution) and the current best objective value over time. The time axis is presented in logarithmic scale for better readability. Instead of iterations, time is used to show bound progression. The evaluation of the bound progression showed that using tighter formulations, less iterations per second can be performed compared to the original formulation. This is expected as the tighter formulations consist of more equations to be solved. The graphs in Fig. 5 show that using the tighter formulations a much smaller gap between current best solution and the lower bound can be obtained at any time. Only

during the first seconds in the solution process of case-study 2 and 6, the tighter formulations show a bigger duality gap than the original formulation. Formulations 3 and 4 shows a very similar behaviour in terms of bound progression throughout all of the solved case-studies. Except for case-study 1, where formulation 4 resulted in a slightly lower gap and overall computation time, formulation 3 shows the best bound progression. It needs to be stated, that for all of the small case-studies, the solver could find an objective value that corresponds to the global optimal solution after several seconds.

The results show that the time needed to find the globally optimal solution for the small case-studies (CS 1–6) can be reduced with all of the tightened formulations. Using formulation 2 the median value of the computation time was reduced to about 31% compared to the original formulation. For the tighter formulations 3 and 4 the median value lies at about 3.2% and 3.5% respectively. The impact of the tightened formulations varies for each individual case-study. For case-study 6 the tightened formulations reduced the computation time to about 30.8%–78.4% of the original formulation whereas for case-study 5 the computation could be reduced to 0.65%–1.29%. The reduction could potentially be even more significant as the original formulation did not converge to the global optimum within the time limit of 8 hours and thus the time limit was used to calculate the reduction.

3.4. Impact on residual gap and objective value

For analysis of the impact of the proposed tightened formulations on TAC and duality gap, optimization was performed on five case-studies (CS 7–11) which consist of 7–39 process streams. In neither of these case-studies the gap could be closed and thus global optima cannot be guaranteed. The solutions in terms of TAC and the remaining gap obtained at the time limit of 8 h are presented in Tables 4 and 5 respectively.

The comparison of the obtained objective values (TAC) shows that tightening of the model does not necessarily improve the best integer solution found at a given time. After the time limit was reached, the median lies in the range of 99.56%–100.24% of the

Table 4
TAC (€) obtained after the time limit was reached for case-studies 7–11.

CS	Formulation			
	1	2	3	4
7	6,338,197	6,338,160	6,354,342	6,336,493
8	1,525,075	1,550,857	1,518,387	1,548,295
9	464,434	471,708	459,696	465,568
10	1,336,749	1,326,827	1,328,078	1,330,576
11	2,263,822	2,248,362	2,412,683	2,426,809

Table 5
Duality gap (-) after the time limit was reached for case-studies 7–11.

CS	Formulation			
	1	2	3	4
7	0.16	0.17	0.02	0.01
8	0.57	0.51	0.26	0.27
9	0.59	0.47	0.38	0.38
10	0.45	0.22	0.24	0.22
11	0.88	0.80	0.50	0.50

original formulation. The largest improvement could be obtained for case-study 8 and formulation 3 with 1.02%. The worst results for the objective values using tightened formulations were obtained for case-study 10 which is the largest of the case-studies. Formulation 3 resulted in an objective value 6.58% higher than using the original formulation. Formulation 4 resulted in an objective value higher by 7.2%.

The median of the duality gap decreases by 12% for formulation 2, by 46% for formulation 3 and by 50% for formulation 4 compared to the original formulation. For case-study 7 which consists of 7 process streams the residual gap could be reduced to 2% using formulation 3 and to 1% using formulation 4 compared to 16% with the original formulation without tightening measures. This shows that tightening of the problem can drastically reduce the gap and thus the uncertainty of how much better the global optimal solu-

tion might be compared to the best integer feasible solution found when the solver terminated.

This leads to the conclusion that tighter formulations can be solved faster to global optimality even though the search paths may be altered in a way that the best possible integer solutions found before the global optimum was obtained, do not necessarily have to be better compared to the solutions found using the original formulation without tightening measures.

4. Conclusion

In this paper possibilities for the tightening of the classic stage-wise superstructure formulation proposed by Yee and Grossmann (1990) were presented that are directly implemented in the model. This makes the implementation independent of the solution algorithm used to solve the underlying MINLP problem.

The proposed formulations help the solver with lower bound progression and yield a reduction of computation time for global optimization of small scale HENS problems. For some of the case-studies computation time could be reduced by more than an order of magnitude. For larger case-studies, that could not be solved to global optimality, tight variable bounds combined with additional inequality constraints showed to reduce the duality gap significantly faster, although this does not imply that the best objective value obtained after a given time is also reduced.

Nevertheless, model analysis in combination with the introduction of additional tightening constraints derived from physical insights showed to be worthwhile in terms of computation time and gap. Measures for problem tightening similar to the ones presented in this paper might also be applicable to other MI(N)LP problems.

Acknowledgements

This paper and the corresponding project were initiated and could be realized by means of the endowed professorship through the cooperation between AIT (Austrian Institute of Technology) and TU Wien (Vienna University of Technology) in the research-field of Industrial Energy Systems.

Appendix A

Stage-wise superstructure formulation (Yee and Grossmann, 1990)

$$\begin{aligned} \min TAC = & \underbrace{\sum_i c_{cui} q_{cui} + \sum_j c_{hu} q_{huj}}_{\text{energy costs}} + \underbrace{\sum_i \sum_j \sum_k c_f z_{ijk} + \sum_i c_f z_{cui} + \sum_j c_f z_{huj}}_{\text{step-fixed investment costs}} \\ & + \underbrace{\sum_i \sum_j \sum_k c \left(\frac{q_{ijk}}{U_{ij} LMTD_{ijk}} \right)^\beta + \sum_i c \left(\frac{q_{cui}}{U_{cui} LMTD_{cui}} \right)^\beta + \sum_j c \left(\frac{q_{huj}}{U_{huj} LMTD_{huj}} \right)^\beta}_{\text{variable investment costs}} \end{aligned}$$

subject to

$$\left. \begin{aligned} \sum_j \sum_k q_{ijk} + q_{cui} &= F_i (T_i^{in} - T_i^{out}), i \in HP \\ \sum_i \sum_k q_{ijk} + q_{huj} &= F_j (T_j^{out} - T_j^{in}), j \in CP \end{aligned} \right\} \text{stream-wise energy balance}$$

$$\left. \begin{aligned} \sum_i q_{ijk} &= F_i (T_{ik} - T_{i,k+1}), i \in HP \\ \sum_j q_{ijk} &= F_j (T_{jk} - T_{j,k+1}), j \in CP \end{aligned} \right\} \text{energy balance for each stage}$$

$$\left. \begin{aligned} T_{i,k=1} &= T_i^{in}, T_{j,k=NOK} = T_j^{in} \\ T_{ik} &\geq T_{i,k+1}, T_{jk} \geq T_{j,k+1} \\ T_{i,k=NOK+1} &\geq T_i^{out}, T_{j,k=1} \geq T_j^{out} \end{aligned} \right\} \text{assignment of inlet temperatures}$$

$$\left. \begin{aligned} q_{cui} &= F_i (T_{i,k=NOK+1} - T_i^{out}) \\ q_{huj} &= F_j (T_j^{out} - T_{j,k=1}) \end{aligned} \right\} \text{monotonic decrease in Temperature}$$

$$\left. \begin{aligned} \Delta T_{ijk} &\geq \Delta T_{min}, \Delta T_{cui} \geq \Delta T_{min}, \Delta T_{huj} \geq \Delta T_{min} \\ q_{ijk} &\leq \Omega_{ij} z_{ijk}, q_{cui} \leq \Omega_{cui} z_{cui}, q_{huj} \leq \Omega_{huj} z_{huj} \end{aligned} \right\} \text{utility heat loads}$$

$$\left. \begin{aligned} \Delta T_{ijk} &\leq T_{ik} - T_{jk} + \Gamma_{ij} (1 - z_{ijk}) \\ \Delta T_{ij,k+1} &\leq T_{i,k+1} - T_{j,k+1} + \Gamma_{ij} (1 - z_{ijk}) \\ \Delta T_{cui1} &\leq T_{i,k=NOK} - T_{cui}^{out} + \Gamma_{cui} (1 - z_{cui}) \\ \Delta T_{cui2} &\leq T_i^{out} - T_{cui}^{in} + \Gamma_{cui} (1 - z_{cui}) \\ \Delta T_{huj1} &\leq T_{hu}^{out} - T_{j,k=1} + \Gamma_{huj} (1 - z_{huj}) \\ \Delta T_{huj2} &\leq T_{hu}^{in} - T_j^{out} + \Gamma_{huj} (1 - z_{huj}) \end{aligned} \right\} \text{lower bounds for temperature differences}$$

$$\left. \begin{aligned} LMTD_{ijk} &= \frac{\Delta T_{ijk} - \Delta T_{ij,k+1}}{\ln \frac{\Delta T_{ijk}}{\Delta T_{ij,k+1}}} \\ LMTD_{cui} &= \frac{\Delta T_{cui1} - \Delta T_{cui2}}{\ln \frac{\Delta T_{cui1}}{\Delta T_{cui2}}} \\ LMTD_{huj} &= \frac{\Delta T_{huj1} - \Delta T_{huj2}}{\ln \frac{\Delta T_{huj1}}{\Delta T_{huj2}}} \end{aligned} \right\} \text{upper bounds for heat loads}$$

$$\left. \begin{aligned} LMTD_{ijk} &= \frac{\Delta T_{ijk} - \Delta T_{ij,k+1}}{\ln \frac{\Delta T_{ijk}}{\Delta T_{ij,k+1}}} \\ LMTD_{cui} &= \frac{\Delta T_{cui1} - \Delta T_{cui2}}{\ln \frac{\Delta T_{cui1}}{\Delta T_{cui2}}} \\ LMTD_{huj} &= \frac{\Delta T_{huj1} - \Delta T_{huj2}}{\ln \frac{\Delta T_{huj1}}{\Delta T_{huj2}}} \end{aligned} \right\} \text{upper bounds temperature differences}$$

$$\left. \begin{aligned} T_i^{out} &\leq T_{ik} \leq T_i^{in}, T_j^{in} \leq T_{jk} \leq T_j^{out} \\ q_{ijk}, q_{cui}, q_{huj} &\geq 0 \\ z_{ijk}, z_{cui}, z_{huj} &\in [0, 1] \end{aligned} \right\} \text{definition of LMTD for process-process heat exchangers}$$

$$\left. \begin{aligned} T_i^{out} &\leq T_{ik} \leq T_i^{in}, T_j^{in} \leq T_{jk} \leq T_j^{out} \\ q_{ijk}, q_{cui}, q_{huj} &\geq 0 \\ z_{ijk}, z_{cui}, z_{huj} &\in [0, 1] \end{aligned} \right\} \text{definition of LMTD for utility heat exchangers}$$

$$\left. \begin{aligned} T_i^{out} &\leq T_{ik} \leq T_i^{in}, T_j^{in} \leq T_{jk} \leq T_j^{out} \\ q_{ijk}, q_{cui}, q_{huj} &\geq 0 \\ z_{ijk}, z_{cui}, z_{huj} &\in [0, 1] \end{aligned} \right\} \text{upper temperature bounds}$$

$$\left. \begin{aligned} q_{ijk}, q_{cui}, q_{huj} &\geq 0 \\ z_{ijk}, z_{cui}, z_{huj} &\in [0, 1] \end{aligned} \right\} \text{non-negativity constraints}$$

$$\left. \begin{aligned} z_{ijk}, z_{cui}, z_{huj} &\in [0, 1] \end{aligned} \right\} \text{integrality constraints}$$

References

- Ahmad, S., Linnhoff, B., Smith, R., 1990. Cost optimum heat exchanger networks—2. targets and design for detailed capital cost models. *Comput. Chem. Eng.* 14 (7), 751–767.
- Anantharaman, R., Nastad, I., Nygreen, B., Gundersen, T., 2010. The sequential framework for heat exchanger network synthesis—the minimum number of units sub-problem. *Comput. Chem. Eng.* 34 (11), 1822–1830. doi:10.1016/j.compchemeng.2009.12.002.
- Bergamini, M.L., Scenna, N.J., Aguirre, P.A., 2007. Global optimal structures of heat exchanger networks by piecewise relaxation. *Ind. Eng. Chem. Res.* 46 (6), 1752–1763. doi:10.1021/ie061288p.
- Björk, K.-M., Nordman, R., 2005. Solving large-scale retrofit heat exchanger network synthesis problems with mathematical optimization methods. *Chem. Eng. Process.* 44 (8), 869–876. doi:10.1016/j.ccep.2004.09.005.
- Björk, K.-M., Westerlund, T., 2002. Global optimization of heat exchanger network synthesis problems with and without the isothermal mixing assumption. *Comput. Chem. Eng.* 26 (11), 1581–1593. doi:10.1016/S0098-1354(02)00129-1.
- Bogataj, M., Kravanja, Z., 2012. An alternative strategy for global optimization of heat exchanger networks. *Appl. Therm. Eng.* 43, 75–90. doi:10.1016/j.applthermaleng.2011.12.015.
- Chen, J., 1987. Comments on improvements on a replacement for the logarithmic mean. *Chem. Eng. Sci.* 42 (10), 2488–2489. doi:10.1016/0009-2509(87)80128-8.
- Ciric, A.R., Floudas, C.A., 1991. Heat exchanger network synthesis without decomposition. *Comput. Chem. Eng.* 15 (6), 385–396. doi:10.1016/0098-1354(91)87017-4.
- Czyzyk, J., Mesnier, M.P., Moré, J.J., 1998. The NEOS server. *IEEE J. Comput. Sci. Eng.* 5 (3), 68–75.
- Dolan, E.D., 2001. The NEOS Server 4.0 Administrative Guide. Technical Memorandum ANL/MCS-TM-250. Mathematics and Computer Science Division, Argonne National Laboratory.
- Furman, K.C., Sahinidis, N.V., 2001. Computational complexity of heat exchanger network synthesis. *Comput. Chem. Eng.* 25 (9–10), 1371–1390. doi:10.1016/S0098-1354(01)00681-0.
- Gropp, W., Moré, J.J., 1997. Optimization environments and the NEOS server. In: Buhman, M.D., Iserles, A. (Eds.), *Approximation Theory and Optimization*. Cambridge University Press, pp. 167–182.
- Gundersen, T., 2013. Targets and heat exchanger network design. In: Klimes, J.J. (Ed.), *Handbook of Process Integration (PI)*. Woodhead Publishing Ltd., Oxford, pp. 129–167. Ch. 4.
- Huo, Z., Zhao, L., Yin, H., Ye, J., 2012. A hybrid optimization strategy for simultaneous synthesis of heat exchanger network. *Korean J. Chem. Eng.* 29 (10), 1298–1309. doi:10.1007/s11814-012-0007-2.
- Isafiade, A.J., Short, M., 2016. Simultaneous synthesis of flexible heat exchanger networks for unequal multi-period operations. *Process Saf. Environ. Prot.* 103, 377–390. doi:10.1016/j.psep.2016.04.021.
- Lin, B., Miller, D.C., 2004. Solving heat exchanger network synthesis problems with tabu search. *Comput. Chem. Eng.* 28 (8), 1451–1464. doi:10.1016/j.compchemeng.2003.10.004.
- Linnhoff, B., 1994. A User Guide on Process Integration for the Efficient Use of Energy, Rev. 1st ed. Institution of Chemical Engineers, Rugby.
- Linnhoff, B., Flower, J.R., 1978. Synthesis of heat exchanger networks: II. Evolutionary generation of networks with various criteria of optimality. *AIChE J.* 24 (4), 642–654. doi:10.1002/aic.690240412.
- Ma, X., Yao, P., Luo, X., Roetzel, W., 2008. Synthesis of multi-stream heat exchanger network for multi-period operation with genetic/simulated annealing algorithms. *Appl. Therm. Eng.* 28 (8–9), 809–823. doi:10.1016/j.applthermaleng.2007.07.015.
- Puranik, Y., Sahinidis, N.V., 2017. Domain reduction techniques for global NLP and MINLP optimization. *Constraints* 22 (3), 338–376. doi:10.1007/s10601-016-9267-5.
- Saboo, A., Morari, M., Colberg, R., 1986. RESHEX: an interactive software package for the synthesis and analysis of resilient heat-exchanger networks—II: discussion of area targeting and network synthesis algorithms. *Comput. Chem. Eng.* 10 (6), 591–599.
- Sahinidis, N. V., 2014. BARON 14.3.1: Global Optimization of Mixed-Integer Nonlinear Programs, User's Manual.
- Soršak, A., Kravanja, Z., 2002. Simultaneous MINLP synthesis of heat exchanger networks comprising different exchanger types. *Comput. Chem. Eng.* 26 (4–5), 599–615. doi:10.1016/S0098-1354(01)00779-7.
- Tawarmalani, M., Sahinidis, N.V., 2005. A polyhedral branch-and-cut approach to global optimization. *Math. Program.* 103, 225–249.
- Umeda, T., Harada, T., Shiroko, K., 1979. A thermodynamic approach to the synthesis of heat integration systems in chemical processes. *Comput. Chem. Eng.* 3 (1–4), 273–282. doi:10.1016/0098-1354(79)80046-0.
- Yee, T.F., Grossmann, I.E., 1990. Simultaneous optimization models for heat integration—II. Heat exchanger network synthesis. *Comput. Chem. Eng.* 14 (10), 1165–1184.
- Yerramsetty, K.M., Murty, C., 2008. Synthesis of cost-optimal heat exchanger networks using differential evolution. *Comput. Chem. Eng.* 32 (8), 1861–1876. doi:10.1016/j.compchemeng.2007.10.005.
- Zamora, J.M., Grossmann, I.E., 1998. A global MINLP optimization algorithm for the synthesis of heat exchanger networks with no stream splits. *Comput. Chem. Eng.* 22 (3), 367–384. doi:10.1016/S0098-1354(96)00346-8.
- Zhang, W.V.N., 2006. Design of flexible heat exchanger network for multi-period operation. *Chem. Eng. Sci.* 61 (23), 7730–7753. doi:10.1016/j.ces.2006.08.043.
- Zhu, X.X., 1997. Automated design method for heat exchanger network using block decomposition and heuristic rules. *Comput. Chem. Eng.* 21 (10), 1095–1104. doi:10.1016/S0098-1354(96)00320-1.

5.3 Paper 3

Full paper conference contribution in
Proceedings of the 12th Conference on Sustainable Development of Energy, Water and Environment Systems

Tightening of MINLP Superstructure Relaxation for Faster Solution of Heat Exchanger Network Synthesis Problems

Anton Beck
Center for Energy
Austrian Institute of Technology, Vienna, Austria
e-mail: anton.beck@ait.ac.at

René Hofmann*
Institute of Thermodynamics and Energy Systems
Technische Universität Wien, Vienna, Austria
e-mail: rene.hofmann@tuwien.ac.at

ABSTRACT

Heat exchanger network synthesis is a major topic when it comes to heat integration in industrial processes. Mixed Integer Nonlinear Programming (MINLP) superstructures in various forms have been used for decades to find cost optimal heat exchanger networks. The algorithms used for optimization of MINLP problems solve Mixed Integer Linear Programming (MILP) and Nonlinear Programming (NLP) sub-problems iteratively. If these sub-problems are tightened, which means that the solution space is reduced but still includes all physically feasible solutions, the algorithm can potentially go through the solution space faster as branches can be excluded from the set of potentially optimal solutions earlier.

In this work, the impact of additional inequality constraints was investigated. Comparison with the standard formulation used in most of literature shows that the tighter formulations yield solutions faster and a lower duality gap if the test cases cannot be solved to optimality. Also, a linearized model is proposed and tightening measures are tested.

KEYWORDS

mathematical programming, heat integration, heat exchanger networks, optimization

INTRODUCTION

Different superstructure formulations were proposed in the early 90s that first allowed simultaneous consideration of the number of heat exchangers (HEX) involved, their respective HEX area requirements and costs for utilities [1,2]. The simultaneous heat exchanger network synthesis problem (HENS) is one of many NP-hard¹ MINLP problems [3]. Especially global optima are hard to find even for small problems and with state of the art solvers available [4]. Specialized algorithms for the solution of simultaneous HENS problems have been proposed that incorporate specific properties of the problem to push the limits of problem size for which global optima can be obtained. Zamora and Grossmann [5] presented an outer approximation branch and bound algorithm that uses convex underrelaxations to solve the non-convex MINLP superstructure proposed by Yee and Grossmann [1] to global optimality with the restriction that no stream splits are allowed. Björk and Westerlund [6] presented a global optimization procedure for the same superstructure formulation that allows for stream splits and non-

* Corresponding author

¹ NP-hard ("Non-deterministic Polynomial acceptable problems"-hard) problems are characterized as being at least as hard as the NP-complete problems. [3]

isothermal mixing. Bergamini et al. [7] developed a methodology for global optimization based on outer approximation methods and physical insights. They constructed two lower bounding convex MINLP problems including piecewise underestimators of the nonconvex terms which provide solutions used to initialize a reduced NLP problem. Bogataj and Kravanja [8] proposed an approach for obtaining globally optimal solutions to the simultaneous HENS problem which uses an aggregated substructure to reduce the number of nonconvex terms, which need to be convexified in order to derive a convex underestimating problem.

Tightening of the relaxed sub-problems that need to be solved during the optimization process potentially helps the solver as infeasible branches or branches that yield no improvement on the current objective value can be excluded from the search space more quickly. Bergamini et al. [7] incorporated linear inequality constraints that form a lower bound for the total HEX area, stream-wise HEX areas and total number of HEX units in their global optimization methodology. Anantharaman et al. [9] used physically feasible upper bounds for the maximum transferrable heat of individual stream pairs. They also derived lower bounds for stream-wise HEX matches within a MILP transshipment model for the identification of the overall minimum number of HEX. In the case that no specialized algorithms are available global general-purpose solvers can be used to solve HENS problems.

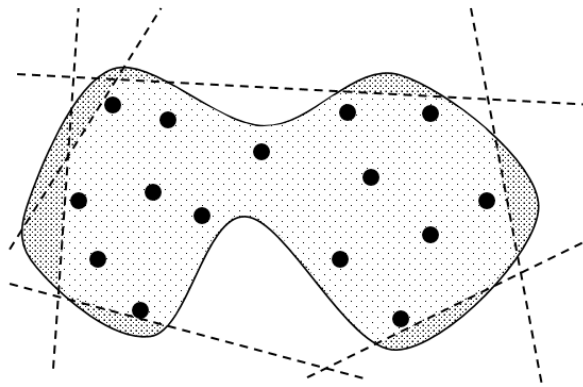


Figure 1: Schematic illustration of the reduced nonlinear nonconvex solution space. Black dots represent feasible integer solutions. Dashed lines are additional linear inequality constraints.

Analysis of the MINLP superstructure formulation proposed by Yee and Grossmann [1] yields potentials for tightening of existing constraints and introduction of additional inequality constraints that tighten the relaxations involved in the solution process. These tightening measures are introduced to the superstructure model prior to optimization and thus can be used with any global MINLP solver. A schematic illustration of the solution space of the tightened problem is shown in Figure 1. The model modifications are tested with various case-studies and the impact of these measures is analysed. Also, a linearized version of the MINLP superstructure is investigated in combination with the proposed tightening measures.

TIGHTENING OF THE MODEL

Tightening measures proposed in this paper are based on the MINLP superstructure formulation by Yee and Grossmann [1]. The objective of this formulation is to minimize the total annual costs (TAC) which consist of annualized investment costs and energy costs (Eq. (1)).

$$\begin{aligned} \min TAC = & \sum_i c_{cui} q_{cui} + \sum_j c_{hu} q_{huj} + \sum_i \sum_j \sum_k c_f z_{ijk} + \sum_i c_f z_{cui} + \sum_j c_f z_{huj} + \\ & \sum_i \sum_j \sum_k c \left(\frac{q_{ijk}}{U_{ij} LMTD_{ijk}} \right)^\beta + \sum_i c \left(\frac{q_{cui}}{U_{cui} LMTD_{cui}} \right)^\beta + \sum_j c \left(\frac{q_{huj}}{U_{huj} LMTD_{huj}} \right)^\beta \end{aligned} \quad (1)$$

$$\begin{aligned} & \underbrace{\sum_i \sum_j \sum_k c \left(\frac{q_{ijk}}{U_{ij} LMTD_{ijk}} \right)^\beta}_{A_{red,ijk}=A_{ijk}^\beta} + \underbrace{\sum_i c \left(\frac{q_{cui}}{U_{cui} LMTD_{cui}} \right)^\beta}_{A_{red,cui}=A_{cui}^\beta} + \underbrace{\sum_j c \left(\frac{q_{huj}}{U_{huj} LMTD_{huj}} \right)^\beta}_{A_{red,huj}=A_{huj}^\beta} \end{aligned}$$

In Eq. (1) q_{ijk} , q_{cui} and q_{huj} are the heat flows between process streams and utility heat loads, U_{ij} , U_{cui} and U_{huj} are heat transfer coefficients, $LMTD_{ijk}$, $LMTD_{cui}$ and $LMTD_{huj}$ are the logarithmic mean temperature differences within each potential HEX, c_{cui} and c_{hu} are the cost coefficients for utility consumption, c_f and c are cost coefficients for step-fixed and variable investment costs and β is the cost exponent for HEX areas. The model consists of energy balances for each process stream

$$\sum_j \sum_k q_{ijk} + q_{cui} = F_i (T_i^{in} - T_i^{out}), \quad i \in HP \quad (2)$$

$$\sum_i \sum_k q_{ijk} + q_{huj} = F_j (T_j^{out} - T_j^{in}), \quad j \in CP \quad (3)$$

where F_i and F_j are the specific heat flows, T_i^{in} and T_j^{in} are the inlet temperatures and T_i^{out} and T_j^{out} are the outlet temperatures of the hot and cold streams. Also, energy balances are calculated for each temperature stage k with the temperature nodes t_{ik} and t_{jk}

$$\sum_i q_{ijk} = F_i (t_{ik} - t_{i,k+1}), \quad i \in HP \quad (4)$$

$$\sum_j q_{ijk} = F_j (t_{jk} - t_{j,k+1}), \quad j \in CP \quad (5)$$

Inlet temperatures are assigned to the temperature nodes $t_{i,k=1}$ and $t_{j,k=NOK}$ by

$$t_{i,k=1} = T_i^{in}, \quad t_{j,k=NOK} = T_j^{in}. \quad (6)$$

Monotonic decrease in temperature is assured by

$$t_{ik} \geq t_{i,k+1}, \quad t_{jk} \geq t_{j,k+1} \quad (7)$$

and

$$t_{i,k=NOK+1} \geq T_i^{out}, \quad t_{j,k=1} \geq T_j^{out}. \quad (8)$$

Utility heat loads q_{cui} and q_{huj} are calculated by

$$q_{cui} = F_i (t_{i,k=NOK+1} - T_i^{out}), \quad q_{huj} = F_j (T_j^{out} - t_{j,k=1}). \quad (9)$$

Variable bounds are set by

$$dt_{ijk} \geq dTmin, \quad dt_{cui} \geq dTmin, \quad dt_{huj} \geq dTmin \quad (10)$$

$$T_i^{out} \leq t_{ik} \leq T_i^{in}, \quad T_j^{in} \leq t_{jk} \leq T_j^{out} \quad (11)$$

$$q_{ijk}, q_{cui}, q_{huj} \geq 0. \quad (12)$$

In order to ensure physically feasible heat transfer logical constraints involving the binary variables z_{ijk} , z_{cui} and z_{huj} are used (Eq. (13)).

$$z_{ijk}, z_{cui}, z_{huj} \in 0,1 \quad (13)$$

The logical constraints for the transferred energy q_{ijk} , q_{cui} and q_{huj} for each HEX match are stated as

$$q_{ijk} \leq \Omega_{ij} z_{ijk}, \quad q_{cui} \leq \Omega_{cui} z_{cui}, \quad q_{huj} \leq \Omega_{huj} z_{huj}. \quad (14)$$

In this equation Ω_{ij} is an upper bound that is used to keep the transferred heat q_{ijk} in bounds and to make sure that for $z_{ijk} = 0$ no heat is transferred. The binary variables z_{ijk} represent the existence of the HEX. The parameter Ω_{ij} is set to the minimum of the heat requirements of the streams involved in the match as stated in Eq. (15),

$$\Omega_{ij} = \min\{F_i(T_i^{in} - T_i^{out}), F_j(T_j^{out} - T_j^{in})\}. \quad (15)$$

The values for Ω_{cui} and Ω_{huj} are set to the heat content of the hot and cold streams respectively. To ensure that the variables representing the temperature differences dt_{ijk} and $dt_{ij,k+1}$ can have positive values even in the case where the cold stream is hotter than the hot stream ($t_{jk} > t_{ik}$) and the temperature differences in stage k really are negative and thus no feasible heat transfer from the hot stream to the cold stream can take place the inequality constraints Eq. (16) and Eq. (17) are used.

$$dt_{ijk} \leq t_{ik} - t_{jk} + \Gamma_{ij} (1 - z_{ijk}) \quad (16)$$

$$dt_{ij,k+1} \leq t_{i,k+1} - t_{j,k+1} + \Gamma_{ij} (1 - z_{ijk}) \quad (17)$$

Γ_{ij} is a sufficiently large positive real number that ensures that dt_{ijk} and $dt_{ij,k+1}$ are greater than their lower bound $dTmin$ (Eq. (10)) in the case that z_{ijk} is zero. Vice versa z_{ijk} is forced to zero if no feasible heat transfer is possible due to negative real temperature differences. The parameter Γ_{ij} is usually calculated by

$$\Gamma_{ij} = \max\{T_j^{out} - T_j^{in} + dTmin, 0\}. \quad (18)$$

Similarly, logical constraints are used to ensure that the temperature differences in the potential utility exchangers are greater than $dTmin$.

$$dt_{cui1} \leq t_{i,k=NOK} - t_{cu}^{out} + \Gamma_{cui} (1 - z_{cui}) \quad (19)$$

$$dt_{cui2} \leq T_i^{out} - t_{cu}^{in} + \Gamma_{cui} (1 - z_{cui}) \quad (20)$$

$$dt_{huj1} \leq t_{hu}^{out} - t_{j,k=1} + \Gamma_{huj} (1 - z_{huj}) \quad (21)$$

$$dt_{huj2} \leq t_{hu}^{in} - T_j^{out} + \Gamma_{huj} (1 - z_{huj}) \quad (22)$$

For the calculation of the logarithmic temperature differences the approximation proposed by Chen [10] is used.

$$LMTD_{ijk} = \left(dt_{ijk} dt_{ij,k+1} \frac{dt_{ijk} + dt_{ij,k+1}}{2} \right)^{\frac{1}{3}}, \quad (23)$$

$$LMTD_{cui} = \left(dt_{cui1} dt_{cui2} \frac{dt_{cui1} + dt_{cui2}}{2} \right)^{\frac{1}{3}}, \quad (24)$$

$$LMTD_{cui} = \left(dt_{huj1} dt_{huj2} \frac{dt_{huj1} + dt_{huj2}}{2} \right)^{\frac{1}{3}} \quad (25)$$

TIGHTER MODEL CONSTRAINTS

Parameters Ω and Γ have a lower limit to where the physically feasible solution space of the model is not restricted. The lower limit for Ω_{ij} for process-to-process heat exchange is obtained by calculating the maximum transferable heat between each stream pair q_{jik}^{max} . This can be done by performing pinch analysis on each stream pair. If the stream pair forms a threshold problem (reduction of the approach temperature doesn't decrease possible heat transfer between the process streams) the minimum value of the heat flow of both process streams is the maximum transferable heat between the two process streams (Eq. (15)).

In order to tighten the constraints for feasible temperature differences as much as possible additional Γ values can be calculated for the stages $k = 1$ and $k = NOK$. This results in three values for Γ for each potential stream match. The lower limit for Γ_{ijk} depends on the stage k and on whether the temperature difference at the hot or cold side of the HEX is calculated.

- $k = 1$, hot side of HEX: As the inlet temperature of the hot stream corresponds to the inlet temperature into the HEX in stage 1 $\Gamma_{ij,k=1}^{hot}$ is the maximum negative temperature difference between hot and cold stream plus $dTmin$

$$\Gamma_{ij,k=1}^{hot} = \max \{ T_j^{out} - T_i^{in} + dTmin, 0 \} \quad (26)$$

- $k = NOK$, cold side of HEX: Similarly, as the inlet temperature of the cold stream is known the maximum negative temperature difference between hot and cold stream plus $dTmin$ is

$$\Gamma_{ij,k=NOK+1}^{cold} = \max \{ T_j^{in} - T_i^{out} + dTmin, 0 \} \quad (27)$$

- In all other cases ($k \neq 1, NOK + 1$), only the upper and lower limits are known

$$\Gamma_{ijk} = \max \{ T_j^{out} - T_j^{out} + dTmin, 0 \} \quad (28)$$

UPPER BOUNDS FOR HEAT RECOVERY

A rigorous upper bound for possible heat recovery q_{rec}^{max} (Eq. (29)) can be derived from pinch analysis as no more internal heat recovery is possible than the energy target at $dTmin$ [11].

$$\sum_i \sum_j \sum_k q_{ijk} \leq q_{rec}^{max} \quad (29)$$

The upper bounds for heat transfer for the smallest possible subsystems consisting of only one hot and one cold stream $q_{rec,ij}^{max}$ are equivalent to the tightest possible bounds for pair-wise maximum heat transfer Ω_{ij} .

$$\sum_k q_{ijk} \leq q_{rec,ij}^{max} = \Omega_{ij} \quad (30)$$

LINEAR CONSTRAINTS FOR TEMPERATURE DIFFERENCES

Within the relaxed problem, the upper bound for the transferred heat q_{ijk} scales linearly with the binary variable z_{ijk} as can be seen in Eq. (14). In addition, the upper limit for the temperature differences dt_{ijk} and $dt_{ij,k+1}$ increases linearly as z_{ijk} decrease (Eqs. (16,17)) so that the upper limit for $LMTD_{ijk}$ also increases, leading to smaller HEX areas within the Linear Programming (LP) relaxed problem. Introducing new constraints that limit dt_{ijk} and $dt_{ij,k+1}$ can tighten this formulation. For these constraints to be viable additional variables must be introduced. Instead of $NOK + 1$ temperature nodes for each stream $2NOK$ nodes are needed to ensure correct temperature differences. These additional constraints are stated as

$$dt_{ij,2k-1} \leq dTmin + (\Gamma_{2,ij} - dTmin) z_{ijk}, \quad (31)$$

$$dt_{ij,2k} \leq dTmin + (\Gamma_{2,ij} - dTmin) z_{ijk}, \quad (32)$$

$$\Gamma_{2,ij} = \min\{T_i^{in} - T_j^{in}, 0\}. \quad (33)$$

The Eqs. (34-35) lower the upper limit for the temperature differences for each potential HEX if z_{ijk} decreases. This way the objective values within the LP relaxed problem are increased and thus the formulation is tightened.

Analysis of the pair-wise maximum temperature differences in dependence of the transferred heat can be used to reduce the upper limit for possible temperature differences as the transferred heat increases. The functions for the upper limit for temperature differences $dt_{ij,1}^{max}$ and $dt_{ij,2NOK}^{max}$ are

$$dt_{ij,1}^{max} = (T_i^{in} - T_j^{in}) - \frac{\sum_k q_{ijk}}{F_j} \quad (34)$$

and

$$dt_{ij,2NOK}^{max} = (T_i^{in} - T_j^{in}) - \frac{\sum_k q_{ijk}}{F_i}. \quad (35)$$

In the first stage $k = 1$ at the hot side of the exchanger the upper bound is $dt_{ij,1}^{max}$.

$$dt_{ij,1} \leq dt_{ij,1}^{max} \quad (36)$$

An upper bound for the temperature difference $dt_{ij,2NOK}$ in the last stage $k = NOK$ is $dt_{ij,2NOK}^{max}$.

$$dt_{ij,2NOK} \leq dt_{ij,2NOK}^{max} \quad (37)$$

For the intermediate stages $1 < K < NOK$ the temperature difference dt can be constrained by

$$dt_{ij,2K} \leq dt_{ij,1}^{max} - \left(\frac{1}{F_i} - \frac{1}{F_j}\right) \sum_{k \leq K} q_{ijk} \quad (38)$$

and

$$dt_{ij,2(K+1)-1} \leq dt_{ij,1}^{max} - \left(\frac{1}{F_i} - \frac{1}{F_j}\right) \sum_{k \leq K} q_{ijk}. \quad (39)$$

LINEARIZED MODEL

To test the different sets of additional constraints within a strictly linear model, a linearized version of the MINLP superstructure formulation was generated. In this model an inner approximation of $LMTD$ is used with a maximum relative difference of 1%. This relative difference can be arbitrarily low but an increasing number of linear inequality constraints is needed with decreasing maximum relative difference. The reduced HEX area $A_{red,ijk}$ (Eq. (1)) which considers the cost exponent β and the HEX area A for every possible match directly is approximated by multiple linear constraints using a least-squares fit. The domain for which this approximation is carried out is defined by

$$0.2 q_{rec,ij}^{max} \leq q_{ijk} \leq q_{rec,ij}^{max} \quad (40)$$

and

$$dTmin \leq LMTD_{ijk} \leq \Gamma_{2,ij} \quad (41)$$

The domain is further reduced as both the minimum and maximum feasible values for $LMTD_{ijk}$ are functions of the transferred heat q_{ijk} and thus data points lying outside of the feasible range are excluded from the approximation. The restriction of the approximation domain of $0.2 q_{rec,ij}^{max} \leq q_{ijk}$ leads to overestimation of the HEX area with HEX that transfer only small amounts of their potential heat transfer. The binary variables z_{ijk} that determine whether the HEX exists are used to switch on/off the constraints, allowing the HEX area to be zero if no HEX exists. To ensure physical feasibility of the solution a NLP stage is solved that is initialised with the solution of the linear superstructure model. No changes in the network structure are possible.

CASE-STUDIES

Six case-studies taken from literature are used to evaluate the proposed tightening measures. The case-studies increase in size ranging from 4 to 39 process streams. Case-studies 1, 3, 5 and 6 were also used by Escobar et al. [12] for a case-study comparison. Case-study 1 is adapted from the work of Gundersen [13] who used this example for HENS using pinch-methodology. Björk et al. [6,14] presented the case-studies 3 and 6 for their approaches for HENS of large-scale problems. Case-study 5 was first presented by Sorsak and Kravanja [15] who used different types of HEX within HENS. The case-studies 2 and 4 are adapted from multi-period HENS problems presented by Zhang and Verheyen [16] and Ma et al. [17]. The stream data for case-study 2 was presented by Isafiade et al. [18] who proposed a single representative operation period for the multi-period case-study of Zhang and Verheyen [16].

RESULTS

In this section measures that tightening the model are evaluated for the MINLP superstructure and the linearized model. The MINLP models were solved using BARON [19,20] (CPLEX is used as MILP solver and CONOPT is used to solve the NLP sub-problem). The linearized model was solved with CPLEX. All solvers were used with their default settings.

For each case-study two sets of tightening constraints and modifications were compared to the formulation without any tightening measures:

- Original Formulation: Here, the standard constraints and parameters from the original superstructure formulation (Eq. (1-25)) are used.

- Measure 1: The parameters Ω and Γ used within the constraints of the original formulation are adjusted (Eqs. (26-28)). Also, constraints for maximum transferrable heat for the total process (Eq. (29)) and for each stream pair (Eq. (30)) are added.
- Measure 2: Additional constraints for temperature differences are added (Eqs. (31-39)) and additional variables for temperature differences are added accordingly.

All optimization runs were performed on the NEOS server cluster [21–23] except case study 1 and 3 which were performed on an Intel Core i7-6700HQ with 8GB RAM due to problems related to the node files generated by CPLEX. Each optimization problem was run three times. The best solutions and lowest computational times are presented in

Table 1. The best values obtained for each case study are displayed in bold font. The time limit was set to 7200 seconds and the stopping criteria for relative and absolute duality gap was set to zero.

Table 1: Case-study results

case-study	Measure	TAC		time (s)		gap (%)	
		MINLP	MILP+NLP	MINLP	MILP	MINLP	MILP
1*	orig.	360,822	366,240	5945.16	0.11	0.00	0.00
	1	360,822	366,240	3097.20	0.06	0.00	0.00
	2	360,822	366,240	880.82	0.06	0.00	0.00
2	orig.	6,338,159	6,336,493	limit	0.30	0.23	0.00
	1	6,336,493	6,336,493	limit	0.58	0.26	0.00
	2	6,336,493	6,336,493	limit	0.46	0.24	0.00
3*	orig.	1,548,012	1,518,883	limit	949.47	0.59	0.00
	1	1,525,116	1,513,731	limit	limit	0.38	0.24
	2	1,527,334	1,513,731	limit	limit	0.37	0.19
4	orig.	463,779	444,487	limit	970.15	0.60	0.00
	1	461,344	444,487	limit	1533.44	0.59	0.00
	2	459,601	444,487	limit	359.77	0.58	0.00
5	orig.	1,328,558	1,316,524	limit	285.79	0.53	0.00
	1	1,320,655	1,316,524	limit	317.85	0.41	0.00
	2	1,315,822	1,312,524	limit	70.03	0.38	0.00
6	orig.	NA	2,062,211	limit	limit	NA	0.70
	1	2,207,221	2,003,360	limit	limit	0.74	0.63
	2	2,165,364	1,983,349	limit	limit	0.73	0.49

*solved on an Intel Core i7-6700HQ with 8GB RAM

The value for TAC obtained after 7200 seconds was equal or lower with the proposed tightening measures for all case-studies. The tightest formulation (measure 2) resulted in the lowest TAC except for case-study 3 where measure 1 resulted in the best objective value. Numerical issues have to be considered interpreting the presented results. Even though the linear model was solved to global optimality (duality gap equal to zero) slightly lower values for TAC were obtained when tighter formulations were used.

Comparison of the computation times needed to solve case-study 1 to global optimality shows that tighter formulations can have a significant impact. Using tightening measure 2 computation time could be reduced by about 85%. The other case-studies could not be solved to global optimality with the MINLP superstructure formulation.

The computation times for the linearized model show that tighter models are not necessarily solved faster. Measure 1 does not have a positive impact regarding computation time in most cases whereas measure 2 reduces computation time for the majority of case-studies.

After 7200 seconds the residual gap between best integer feasible solution found by the solver and theoretical best solution tends to improve for both measure 2 and 3 with slightly lower values for measure 3. Using the linearized superstructure model only case-study 3 with tightening measures and case-study 6 could not be solved to optimality within the time limit. For these cases the same tendency as for the MINLP model can be observed that tighter formulations lower the residual gap.

CONCLUSION

With the proposed tightened formulations of the MINLP model by Yee and Grossmann [1] a reduction of computation time for global optimization of a small scale HENS problem could be obtained. The impact of each tightening measure varies with each case-study and thus a general statement of which tightening measure is most suitable for an individual case-study is not possible without further investigations. For larger case-studies that could not be solved to global optimality tighter formulations showed to reduce the duality gap. Although the results presented in this paper suggest that the best objective value obtained after a given time is lower if the problem is tightened, this might not be true for all possible tightening measures. Investigations with further tightening measures will be carried out to analyze this.

NOMENCLATURE

Abbreviations

HEN	Heat Exchanger Network
HENS	Heat Exchanger Network Synthesis
HEX	Heat Exchanger
LP	Linear Programming
MILP	Mixed Integer Linear Programming
MINLP	Mixed Integer Nonlinear Programming
NLP	Nonlinear Programming
TAC	Total Annual Costs

Sets

CP	set of cold process streams
HP	set of hot process streams

Subscripts

cu	cold utility
hu	hot utility
i	hot stream, $i \in HP$
j	cold stream, $j \in CP$
k	temperature stage, $k=1, \dots, NOK$

Superscripts

cold	cold side of heat exchanger
hot	hot side of heat exchanger
in	inlet
max	maximum value
out	outlet

Variables

A	heat exchanger area	m^2
A_{red}	reduced heat exchanger area	$m^{2\beta}$

dt	temperature difference	°C
LMTD	logarithmic mean temperature difference	°C
q	heat flow	kW
t	temperature	°C
z	binary variable for existence of heat exchanger	-

Parameters

Γ	auxiliary parameter to ensure feasible temperature difference	°C
Γ_2	auxiliary parameter to limit temperature difference	°C
Ω	upper Limit for pairwise heat transfer	kW
dTmin	minimal temperature difference	°C
F	specific heat flow capacity	kW/K
NOK	number of temperature stages	-
T	temperature	°C

References

- 1 Yee TF, Grossmann IE. Simultaneous optimization models for heat integration-II. heat exchanger network synthesis. *Computers & Chemical Engineering* 1990;14(10):1165–84.
- 2 Ciric AR, Floudas CA. Heat exchanger network synthesis without decomposition. *Computers & Chemical Engineering* 1991;15(6):385–96.
- 3 Furman KC, Sahinidis NV. Computational complexity of heat exchanger network synthesis. *Computers & Chemical Engineering* 2001;25(9-10):1371–90.
- 4 Yerramsetty KM, Murty C. Synthesis of cost-optimal heat exchanger networks using differential evolution. *Computers & Chemical Engineering* 2008;32(8):1861–76.
- 5 Zamora JM, Grossmann IE. A global MINLP optimization algorithm for the synthesis of heat exchanger networks with no stream splits. *Computers & Chemical Engineering* 1998;22(3):367–84.
- 6 Björk K-M, Westerlund T. Global optimization of heat exchanger network synthesis problems with and without the isothermal mixing assumption. *Computers & Chemical Engineering* 2002;26(11):1581–93.
- 7 Bergamini ML, Scenna NJ, Aguirre PA. Global Optimal Structures of Heat Exchanger Networks by Piecewise Relaxation. *Ind. Eng. Chem. Res.* 2007;46(6):1752–63.
- 8 Bogataj M, Kravanja Z. An alternative strategy for global optimization of heat exchanger networks. *Applied Thermal Engineering* 2012;43:75–90.
- 9 Anantharaman R, Nastad I, Nygreen B, Gundersen T. The sequential framework for heat exchanger network synthesis—The minimum number of units sub-problem. *Computers & Chemical Engineering* 2010;34(11):1822–30.
- 10 Chen J. Comments on improvements on a replacement for the logarithmic mean. *Chemical Engineering Science* 1987;42(10):2488–9.
- 11 Umeda T, Harada T, Shiroko K. A thermodynamic approach to the synthesis of heat integration systems in chemical processes. *Computers & Chemical Engineering* 1979;3(1-4):273–82.
- 12 Escobar M, Trierweiler JO. Optimal heat exchanger network synthesis: A case study comparison. *Applied Thermal Engineering* 2013;51(1-2):801–26.
- 13 T. Gundersen. A Process Integration PRIMER. SINTEF Energy Research; 2000.
- 14 Björk K-M, Nordman R. Solving large-scale retrofit heat exchanger network synthesis problems with mathematical optimization methods. *Chemical Engineering and Processing: Process Intensification* 2005;44(8):869–76.

- 15 Soršak A, Kravanja Z. Simultaneous MINLP synthesis of heat exchanger networks comprising different exchanger types. *Computers & Chemical Engineering* 2002;26(4-5):599–615.
- 16 Zhang WVN. Design of flexible heat exchanger network for multi-period operation. *Chemical Engineering Science* 2006;61(23):7730–53.
- 17 Ma X, Yao P, Luo X, Roetzel W. Synthesis of multi-stream heat exchanger network for multi-period operation with genetic/simulated annealing algorithms. *Applied Thermal Engineering* 2008;28(8-9):809–23.
- 18 Isafiade AJ, Short M. Simultaneous synthesis of flexible heat exchanger networks for unequal multi-period operations. *Process Safety and Environmental Protection* 2016;103:377–90.
- 19 Sahinidis NV. BARON 14.3.1: Global Optimization of Mixed-Integer Nonlinear Programs, \em User’s Manual; 2014.
- 20 Tawarmalani M, Sahinidis NV. A polyhedral branch-and-cut approach to global optimization. *Mathematical Programming* 2005;103(2):225–49.
- 21 Gropp W, Moré JJ. Optimization Environments and the NEOS Server. In: Buhman MD, Iserles A, editors. *Approximation Theory and Optimization*. Cambridge University Press; 1997, p. 167–182.
- 22 Dolan ED. The NEOS Server 4.0 Administrative Guide. Technical Memorandum; 2001.
- 23 Czyzyk J, Mesnier MP, Moré JJ. The NEOS Server. *IEEE Journal on Computational Science and Engineering* 1998;5(3):68–75.

5.4 Paper 4

Full paper conference contribution in

Proceedings of the 28th European Symposium on Computer Aided Process Engineering

Anton Friedl, Jiří J. Klemeš, Stefan Radl, Petar S. Varbanov, Thomas Wallek (Eds.)
Proceedings of the 28th European Symposium on Computer Aided Process Engineering
June 10th to 13th, 2018, Graz, Austria. © 2018 Elsevier B.V. All rights reserved.
<https://doi.org/10.1016/B978-0-444-64235-6.50234-5>

Extensions for Multi-Period MINLP Superstructure Formulation for Integration of Thermal Energy Storages in Industrial Processes

Anton Beck^a and René Hofmann^{a,b,*}

^a*AIT Austrian Institute of Technology GmbH, Center for Energy, Sustainable Thermal Energy Systems, Giefinggasse 2, 1210 Wien, Austria*

^b*Technische Universität Wien, Institute for Energy Systems and Thermodynamics, Getreidemarkt 9/BA, 1060 Wien, Austria*
Rene.Hofmann@tuwien.ac.at

Abstract

In this paper, extensions to the MINLP superstructure formulation for multi-period heat exchanger network synthesis (HENS) proposed by Zhang (2006) which is based on the work by Yee and Grossmann (1990) are introduced. These modifications allow for simultaneous HENS including storage-subsystems with different characteristics. Besides stratified tanks and two-tank systems models for latent heat thermal storages (LHTS) and sensible storages are presented. Also, a sequential targeting procedure for the integration of storages is presented which combines insights from pinch analysis methods and a MINLP-formulation to calculate an approximation for optimal storage size and melting temperature. The results of the proposed integration procedure for thermal energy storages is demonstrated using a case study adapted from literature.

Keywords: Mathematical Programming, Heat Integration, Thermal Energy Storage, Latent Heat Thermal Storage, Pinch Analysis

1. Introduction

The synthesis of cost-efficient heat exchanger networks (HENS) has been a topic of scientific interest for several decades now. However, only little research has been done towards the combination with cost-efficient storage integration for multi-period plant operation. Anastasovski (2017) used Pinch Technology for the introduction of two-tank systems in HENS. Storage costs are obtained by variation of storage parameters and temperature differences. Chen and Ciou (2008) proposed a MINLP superstructure formulation for cost-efficient indirect heat recovery using thermal energy storage. A sequential design procedure for HENS with selection of an optimal utility system and storage integration was proposed by Mian et al. (2016). They tried to overcome the drawbacks of the sequential approach by applying the derivative-free hybrid algorithm PGS-COM by Martelli and Amaldi (2014). To our best knowledge, no work has been published on cost-optimal HENS combined with the integration of LHTS or sensible storages with fixed mass. A rigorous optimization procedure for the integration of thermal energy storages such as multi-tank systems but also LHTS might be a door opener for industrial application of these heat recovery systems. In this paper an extension to the simultaneous MINLP superstructure formulation for multi-period HENS proposed by Zhang (2006) is presented that allows for storage integration with different characteristics. For the integration of LHTS and sensible storages with fixed mass such as fluidized bed regenerators (FBR) a targeting stage is proposed to identify (sub)-optimal storage mass.

2. Storage Integration Algorithm

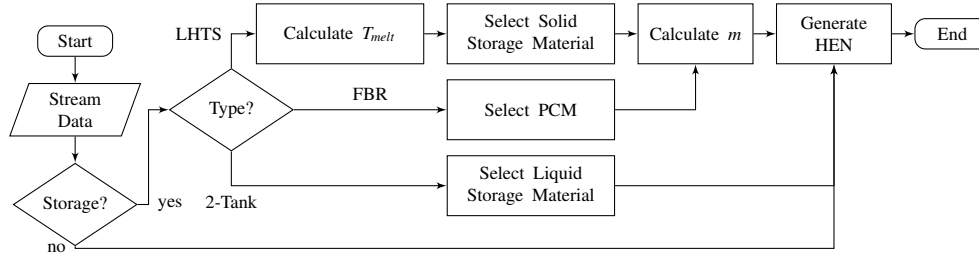


Figure 1: Flow chart for the storage integration algorithm

The combination of simultaneous HENS for multi-period problems and the integration of thermal energy storages leads to a highly complex optimization problem. To reduce problem complexity a storage integration algorithm is proposed which splits the selection of the storage type, storage material and storage mass and thus storage capacity into individual problems. These are treated sequentially according to Fig. 1. A MILP targeting formulation described in section 2.1 is used to calculate the phase change temperature T_{melt} for LHTS which is then used to manually select a suitable phase change material. Also, storage materials for the FBR and two-tank system are selected by the user. For storages with fixed storage mass and variable storage temperature (LHTS, FBR) the target formulation is then used to find the optimal storage size. Finally, the extended MINLP superstructure formulation for multi-period HENS and storage integration (section 2.3) is set up with the predefined storage parameters to find the cost-optimal mixed heat recovery system.

2.1. Storage Target

The targeting procedure for the integration of sensible and latent thermal energy storage with fixed storage mass is formulated as a MILP model which is based on modified Grand Composite Curves (mGCC) which are similar to the shifted Grand Composite Curves (GCC) proposed by Bandyopadhyay et al. (2010) for total site integration. These curves are obtained by removing the "pockets" from the GCC, splitting it at the pinch point and shifting the two new curves back by $\Delta T_{min}/2$. The mGCCs, just like the GCC, provide information at which temperature heating or cooling can be supplied to the process. Within the MILP model the mGCCs for every operation period are then formulated as piecewise linear functions using binary variables. The optimal trade-off between storage size and external utility is then found by variation of the storage size and solving the MILP formulation until no improvement of the objective value can be obtained. No individual process streams and no individual heat exchangers are considered which makes the problem relatively easy to solve.

2.2. Storage Models

In this work generic models for LHTS, FBR and two-tank or stratified tank systems are presented which can be used in both the targeting formulation and the extended superstructure. All storages are modelled as a mass points (uniform temperature in the storage), process streams are connected to the storages by an intermediate storage cycle (ISC) via heat exchangers (HEXs), the storage state is equal at the beginning and the end of the process duration and the storage temperature during each time interval is considered to be equal to the storage temperature at the end of each individual time interval. The model equations for the cumulated storage energy and the ISC are equal for all storage types. The cumulated energy for each operation period $Q_{cum,p}$ in the storages is calculated as

$$Q_{cum,P} = Q_{shift} + \sum_{p=1,\dots,P} \dot{Q}_{charge,p} \Delta t_p - \sum_{p=1,\dots,P} \dot{Q}_{discharge,p} \Delta t_p, \quad Q_{shift} \geq 0, \quad P = 1, \dots, NOP \quad (1)$$

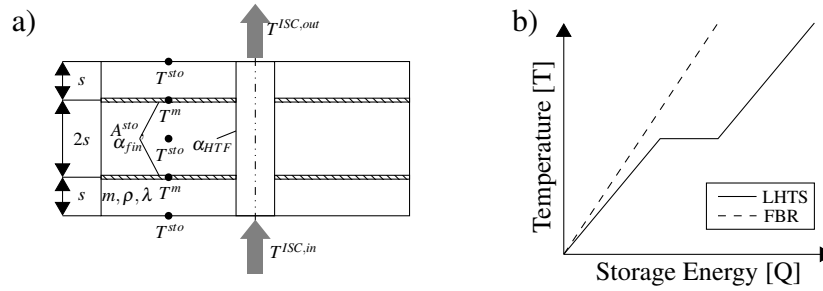


Figure 2: Schematic storage model and QT-characteristics for LHTS and FBR

where Q_{shift} is the storage load at the beginning of the storage cycle. $\dot{Q}_{charge,p}$ and $\dot{Q}_{discharge,p}$ are the charging and discharging loads of operation period p with the duration Δt_p . NOP is the number of operation periods. Simultaneous charging and discharging is not allowed and is prohibited by the constraints $z_{ikp}^{ISC} \leq 1 - y_p$ and $z_{jkp}^{ISC} \leq y_p$ where y_p are binaries that decide whether the storage is charged or discharged. The binary variables z_{ikp}^{ISC} and z_{jkp}^{ISC} determine whether the HEXs between the process streams (hot process stream i , cold process stream j) and the ISC are active in temperature stage k . For the two-tank model no HEX between the ISC and the storage vessels is needed as the heat transfer fluid (HTF) is stored directly. The lower and upper temperatures in the ISC correspond to the temperatures of the hot and cold storage tanks ($T_p^{ISC,hot} = T^{sto,hot}$, and $T_p^{ISC,cold} = T^{sto,cold}$). The minimum storage mass m is calculated by the nonlinear equation

$$Q_{cum}^{ub} - Q_{cum}^{lb} = (T^{sto,hot} - T^{sto,cold})cpm \quad (2)$$

where Q_{cum}^{ub} and Q_{cum}^{lb} are the maximum and minimum values of $Q_{cum,p}$. Opposed to two-tank systems in LHTS and FBR a HEX between the ISC and the storage is needed which is used for both charging and discharging. The necessary heat transfer area A^{sto} for this HEX is calculated by

$$A^{sto} \geq \frac{\sum_i \sum_k \dot{Q}_{ikp}^{ISC} + \sum_j \sum_k \dot{Q}_{jkp}^{ISC}}{U \Delta T_p^{sto}} \quad (3)$$

where \dot{Q}_{ikp}^{ISC} and \dot{Q}_{jkp}^{ISC} are the heat loads from the process streams to the ISC, ΔT_p^{sto} is the temperature difference between the storage fins T^m and the storage material T^{sto} , and U is the overall heat transfer coefficient in the storage HEX. ΔT_p^{sto} is calculated by

$$\Delta T_p^{sto} \leq T_p^{sto} - T_p^m + \Gamma y_p, \quad \Delta T_p^{sto} \leq T_p^m - T_p^{sto} + \Gamma (1 - y_p) \quad (4)$$

where Γ is a sufficiently large number used to activate and deactivate Eq. (4). The overall heat transfer coefficient U is derived from a simple model according to Fig. 2. The LHTS and FBR are modelled as shell and tube storages with radial fins that stretch out to the shell. It is assumed that the tube area is negligible compared to the fin area and thus all heat transfer is performed by the fins which are assumed to operate at the arithmetic mean of the HTF in- and outlet temperatures ($T^m = (T^{ISC,in} + T^{ISC,out})/2$). The characteristic length s for heat conduction is then calculated by $s = \frac{m}{A^{sto}\rho}$. The heat transfer coefficients from HTF to the fins α_{HTF} and from the fins to the storage medium α_{sto} are assumed to be infinite for the LHTS. This way the overall heat transfer coefficient is a function of the HEX area A^{sto} , the storage mass m , the thermal conductivity of the storage material λ and its density ρ . For the FBR model heat conduction is assumed to be negligible and a constant heat transfer coefficient between the fins and the storage material α_{sto} is assumed.

Table 1: Stream data and cost coefficients

	T _{in} (°C)	T _{out} (°C)	CP (kW/K)	Start (h)	End (h)
H1	170	50	3	0.3	0.8
H2	190	80	4	0.25	1
C1	100	160	8	0	0.5
C2	40	155	10	0.5	0.7
UT h	250	250	-	-	-
UT c	10	15	-	-	-

Exchanger cost = $1000+175[A(m^2)]^\beta \text{€y}^{-1}$, Storage cost (LHTS/FBR/2-tank) = $10,000/20,000/6,000[m(kg)/\rho(kg/m^3)]+50.7[A(m^2)]^\beta \text{€y}^{-1}$, $\beta = 0.6$, hot utility cost = $252 \text{€y}^{-1} \text{ kW}^{-1}$, cold utility cost = $22.68 \text{€y}^{-1} \text{ kW}^{-1}$, $dT_{min} = 5^\circ\text{C}$, years $y = 3$

Table 2: Storage material properties

	LHTS	FBR	2-tank
Material	Erythritol ^a	Quartz sand	Therm. oil
cp_s (kJ/kgK)	1.38	0.83	-
cp_l (kJ/kgK)	2.76	-	2
Δh (kJ/kg)	339.8	-	-
λ_s (W/mK)	0.733	-	-
λ_l (W/mK)	0.326	-	-
ρ (kg/m ³)	1390*	1300	1000
	(1480, 1300)		
T_{melt} (°C)	117.7	-	-

*average value, ^aF. Agyenim and I. Knight (2007)

$$U_{LHTS} = \frac{1}{\underbrace{\frac{1}{\alpha_{sto}} + \frac{s}{\lambda}}_0 + \underbrace{\frac{1}{\alpha_{HTF}}}_0} = \frac{\lambda}{s} = \frac{\lambda A^{sto} \rho}{m}, \quad U_{FBR} = \frac{1}{\underbrace{\frac{1}{\alpha_{sto}} + \frac{s}{\lambda}}_0 + \underbrace{\frac{1}{\alpha_{HTF}}}_0} = \alpha_{sto} = const. \quad (5)$$

For the LHTS different values for λ and thus U_{LHTS} are used for solid, liquid and transition phase, where for the transition the average of the solid and liquid values is used. Eq. (3) is adapted using the binary variables which are also used to model the piecewise linear QT-characteristics. This characteristic shown in Fig. 2 provides a relation between the storage temperature and the stored energy and depends on storage mass, specific heat cp , phase change enthalpy Δh and melting temperature T_{melt} . For FBR this characteristic is linear for fixed storage mass.

2.3. Extended Superstructure

In this paper a multi-period formulation based on the MINLP superstructure proposed by Zhang (2006) is used and extended for storage integration. The objective function in the extended version considers HEX between process streams and ISC, storage HEX in the case of LHTS or FBR and the mass of the storage material. The costs for storage construction and storage equipment are assumed to be proportional to the mass of the storage material and are considered in the cost coefficient for storage mass.

3. Example

To demonstrate the integration procedure a slightly adapted version of an example from Kemp (2007) was investigated. The example consists of two hot and two cold process streams with different start and end times leading to 6 operation periods. The process is assumed to be cyclic with a cycle duration of one hour. For higher accuracy for storage heat flows of LHTS and FBR all operation periods were split into two periods with equal durations. The stream data and cost coefficients, which are rough estimates based on material costs, are presented in Table 1.

In the targeting phase for the integration of a LHTS system an ideal phase change temperature for the PCM of 120°C was found. The sugar alcohol Erythritol with a phase change temperature of 117.7°C was then selected as storage material. For the FBR quartz sand and for the two-tank system thermal oil were selected as storage materials. The properties of the selected storage materials are shown in Table 2. The heat transfer coefficient between the fins and the storage material in the FBR was assumed to be $0.3 \text{ kW/m}^2\text{K}$ based on the work by Molerus et al. (1995). The obtained targets for ideal storage masses for LHTS and FBR were 710.3 kg and 1725.5 kg respectively. After material selection and targeting for storage mass the extended multi-period MINLP superstructure was solved using the local MINLP solver DICOPT (DIcrete and Continuous Optimizer)

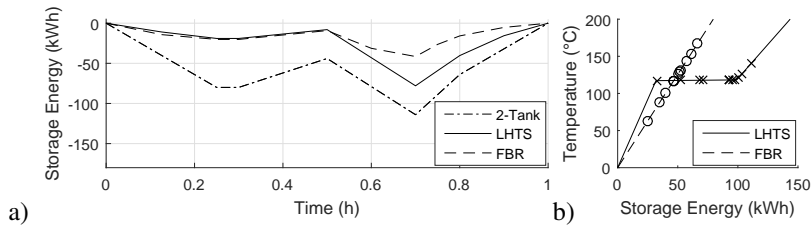


Figure 3: a) Cumulated storage energy over process duration for two-tank system, LHTS and FBR, b) QT-diagram with storage states

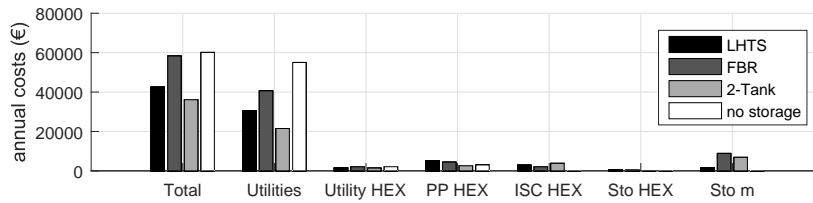


Figure 4: Annual cost analysis for the obtained HEN with LHTS, FBR, two-tank system and without storage integration (PP= direct heat integration)

which is based on the outer approximation method with equality relaxation strategies presented by Viswanathan and Grossmann (1990). DICOPT was initialized using an approximate solution obtained by solving a linearized version of the formulation.

Fig. 3 a) shows the cumulated storage energy over time. Using the two-tank system the highest heat recovery was obtained followed by the LHTS system. The integration of the FBR yielded the lowest heat recovery which can also be seen from the utility costs in Fig. 4. In Fig. 3 b) a QT-diagram is presented which shows that the LHTS system operates in phase transition and in the liquid phase of the storage medium. The temperature range within the storage is small compared to the FBR where the storage temperature ranges from 62.5 to 166.8 °C. The two-tank system operates at 165 and 105 °C and the optimal storage mass is 3420 kg.

Comparison of the annual costs of the optimized heat recovery systems and the HEN without storage integration (Fig. 4) shows that the two-tank system is the most cost-efficient solution with total annual costs of 36,122 € compared to 60,116 € for the case without storage. Although, the costs for the storage vessels of the two-tank system exceed the cost for the LHTS, higher heat recovery can be obtained which makes the storage more cost-efficient. The least cost-efficient storage is the FBR with high costs for the storage vessel and low heat recovery. The HENs for all cases are presented in Fig. 5. The HENs with LHTS and two-tank system have one less utility exchanger than the HEN without storage integration. All four process streams are connected to the ISC. Using the FBR no reduction in the the number of utility HEXs was obtained.

4. Conclusion

The proposed procedure for storage integration allows for simultaneous optimization of HENs and storage subsystems. Storage models for two-tank systems, LHTS and FBR that will be validated in future work were presented that can be included in superstructure formulations for HENS. This allows for scenario analysis of different types of storages. The proposed targeting procedure helps to select a PCM with a suitable melting temperature for LHTS and to reduce problem complexity by providing estimates for optimal storage size. In the presented example a conventional two-tank storage system resulted in the lowest annual costs. Although, other storage systems might

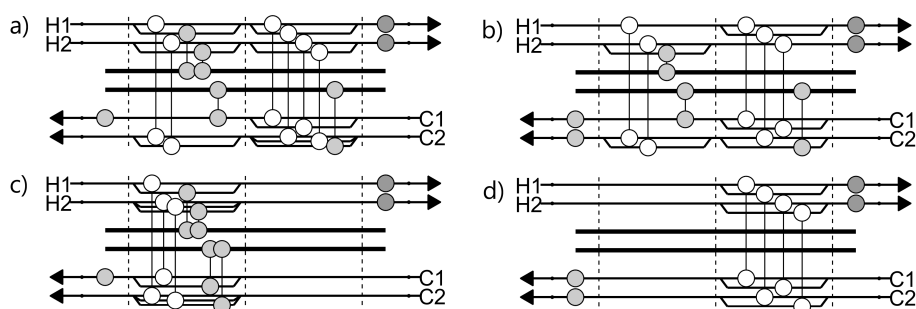


Figure 5: Optimal HENs: a) LHTS, b) FBR, c) two-tank system d) no storage

be the better alternative if condensing and evaporating process streams are considered or for high temperature application. Whether storage integration is worthwhile highly depends on the costs for storage equipment and additional utilities. Also, low period durations for cyclic processes favour the integration of storage systems as higher heat recovery per storage volume can be obtained.

5. Acknowledgement

This integration method of thermal energy storages and the corresponding project were initiated and could be realized by means of the endowed professorship through the cooperation between AIT (Austrian Institute of Technology) and TU Wien (Vienna University of Technology) in the research-field of Industrial Energy Systems.

References

- A. Anastasovski, 2017. Design of heat storage units for use in repeatable time slices. *Applied Thermal Engineering* 112, 1590–1600.
- S. Bandyopadhyay, J. Varghese, V. Bansal, 2010. Targeting for cogeneration potential through total site integration. *Applied Thermal Engineering* 30 (1), 6–14.
- C.-L. Chen, Y.-J. Ciou, 2008. Design and optimization of indirect energy storage systems for batch process plants. *Industrial & Engineering Chemistry Research* 47 (14), 4817–4829.
- M. F. Agyenim, I. Knight, 2007. The use of phase change material (pcm) to improve the coefficient of performance of a chiller for meeting domestic cooling in wales. 2nd PALENC Conference and 28th AIVC Conference on Building Low Energy Cooling and Advanced Ventilation Technologies in the 21st Century, September 2007, Crete island, Greece 1.
- I. C. Kemp, 2007. *Pinch Analysis and Process Integration*. Elsevier.
- E. Martelli, E. Amaldi, 2014. Pgs-com: A hybrid method for constrained non-smooth black-box optimization problems. *Computers & Chemical Engineering* 63, 108–139.
- A. Mian, E. Martelli, F. Maréchal, 2016. Multi-period sequential synthesis of heat exchanger networks and utility systems including storages. In: 26th European Symposium on Computer Aided Process Engineering. Vol. 38 of *Computer Aided Chemical Engineering*. Elsevier, pp. 967–972.
- O. Molerus, A. Burschka, S. Dietz, 1995. Particle migration at solid surfaces and heat transfer in bubbling fluidized beds—ii. prediction of heat transfer in bubbling fluidized beds. *Chemical Engineering Science* 50 (5), 879–885.
- J. Viswanathan, I. Grossmann, 1990. A combined penalty function and outer-approximation method for minlp optimization. *Computers & Chemical Engineering* 14 (7), 769 – 782.
URL <http://www.sciencedirect.com/science/article/pii/0098135490870854>
- T. F. Yee, I. E. Grossmann, 1990. Simultaneous optimization models for heat integration-ii. heat exchanger network synthesis. *Computers & Chemical Engineering* 14 (10), 1165–1184.
- W. V. N. Zhang, 2006. Design of flexible heat exchanger network for multi-period operation. *Chemical Engineering Science* 61 (23), 7730–7753.

5.5 Paper 5

Full paper journal contribution in
Applied Thermal Engineering
(2017 Impact Factor: 3.771)



Contents lists available at ScienceDirect

Applied Thermal Engineering

journal homepage: www.elsevier.com/locate/apthermeng

Research Paper

A sequential approach for integration of multiple thermal energy storages with fixed mass and variable temperature

Anton Beck^a, René Hofmann^{a,b,*}^a AIT Austrian Institute of Technology GmbH, Center for Energy, Sustainable Thermal Energy Systems, Giefinggasse 2, 1210 Wien, Austria^b Technische Universität Wien, Institute for Energy Systems and Thermodynamics, Getreidemarkt 9/BA, 1060 Wien, Austria

HIGHLIGHTS

- Analysis of pressurized water storages (> 100 °C): moderate costs for low pressures.
- Introduction of the first model for process integration of multiple FMVT storages.
- Introduction of a simplified model for sizing of FMVT storages.
- With pressurized water storages reduction of hot utility demand (~50%) achieved.

ARTICLE INFO

Keywords:

Mathematical programming
Heat integration
Thermal energy storage
Pressurized water storage

ABSTRACT

Heat recovery in industrial processes is gaining importance as climate goals push industries to increase their energy efficiency. But also potential economic benefits give incentives to increase waste heat recovery and thus energy efficiency. The various available thermal energy storage technologies yield high potentials to increase energy efficiency in industrial processes. However, storages with fixed mass and variable temperature are rarely considered for storage integration using process integration methods.

In this paper, a sequential approach using mathematical programming formulations combined with insights from pinch-analysis is proposed that allows to find cost efficient heat recovery systems incorporating storages with fixed mass and variable temperature. The procedure is demonstrated by integration of pressurized water storages into two industrial process examples taken from literature. For both examples hot utility demand could be reduced by about 50% compared to solutions without storage integration.

1. Introduction

Energy saving potentials in industry comprise highly economical measures with short payback times according to a recent EU report [1]. The efficient use of thermal energy in industry is not only beneficial for the environment due to decreased usage of fossil fuels and thus mitigation of green house gas emissions but often leads to economical benefits. This is why a lot of work has been done in the field of process integration in the last decades, as shown by recent review papers by Morar and Agachi [2] and Klemes et al. [3]. According to Fernandez et al. [4] the implementation of batch processes in industry is increasing due to its flexibility and adaptability. These batch processes show time dependent behaviour which means that the temperature levels and heat loads of sources and sinks may change over time or that heat sources and sinks may not occur simultaneously and thus no direct

heat recovery using heat exchangers (HEX) is possible. Several approaches have been developed in the past to identify and ultimately to exploit heat recovery potentials in time-dependent processes using thermal energy storages. Fernandez et al. [4] noted in their review paper about process integration in batch processes that in this century's research the utilization of thermal energy storages has increased significantly.

Stoltze et al. [5] distinguish between storages with variable mass and fixed temperature (VMFT) such as storage systems with multiple storage tanks or stratified tanks, fixed mass and fixed temperature (FMFT) such as ideal latent heat thermal energy storages (LHTS) and fixed mass and variable temperature (FMVT) such as regenerators with homogeneous temperature distribution. They focused on storages of the VMFT class as they claimed that the other types are not suitable for the processes discussed in their paper and because of limited heat recovery

* Corresponding author at: Technische Universität Wien, Institute for Energy Systems and Thermodynamics, Getreidemarkt 9/BA, 1060 Wien, Austria.

E-mail address: Rene.Hofmann@tuwien.ac.at (R. Hofmann).

URL: <http://www.tuwien.ac.at> (R. Hofmann).

<https://doi.org/10.1016/j.applthermaleng.2018.11.039>

Received 10 August 2018; Received in revised form 23 October 2018; Accepted 10 November 2018

Available online 13 November 2018

1359-4311/ © 2018 Elsevier Ltd. All rights reserved.

Nomenclature		x_0	initial vapour fraction (kg/kg)
Acronyms		y	annualization factor (-)
Parameters		Subscripts	
CC	Composite Curves	i	hot stream
CS	case-study	j	cold stream
FMFT	fixed mass fixed temperature	k	temperature stage
FMVT	fixed mass variable temperature	m	segment of hot mGCC
GCC	Grand Composite Curves	max	maximum value
HENS	heat exchanger network synthesis	min	minimum value
HEX	heat exchanger	n	segment of cold mGCC
ISC	intermediate storage cycle	s	storage
LHTS	latent heat thermal energy storage	t	time interval
mGCC	modified Grand Composite Curves	Superscripts	
MINLP	mixed integer nonlinear programming	c	cold
SCC	Storage Composite Curves	h	hot
TAC	total annual costs	in	inlet
TAM	time average method	ISC	intermediate storage cycle
VMFT	variable mass fixed temperature	out	outlet
		SCC	storage composite curve
α	coefficients for polynomial fit	STO	storage
β	cost exponent (-)	TOT	total
ΔT_{min}	minimum approach temperature (°C)	UT	utility
\dot{m}	mass flow of process streams (kg/s)	Variables	
Γ	big-M coefficients	ΔT	temperature difference (°C)
λ	coefficients for polynomial fit	\dot{Q}	heat flow (kW)
ρ_{steel}	steel price (kg/m ³)	$LMTD$	logarithmic mean temperature difference (°C)
σ_r	radial stress (N/mm ²)	TAC	total annual costs (€)
σ_t	tangential stress (N/mm ²)	A	heat exchanger area (m ²)
σ_{steel}	maximal stress (€/kg)	d	diameter (m)
τ	time interval duration (s)	l	length (m)
a	coefficient for modelling of mGCC (kW/K)	m	mass (kg)
b	coefficient for modelling of mGCC (kW/K)	p	pressure (Pa)
c^{fix}	costs for HEX installation (€)	Q	energy (kWh)
c^{var}	specific costs for HEX area €/m ²)	Q^{shift}	energy shifting initial storage temperature (kWh)
c_p	specific heat capacity (kW/kg K)	s	wall thickness (m)
C_s	annual storage costs (€)	T	temperature (°C)
C_{steel}	steel price (€/kg)	V	volume (m ³)
CP	set of cold process streams	x	binary variables for activating segments of the mGCCs (-)
HP	set of hot process streams	y^{ass}	binary variables for identification of SCC (-)
M_t	number of segments of hot mGCC	z	binary variables for existence of heat exchanger (-)
N_t	number of segments of cold mGCC	z^{switch}	binary variables to determine charging/discharging
NOK	number of temperature stages		
NOP	number of time intervals		
NOS	number of storages		
U	heat transfer coefficient (kW/m ² K)		

potential. However, De Boer et al. [6] investigated the potentials for integration of a latent heat storage with a melting temperature of 140°C and sensible heat storages using concrete as storage material and found that the implementation of FMVT systems could save up to 70% of the energy consumption without any other modification on the process manufacturing. The potentials for the different storages were obtained using a thermal model of a predefined integration scheme.

A more systematic approach is the time average method (TAM), which was one of the first approaches to quantify heat recovery potentials using storages. In this method, all streams are treated as if they occurred simultaneously and their heating and cooling demands are considered in terms of energy. The energy targets calculated using pinch-analysis yield the theoretical maximum for heat recovery. Both Stolze et al. [5] and Kruppenacher et al. [7] used the time-average approach in their works on storage integration. Stolze et al. [5] showed

that usually only few storage tanks are necessary to fulfill energy targets obtained using TAM. Similarly, Kruppenacher et al. [7] proposed a heuristic approach to identify the minimum number of storage tanks to obtain maximum energy recovery.

One of the few works considering integration of FMVT and FMFT storages was done by Anastovski [8] who introduced warm water storage tanks into an industrial process with cyclic operation. He used an iterative approach based on heat cascade analysis, pinch-analysis and cost evaluation. Walmsley et al. [9] did not use FMVT or FMFT storages for heat recovery in a dairy plant but they concluded that variable tank temperature levels in a multi-tank system yield better heat recovery potentials compared to constant temperature systems.

In contrast to methods based on pinch-analysis principles, mathematical programming approaches for storage integration have been developed. One major advantage of mathematical programming is that

it allows flexible modelling of the energy systems in concern. For example, Chen et al. [10] proposed a mixed integer nonlinear programming (MINLP) superstructure formulation for cost-efficient indirect heat recovery in batch processes using multiple storage tanks (VMFT). Sebelebe and Majoz [11] presented a mathematical programming formulation that is aimed at minimizing energy consumption in multi-purpose batch plants through multiple heat storage vessels. In their paper they investigate the optimal number of heat storage vessels as well as design parameter. Another approach for cost efficient integration of thermal storages was proposed by Yang et al. [12] who combined nonlinear programming and a graphical approach for cost-efficient integration of VMFT storages.

Despite all the work that has been done, FMVT storage systems for industrial waste heat recovery have not been considered in combination with process integration methods in a systematic way even though for processes, where multi-tank or stratified tank systems cannot be used, FMVT might be a promising alternative. In order to identify cost-efficient integration of FMVT systems in industry, systematic methods need to be developed. Graphical approaches such as pinch-analysis cannot handle the changing temperature levels of FMVT storages appropriately because storage volume, heat loads and storage temperature need to be considered simultaneously. For this reason, mathematical programming and hybrid approaches that also use insights from pinch-analysis for simplification of the problems are promising tools for the integration of FMVT storage systems.

2. Scope of this paper

In this paper, the problem of cost efficient integration of thermal energy storages with fixed mass and variable temperature is addressed. Therefore, a commonly used MINLP superstructure formulation proposed by Yee and Grossman [13] is extended for the integration of thermal energy storages. This extension is presented in Section 3. However, simultaneous optimization of the heat exchanger network (HEN) and the storage systems including storage sizes and temperature levels increases the complexity of the problem significantly compared to the original superstructure formulation for heat exchanger network synthesis (HENS) which is already an NP-hard problem [14]. For this reason, a sequential approach is presented that splits the problem into storage sizing and HENS:

1. First, the storage sizes are optimized using a novel MINLP formulation. This formulation is a hybrid approach that combines pinch-analysis principles and mathematical programming. It is based on modified Grand Composite Curves (mGCC) which are modelled as constraints for heat recovery (Section 4). This formulation is much easier to solve compared to the extended HENS problem as it does not consider heat exchanger (HEX) areas and has less combinatorial difficulty.
2. Then the extended simultaneous stage-wise superstructure model for HENS is solved with fixed storage sizes obtained in step 1 which eliminates nonlinear constraints and thus can be solved much faster.

The novel approach is demonstrated by means of two example cases taken from literature. Pressurized water storages which are described in this paper are used as closed loop thermal storage system. A cost function for this storage type is derived that considers material costs as a function of the maximum pressure in the storage vessel and its volume. This type of storage was also used for integration of solar thermal energy by Kulkarni et al. [15].

It needs to be stated that the proposed integration approach is not restricted to pressurized water storages but can be used for the integration of other thermal energy storages with fixed mass and variable temperature. Beck and Hofmann [16] used a simplified version of the procedure and the mathematical programming models for integration of single storage units and their comparison.

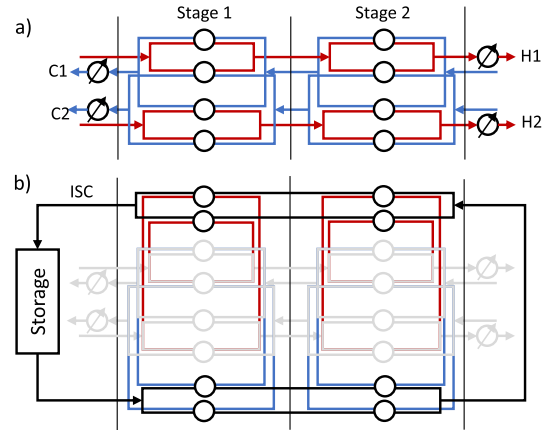


Fig. 1. (a) Basic superstructure, (b) extended superstructure.

3. Extended superstructure for HENS

In this work, a multi-period formulation proposed by Zhang and Verheyen [17], which is based on the MINLP superstructure proposed by Yee and Grossmann [13] (Fig. 1(a)), is extended for the possibility of storage integration. In this stage-wise superstructure isothermal mixing is assumed and utility cooling and heating is only possible outside the predefined temperature stages. Escobar et al. [18] showed that despite this simplifying assumptions the superstructure proposed by Yee and Grossmann [13] yields better results and can be solved faster for many problems compared to the superstructure without isothermal mixing assumption proposed by Ciric and Floudas [19].

The proposed extensions to the superstructure are shown in Fig. 1(b) for a simple problem with two hot and cold streams, two temperature stages and a single FMVT storage. In each temperature stage heat exchangers can be placed that connect the process streams to intermediate storage cycles (ISCs). The ISCs are used to transfer heat from the process streams to the storages and are assumed to have no thermal capacity.

The objective for the extended superstructure formulation is to minimize total annual costs (TAC) and thus the objective function can be written as

$$\begin{aligned}
 \min TAC = & \underbrace{\sum_t \left(\sum_i c^{UTc} \dot{Q}_{it}^{UTc} + \sum_j c^{UTh} \dot{Q}_{jt}^{UTh} \right)}_{\text{energy costs}} \tau_t \\
 & + \underbrace{c^{fix} \left(\sum_i \sum_j \sum_k z_{ijk} + \sum_i z_i^{UTc} + \sum_j z_j^{UTh} \right)}_{\text{fixed costs for HEX connecting process streams and utility HEX}} \\
 & + \underbrace{c^{var} \left(\sum_i \sum_j \sum_k A_{ijk}^\beta + \sum_i A_i^{UTc \beta} + \sum_j A_j^{UTh \beta} \right)}_{\text{variable costs for HEX connecting process streams and utility HEX}} \\
 & + \underbrace{c^{fix} \left(\sum_s \left(\sum_i \sum_k z_{iks}^{ISCC} + \sum_j \sum_k z_{jks}^{ISCh} \right) \right)}_{\text{fixed costs for HEX connecting streams to ISCs}} \\
 & + \underbrace{c^{var} \left(\sum_s \left(\sum_i A_{is}^{ISCC \beta} + \sum_j A_{js}^{ISCh \beta} \right) \right)}_{\text{variable costs for HEX connecting streams to ISCs}} \\
 & + \underbrace{\sum_s C_s}_{\text{storage costs}} + \underbrace{c^{var} \sum_s A_s^{STO \beta}}_{\text{variable costs for storage HEX}} \\
 \forall s = 1, \dots, NOS, k = 1, \dots, NOK, t = 1, \dots, NOP, \\
 i \in HP, j \in CP.
 \end{aligned} \tag{1}$$

The terms in this objective function can be divided into energy costs, costs for heat exchangers and costs for storages. Energy costs are made up by the cost coefficients c^{UTc} and c^{UTh} for utility consumption

and the utility heat loads \dot{Q}_{it}^{UTc} and \dot{Q}_{jt}^{UTh} multiplied by operating period durations τ_i . Costs for heat exchangers are divided into fixed and variable costs. c^{fix} is the cost coefficient for the installation of HEX and c^{var} is the coefficient for variable HEX areas. The cost exponent β describes the degressive behaviour of HEX area costs. The binary variables z_{ijk} , z_{it}^{UTc} , z_j^{UTh} , z_{iks}^{ISCc} and z_{jks}^{ISCh} determine whether a HEX is placed in the superstructure. The HEX areas are represented by the continuous variables A_{ijk} , A_{it}^{UTc} , A_j^{UTh} , A_{is}^{ISCc} and A_{js}^{ISCh} . The heat transfer A_s^{STO} is only considered for FMVT storages where the heat transfer fluid is not also the storage material. If the heat transfer fluid in the ISCs is also the storage material, no heat exchange inside the storage vessels needs to be considered. C_s are the costs for the storage units and are calculated depending on the storage types that are integrated. NOK is the number of temperature intervals, NOP is the number of operating periods, NOS is the number of thermal energy storages and HP and CP are the sets of hot and cold process streams.

In the following, the most important constraints for the superstructure extension are presented. The full model for the extended superstructure can be found in Appendix A of this paper.

3.1. Energy balances

The total heat balances for each process stream are altered to consider storage heat loads.

$$\begin{aligned} (T_{it}^{in} - T_{it}^{out})c_{p,it}\dot{m}_{it} &= \sum_k \sum_j \dot{Q}_{ijkt} + \dot{Q}_{it}^{UTc} + \sum_k \sum_s \dot{Q}_{ikst}^{ISCc}, \\ (T_{jt}^{out} - T_{jt}^{in})c_{p,jt}\dot{m}_{jt} &= \sum_k \sum_i \dot{Q}_{ijkt} + \dot{Q}_{jt}^{UTh} + \sum_k \sum_s \dot{Q}_{jkst}^{ISCh}, \\ \forall t = 1, \dots, NOP, s = 1, \dots, NOS, k = 1, \dots, NOK, \\ i \in HP, j \in CP \end{aligned} \quad (2)$$

In Eq. (2) T^{in} and T^{out} are the inlet and outlet temperatures of the hot streams i and cold streams j respectively. $c_{p,it}$ and $c_{p,jt}$ are the heat capacities of the hot and cold streams with the corresponding mass flows \dot{m}_{it} and \dot{m}_{jt} . \dot{Q}_{ijkt} are the transferred heat flows between hot stream i and cold stream j in the temperature interval k and operating period t . The total heat balances for each temperature interval k are

$$\begin{aligned} (T_{ikt} - T_{i,k+1,t})c_{p,it}\dot{m}_{it} &= \sum_j \dot{Q}_{ijkt} + \sum_s \dot{Q}_{ikst}^{ISCc}, \\ (T_{jkt} - T_{j,k+1,t})c_{p,jt}\dot{m}_{jt} &= \sum_i \dot{Q}_{ijkt} + \sum_s \dot{Q}_{jkst}^{ISCh}, \\ \forall t = 1, \dots, NOP, s = 1, \dots, NOS, k = 1, \dots, NOK, \\ i \in HP, j \in CP \end{aligned} \quad (3)$$

where T_{ikt} and T_{jkt} are the temperatures of hot and cold streams respectively at the beginning of each temperature interval k . $T_{i,k+1,t}$ and $T_{j,k+1,t}$ are the temperatures of hot and cold streams respectively at the end of each temperature interval.

3.2. Connection to the ISCs

Similar to the logical constraints for heat loads in the basic superstructure formulation presented in the Appendix, the constraints for heat loads in the HEX connecting process streams and the ISCs (\dot{Q}_{ikst}^{ISCc} and \dot{Q}_{jkst}^{ISCh}) are modelled using big-M formulations. These are also used to restrict matches between process streams and the ISC with insufficient temperature differences and to ensure that the variables for temperature differences at the hot and cold end of HEX always have positive values.

$$\begin{aligned} \Delta T_{jst}^{ISCh1} &\leq T_{st}^{ISC,in} - T_{jkt} + \Gamma_{js}^{T,ISC}(1 - z_{jkst}^{ISCh}), \\ \Delta T_{jst}^{ISCh2} &\leq T_{st}^{ISC,out} - T_{j,k+1,t} + \Gamma_{js}^{T,ISC}(1 - z_{jkst}^{ISCh}), \\ \Delta T_{ist}^{ISCc1} &\leq T_{ikt} - T_{st}^{ISC,in} + \Gamma_{is}^{T,ISC}(1 - z_{ikst}^{ISCc}), \\ \Delta T_{ist}^{ISCc2} &\leq T_{i,k+1,t} - T_{st}^{ISC,out} + \Gamma_{is}^{T,ISC}(1 - z_{ikst}^{ISCc}), \\ \forall t = 1, \dots, NOP, s = 1, \dots, NOS, k = 1, \dots, NOK, \\ i \in P, j \in CP. \end{aligned} \quad (4)$$

The coefficients $\Gamma^{T,ISC}$ need to be sufficiently large to ensure positive values for the temperature differences ΔT^{ISCh} and ΔT^{ISCc} and feasible heat transfer. The superscripts 1 and 2 represent variables at the hot and cold side of heat exchangers and $T_{st}^{ISC,in}$ and $T_{st}^{ISC,out}$ are the ISC temperatures entering and leaving the storage vessels. HEX areas A_{js}^{ISCh} and A_{is}^{ISCc} are modelled using the temperature differences in Eq. (4) and the heat loads \dot{Q}_{ikst}^{ISCc} and \dot{Q}_{jkst}^{ISCh} .

In the extended superstructure only one exchanger is allowed for each match between the ISCs and process streams. This simplification tightens the problem and makes it more compact because only one nonlinear constraint needs to be satisfied for modelling of the HEX areas A_{js}^{ISCh} and A_{is}^{ISCc} instead of NOK for each possible match and operating period.

3.3. Storage models

The storage models presented in this section are used for both the extended superstructure formulation for HENS and the storage sizing MINLP model presented in Section 4.

When it comes to FMVT storages, two different types can be distinguished (Fig. 2):

- Storages that are charged **indirectly** through heat exchange (HTF and storage material are different)
- Storages that are charged **directly** (HTF and storage material are the same)

If the storages are charged indirectly, the required heat transfer area can be calculated by

$$\begin{aligned} A_s^{STO} &\geq \frac{\sum_i \dot{Q}_{ist}^{ISCc} + \sum_j \dot{Q}_{jst}^{ISCh}}{U_s^{STO} LMTD_{st}^{STO}}, \\ \forall t = 1, \dots, NOP, s = 1, \dots, NOS, k = 1, \dots, NOK, \\ i \in HP, j \in CP. \end{aligned} \quad (5)$$

The logarithmic mean temperature differences inside the storages are modelled using logical constraints involving binary variables and the temperature levels of the storages and the ISCs.

Storage systems that are charged directly do not need heat transfer

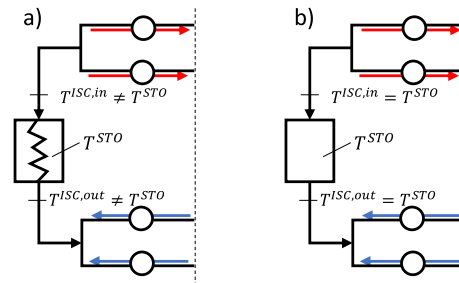


Fig. 2. FMVT storages charged (a) indirectly, (b) directly.

inside the storage vessels and thus the constraints in Eq. (5) are not necessary. Also, in this case the temperatures in the ISCs ($T^{ISC,in}$ and $T^{ISC,out}$) are equal to T^{STO} , which simplifies Eq. (4).

The relation between storage temperature and stored energy is described by the bi-linear equality constraints

$$T_{st}^{STO} c_p m_s = Q_{st}^{STO} + Q_s^{shift}, \quad \forall t = 1, \dots, NOP, s = 1, \dots, NOS \quad (6)$$

with the storages specific heat capacity c_p and the mass of storage material m_s . Q_{st}^{STO} is the cumulated energy after period t for storage s and Q_s^{shift} allows storages to have any initial temperature. Q_{st}^{STO} is obtained by the summation of the charging and discharging heat loads between the storages and the ISCs in the previous time periods with durations τ

$$Q_{st}^{STO} = \sum_{r=1}^t \left(\dot{Q}_{sr}^{ISCc} - \dot{Q}_{sr}^{ISCh} \right) \tau_r, \quad \forall t = 1, \dots, NOP, s = 1, \dots, NOS \quad (7)$$

where

$$\dot{Q}_{st}^{ISCh} = \sum_j \sum_k \dot{Q}_{jkst}^{ISCh}, \quad \dot{Q}_{st}^{ISCc} = \sum_i \sum_k \dot{Q}_{ikst}^{ISCc}, \quad \forall t = 1, \dots, NOP, k = 1, \dots, NOK, s = 1, \dots, NOS, \quad i \in HP, j \in CP. \quad (8)$$

To model cyclic operation the additional constraint is introduced that the cumulated storage energy Q_{st}^{STO} is equal to zero at $t = NOP$. Another restriction is that the storages cannot be charged and discharged at the same time. This is modelled using logical constraints that force either charging or discharging heat loads to zero.

FMVT storages gradually change their temperature within operating periods of charging or discharging and thus a proper control strategy and the possibility for HEX by-passes is required to keep heat loads constant within the individual operating periods. Temperature differences for heat exchange (Eqs. (4) and (5)) are calculated using the storage temperatures at the end of each operating period, which corresponds to safe-side modelling and ensures feasibility. Also, homogeneous temperature in the storage and constant specific heat capacities are assumed and heat losses are neglected.

Depending on the system, storage costs C_s used in the objective function Eq. (1) may be very different depending on the storage systems to be integrated and thus a general cost function cannot be provided. A cost-function for the pressurized storage system presented in this paper are derived in Section 5.

4. MINLP formulation for storage sizing

As stated earlier, the extended superstructure formulation presented in Section 3 is difficult to solve because of several nonlinear constraints and its combinatorial complexity. For this reason, an MINLP formulation is introduced that allows to calculate storage sizes and storage mass m_s which can then be used as a fixed parameter within the extended superstructure formulation in Eq. (6). This significantly reduces the number of nonlinear constraints and thus allows the superstructure to be solved much faster.

The idea behind this MINLP formulation is to use insights from pinch-analysis combined with mathematical programming to find optimal storage sizes and storage operation.

4.1. Modified grand composite curves

The MINLP formulation for storage sizing is based on mGCCs which are similar to the shifted Grand Composite Curves (GCC) proposed by

Bandyopadhyay et al. [20] for total-site integration. They determine necessary heating and cooling loads and the temperature levels at which they can be supplied.

In order to obtain mGCCs, first, Composite Curves are calculated using a minimal allowable temperature difference ΔT_{min} (Fig. 3 left). Then, GCCs are derived by shifting both hot and cold Composite Curves by $\Delta T_{min}/2$ so that they touch at the pinch point and then calculating the horizontal difference between the two Composite Curves (Fig. 3 middle). The so called heat recovery pockets are removed and the GCC is split at the pinch point. Finally, the mGCCs are obtained by shifting the split curves back by $\Delta T_{min}/2$. The mGCCs are calculated for every operating period. Within the MINLP formulation the mGCCs are modelled as piecewise linear constraints for storage temperatures and heat loads.

4.2. Mathematical model

The objective of the MINLP formulation for storage sizing is to minimize TAC considering the trade-off between storage costs and costs for residual utilities. No individual HEX are considered which makes the problem relatively easy to solve compared to the superstructure formulation. However, for problems where investment costs for HEX are high compared to energy costs, the results from the MINLP for storage sizing might not correspond to real cost-optimal storage sizes for HENS. The objective function for the storage sizing MINLP can be stated as

$$\min TAC = \sum_t (\dot{Q}_t^{UTh} c^{UTh} + \dot{Q}_t^{UTc} c^{UTc}) \tau_t + \sum_s C_s, \quad \forall t = 1, \dots, NOP, s = 1, \dots, NOS, \quad (9)$$

where \dot{Q}_t^{UTh} and \dot{Q}_t^{UTc} are the hot and cold utility heat loads in period t and c^{UTh} and c^{UTc} are the cost coefficients for utility consumption. Again, C_s are the costs for each storage s which depend on the storage systems that should be integrated.

If only a single storage system is to be integrated, the mGCCs can be interpreted as an upper bound for the heat load of the storage depending on the storage temperature. However, if more storage systems should be integrated simultaneously, storage heat load cascades need to be modelled.

To illustrate this idea, a graphical representation of the solution for a simple example with two operating periods is presented in Fig. 4 which was obtained using the global optimization solver Baron. The grey areas defined by the mGCCs and the upper and lower bounds for storage temperatures show the feasible temperature range and the corresponding feasible storage charging and discharging heat loads. The numbered lines in this Figure represent storage temperatures after

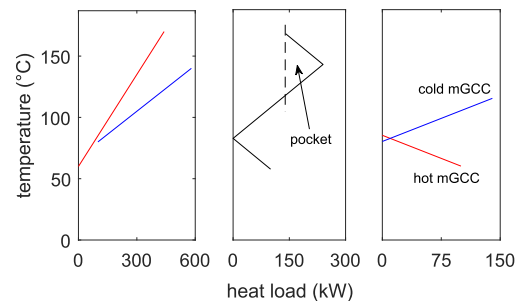


Fig. 3. Left: Composite Curves, middle: Grand Composite Curves, right: modified Grand Composite Curves.

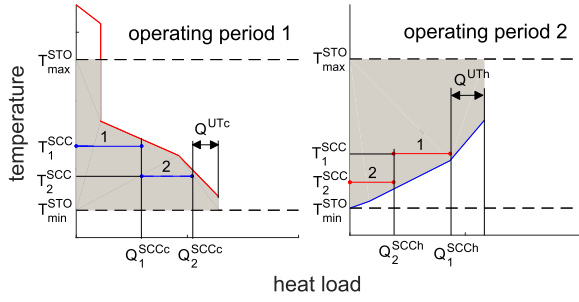


Fig. 4. mGCCs for a small example with two operating periods and a solution for storage temperatures and heat loads; feasible range for temperature and heat loads is marked in grey.

the respective operating periods and the corresponding heat loads. These lines can be interpreted as storage composite curves (SCC) as they are constructed the same way as standard composite curves. In this small example, both storage 1 and 2 are charged during operating period 1 and storage 1 has the higher end-temperature. This means that the mGCC yields an upper bound for the heat load of storage 1 and an upper bound for the cumulated energy of storage 1 and storage 2. Both storages are discharged during operating period 2. Here, the mGCC yields an upper bound for the heat load of storage 2 with the lowest end-temperature and an upper bound for the cumulated heat loads for storages 1 and 2. For this reason storage heat load cascades need to be modelled for both charging (\dot{Q}_1^{SCCc} and \dot{Q}_2^{SCCc}) and discharging (\dot{Q}_1^{SCCh} and \dot{Q}_2^{SCCh}). In the following, two different model formulations for storage heat load cascades are presented.

Model A: A restriction is introduced that ensures a monotonic decrease in storage temperature from storage s to storage $s + 1$. This means that storage $s + 1$ cannot be hotter than storage s in any operating period.

$$T_{st}^{STO} > T_{s+1,t}^{STO} \quad \forall s = 1, \dots, NOS - 1, t = 1, \dots, NOP \quad (10)$$

In this formulation storage temperatures T_{st}^{STO} are already sorted due to the restriction of monotonic decrease in temperatures and thus the sorted temperatures T_{st}^{SCC} are simply modelled by

$$T_{st}^{SCC} = T_{st}^{STO}, \quad \forall s = 1, \dots, NOS, t = 1, \dots, NOP. \quad (11)$$

With this restriction, the storage heat load cascades for charging and discharging can be modelled using the following constraints

$$\dot{Q}_{st}^{SCCc} = \sum_{s^*=1}^s \dot{Q}_{s^*,t}^{ISCc}, \quad \forall s, s^* = 1, \dots, NOS, t = 1, \dots, NOP \quad (12)$$

$$\dot{Q}_{st}^{SCCh} = \sum_{s^*=1}^s \dot{Q}_{NOS+1-s^*,t}^{ISCh}, \quad \forall s, s^* = 1, \dots, NOS, t = 1, \dots, NOP. \quad (13)$$

Model B: If the restriction of monotonic decrease in storage temperatures should be avoided, additional continuous and binary variables need to be introduced. Those binary variables are used within assignment matrices of the size $NOS \times NOS$ for sorting storage temperatures and modelling of storage heat load cascades. Compared to **Model A**, more binary variables are needed and the problem's complexity increases significantly. The inequality constraints necessary to model the sorted temperatures T_{st}^{SCC} and the corresponding storage heat

load cascades in **Model B** are presented in **Appendix B** of this paper.

As stated before, the maximum storage heat loads are constrained by the mGCCs. Depending on the shape of the mGCCs, binary variables are necessary to model them. If the shape of the mGCC is convex in the allowed storage operating temperature range no binary variables need to be introduced. If the mGCCs are non-convex, they are modelled using a big-M formulation and the binary variables x_n and x_m . Here, the modified big-M formulation proposed by Trespalacios and Grossmann [21] is used, as it is tighter than the general big-M formulation. The resulting inequality constraints for storage heat loads can be stated as

$$\dot{Q}_{st}^{SCCh} \leq a_{m,t} + b_{m,t} \left(T_{st}^{STO} - \Delta T_{min} \right) + \sum_{\tilde{m}_i=1}^{M_t} x_{\tilde{m}_i,t} \Gamma_{\tilde{m}_i,t}, \quad \forall s = 1, \dots, NOS, t = 1, \dots, NOP, m_t = 1, \dots, M_t, \quad (14)$$

$$\dot{Q}_{st}^{SCCc} \leq a_{n,t} + b_{n,t} \left(T_{st}^{STO} + \Delta T_{min} \right) + \sum_{\tilde{n}_i=1}^{N_t} x_{\tilde{n}_i,t} \Gamma_{\tilde{n}_i,t}, \quad \forall s = 1, \dots, NOS, t = 1, \dots, NOP, n_t = 1, \dots, N_t. \quad (15)$$

M_t and N_t are the numbers of piece-wise linear equations of the hot and cold mGCC in operating period t . Γ_{m_t} and Γ_{n_t} are suitable (smallest possible) coefficients to activate/deactivate equations. There can only be one active piece-wise linear inequality constraint so the sum of the binary variables x_{m_t} and x_{n_t} for each operating period and mGCC is equal to 1.

$$\sum_{m_t} x_{m_t} = 1, \quad \sum_{n_t} x_{n_t} = 1, \quad \forall t = 1, \dots, NOP, n_t = 1, \dots, N_t, m_t = 1, \dots, M_t. \quad (16)$$

The total heating and cooling demands have to be either provided by storages or by external utilities.

$$\dot{Q}_t^{TOTh} = \sum_s \dot{Q}_{st}^{ISCh} + \dot{Q}_t^{UTh}, \quad \forall t = 1, \dots, NOP, s = 1, \dots, NOS, \quad (17)$$

$$\dot{Q}_t^{TOTc} = \sum_s \dot{Q}_{st}^{ISCc} + \dot{Q}_t^{UTc}, \quad \forall t = 1, \dots, NOP, s = 1, \dots, NOS. \quad (18)$$

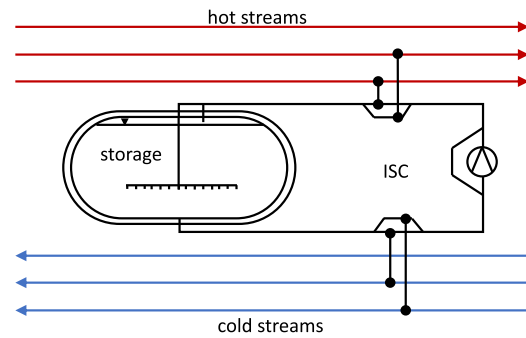


Fig. 5. Schematic integration of a pressurized water storage for industrial heat recovery.

5. Pressurized water storage (FMVT)

In this section, a pressurized water storage system is described and a cost function for the pressure vessel is derived. In Section 6 this storage system is integrated into two industrial example processes to demonstrate the effectiveness of the proposed storage integration procedure.

5.1. Storage description

The pressurized water storage consists of a pressure vessel filled with boiling water and saturated steam. When the storage is charged, boiling water from inside of the storage vessel is pumped through HEX connecting the ISC to the process streams and back into the storage (Fig. 5). This causes both temperature and pressure in the storage to increase. When discharged, steam is taken from the storage and condensed in a HEX connecting the ISC to cold process streams.

The main advantage of pressurized water storages compared to hot water storages is the higher storage temperature. Typically, unpressurized hot water storages only work below 100 °C. However, with multi-tank systems generally higher heat recovery can be obtained because the in and outlet temperatures of the storage subsystems can be kept constant and heat can be recovered over a wider temperature range as stated by Stoltze et al. [5]. When it comes to storage temperatures above 100 °C multi-tank or stratified tank storages using thermal oil with a temperature range up to 400–500 °C can be considered. These storage systems have comparably low energy density due to the low specific heat capacity of thermal oil compared to water (c_p water 4.190 kJ/kg K, c_p oil rd. 2 kJ/kg K). Another storage type that can operate at temperatures above 100 °C is latent heat thermal energy storages (LHTS). LHTS are of special interest if energy should be stored within a small temperature range around the melting temperature of the storage material. This storage type is charged and discharged indirectly and thus double heat transfer is necessary. First, heat needs to be transferred from the process streams to the heat transfer fluid in the ISC and then further on to the storage material. With closed system pressurized water storages no HEX area is needed because they are charged directly.

5.2. Storage characteristics

The storage medium in pressurized water storages is in a two-phase state, which means that a fraction of water is evaporated. The steam fraction has to be as low as possible to obtain the highest energy density. In Fig. 6 the volume specific energy for two different temperature differences is shown as a function of the initial steam fraction x_0 (steam fraction at 100 °C). As can be seen, the maximum energy density has its maximum at very low values for $x_0 > 0$. However, the optimum x_0 depends on the difference between maximum and minimum storage temperature. For very low values of x_0 if a certain pressure is reached all the steam in the pressure vessel condenses due to the isochoric change of state. This behaviour is shown in Fig. 7 for $x_0 = 0.0001$ and means that at the same maximum pressure, lower temperatures and thus lower energy densities can be realized (Fig. 6). Specific energy and other properties of pressurized water were calculated using CoolProp for Matlab [22].

5.3. Storage costs

The main cost driver for the storage vessel is the steel mass needed for construction. The wall thickness of the pressure vessel for a given material is mainly a function of the maximum pressure p_{max} in the storage. For a cylindrical pressure vessel the mean tangential stress within the wall σ_t depends on the pressure inside the pressure vessel,

the inner diameter of the wall d and the wall thickness s [23].

$$\sigma_t = \frac{pd}{2s} \quad (19)$$

The radial stress at the inside of the vessel is equal to $-p$ and on the outside equal to 0. The mean radial stress σ_r is then given by

$$\sigma_r = -\frac{p}{2}. \quad (20)$$

The equivalent stress σ_v results from the shear stress hypothesis.

$$\sigma_v = \sigma_{max} - \sigma_{min} = \sigma_t - \sigma_r = \frac{pd}{2s} + \frac{p}{2} = \frac{p(d+s)}{2s}. \quad (21)$$

The minimal wall thickness s_{min} can then be calculated as

$$s_{min} = \frac{p(d+s)}{2\sigma_{steel}} + s_1. \quad (22)$$

Here, σ_{steel} is the maximum stress depending on the material used for construction. The safety coefficient s_1 is added to ensure that the wall endures slight deviations from the maximum stresses and corrosion and also helps to find definite solutions for the minimization of storage material. As can be seen from Eq. (22), $s_{min}(p)$ is a linear function. However, if s_{min} is expressed as $s_{min}(T^{STO})$ a nonlinear function is obtained. For the closed system pressurized water system and a fixed value for the initial steam content x_0 a polynomial approximation can be found for the relation between storage temperature T^{STO} and storage pressure p . A 3rd-order polynomial (Eq. (23)) yields a sufficiently good approximation.

$$p = \alpha_1 T^3 + \alpha_2 T^2 + \alpha_3 T + \alpha_4 \quad (23)$$

With the assumption of a cylindrical storage vessel the steel mass m_{steel} is the following function of the wall thickness $s_{min}(T^{STO})$, the inner diameter of the vessel d , the length of the storage l and the steel density ρ_{steel} .

$$m_{steel} = \left(\left(\frac{d+2s_{min}}{2} \right)^2 - \left(\frac{d}{2} \right)^2 \right) \pi l \rho_{steel} + 2 \left(\frac{d}{2} \right)^2 \pi s_{min} \rho_{steel} \quad (24)$$

The correlation between storage volume V_s and the storage parameters d and l and the mass of storage material m_s and its density ρ_s is given by

$$V_s = \frac{d^2}{4} l \pi = \frac{m_s}{\rho_s}. \quad (25)$$

Assuming the costs for the storage vessel C_s is only a function of the steel mass m_{steel} , the costs can be calculated as

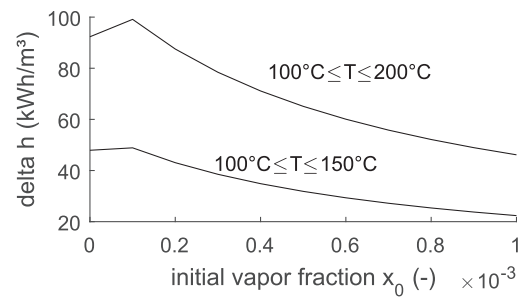


Fig. 6. Specific heat capacity of the pressurized water storage as a function of the initial vapor fraction x_0 .

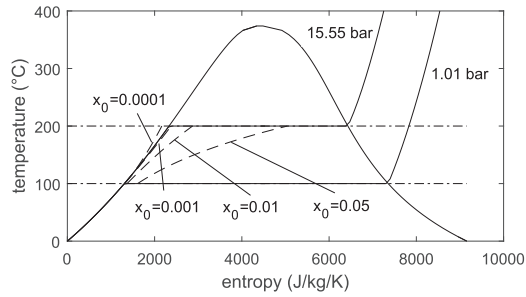


Fig. 7. Propagation of initial vapor fraction x_0 at 100 °C in the pressurized water storage for various values in the T-S diagram.

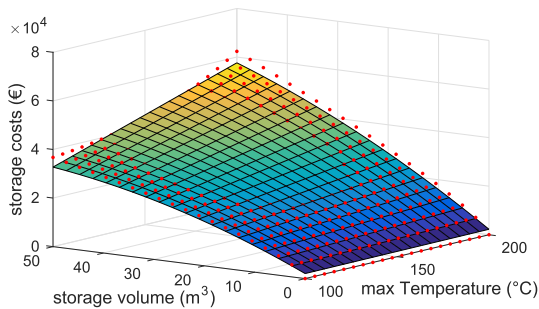


Fig. 8. Storage costs, calculated with $\rho_{steel} = 7850 \text{ kg/m}^3$, $s_1 = 0.01 \text{ m}$, $\sigma_{steel} = 350 \text{ MPa}$ and specific material costs $c_{steel} = 6 \text{ €/kg}$ - real values (red dots) and quadratic fit (surface). (For interpretation of the references to colour in this figure legend, the reader is referred to the web version of this article.)

Table 1

Case-study 1: Stream data and cost coefficients.

	T^{in} (°C)	T^{out} (°C)	$\dot{m} c_p$ (kW/K)	Start (h)	End (h)
H1	170	50	3	0.3	0.8
H2	190	80	4	0.25	1
C1	100	160	8	0	0.5
C2	40	155	10	0.5	0.7
UT h	250	250	-	-	-
UT c	10	15	-	-	-

Exchanger cost = $1000 + 175[A(m^2)]^\beta \text{€y}^{-1}$, $\beta = 0.6$, hot utility cost = 252 €kW^{-1} , cold utility cost = 22.68 €kW^{-1} , $\Delta T_{min} = 5 \text{ °C}$, heat transfer coefficients: $U = 0.5$, $U^{Th/c} = 0.5$, $U^{SCH/c} = 0.89 \text{ kW/m}^2 \text{ K}$, storage cost coefficients: $\lambda_1 = 5745$, $\lambda_2 = 5.13$, $\lambda_3 = 290.5$, $\lambda_4 = 3.08$, $\lambda_5 = -0.78$, storage material: $c_p = 4.26 \text{ kWh/kg}$, $\rho_s = 862 \text{ kg/m}^3$

$$C_s = f^*(V_s, T_{max,s}^{STO}) \quad (26)$$

where $f^*(V, T_{max}^{STO})$ is a quadratic function obtained by least squares fitting of the data points obtained from minimizing $m_{steel}(l, d, T_{max}^{STO})$

$$f^*(V, T_{max}^{STO}) = \lambda_1 + \lambda_2 V + \lambda_3 T_{max}^{STO} + \lambda_4 T_{max}^{STO} V + \lambda_5 V^2 \quad (27)$$

The data points for minimum storage costs at a given storage volume V and a given maximum storage temperature T_{max}^{STO} and the corresponding quadratic fit are shown in Fig. 8. A better fit could have been obtained using polynomials of higher order. However, in this case for terms including T_{max}^{STO} a linear fit was considered to ensure monotonic increase of storage costs. The values for steel density ($\rho_{steel} = 7850 \text{ kg/m}^3$) and maximum allowable stress ($\sigma_{steel} = 350 \text{ MPa}$) used within the

cost function derived for the pressurized water storage are based on typical values for stainless steel. The specific material costs ($c_{steel} = 6 \text{ €/kg}$) are a rough estimate that includes costs for manufacturing of the pressure vessels.

6. Examples

In this section, the proposed two step integration procedure is demonstrated by means of two case-studies.

The first case-study is a slightly adapted version of an example taken from Kemp [24]. The example consists of two hot and two cold process streams with different start and end times leading to 6 different operation periods. The process is assumed to be cyclic with a cycle duration of one hour and both direct and indirect heat recovery is possible. The stream data and the cost coefficients used for this case-study are presented in Table 1.

The second test case is taken from Jung et al. [25]. This problem was originally used to demonstrate a rescheduling algorithm. However, in this paper heat is recovered using FMVT heat storages. The example consists of five hot and eight cold process streams with different start and end times leading to 11 operation periods where at least one process stream is active. There are only two operating periods where hot and cold streams coexist, however, in these instances no direct heat recovery is possible due to the fact that the streams are condensing and evaporating at the same temperature and thus no sufficient driving temperature differences for direct heat exchange are present. The process is a batch process with a batch duration of 13.5 h. The stream data and cost coefficients are presented in Table 2.

TAM targets for these case-studies (Fig. 9) show that for both cases there is heat recovery potential at temperature levels above 100 °C and thus for integration of the presented pressurized water storages.

6.1. Model and solver parameters

In the first step, the proposed MINLP formulation for storage sizing (Model A) was used to simultaneously calculate storage sizes and the corresponding storage masses for up to three storages. This formulation

Table 2

Case-study 2: Stream data and cost coefficients.

	T^{in} (°C)	T^{out} (°C)	$\dot{m} c_p$ (kW/K)	Start (h)	End (h)
H1	105	80	7.648	1.5	1.75
H2	105	80	7.648	8.5	8.75
H3	120	119	536.5	11	13
H4	120	100	7.72	13	13.5
H5	128	127	273.4	3	6
C1	0	33	4.894	0	0.4
C2	0	33	4.894	7	7.4
C3	33	85	3.115	0.4	1
C4	33	85	3.115	7.4	8
C5	20	120	5.36	10.3	11
C6	119	120	536.5	11	13
C7	60	128	0.912	2	3
C8	127	128	273.4	3	6
UT h	150	150	-	-	-
UT c	10	15	-	-	-

Exchanger cost = $1600 + 210[A(m^2)]^\beta \text{€y}^{-1}$, $\beta = 0.95$, hot utility cost = 250 €kW^{-1} , cold utility cost = 25 €kW^{-1} , $\Delta T_{min} = 2.5 \text{ °C}$, heat transfer coefficients: $U = 0.5$, $U^{Th/c} = 0.5$, $U^{SCH/c} = 0.89 \text{ kW/m}^2 \text{ K}$, storage cost coefficients: $\lambda_1 = 6087$, $\lambda_2 = 2.65$, $\lambda_3 = 399.6$, $\lambda_4 = 2.11$, $\lambda_5 = -0.78$, storage material: $c_p = 4.24 \text{ kWh/kg}$, $\rho_s = 885.2 \text{ kg/m}^3$.

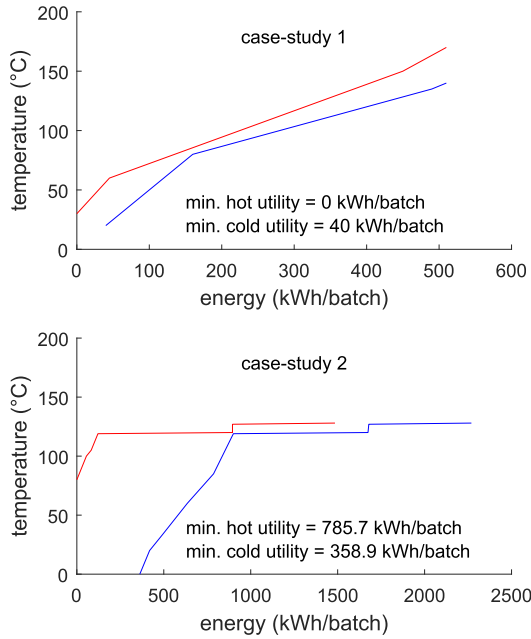


Fig. 9. TAM composite curves and utility targets for both case-studies.

Table 3

Case-study 1: Results for an annualization factor of $\gamma = 5$. Best values for TAC are highlighted in bold font.

sto	V^{TOT} m ³	V m ³	Sizing TAC €/y	HENS TAC €/y	HENS Q^{UTh} (kWh/b)	HENS T_{max}^{STO} °C
0	—	—	—	57,995	197.00	—
1	14.4	14.4	31,629	40,379	115.77	105.8
2	10.3	5.2	31,377	38,104	101.41	127.6
		5.1				105.9
3	8.7	3.0	32,184	39,053	100.00	112.8
		2.9				103.5
		2.8				132.9

was solved using global optimization solver BARON [26,27] with a relative gap of 10% as termination criteria.

In the second step, a linearized version of the extended superstructure formulation was solved with these fixed storage masses using the MILP solver CPLEX. The linearization was carried out using the approach proposed by Beck and Hofmann [28]. For cost calculation and to ensure physical feasibility HEX areas obtained with the linearized superstructure were then recalculated to correspond to their actual values.

The superstructure formulation was initialized with 3 temperature stages for heat exchangers connecting two process streams for case-study 1 and with 2 temperature stages for case-study 2. Heat exchangers connecting process streams and the ISCs could be placed in 5 and 4 stages respectively.

Different maximum storage temperatures were set for each case-study. For case-study 1 it was set to 160 °C whereas in case-study 2 it was set to 130 °C. These upper bounds for storage temperatures were set to be approximately the maximum possible supply temperatures that occur in the respective case studies. The vapour quality within the storages was set so it corresponds to 95% liquid water volume at the maximum storage temperatures. This means that the mixed density of water and steam within the storage ρ_s depends on the maximum allowed temperature in the storage. Function Eq. (27) was used for storage cost and the coefficients λ were adapted accordingly for each case-study. The used values for λ are presented in Tables 1 and 2.

6.2. Results for case-study 1

For case-study 1, The TAC obtained with the MINLP formulation for storage sizing and the TAC obtained with the extended superstructure formulation with fixed storage sizes for an annualization factor of $\gamma = 5$ are presented in Table 3. The best TAC for the storage sizing MINLP were obtained using two storages which resulted in slightly lower costs (31,377 €/y) compared to the solution for one storage system (31,629 €/y). Introduction of a third storage increased costs for the system to 32,184 €/y. In this case-study, the optimal total storage volume found by the solver decreases with an increasing number of storages.

In Fig. 10, a graphical representation of the solutions obtained for the sizing MINLP is presented. In this figure, the heat loads for the individual storages and the resulting end-temperatures are shown for

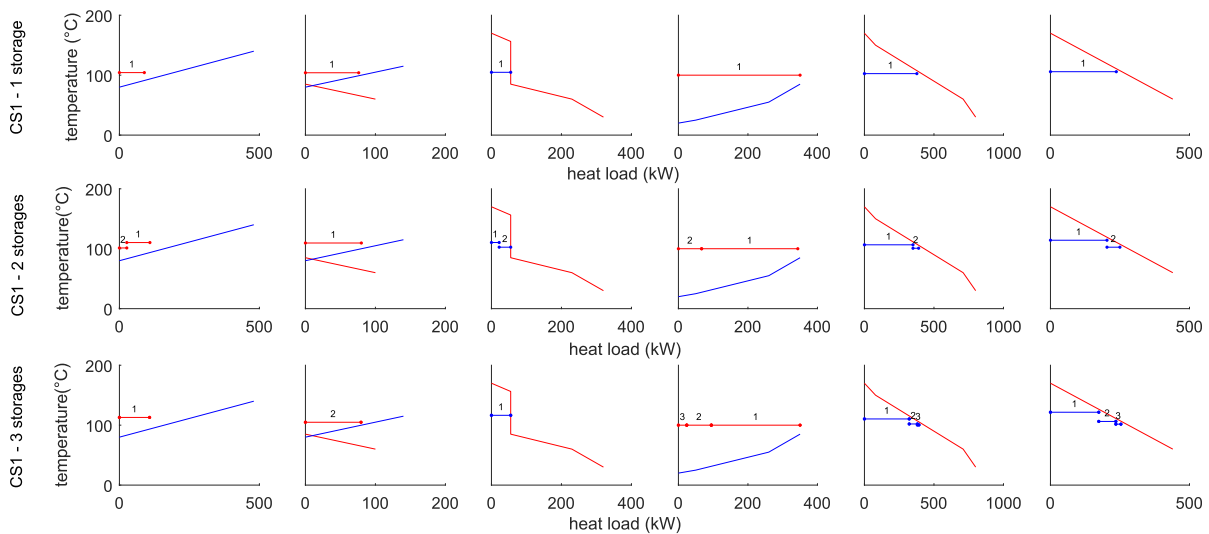


Fig. 10. Results for storage sizing MINLP formulation for case-study 1 and an annualization factor of $\gamma = 5$; numbered lines represent the respective storage temperatures and heat loads.

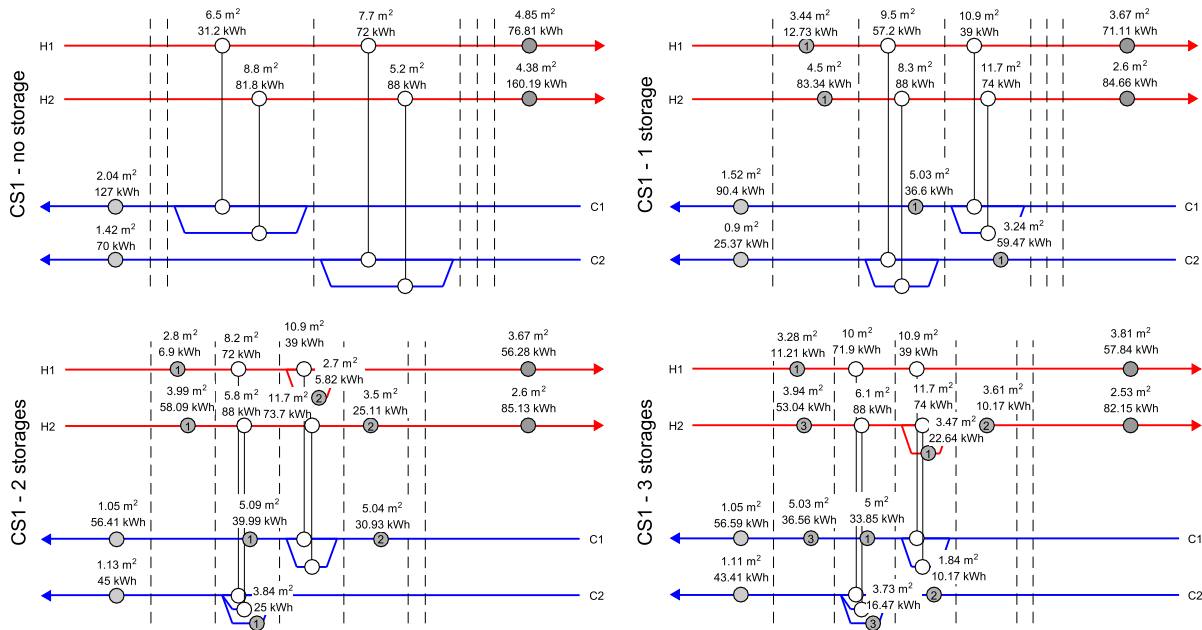


Fig. 11. HEN for case-study 1 and an annualization factor of $y = 5$; numbered HEX represent connections to the respective thermal energy storages.

Table 4

Case-study 2: Results for various annualization factors y . Best values for TAC for $y = 5$ are highlighted in bold font.

y	sto	V^{TOT} m ³	V m ³	T_{max}^{STO} °C	Sizing TAC €	HENS TAC €	HENS Q^{LTh} (kWh/b)
5	0	—	—	—	—	59,810	2,654
	1	17.41	17.41	125.0	43,299	54,817	2003
	2	21.44	3.99	124.8	43,835	56,816	1961
3	22.38	1.13	123.2	44,940	57,830	1983	
		3.89	115.9				
		17.36	121.5				
10	2	165.77	147.98	124.9	40,335	49,572	1530
			17.78	124.4			
15	2	279.65 ^a	250.00	124.7	35,435	42,401	1319
			29.65	116.6			
20	2	286.59 ^a	250.00	124.7	32,969	38,095	1298
			36.59	116.9			

^a At least one storage is at the volume limit of 250 m³.

each operating period. The maximum temperatures of the storage systems increase with the number of storages, which was expected as the feasible temperature range for smaller storage systems is higher compared to larger storages. Especially in the last operating period it becomes apparent that several smaller storages can fit the hot mGCC better and thus yield higher heat recovery potential. However, higher maximum storage temperatures also result in higher maximum pressures. This in return requires thicker storage walls and results in higher storage costs. Most storages in this case-study operate in a relatively low temperature range only slightly above 100 °C.

The results for the extended superstructure formulation show that for case-study 1 the introduction of one storage system improves the TAC from 57,995 €/y to 40,379 €/y. Introduction of a second storage

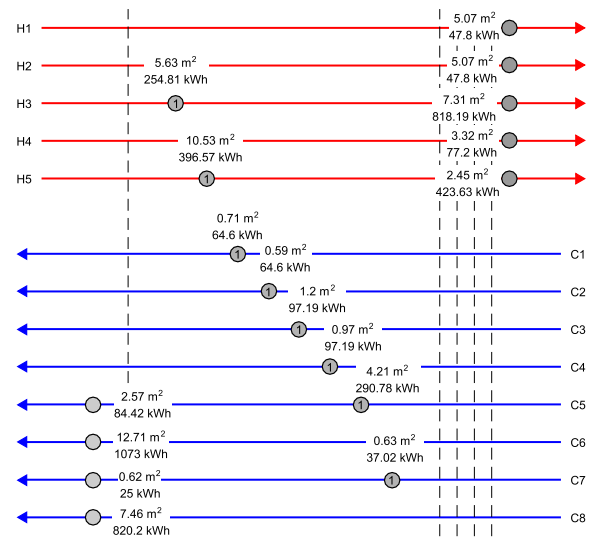


Fig. 12. HEN for case-study 2 and an annualization factor of 5; numbered HEX represent connections to the thermal energy storage.

yields slight improvements in terms of TAC (38,104 €/y) whereas the introduction of a third storage does not improve the solution any further (39,053 €/y). This corresponds to solutions for the storage sizing MINLP formulation where the TAC were also lowest using two storage systems. The optimal HENs obtained for different numbers of storages, also the complexity of the optimal HEN is increased. The HEN with the lowest TAC (two storages) uses 7 HEX to connect the ISCs and the process streams compared to 4 HEX when only one storage was

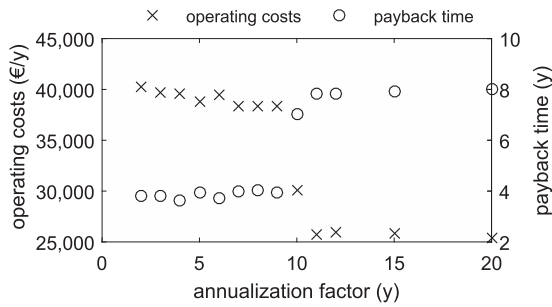


Fig. 13. Resulting operating costs and payback time for storage integration using two storages for case-study 2.

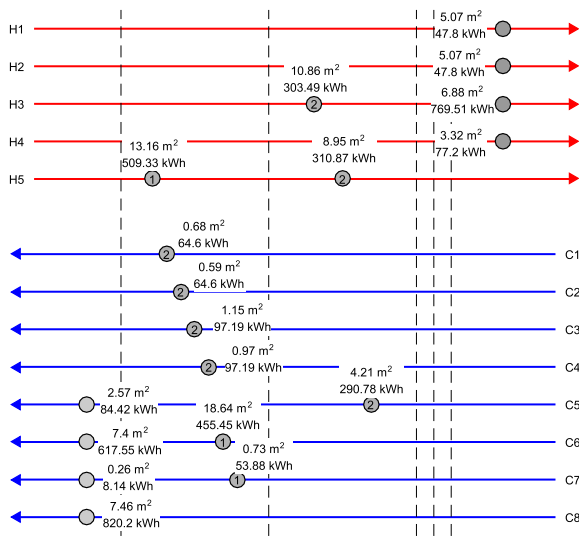


Fig. 14. HEN for case-study 2 and an annualization factor of 10; numbered HEX represent connections to the thermal energy storages.

considered. Introduction of a third storage increases the number of HEX to 8.

The demand for external heating Q^{UTh} is shown in Table 3. It can be seen that the introduction of a third storage system merely reduces the heating demand from 101.41 kWh/batch to 100 kWh/batch. Obviously investment costs in extra HEX and an additional storage vessel is not worthwhile and results in the highest TAC of all HEN including storages.

6.3. Results for case-study 2

The results for case-study 2 are presented in Table 4. For an annualization factor of $y = 5$ the results show that introduction of more than one storage system does not yield better TAC for both the MINLP formulation for storage sizing and the superstructure formulation and only slight improvements on utility consumption Q^{UTh} could be achieved. The HEN with the lowest TAC for an annualization factor of $y = 5$ is presented in Fig. 12. It uses one storage and improved the TAC from 59,810€/y to 54,817€/y. It needs to be mentioned that in this HEN the cold stream C6, which is an evaporating stream with an inlet temperature of 119 °C and an outlet temperature of 120 °C is not connected to the ISC. However, in the TAM composite curves shown in

Fig. 9 there is clearly heat recovery potential in this temperature range (almost horizontal cold composite curve). For this reason, the impact of the annualization factor on the optimal solutions found by the solvers was studied.

Table 4 shows that with two storages and an annualization factor of $y = 10$ the hot utility demand could be reduced to 1530 kWh/batch compared to 1961 kWh/batch obtained with an annualization factor of $y = 5$. An increase of the annualization factor to $y = 15$ yields further reduction of the hot utility demand to 1319 kWh/batch. However with $y = 15$ one of the storages reached the limit for storage volume of 250 m³. An increase of the annualization factor to $y = 20$ does not yield a significant further reduction of hot utility demand. If storage size would not have been constrained, even higher heat recovery would have been possible. In Fig. 13 the obtained operating costs and the resulting payback time for the investment in HEX and storages are presented for various annualization factors ranging from $y = 2$ to $y = 20$. Starting from an annualization factor of $y = 10$ significant reductions of operating costs could be achieved. However, payback periods increase significantly up to 8 years. Fig. 14 shows that for $y = 10$ the connection of stream C6 to one of the storage systems is economically feasible and the process stream H5 does not need external cooling.

7. Conclusion

In this paper, a novel approach for the integration of thermal energy storages with fixed mass and virable temperature was proposed. In the first step a novel MINLP formulation for storage sizing combining insights from pinch-analysis and mathematical programming is solved to obtain optimized storage sizes. Then, an extended superstructure formulation for HENS is initialized and solved with these fixed storage sizes.

The proposed formulation can be used for the integration of multiple storage systems which is demonstrated for pressurized water storages which are operated as closed loop systems.

By means of two case-studies taken from literature it could be shown that using the presented sequential approach FMVT storages can be integrated into heat recovery networks. The integration of multiple storages can yield cost benefits due to higher heat recovery potentials. However, at a certain point storage integration becomes economically infeasible if low payback times need to be obtained.

The results presented in this paper also show, that for optimization models minimizing TAC, the annualization factor plays an important role. For case study 2, an annualization factor of 10 and higher yields solutions for storage integration with considerably increased heat recovery up to 50%. However, payback time for equipment integration then goes up to values as high as 8 years, which might not be economically feasible for industrial application. This shows, that analysis of the impact of the annualization factor on payback-time can provide important information for energy efficiency projects.

For real-life implementation of the proposed pressurized water storages operability constraints need to be investigated in future works. Also, a control strategy for feasible operation of FMVT storages needs to be developed.

Acknowledgement

The idea of this paper and the corresponding work were initiated and realized by means of the endowed professorship through the cooperation between TU Wien and AIT Austrian Institute of Technology GmbH in the research area of Industrial Energy Systems.

Appendix A. Extended superstructure MINLP formulation

A.1. Objective function

$$\begin{aligned}
 \min TAC = & \underbrace{\sum_t \left(\sum_i c^{UTc} \dot{Q}_{it}^{UTc} + \sum_j c^{UTh} \dot{Q}_{jt}^{UTh} \right)}_{\text{energy costs}} \tau_t \\
 & + \underbrace{c^{fix} \left(\sum_i \sum_j \sum_k z_{ijk} + \sum_i z_i^{UTc} + \sum_j z_j^{UTh} \right)}_{\text{fixed costs for HEX connecting process streams and utility HEX}} \\
 & + \underbrace{c^{var} \left(\sum_i \sum_j \sum_k A_{ijk}^\beta + \sum_i A_i^{UTc \beta} + \sum_j A_j^{UTh \beta} \right)}_{\text{variable costs for HEX connecting process streams and utility HEX}} \\
 & + \underbrace{c^{fix} \left(\sum_s \left(\sum_i \sum_k z_{iks}^{IScC} + \sum_j \sum_k z_{jks}^{ISCh} \right) \right)}_{\text{fixed costs for HEX connecting streams to ISCs}} \\
 & + \underbrace{c^{var} \left(\sum_s \left(\sum_i A_{is}^{IScC \beta} + \sum_j A_{js}^{ISCh \beta} \right) \right)}_{\text{variable costs for HEX connecting streams to ISCs}} \\
 & + \underbrace{\sum_s C_s}_{\text{storage costs}} + \underbrace{c^{var} \sum_s A_s^{STO \beta}}_{\text{variable costs for storage HEX}} \\
 \forall s = 1, \dots, NOS, k = 1, \dots, NOK, t = 1, \dots, NOP, \\
 i \in HP, j \in CP.
 \end{aligned} \tag{A.1}$$

A.2. Constraints

Stream-wise energy balances:

$$\begin{aligned}
 (T_{it}^{in} - T_{it}^{out}) c_{p,it} \dot{m}_{it} = & \\
 \sum_k \sum_j \dot{Q}_{ykt} + \dot{Q}_{it}^{UTc} + \sum_k \sum_s \dot{Q}_{ikts}^{IScC}, & \\
 (T_{jt}^{out} - T_{jt}^{in}) c_{p,jt} \dot{m}_{jt} = & \\
 \sum_k \sum_i \dot{Q}_{ykt} + \dot{Q}_{jt}^{UTh} + \sum_k \sum_s \dot{Q}_{jks}^{ISCh}, & \\
 \forall t = 1, \dots, NOP, s = 1, \dots, NOS, k = 1, \dots, NOK, \\
 i \in HP, j \in CP
 \end{aligned} \tag{A.2}$$

Stage-wise energy balances:

$$\begin{aligned}
 \left(T_{ikt} - T_{i,k+1,t} \right) c_{p,it} \dot{m}_{it} = & \sum_j \dot{Q}_{ykt} + \sum_s \dot{Q}_{ikts}^{IScC}, \\
 \left(T_{jkt} - T_{j,k+1,t} \right) c_{p,jt} \dot{m}_{jt} = & \sum_i \dot{Q}_{ykt} + \sum_s \dot{Q}_{jks}^{ISCh} \\
 \forall t = 1, \dots, NOP, s = 1, \dots, NOS, k = 1, \dots, NOK, \\
 i \in HP, j \in CP
 \end{aligned} \tag{A.3}$$

Inlet temperatures:

$$\begin{aligned}
 T_{it}^{in} = T_{i,k=1,t}, \quad T_{jt}^{in} = T_{j,NOK+1,t} \\
 \forall t = 1, \dots, NOP, k = 1, \dots, NOK, i \in HP, j \in CP.
 \end{aligned} \tag{A.4}$$

Monotonic temperature decrease:

$$\begin{aligned}
 T_{ikt} \geq T_{i,k+1,t}, \quad T_{i,NOK+1,t} \geq T_{it}^{out}, \\
 \forall t = 1, \dots, NOP, k = 1, \dots, NOK, i \in HP
 \end{aligned} \tag{A.5}$$

$$\begin{aligned}
 T_{jkt} \geq T_{j,k+1,t}, \quad T_{jt}^{out} \geq T_{j,k=1,t} \\
 \forall t = 1, \dots, NOP, k = 1, \dots, NOK, j \in CP.
 \end{aligned} \tag{A.6}$$

Utility demands:

$$\begin{aligned}
 (T_{i,NOK+1,t} - T_{it}^{out}) c_{p,it} \dot{m}_{it} = \dot{Q}_{it}^{UTc} \\
 \forall t = 1, \dots, NOP, k = 1, \dots, NOK, i \in HP
 \end{aligned} \tag{A.7}$$

$$(T_{jt}^{out} - T_{j,k=1,t})c_{p,jt}\dot{m}_{jt} = \dot{Q}_{jt}^{UTH} \quad \forall t = 1, \dots, NOP, k = 1, \dots, NOK, j \in CP. \quad (A.8)$$

Logical constraints for heat loads:

$$\begin{aligned} \dot{Q}_{ijkt} - \Gamma_{ijt}^Q z_{ijkt} &\leq 0, \quad z_{ijk} \geq z_{ijkt}, \\ \dot{Q}_{it}^{UTc} - \Gamma_{it}^{Q,UTc} z_{it}^{UTc} &\leq 0, \quad z_i^{UTc} \geq z_{it}^{UTc}, \\ \dot{Q}_{jt}^{UTH} - \Gamma_{jt}^{Q,UTH} z_{jt}^{UTH} &\leq 0, \quad z_j^{UTH} \geq z_{jt}^{UTH}, \\ &\forall t = 1, \dots, NOP, k = 1, \dots, NOK, i \in HP, j \in CP \end{aligned} \quad (A.9)$$

Temperature differences:

$$\begin{aligned} \Delta T_{ijkt} &\leq T_{ikt} - T_{jkt} + \Gamma_{ijt}^T (1 - z_{ijkt}), \\ \Delta T_{ij,k+1,t} &\leq T_{i,k+1,t} - T_{j,k+1,t} + \Gamma_{ijt}^T (1 - z_{ijkt}), \\ \Delta T_{it}^{UTc} &\leq T_{i,NOK+1,t} - T^{UTc,out} + \Gamma_{it}^{T,UTc} (1 - z_{it}^{UTc}), \\ \Delta T_{jt}^{UTH} &\leq T^{UTH,out} - T_{j,k=1,t} + \Gamma_{jt}^{T,UTH} (1 - z_{jt}^{UTH}), \\ &\forall t = 1, \dots, NOP, s = 1, \dots, NOS, k = 1, \dots, NOK, \\ &\quad i \in HP, j \in CP. \end{aligned} \quad (A.10)$$

Minimum temperature differences:

$$\begin{aligned} \Delta T_{ijkt} &\geq \Delta T_{min}, \quad \Delta T_{it}^{UTc} \geq \Delta T_{min}, \quad \Delta T_{jt}^{UTH} \geq \Delta T_{min}, \\ &\forall t = 1, \dots, NOP, s = 1, \dots, NOS, k = 1, \dots, NOK, \\ &\quad i \in HP, j \in CP \end{aligned} \quad (A.11)$$

Logarithmic mean temperature differences (Chen approximation [29]):

$$\begin{aligned} LMTD_{ijkt} &= \left(\Delta T_{ijkt} \Delta T_{ij,k+1,t} \frac{\Delta T_{ijkt} + \Delta T_{ij,k+1,t}}{2} \right)^{\frac{1}{3}}, \\ LMTD_{it}^{UTc} &= \left(\Delta T_{it}^{UTc} \left(T_{it}^{out} - T^{UTc,in} \right) \frac{\Delta T_{it}^{UTc} + (T_{it}^{out} - T^{UTc,in})}{2} \right)^{\frac{1}{3}}, \\ LMTD_{jt}^{UTH} &= \left(\Delta T_{jt}^{UTH} \left(T^{UTH,in} - T_{jt}^{out} \right) \frac{\Delta T_{jt}^{UTH} + (T^{UTH,in} - T_{jt}^{out})}{2} \right)^{\frac{1}{3}}, \\ &\forall t = 1, \dots, NOP, k = 1, \dots, NOK, \\ &\quad i \in HP, j \in CP \end{aligned} \quad (A.12)$$

Minimum temperature differences LMTD:

$$\begin{aligned} LMTD_{ijkt} &\geq \Delta T_{min}, \\ LMTD_{it}^{UTc} &\geq \Delta T_{min}, \quad LMTD_{jt}^{UTH} \geq \Delta T_{min}, \\ &\forall t = 1, \dots, NOP, s = 1, \dots, NOS, k = 1, \dots, NOK, \\ &\quad i \in HP, j \in CP \end{aligned} \quad (A.13)$$

HEX areas:

$$A_{ijk} \geq \frac{\dot{Q}_{ijkt}}{U_{ijkt} LMTD_{ijkt}}, \quad \forall t = 1, \dots, NOP, k = 1, \dots, NOK, i \in HP, j \in CP \quad (A.14)$$

$$A_i^{UTc} \geq \frac{\dot{Q}_i^{UTc}}{U_i^{UTc} LMTD_{it}^{UTc}}, \quad A_j^{UTH} \geq \frac{\dot{Q}_j^{UTH}}{U_j^{UTH} LMTD_{jt}^{UTH}}, \quad \forall t = 1, \dots, NOP, s = 1, \dots, NOS, k = 1, \dots, NOK, i \in HP, j \in CP. \quad (A.15)$$

Heat loads ISC:

$$\begin{aligned} \dot{Q}_{ikst}^{ISC} - \Gamma_{it}^{Q,ISC} z_{ikst}^{ISC} &\leq 0, \quad z_{iks}^{ISC} \geq z_{ikst}^{ISC}, \\ \dot{Q}_{jkst}^{ISCh} - \Gamma_{jt}^{Q,ISCh} z_{jkst}^{ISCh} &\leq 0, \quad z_{jks}^{ISCh} \geq z_{jkst}^{ISCh}, \\ &\forall t = 1, \dots, NOP, s = 1, \dots, NOS, k = 1, \dots, NOK, \\ &\quad i \in HP, j \in CP. \end{aligned} \quad (A.16)$$

Logical constraints for heat loads ISC:

$$\begin{aligned} \sum_k \dot{Q}_{ikst}^{IScC} &\leq \Gamma_i^{Q,IScC} \left(1 - z_{st}^{switch}\right), \\ \sum_k \dot{Q}_{jkst}^{ISCh} &\leq \Gamma_j^{Q,ISCh} (z_{st}^{switch}), \\ \forall t = 1, \dots, NOP, s = 1, \dots, NOS, k = 1, \dots, NOK, \\ i &\in HP, j \in CP. \end{aligned} \quad (A.17)$$

Temperature differences ISC:

$$\begin{aligned} \Delta T_{jst}^{ISCh1} &\leq T_{st}^{ISc,in} - T_{jkt} + \Gamma_{js}^{T,ISc} (1 - z_{jkst}^{ISCh}), \\ \Delta T_{jst}^{ISCh2} &\leq T_{st}^{ISc,out} - T_{j,k+1,t} + \Gamma_{js}^{T,ISc} (1 - z_{jkst}^{ISCh}), \\ \Delta T_{ist}^{IScC1} &\leq T_{ikt} - T_{st}^{ISc,in} + \Gamma_{is}^{T,ISc} (1 - z_{ikst}^{IScC}), \\ \Delta T_{ist}^{IScC2} &\leq T_{i,k+1,t} - T_{st}^{ISc,out} + \Gamma_{is}^{T,ISc} (1 - z_{ikst}^{IScC}), \\ \forall t = 1, \dots, NOP, s = 1, \dots, NOS, k = 1, \dots, NOK, \\ i &\in P, j \in CP. \end{aligned} \quad (A.18)$$

Minimum temperature differences ISC:

$$\begin{aligned} \Delta T_{ist}^{IScC1} &\geq \Delta T_{min}, \quad \Delta T_{jst}^{ISCh1} \geq \Delta T_{min}, \\ \Delta T_{ist}^{IScC2} &\geq \Delta T_{min}, \quad \Delta T_{jst}^{ISCh2} \geq \Delta T_{min}, \\ \forall t = 1, \dots, NOP, s = 1, \dots, NOS, k = 1, \dots, NOK, \\ i &\in HP, j \in CP \end{aligned} \quad (A.19)$$

Logarithmic mean temperature differences ISC (Chen approximation [29]):

$$\begin{aligned} LMTD_{ist}^{IScC} &\leq \\ &\left(\Delta T_{ist}^{IScC1} \Delta T_{ist}^{IScC2} \frac{\Delta T_{ist}^{IScC1} + \Delta T_{ist}^{IScC2}}{2} \right)^{\frac{1}{3}}, \\ \forall t = 1, \dots, NOP, s = 1, \dots, NOS, k = 1, \dots, NOK, \\ i &\in HP \end{aligned} \quad (A.20)$$

$$\begin{aligned} LMTD_{jst}^{ISCh} &\leq \\ &\left(\Delta T_{jst}^{ISCh1} \Delta T_{jst}^{ISCh2} \frac{\Delta T_{jst}^{ISCh1} + \Delta T_{jst}^{ISCh2}}{2} \right)^{\frac{1}{3}}, \\ \forall t = 1, \dots, NOP, s = 1, \dots, NOS, k = 1, \dots, NOK, \\ j &\in CP. \end{aligned} \quad (A.21)$$

Minimum temperature differences LMTD ISC:

$$\begin{aligned} LMTD_{ist}^{IScC} &\geq \Delta T_{min}, \quad LMTD_{jst}^{ISCh} \geq \Delta T_{min}, \\ \forall t = 1, \dots, NOP, s = 1, \dots, NOS, k = 1, \dots, NOK, \\ i &\in HP, j \in CP \end{aligned} \quad (A.22)$$

Constraints for number of HEX for ISC:

$$\begin{aligned} \sum_k z_{ikst}^{IScC} &\leq 1, \quad \sum_k z_{jkst}^{ISCh} \leq 1, \\ \forall t = 1, \dots, NOP, s = 1, \dots, NOS, k = 1, \dots, NOK, \\ i &\in HP, j \in CP. \end{aligned} \quad (A.23)$$

Heat exchanger areas ISC:

$$\begin{aligned} A_{is}^{IScC} &\geq \frac{\sum_k \dot{Q}_{ikst}^{IScC}}{U_{is}^{IScC} LMTD_{ist}^{IScC}}, \\ \forall t = 1, \dots, NOP, s = 1, \dots, NOS, \\ k = 1, \dots, NOK, i &\in HP \end{aligned} \quad (A.24)$$

$$\begin{aligned} A_{js}^{ISCh} &\geq \frac{\sum_k \dot{Q}_{jkst}^{ISCh}}{U_{js}^{ISCh} LMTD_{jst}^{ISCh}}, \\ \forall t = 1, \dots, NOP, s = 1, \dots, NOS, \\ k = 1, \dots, NOK, j &\in CP. \end{aligned} \quad (A.25)$$

Heat transfer area inside indirect storages:

$$A_s^{STO} \geq \frac{\sum_i \dot{Q}_{st}^{ISCc} + \sum_j \dot{Q}_{st}^{ISCh}}{U_s^{STO} LMTD_{st}^{STO}}$$

$$\forall t = 1, \dots, NOP, s = 1, \dots, NOS, k = 1, \dots, NOK,$$

$$i \in HP, j \in CP. \quad (A.26)$$

Temperature difference inside the storages:

$$\Delta T_{st}^{STOh1} \leq T_{st}^{ISC,in} - T_{st}^{STO} + \Gamma^{STO}(z_{st}^{switch}),$$

$$\Delta T_{st}^{STOh2} \leq T_{st}^{ISC,out} - T_{st}^{STO} + \Gamma^{STO}(z_{st}^{switch}),$$

$$\Delta T_{st}^{STOc1} \leq T_{st}^{STO} - T_{st}^{ISC,in} + \Gamma^{STO}(1 - z_{st}^{switch}),$$

$$\Delta T_{st}^{STOc2} \leq T_{st}^{STO} - T_{st}^{ISC,out} + \Gamma^{STO}(1 - z_{st}^{switch}),$$

$$\forall t = 1, \dots, NOP, s = 1, \dots, NOS, \quad (A.27)$$

Logarithmic temperature difference inside the storages (Chen approximation [29]):

$$LMTD_{st}^{STO} \leq \left(\Delta T_{st}^{STOh1} \Delta T_{st}^{STOh2} \frac{\Delta T_{st}^{STOh1} + \Delta T_{st}^{STOh2}}{2} \right)^{\frac{1}{3}},$$

$$LMTD_{st}^{STO} \leq \left(\Delta T_{st}^{STOc1} \Delta T_{st}^{STOc2} \frac{\Delta T_{st}^{STOc1} + \Delta T_{st}^{STOc2}}{2} \right)^{\frac{1}{3}},$$

$$\forall t = 1, \dots, NOP, s = 1, \dots, NOS, \quad (A.28)$$

In addition, constraints that describe the thermodynamic state of the storages and the connection between storage and ISC are necessary (Eqs. (6) and (7)).

Appendix B. Storage sizing MINLP formulation

Heat load constraints (mGCC):

$$\dot{Q}_{st}^{SCCh} \leq a_{m_t} + b_{m_t} T_{st}^{STO} + \sum_{\tilde{m}_t=1}^{M_t} x_{\tilde{m}_t,t} \Gamma_{\tilde{m}_t,t},$$

$$\forall s = 1, \dots, NOS, t = 1, \dots, NOP, m_t = 1, \dots, M_t, \quad (B.1)$$

$$\dot{Q}_{st}^{SCCc} \leq a_{n_t} + b_{n_t} T_{st}^{STO} + \sum_{\tilde{n}_t=1}^{N_t} x_{\tilde{n}_t,t} \Gamma_{\tilde{n}_t,t},$$

$$\forall s = 1, \dots, NOS, t = 1, \dots, NOP, n_t = 1, \dots, N_t. \quad (B.2)$$

The MINLP formulation can be formulated in a compact way, if Γ_{n_t} and Γ_{m_t} are chosen appropriately.

Constraints for activity of mGCC segments:

$$\sum_{m_t} x_{m_t} = 1, \quad \sum_{n_t} x_{n_t} = 1,$$

$$\forall t = 1, \dots, NOP, n_t = 1, \dots, N_t, m_t = 1, \dots, M_t. \quad (B.3)$$

Utilities demand:

$$\dot{Q}_t^{TOTh} = \sum_s \dot{Q}_{st}^{ISCh} + \dot{Q}_t^{UTh},$$

$$\forall t = 1, \dots, NOP, s = 1, \dots, NOS, \quad (B.4)$$

$$\dot{Q}_t^{TOTc} = \sum_s \dot{Q}_{st}^{ISCc} + \dot{Q}_t^{UTc},$$

$$\forall t = 1, \dots, NOP, s = 1, \dots, NOS. \quad (B.5)$$

B.1. Model A

Monotonic temperature decrease:

$$T_{st}^{STO} > T_{s+1,t}^{STO}, \quad \forall s = 1, \dots, NOS - 1, t = 1, \dots, NOP \quad (B.6)$$

Cumulated storage heat loads:

$$T_{st}^{SCC} = T_{st}^{STO}, \quad \forall s = 1, \dots, NOS, t = 1, \dots, NOP \quad (B.7)$$

$$\dot{Q}_{st}^{SCCc} = \sum_{s^*=1}^s \dot{Q}_{s^*t}^{ISCc},$$

$$\forall s, s^* = 1, \dots, NOS, t = 1, \dots, NOP \quad (B.8)$$

$$\dot{Q}_{st}^{SCCh} = \sum_{s^*=1}^s \dot{Q}_{NOS+1-s^*,t}^{ISCh}, \quad \forall s, s^* = 1, \dots, NOS, t = 1, \dots, NOP \quad (B.9)$$

B.2. Model B

Cumulated storage heat loads and temperature cascade:

For $s = 1$:

$$\dot{Q}_{st}^{SCCc} \geq \dot{Q}_{s^*,t}^{ISCc} + (y_{s,s^*,t}^{ass} - 1)\dot{Q}_{max,t}, \quad \forall s, s^* = 1, \dots, NOS, t = 1, \dots, NOP \quad (B.10)$$

$$\dot{Q}_{st}^{SCCh} \geq \dot{Q}_{s^*,t}^{ISCh} + (y_{NOS+1-s^*,t}^{ass} - 1)\dot{Q}_{max,t}, \quad \forall s, s^* = 1, \dots, NOS, t = 1, \dots, NOP \quad (B.11)$$

$$T_{st}^{SCC} \geq T_{s^*,t}^{STO} + (y_{s,s^*,t}^{ass} - 1)\Delta T_{max}, \quad \forall s, s^* = 1, \dots, NOS, t = 1, \dots, NOP \quad (B.12)$$

For $1 < s < NOS$:

$$\dot{Q}_{st}^{SCCc} \geq \dot{Q}_{s-1,t}^{SCCc} + \dot{Q}_{s^*,t}^{ISCc} + (y_{s,s^*,t}^{ass} - 1)\dot{Q}_{max,t}, \quad \forall s, s^* = 1, \dots, NOS, t = 1, \dots, NOP \quad (B.13)$$

$$\dot{Q}_{st}^{SCCh} \geq \dot{Q}_{s-1,t}^{SCCh} + \dot{Q}_{s^*,t}^{ISCh} + (y_{NOS+1-s^*,t}^{ass} - 1)\dot{Q}_{max,t}, \quad \forall s, s^* = 1, \dots, NOS, t = 1, \dots, NOP \quad (B.14)$$

$$T_{st}^{SCC} \geq T_{s^*,t}^{STO} + (y_{s,s^*,t}^{ass} - 1)\Delta T_{max}, \quad \forall s, s^* = 1, \dots, NOS, t = 1, \dots, NOP \quad (B.15)$$

For $s = NOS$:

$$\dot{Q}_{st}^{SCCc} \geq \sum_{s^*} \dot{Q}_{s^*,t}^{ISCc}, \quad \forall s, s^* = 1, \dots, NOS, t = 1, \dots, NOP \quad (B.16)$$

$$\dot{Q}_{st}^{SCCh} \geq \sum_{s^*} \dot{Q}_{s^*,t}^{ISCh}, \quad \forall s, s^* = 1, \dots, NOS, t = 1, \dots, NOP \quad (B.17)$$

$$T_{st}^{SCC} \geq T_{s^*,t}^{STO}, \quad \forall s, s^* = 1, \dots, NOS, t = 1, \dots, NOP \quad (B.18)$$

Constraints for assignment matrices:

$$\sum_s y_{s,s^*,t}^{ass} = 1, \quad \sum_{s^*} y_{s,s^*,t}^{ass} = 1, \quad \forall s, s^* = 1, \dots, NOS, t = 1, \dots, NOP \quad (B.19)$$

References

- [1] C. R. Wolfgang Eichhammer, Enhancing the impact of energy audits and energy management in the European Union: a review of article 8 of the energy efficiency directive, The European Council for an Energy Efficient Economy (eceee) & Fraunhofer ISI, 2016.
- [2] M. Morar, P.S. Agachi, Review: important contributions in development and improvement of the heat integration techniques, *Comput. Chem. Eng.* 34 (8) (2010) 1171–1179, <https://doi.org/10.1016/j.compchemeng.2010.02.038>.
- [3] J.J. Klemes, P.S. Varbanov, P. Kapustenko, New developments in heat integration and intensification, including total site, waste-to-energy, supply chains and fundamental concepts, *Appl. Therm. Eng.* 61 (1) (2013) 1–6, <https://doi.org/10.1016/j.applthermaleng.2013.05.003>.
- [4] I. Fernández, C.J. Renedo, S.F. Pérez, A. Ortiz, M. Mañana, A review: energy recovery in batch processes, *Renew. Sustain. Energy Rev.* 16 (4) (2012) 2260–2277, <https://doi.org/10.1016/j.rser.2012.01.017>.
- [5] S. Stoltze, J. Mikkelsen, B. Lorentzen, P. Peterson, B. Qvale, Waste-heat recovery in batch process using heat storage, *J. Energy Resour. Technol.* 117 (2) (1995) 142–149.
- [6] R. De Boer, S. Smeding, P. Bach, G. de Jooide, Heat storage systems for use in an industrial batch process: (results of) a case study, in: 10th International Conference on Thermal Energy Storage, ECOSTOCK, Stockton, NJ, USA, 2006.
- [7] P. Krummenacher, D. Favrat, Indirect and mixed direct-indirect heat integration of batch processes based on pinch analysis, *Int. J. Appl. Thermodynam.* (4) (2001) 135–143.
- [8] A. Anastasovski, Design of heat storage units for use in repeatable time slices, *Appl. Therm. Eng.* 112 (2017) 1590–1600, <https://doi.org/10.1016/j.applthermaleng.2016.10.086>.
- [9] T.G. Walmsley, M.R. Walmsley, M.J. Atkins, J.R. Neale, Integration of industrial solar and gaseous waste heat into heat recovery loops using constant and variable temperature storage, *Energy* 75 (2014) 53–67, <https://doi.org/10.1016/j.energy.2014.01.103>.
- [10] C.-L. Chen, Y.-J. Ciou, Design and optimization of indirect energy storage systems for batch process plants, *Ind. Eng. Chem. Res.* 47 (14) (2008) 4817–4829, <https://doi.org/10.1021/ie0710667>.
- [11] N. Sebelebe, T. Majoji, Heat integration of multipurpose batch plants through multiple heat storage vessels, *Comput. Chem. Eng.* 106 (2017) 269–285, <https://doi.org/10.1016/j.compchemeng.2017.06.007>.
- [12] P. Yang, L.-L. Liu, J. Du, J.-L. Li, Q.-w. Meng, Heat exchanger network synthesis for batch processes by involving heat storages with cost targets, *Appl. Therm. Eng.* 70 (2) (2014) 1276–1282, <https://doi.org/10.1016/j.applthermaleng.2014.05.041>.
- [13] T.F. Yee, I.E. Grossmann, Simultaneous optimization models for heat integration-ii. heat exchanger network synthesis, *Comput. Chem. Eng.* 14 (10) (1990) 1165–1184.
- [14] K.C. Furman, N.V. Sahinidis, Computational complexity of heat exchanger network synthesis, *Comput. Chem. Eng.* 25 (9-10) (2001) 1371–1390, [https://doi.org/10.1016/S0098-5266\(01\)00137-1](https://doi.org/10.1016/S0098-5266(01)00137-1).

- 1016/S0098-1354(01)00681-0.
- [15] G.N. Kulkarni, S.B. Kedare, S. Bandyopadhyay, Design of solar thermal systems utilizing pressurized hot water storage for industrial applications, *Sol. Energy* 82 (8) (2008) 686–699, <https://doi.org/10.1016/j.solener.2008.02.011>.
- [16] A. Beck, R. Hofmann, Extensions for multi-period minlp superstructure formulation for integration of thermal energy storages in industrial processes, in: A. Friedl, J.J. Klemeš, S. Radl, P.S. Varbanov, T. Wallek (Eds.), 28th European Symposium on Computer Aided Process Engineering, *Computer Aided Chemical Engineering*, vol. 43, Elsevier, 2018, pp. 1335–1340, <https://doi.org/10.1016/B978-0-444-64235-6.50234-5>.
- [17] W.V.N. Zhang, Design of flexible heat exchanger network for multi-period operation, *Chem. Eng. Sci.* 61 (23) (2006) 7730–7753, <https://doi.org/10.1016/j.ces.2006.08.043>.
- [18] M. Escobar, J.O. Trierweiler, Optimal heat exchanger network synthesis: a case study comparison, *Appl. Therm. Eng.* 51 (1–2) (2013) 801–826, <https://doi.org/10.1016/j.applthermaleng.2012.10.022>.
- [19] A. Ciric, C. Floudas, Heat exchanger network synthesis without decomposition, *Comput. Chem. Eng.* 15 (6) (1991) 385–396, [https://doi.org/10.1016/0098-1354\(91\)87017-4](https://doi.org/10.1016/0098-1354(91)87017-4).
- [20] S. Bandyopadhyay, J. Varghese, V. Bansal, Targeting for cogeneration potential through total site integration, *Appl. Therm. Eng.* 30 (1) (2010) 6–14, <https://doi.org/10.1016/j.applthermaleng.2009.03.007>.
- [21] F. Trespalacios, I.E. Grossmann, Improved big-m reformulation for generalized disjunctive programs, *Comput. Chem. Eng.* 76 (2015) 98–103.
- [22] I.H. Bell, J. Wronski, S. Quoilin, V. Lemort, Pure and pseudo-pure fluid thermo-physical property evaluation and the open-source thermophysical property library coolprop, *Ind. Eng. Chem. Res.* 53 (6) (2014) 2498–2508, <https://doi.org/10.1021/ie4033999> arXiv:<http://pubs.acs.org/doi/pdf/10.1021/ie4033999>.
- [23] S. Schwaigerer, G. Mühlenbeck, *Festigkeitsberechnung: im Dampfkessel-, Behälter- und Rohrleitungsbau*, Springer, Berlin Heidelberg, 2013.
- [24] I.C. Kemp, *Pinch Analysis and Process Integration*, Elsevier, 2007, <https://doi.org/10.1016/B978-0-7506-8260-2.X5001-9>.
- [25] S.-H. Jung, I.-B. Lee, D.R. Yang, K.S. Chang, Synthesis of maximum energy recovery networks in batch processes, *Kor. J. Chem. Eng.* 11 (3) (1994) 162–171, <https://doi.org/10.1007/BF02697461>.
- [26] M. Tawarmalani, N.V. Sahinidis, A polyhedral branch-and-cut approach to global optimization, *Math. Program.* 103 (2005) 225–249.
- [27] N.V. Sahinidis, BARON 14.3.1: Global Optimization of Mixed-Integer Nonlinear Programs, *User's Manual*, 2014.
- [28] A. Beck, R. Hofmann, A novel approach for linearization of a minlp stage-wise superstructure formulation, *Comput. Chem. Eng.* 112 (2018) 17–26, <https://doi.org/10.1016/j.compchemeng.2018.01.010>.
- [29] J. Chen, Comments on improvements on a replacement for the logarithmic mean, *Chem. Eng. Sci.* 42 (10) (1987) 2488–2489, [https://doi.org/10.1016/0009-2509\(87\)80128-8](https://doi.org/10.1016/0009-2509(87)80128-8).

5.6 Paper 6

Full paper conference contribution in
Proceedings of the International Sustainable Energy Conference 2018

PROCESS INTEGRATION IN A DAIRY FACTORY CONSIDERING THERMAL ENERGY STORAGES – A COMPARISON OF TWO DIFFERENT APPROACHES

Anton Beck^a, Wolfgang Glatzl^b, Jürgen Fluch^b, René Hofmann^{*,a,c}

^a Austrian Institute of Technology GmbH, Center for Energy, Giefinggasse 2, A-1210 Vienna, Austria

^b AEE - INTEC, Industrial Processes and Energy Systems, Feldgasse 19, A-8200 Gleisdorf, Austria

^c TU Wien, Institute for Energy Systems and Thermodynamics, Getreidemarkt 9/BA, A-1060 Vienna, Austria

*Phone: +

*E-Mail: rene.hofmann@tuwien.ac.at / rene.hofmann@ait.ac.at

1 ABSTRACT

In this paper, heat integration for a dairy factory is performed using two different approaches with storage integration capabilities. The use-case consists of 36 process streams which can be considered large-scale. Stream data is available for a period of three weeks with high temporal resolution. Even though a slightly different data basis is needed, both approaches yield comparable results which are analyzed in this paper. The first approach considered in this work is the software tool SOCO which is based on pinch-analysis for time-dependent process streams. It incorporates a flowsheet simulation environment for detailed storage simulation. The second approach is based on mathematical programming and cost-driven superstructure optimization using simple storage models. The best results obtained using both approaches are compared regarding heat exchanger networks, storage integration and economic data. Also, potential synergies between the two approaches are identified that could further improve solutions.

2 INTRODUCTION

Heat integration with the goal of reducing energy consumption and costs has been a research topic for several decades now (Kemp, 2007). Since process integration became a major topic in process engineering, two distinct approaches were intensively studied. On the one hand graphical approaches based on composite curves and the idea of the pinch point were developed and on the other hand mathematical optimization formulations were used to find optimal process integration solutions by minimization of either energy consumption or costs. Heat integration in batch and time-dependent processes has been a topic of scientific interest since the 1980s but only since the turn of the century storage integration has been intensively studied.

For solving time-dependent problems, complex optimization principles are needed. There are two major approaches to overcome non-simultaneous heating and cooling demands - rescheduling of process tasks and heat integration using thermal energy storages (TES). Generally, TES are indispensable and necessary for significantly increasing the resource and energy efficiencies in complex and volatile energy systems. Anastasovski (2017) used Pinch Technology for the integration of two-tank storage systems under economic considerations. Storage costs are optimized by variation of storage parameters and temperature differences. Another approach for storage integration using Pinch Analysis methods was proposed by Krummenacher (2001). A method was proposed that allows to identify the minimum number of storage tanks for a given heat recovery. This method was later on implemented in the process integration software PinCH (Olsen, et al., 2016). Opposed to integration methods based on Pinch Analysis Chen and Ciou (2008) proposed a MINLP superstructure formulation for cost-efficient indirect heat recovery using TES. Also, a sequential design procedure for heat exchanger network synthesis (HENS) with selection of an optimal utility system and storage integration was proposed by Mian et al. (2016). They tried to overcome the drawbacks of the sequential approach by applying a derivative-free hybrid algorithm.

3 PROBLEM STATEMENT

For the integration of TES several approaches with different capabilities have been presented in the past, which have not been thoroughly compared. Within the framework of the IEA IETS Annex 15¹ the project partners AIT and AEE INTEC have developed methods for heat integration with storage capabilities. These methods should be compared and potential synergies should be demonstrated based on a real dairy factory. This use-case can be considered large-scale as it consists of 14 cold and 22 hot process streams. Most of the process streams are discontinuous and some also change start and target temperatures as well as mass flows when active, resulting in a difficult problem for HENS with storage integration.

4 STORAGE INTEGRATION METHODS

The two approaches compared in this paper are AEE INTEC's Storage Optimisation Concepts (SOCO) (Muster-Slawitsch, et al., 2014) and the mathematical programming (MP) framework for heat integration developed by the AIT which are presented in the following. Although these approaches are inherently different, both yield comparable energy recovery systems. A flowchart representation for the individual steps and the corresponding input data is presented in Figure 1.

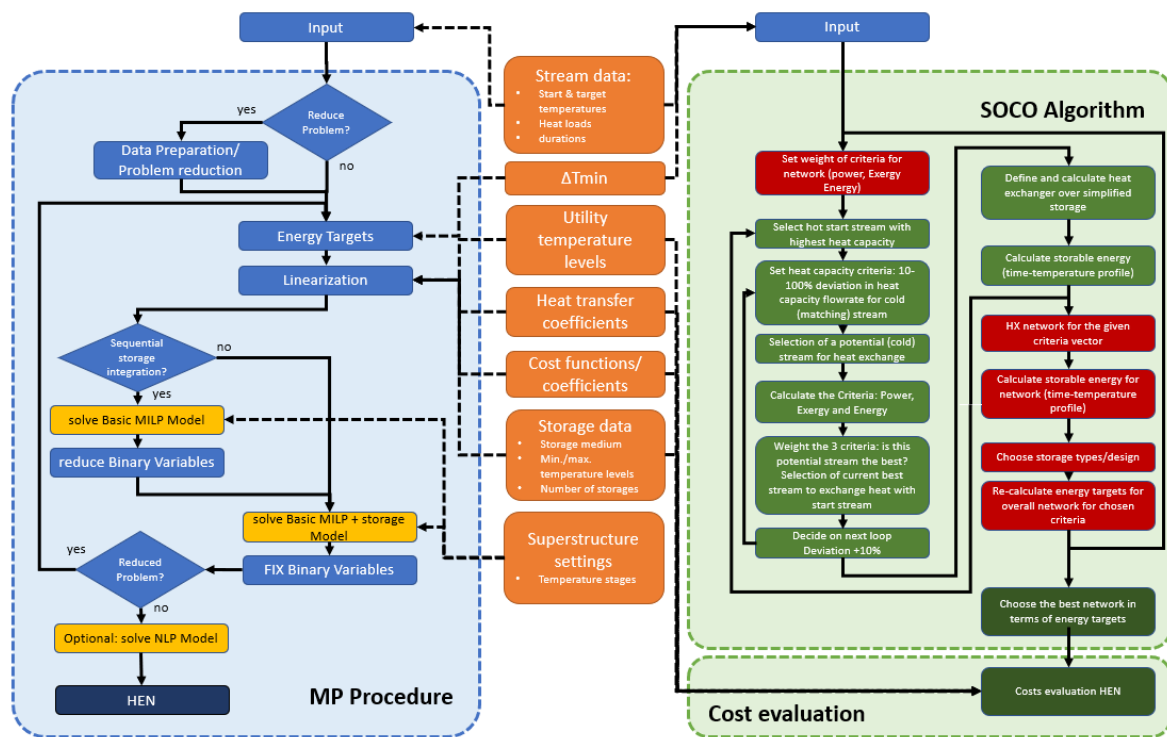


Figure 1: Flowchart SOCO-algorithm and MP procedure

4.1 SOCO

SOCO is a compiled planning tool for optimization and design of heat exchanger and thermal storage systems in complex thermal energy systems that allows to perform heat integration based on Pinch Analysis for time-dependent streams. The SOCO algorithm has been presented by Fluch et al. (2012). The workflow for SOCO can be divided into the following steps:

¹ The IETS (Industrial Energy-Related Technologies and Systems) program unites the IEA (International Energy Agency) activities in this area. The work is organized in Annexes. Annex 15 Phase 2 is the second task on "Industrial Excess Heat Recovery".

1. **Stream data import:** Stream data can be prepared in a suitable spreadsheet template and then imported to SOCO. Temperatures and mass flow can vary in each time step and thus provide full flexibility in the definition of all streams.
2. **HEN Proposal** Based on a deterministic Pinch algorithm (Fluch, et al., 2012) all possible stream combinations are evaluated with and without heat storage. The procedure is re-iterated and the best HEN in terms of total energy recovery, heat exchanger power installed and exergetic use of available streams is selected. The HEN proposal allows the definition of boundary conditions for equipment like minimal and maximal storage size.
3. **HX and heat storage modification:** The proposed heat exchanger and heat storages can be modified manually by the user. The heat storage can be parameterized with volume, insulation (top, mantle, bottom), wall thickness and up to 20 ports with height, shape and diameter.
4. **HEN Design:** SOCO has a build-in flowsheet which allows the design of the HEN as proposed (in step 2) and modified (in step 3). All limitations that were not included in HEN proposal algorithm can now be considered by the planner (e.g. actual location of streams; combinations of multiple proposed heat storages with similar temperature profiles to one heat storage)
5. **HEN Simulation:** The designed HEN in the flowsheet can be simulated. By going back to step 3, the HX and heat storages can be further modified and again simulated. Data of all streams and equipment can be viewed directly in the flowsheet and also exported for further post-processing.

The SOCO storage model allows the definition of two types (fixed level with loading and unloading HX and variable level), detailed insulations definition, ambient and initial temperatures, stratified charging or ports with fixed height.

4.2 Mathematical Programming framework

The second approach is based on an extended MINLP (Mixed Integer Non-Linear Programming) superstructure formulation for cost-optimal heat exchanger network design and storage integration. Both heat exchanger network (HEN) and storage systems are optimized simultaneously allowing for cost-optimal grassroots and retrofit designs. A multi-period extension for the superstructure formulation proposed by Yee & Grossmann (1990) and a simple 0-D model for the two-tank system are used in this paper (Beck & Hofmann, 2018a). The formulation allows to specify forbidden stream matches and also to specify streams as soft-streams, which means that reaching the specified target temperatures is optional. Simplifications for the problem such as reduction of operation periods and reduction of considered process streams are often necessary to handle it rigorously. As these types of combinatorial problems scale poorly with problem size, a linearization approach and tighter model formulations are used as presented by Beck & Hofmann (2017, 2018b). The workflow can be divided into several consecutive steps with different data inputs:

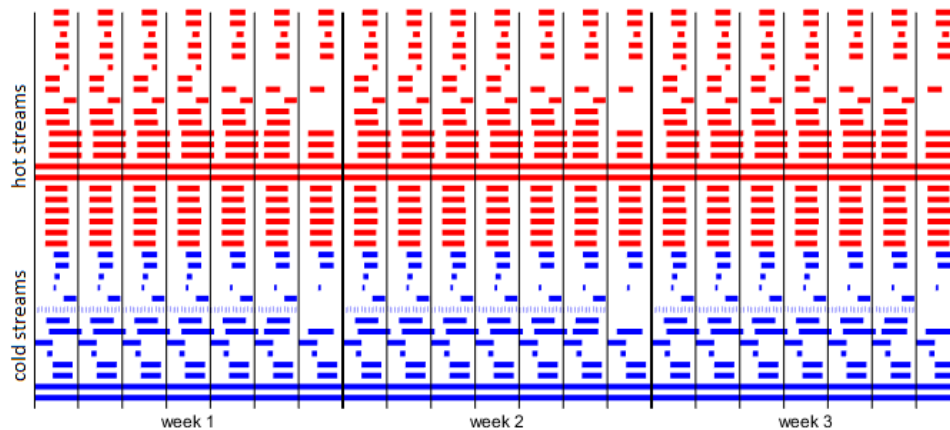
1. **Stream data** must be provided by the user in an appropriate form. Inlet and target temperatures for each process stream and heat capacity flow rates need to be set as well as the duration of each operating period.
2. **Problem reduction:** Depending on the problem size, the problem might need to be reduced due to the poor scaling of simultaneous MI(N)LP problems for HENS. This can be done by reduction of the process streams considered in the HENS problem and by merging consecutive operating periods with equal stream parameters.
3. **Energy targets:** Using the stream data and a user-defined minimum temperature difference ΔT_{min} , energy targets are calculated. These targets are then used for linearization of the original MINLP formulation and to tighten the resulting MILP problem. Also, the energy targets yield information about theoretically possible heat recovery for both storage integration and direct heat recovery.
4. **Linearization:** In the linearization step, the original MINLP superstructure formulation is linearized. Insights from the energy targeting are used to find good approximations of the nonconvex constraints

- 110 used in the original formulation. The user needs to provide heat transfer coefficients, cost coefficients, utilities and storage parameters such as bounds for storage temperatures and storage materials for this step.
- 115 5. **Simultaneous/sequential storage integration:** Next, the user can decide whether storages should be introduced simultaneously with the HEN or if the storage systems should be integrated after an optimal HEN was found. The simultaneous approach might yield a slightly better solution. However, computation time increases significantly.
 6. **Solution for original problem:** In the case, that the problem was reduced, the MILP superstructure for the total problem is solved with fixed binary variables which reduces the problem to an LP formulation.
 - 120 7. **Optional NLP stage:** The user can then decide if an additional NLP problem should be solved, which might yield slight improvements on the LP solution by shifting heat loads and adjusting storage sizes and heat exchanger areas.

125 With the mathematical programming approach, (sub)optimal heat recovery systems for time-dependent processes can be obtained. However, the solution process is time-consuming and thus thorough preparation of the optimization model is needed to avoid solutions that are infeasible for real implementation. This infeasibility might result from stream matches that cannot be allowed for safety reasons or that are economically infeasible due to excessive piping costs that are not considered in the optimization procedure.

5 PROCESS DESCRIPTION

130 The present dairy process has 36 process streams, of which 22 have cooling demand and 14 must be heated. The process streams are active at different time intervals. Some process streams are also subject to changes in process stream parameters such as mass flow, inlet and outlet temperature and specific heat capacity. Data for the process streams are available for a representative period of three weeks (including weekends) with a time resolution of 10 minutes. The stream parameters are periodic with a period of one week. The Gantt chart is shown in Fig. 2.



135 Figure 2: Gantt-chart for the period of available data (all three weeks identical)

140 The days Tuesday to Thursday are identical. On Mondays process streams H12-H14 are not active in the morning. From Friday until Sunday process streams H6, H7 and C3 are inactive. At the weekend the mass flows of the waste heat streams H17-H22 are reduced and the process streams H12-H14 are active only during the day and are not operated as on weekdays until about midnight. On Sunday, process streams H9-H11 and C5-C7 are also inactive. The stream data for the case-study are presented in Table 1. Cooling for hot process streams with a target temperature of 20°C or higher are cooled using cooling water taken from the nearby river.

Table 1: Stream data and cost parameters for use case

	T _{in} (°C)	T _{out} (°C)	m [kg/s]	cp [kJ/kgK]		T _{in} (°C)	T _{out} (°C)	m [kg/s]	cp [kJ/kgK]
H1	8	4	11.11	3.77	H21	44.9	>30	0.02-0.38	4.19
H2	11	4	9.89	3.77	H22	30	>10	0.07-1.47	4.19
H3	5	3	6.94	3.77	C1	33-87	40-94	11.11	3.77
H4	55	8	1.39	2.88	C2	105	110	1.39	2.88
H5	13	8	1.39	2.88	C3	8	21	3.33	2.88
H6	21	11	3.33	2.88	C4	11	28	8.52	3.77
H7	11	6	2.05	3.77	C5	6	70	6.68	3.77
H8	28	6	0.32	3.91	C6	10	40	0.74/1.48	4.19
H9	70	32	6.68	3.77	C7	8	50	3.94	4.09
H10	42	8	3.94	4.09	C8	8	81.5	3.03	4.09
H11	50	8	3.94	4.09	C9	25	90	0.33	3.00
H12	70	5	0.92	4.19	C10	50	77	0.39	4.19
H13	48	5	2.22	4.19	C11	15	65	0.23	4.19
H14	53	5/25	0.22/0.4	3.8/3	C12	15	65	0.54	4.19
H15	140	>60	6.18	1.11	C13	12	102	0.93	4.19
H16	216	>60	0.29	1.11	C14	90	102	0.26	4.19
H17	62.9	>30	0.01-0.3	4.19	HU	150	150		
H18	30	>10	0.12-2.58	4.19	CU1	15	18		
H19	75	>15	0.06-0.55	4.19	CU2	-5	0		
H20	15	>10	3.85-34.69	4.19					

Overall heat transfer coefficient: 4kW/m²K; Utility costs: HU 262.8 €/kW/y, CU1 10 €/kW/y, CU2 292 €/kW/y, Heat exchanger costs: 6133.5*[Area]^{0.219}/y; Storage costs: (756.2*[Volume]+1760)/y; Annualization factor $\gamma=3$; $dT_{min}=2^{\circ}C$

145 Process streams with lower target temperatures are cooled by means of liquid chillers with an energy efficiency ratio of 3 (3kW thermal equivalent to 1kW electric). The hot utility power is steam at 150 °C. The cost coefficients used for operating costs (costs for hot and cold utility) and investment costs (heat exchangers fixed costs and variable costs) and the cost exponent for declining costs for heat transfer surfaces are also summarized in Table 1. A uniform heat transfer coefficient k was chosen for all utility and process flows.

150 **6 PROBLEM SET UP**

6.1 Mathematical Programming procedure

Taking into account active/inactive and variable process flow parameters, 118 different operating states result. In order to carry out a simultaneous design of a cost-efficient HEN, the problem complexity must be reduced for this case-study.

155

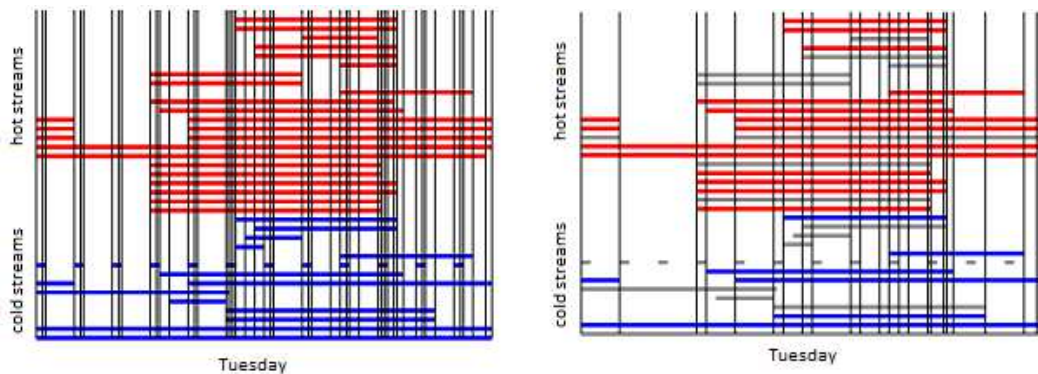


Figure 3: Gantt-chart for Tuesday with time intervals; all streams (left) and reduced streams (right)

160 Tuesday is selected as a representative day for the entire week, since all process streams are active on this day. This reduces the number of different operating states to 45. The 20 process streams with the highest energy content account for about 95% of the total energy content. An analysis is shown in Figure 3. By reducing the problem to 20 process streams, the different operating states are reduced to 23 intervals with constant operating

conditions. The Gantt chart for Tuesday is shown in Figure 2 with individual operating periods for the original and the reduced problem.

To further simplify the problem, the sequential approach is used for storage integration. This means, that first a cost optimal HEN is synthesized and then the storage is introduced to the superstructure. Also, within the superstructure each stream pair may only use one heat exchanger for heat transfer. Three temperature stages were used for the superstructure.

6.2 SOCO

SOCO can use the variable stream data directly for the HEN proposal and HEN simulation. No problem reduction and no exclusion of stream combinations are necessary. Figure 4 shows two examples of the variety of streams.

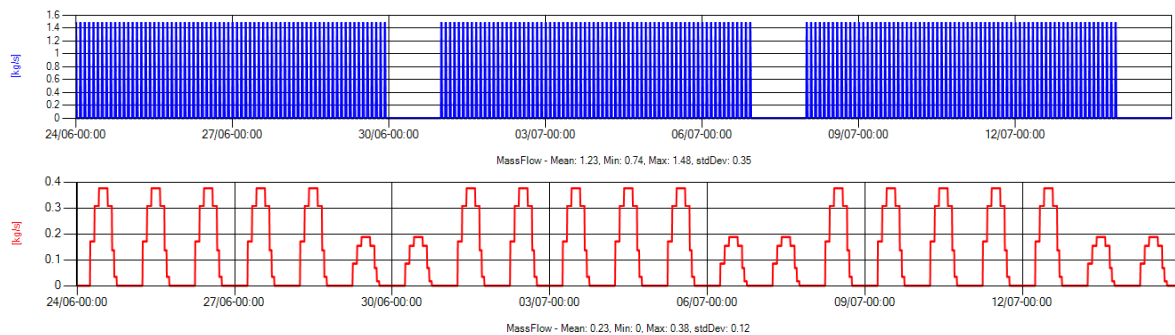


Figure 4: (Top): Cold stream (C6) is active 10 minutes every 2 hours for 6 days a week. (Bottom): Hot stream (H19) is waste heat from a chiller that varies over production day and has reduced load at weekends

7 HEAT EXCHANGER NETWORK AND HEAT RECOVERY

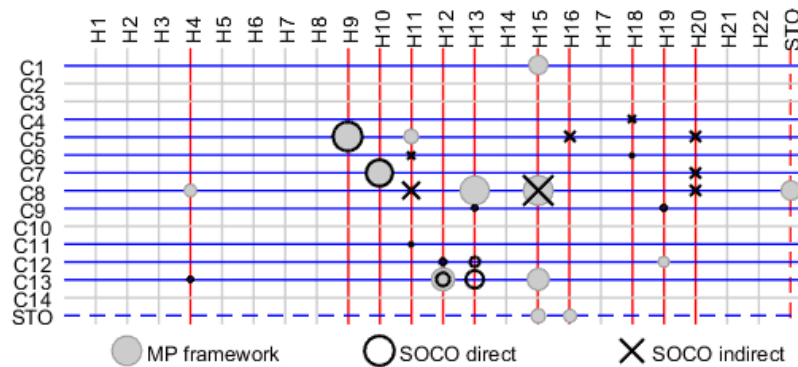
It needs to be mentioned that, although one strength of SOCO is the possibility to adapt the HEN proposal in manifold way in the flowsheet, the HEN proposal was converted directly to the built-in flowsheet area of SOCO to investigate the economic performance of the HEN proposal. The only adaption was the merging of storages with the same hot stream as source. Thereby, 9 proposed storages with 620 m³ volume were merged to 5 storages with 449 m³. The results for the number of HX and the heat recovery achieved with the networks obtained using SOCO and the MP procedure is shown in Table 2. Also, the number of storage units suggested and the approximate computation time for the solution are shown. The results presented for SOCO shows the results of the HEN simulation without further adaptations of the HEN proposal.

The solution found by using the MP framework achieves approximately 83.6% of the heat recovery possible through heat integration by means of heat exchangers and the use of TES compared to 72.3% for the HEN proposed by SOCO. A big difference between the solutions is the use of storages. The MP solution uses one storage subsystem with a 43.14m³ stratified tank whereas with SOCO five storages were proposed. As explained in 4.3, the HEN proposal suggests a set of HX and heat storages depending on energy criteria. Each storage is designed for the combination of two streams. The merging of storages with similar temperature profiles is not performed in the HEN proposal.

Table 2: Number of heat exchangers, storage sizes, heat recovery and computation time for both approaches

	HX utility	HX streams	HX storage	Storages / Vol.	Heat recovery MWh/a	Max. direct/mixed MWh/a	Computation time
MP	26	10	3	1 / 43.14 m ³	13,975.4	14,894.13/16,725.58	rd. 24 hours
SOCO	28	9	15	5 / 449 m ³	12,088.0	14,894.13/16,725.58	rd. 1 second

The number of heat exchangers proposed by SOCO with 52 HX is also higher than the number of HX obtained using rigorous optimization which yields a HEN with 39 HX.



195 Figure 5: Stream combinations with storage integration; MP framework (gray), SOCO direct (dark circle), SOCO indirect (dark X), marker size represents the amount of energy transferred

200 Comparison of the stream combinations proposed by SOCO and the combinations found to be cost-efficient using the MP framework (Figure 5) shows that only four streams combinations are common. Two of them (H9/C5 and H10/C7) transfer approximately the same energy. Using SOCO more heat exchangers with lower total transferred energy were proposed compared to the solution found by the MP framework.

205 In this case study, only 11 of 22 hot streams and 10 of 14 cold streams were considered by either approach. 8 out of these 11 hot streams and 5 out of these 10 cold streams were considered by both approaches. However, 5 out of 6 cold streams and 8 out of 8 hot streams considered by the MP framework were also considered by the SOCO algorithm for heat recovery.

210 Comparison of the annual costs obtained by both approaches (Table 3) shows that rigorous optimization of costs yields lower total annual costs (TAC). This result was expected as in the SOCO proposal cost drivers such as utility costs and heat exchanger costs are not considered but HX are selected by energy criteria. In this case-study it was assumed that process streams with a target temperature lower than 20°C need to be cooled using chillers (CU2 in Table 1) with very high utility costs and thus heat recovery of low grade waste heat is crucial to achieve low operating costs. The focus of SOCO to use rather more storages leads to significantly higher costs in storage and HX for storage.

Table 3: Annual Costs

	OP	HX streams	HX utility	HX storage	Storages	Total
MP	229.6 k€ (68.1%)	35.3 k€ (10.5%)	48.7 k€ (14.4%)	8.9 k€ (2.6%)	14.9 k€ (4.4%)	337.3 k€
SOCO	355.7 k€ (52.1%)	28.6 k€ (4.2%)	74.4 k€ (10.9%)	107.6 k€ (15.8%)	116.2 k€ (17.0%)	682.5 k€

8 POTENTIAL SYNERGIES

215 Even though SOCO does not consider costs in its algorithm for HENS, it selected all but one process streams for heat recovery that were also used in the solution of the MP framework. The SOCO solution process is very fast (seconds) compared to rigorous mathematical optimization (hours/days, depending on problem size) and thus could be used to find a good initial guess for the MP approach. This might speed up the MP approach significantly. Furthermore, the SOCO approach could be used to generate a number of HEN proposals to identify process streams that are likely to be used within the network. The MP model could then be restricted to these process streams for faster solution. The MP solution can then be considered as a global optimum, which cannot be guaranteed by the HEN proposal of SOCO. The MP solution could be drawn in the flowsheet of SOCO to simulate and fine tune the HEN with special attention towards individual storage design.

9 CONCLUSION

225 In this paper, HENs including TES for a large-scale dairy plant were generated using SOCO which is a compiled
planning tool for optimization and design of heat exchanger and thermal storage systems in complex thermal
energy systems developed by AEE INTEC and a mathematical programming framework developed by AIT. The
workflows for both approaches were presented and advantages and disadvantages were discussed. It became clear
230 that rigorous optimization of TAC is very time-consuming and requires thorough data preparation but can find
very good solutions from an economic point of view. SOCO does not require economic data which might be hard
to get in the first place, does not require time-consuming problem setup and can find solutions for both direct and
indirect heat recovery using storages in seconds. However, as it does not consider costs, the HENs obtained yield
higher payback time compared to the rigorous cost-optimization.
Also, possible synergies for both approaches were identified. SOCO might be used to initialize optimization
models with good initial guesses and could also be used for problem reduction which can potentially speed up
235 optimization significantly.

10 REFERENCES

- Anastasovski, A., 2017. Design of Heat Storage Units for use in repeatable Time Slices. *Applied Thermal Engineering*, Band 112, p. 1590–1600.
- 240 Beck, A. & Hofmann, R., 2017. *Tightening of MINLP Superstructure Relaxation for Faster Solution of Heat Exchanger Network Synthesis Problems*. Dubrovnik, -.
- Beck, A. & Hofmann, R., 2018. A Novel Approach for Linearization of a MINLP Stage-Wise Superstructure Formulation. *Computers & Chemical Engineering*, Band 112, p. 17–26.
- Beck, A. & Hofmann, R., 2018a. *Extensions for Multi-Period MINLP Superstructure Formulation for Integration of Thermal Energy Storages in Industrial Processes*. Graz, Austria, Elsevier.
- 245 Beck, A. & Hofmann, R., 2018b. How to tighten a commonly used MINLP superstructure formulation for simultaneous heat exchanger network synthesis. *Computers & Chemical Engineering*, Band 112, p. 48–56.
- Chaturvedi, N. D. & Bandyopadhyay, S., 2012. Minimization of storage requirement in a batch process using pinch analysis. In: *11th International Symposium on Process Systems Engineering*. s.l.:Elsevier, p. 670–674.
- 250 Chen, C.-L. & Ciou, Y.-J., 2008. Design and Optimization of Indirect Energy Storage Systems for Batch Process Plants. *Industrial & Engineering Chemistry Research*, 47(14), p. 4817–4829.
- Fluch, J., Brunner, C. & Muster-Slawitsch, B., 2012. Storage Optimisation Concept in Industries, Commerce and District Heating Businesses. *Chemical Engineering Transactions*, pp. 493-498.
- Kemp, I. C., 2007. *Pinch Analysis and Process Integration*. s.l.:Elsevier.
- 255 krummenacher, p., 2001. *CONTRIBUTION TO THE HEAT INTEGRATION OF BATCH PROCESSES (WITH OR WITHOUT HEAT STORAGE)*, PhD Thesis Nr 2480 (2001). EPFL: s.n.
- Mian, A., Martelli, E. & Maréchal, F., 2016. Multi-period Sequential Synthesis of Heat Exchanger Networks and Utility Systems including storages. In: *26th European Symposium on Computer Aided Process Engineering*. s.l.:Elsevier, p. 967–972.
- 260 Muster-Slawitsch, B., Brunner, C. & Fluch, J., 2014. Application of an advanced pinch methodology for the food and drink production. *Wiley Interdisciplinary Reviews: Energy and Environment*, 3(6), p. 561–574.
- Olsen, D., Abdelouadouda, Y., Wellig, B. & Krummenacher, P., 2016. *Systematic thermal energy storage integration in industry using pinch analysis*. Portoroz, PROCEEDINGS OF ECOS 2016.

Bibliography

- [1] Jane A. Vaselenak, Ignacio Grossmann, and Arthur Westerberg. Heat integration in batch processing. *Industrial & Engineering Chemistry Process Design and Development*, 25, 04 1986.
- [2] Juha Aaltola. Simultaneous synthesis of flexible heat exchanger network. *Applied Thermal Engineering*, 22(8):907–918, 2002.
- [3] International Energy Agency. Technology roadmap energy storage. 2014.
- [4] S. Ahmad, B. Linnhoff, and R. Smith. Cost optimum heat exchanger networks—2. targets and design for detailed capital cost models. *Computers & Chemical Engineering*, 14(7):751–767, 1990.
- [5] R. Anantharaman, I. Nastad, B. Nygreen, and T. Gundersen. The sequential framework for heat exchanger network synthesis—the minimum number of units sub-problem. *Computers & Chemical Engineering*, 34(11):1822–1830, 2010.
- [6] Martin J. Atkins, Michael R.W. Walmsley, and James R. Neale. The challenge of integrating non-continuous processes – milk powder plant case study. *Journal of Cleaner Production*, 18(9):927–934, 2010.
- [7] Suraya Hanim Abu Bakar, Mohd. Kamaruddin Abd. Hamid, Sharifah Rafidah Wan Alwi, and Zainuddin Abdul Manan. Effect of delta temperature minimum contribution in obtaining an operable and flexible heat exchanger network. *Energy Procedia*, 75:3142–3147, 2015.
- [8] Santanu Bandyopadhyay, James Varghese, and Vikas Bansal. Targeting for cogeneration potential through total site integration. *Applied Thermal Engineering*, 30(1):6–14, 2010.
- [9] Riccardo Bergamini, Tuong-Van Nguyen, Fabian Bühler, and Brian Elmegaard. Development of a simplified process integration methodology for retrofit in medium-size industries. *Proceedings of ECOS 2016 - The*

- 29th international conference on efficiency, cost, optimization, simulation and environmental impact of energy systems*, 2016.
- [10] Kaj-Mikael Björk and Roger Nordman. Solving large-scale retrofit heat exchanger network synthesis problems with mathematical optimization methods. *Chemical Engineering and Processing: Process Intensification*, 44(8):869–876, 2005.
- [11] Miloš Bogataj and Zdravko Kravanja. An alternative strategy for global optimization of heat exchanger networks. *Applied Thermal Engineering*, 43:75–90, 2012.
- [12] Raffaele Bolliger, Francesca Palazzi, and François Maréchal. Heat exchanger network (hen) costs and performances estimation for multi-period operation. *Computer Aided Chemical Engineering*, 24, 2008.
- [13] Tobias Boßmann, Wolfgang Eichhammer, and Rainer Elsland. *Policy Report*. Federal Ministry for the Environment, Nature Conservation and Nuclear Safety (BMU), 2012.
- [14] BP Statistical Review of World Energy. *BP Statistical Review of World Energy 2018*. BP, 2018.
- [15] Cheng-Liang Chen and Chia-Yuan Chang. A resource-task network approach for optimal short-term/periodic scheduling and heat integration in multipurpose batch plants. *Applied Thermal Engineering*, 29(5-6):1195–1208, 2009.
- [16] Cheng-Liang Chen and Ying-Jyuan Ciou. Design and optimization of indirect energy storage systems for batch process plants. *Industrial & Engineering Chemistry Research*, 47(14):4817–4829, 2008.
- [17] J.J.J. Chen. Comments on improvements on a replacement for the logarithmic mean. *Chemical Engineering Science*, 42(10):2488–2489, 1987.
- [18] Yang Chen, Ignacio E. Grossmann, and David C. Miller. Computational strategies for large-scale milp transshipment models for heat exchanger network synthesis. *Computers & Chemical Engineering*, 82:68–83, 2015.
- [19] A.R. Ciric and C.A. Floudas. Heat exchanger network synthesis without decomposition. *Computers & Chemical Engineering*, 15(6):385–396, 1991.
- [20] R. C. Cowie. Costing of shell-and-tube heat exchangers.
- [21] Donald Olsen, Y. Abdelouadoud, P. Liem, S. Hoffmann, B. Wellig. Integration of heat pumps in industrial processes with pinch analysis. *Proceedings of the 12th IEA Heat Pump Conference 2017*, 2017.

- [22] Marco Aurelio Dos Santos Bernardes, editor. *Developments in Heat Transfer*. InTech, 2011.
- [23] Wolfgang Eichhammer and Clemens Rohde. Enhancing the impact of energy audits and energy management in the european union: A review of article 8 of the energy efficiency directive. *The European Council for an Energy Efficient Economy (eceee) & Fraunhofer ISI 2016*, 2016.
- [24] Marcelo Escobar, Jorge O. Trierweiler, and Ignacio E. Grossmann. Simultaneous synthesis of heat exchanger networks with operability considerations: Flexibility and controllability. *Computers & Chemical Engineering*, 55:158–180, 2013.
- [25] European Environment Agency. *Trends and projections in Europe 2017: Tracking progress towards Europe’s climate and energy targets*, volume 2017 of *EEA report*. Publications Office of the European Union, Luxembourg, 2017.
- [26] Eurostat. Greenhouse gas emissions by country and sector (infographic), 2018.
- [27] Inmaculada Fernández, Carlos J. Renedo, Severiano F. Pérez, Alfredo Ortiz, and Mario Mañana. A review: Energy recovery in batch processes. *Renewable and Sustainable Energy Reviews*, 16(4):2260–2277, 2012.
- [28] C. A. Floudas, A. R. Ciric, and I. E. Grossmann. Automatic synthesis of optimum heat exchanger network configurations. *AIChE Journal*, 32(2):276–290, 1986.
- [29] Christodoulos A. Floudas. *Nonlinear and mixed-integer optimization: Fundamentals and applications*, volume 12. Oxford University Press, New York, 1995.
- [30] Christodoulos A. Floudas and Ignacio E. Grossmann. Automatic generation of multiperiod heat exchanger network configurations. *Computers & Chemical Engineering*, 11(2):123–142, 1987.
- [31] Juergen Fluch, Brunner Christoph, and Muster-Slawitsch Bettina. Soco - storage optimisation concepts in industries, commerce and district heating businesses. *Chem Eng Trans*, 29:493–498, 01 2012.
- [32] Dominic Chwan Yee Foo, Yin Hoon Chew, and Chew Tin Lee. Minimum units targeting and network evolution for batch heat exchanger network. *Applied Thermal Engineering*, 28(16):2089–2099, 2008.

- [33] Kevin C. Furman and Nikolaos V. Sahinidis. Computational complexity of heat exchanger network synthesis. *Computers & Chemical Engineering*, 25(9-10):1371–1390, 2001.
- [34] Kevin C. Furman and Nikolaos V. Sahinidis. A critical review and annotated bibliography for heat exchanger network synthesis in the 20th century. *Industrial & Engineering Chemistry Research*, 41(10):2335–2370, 2002.
- [35] Dolf Gielen and Michael Taylor. Modelling industrial energy use: The IEAs Energy Technology Perspectives. *Energy Economics*, 29(4):889–912, July 2007.
- [36] T. Gundeepsen and L. Naess. The synthesis of cost optimal heat exchanger networks: An industrial review of the state of the art. *Computers & Chemical Engineering*, 12(6):503 – 530, 1988.
- [37] T. Gundersen, IEA., and Trondheim SINTEF Energy Research. *A Process Integration PRIMER*. SINTEF Energy Research, 2000.
- [38] Ulf Herrmann, Bruce Kelly, and Henry Price. Two-tank molten salt storage for parabolic trough solar power plants. *Energy*, 29(5):883 – 893, 2004. SolarPACES 2002.
- [39] Geoff F. Hewitt and Simon J. Pugh. Approximate design and costing methods for heat exchangers. *Heat Transfer Engineering*, 28(2):76–86, 2007.
- [40] E.C. Hohmann. *Optimum Networks for Heat Exchange*. University Microfilms, 1971.
- [41] Zhaoyi Huo, Liang Zhao, Hongchao Yin, and Jianxiong Ye. A hybrid optimization strategy for simultaneous synthesis of heat exchanger network. *Korean Journal of Chemical Engineering*, 29(10):1298–1309, 2012.
- [42] International Energy Agency. *Capturing the Multiple Benefits of Energy Efficiency*. OECD, 2014.
- [43] Adeniyi J. Isafiade and Michael Short. Simultaneous synthesis of flexible heat exchanger networks for unequal multi-period operations. *Process Safety and Environmental Protection*, 103:377–390, 2016.
- [44] Holger Jensen. Analysis of energy saving potentials in selected eu countries based on a sectorial best-practise approach.

- [45] Jacek Jezowski. Heat exchanger network grassroot and retrofit design. the review of the state-of-the art: part i. heat exchanger network targeting and insight based methods of synthesis. *Hungarian Journal of Industrial Chemistry*, 22:279–294, 01 1994.
- [46] Jacek Jezowski. Heat exchanger network grassroot and retrofit design. the review of the state-of-the art: part ii. heat exchanger network synthesis by mathematical methods and approaches for retrofit design. *Hungarian Journal of Industrial Chemistry*, 22:295–308, 01 1994.
- [47] Da Jiang and Chuei-Tin Chang. A new approach to generate flexible multiperiod heat exchanger network designs with timesharing mechanisms. *Industrial & Engineering Chemistry Research*, 52(10):3794–3804, 2013.
- [48] N. Jiang, S. Bao, and Z. Gao. Heat exchanger network integration using diverse pinch point and mathematical programming. *Chemical Engineering & Technology*, 34(6):985–990, 2011.
- [49] Lixia Kang, Yongzhong Liu, and Le Wu. Synthesis of multi-period heat exchanger networks based on features of sub-period durations. *Energy*, 116:1302–1311, 2016.
- [50] I. C. Kemp. Applications of the time-dependent cascade analysis in process integration. *Heat Recovery Systems and CHP*, 10(4):423–435, 1990.
- [51] I.C. Kemp and A.W. Deakin. Cascade analysis for energy and process integration of batch processes. part 1. calculation of energy targets. *Chemical Engineering Research and Design*, 67:495–509, 09 1989.
- [52] I.C. Kemp and A.W. Deakin. Cascade analysis for energy and process integration of batch processes. part 2. network design and process scheduling. *Chemical Engineering Research and Design*, 67:510–516, 09 1989.
- [53] Jiří Jaromír Klemeš. *Handbook of process integration (PI): Minimisation of energy and water use, waste and emissions*, volume no. 50 of *Woodhead Publishing in energy*. Woodhead Pub, Cambridge, U.K, 2013.
- [54] Klima- und Energiefonds. *Abschlussbericht der Speicherinitiative: Startphase*. Wien, 2016.
- [55] Pierre Krummenacher and Daniel Favrat. Indirect and mixed direct-indirect heat integration of batch processes based on pinch analysis. *International Journal of Applied Thermodynamics*, (4):135–143, 2001.

- [56] Govind N. Kulkarni, Shireesh B. Kedare, and Santanu Bandyopadhyay. Design of solar thermal systems utilizing pressurized hot water storage for industrial applications. *Solar Energy*, 82(8):686–699, 2008.
- [57] H. Kumar. Costing of plate heat exchangers.
- [58] B. Lin and D. C. Miller. Solving heat exchanger network synthesis problems with tabu search. *Computers & Chemical Engineering*, 28(8):1451–1464, 2004.
- [59] B Linnhoff. Pinch analysis - a state-of-the-art overview. *Chemical Engineering Research and Design*, 71:503–522, 09 1993.
- [60] B Linnhoff and S Ahmad. Supertargeting: Optimum synthesis of energy management systems. *Journal of Energy Resources Technology-Transactions of The Asme - J ENERG RESOUR TECHNOL*, 111:121–130, 09 1989.
- [61] B. Linnhoff and S. Ahmad. Cost optimum heat exchanger networks—1. minimum energy and capital using simple models for capital cost. *Computers & Chemical Engineering*, 14(7):729–750, 1990.
- [62] B Linnhoff, G.J. Ashton, and E.D.A. Obeng. Process integration of batch processes. *ICHEME Symposium Series*, 109:221–237, 01 1988.
- [63] B. Linnhoff and E. Hindmarsh. The pinch design method for heat exchanger networks. *Chemical Engineering Science*, 38(5):745 – 763, 1983.
- [64] Bodo Linnhoff and John R. Flower. Synthesis of heat exchanger networks: I. systematic generation of energy optimal networks. *AIChE Journal*, 24(4):633–642, 1978.
- [65] Bodo Linnhoff and John R. Flower. Synthesis of heat exchanger networks: Ii. evolutionary generation of networks with various criteria of optimality. *AIChE Journal*, 24(4):642–654, 1978.
- [66] Bodo Linnhoff, David R. Mason, and Ian Wardle. Understanding heat exchanger networks. *Computers & Chemical Engineering*, 3(1):295 – 302, 1979.
- [67] Roghayeh Lotfi and Ramin B. Boozarjomehry. Superstructure optimization in heat exchanger network (hen) synthesis using modular simulators and a genetic algorithm framework. *Industrial & Engineering Chemistry Research*, 49(10):4731–4737, 2010.

- [68] Xing Luo, Qing-Yun Wen, and Georg Fieg. A hybrid genetic algorithm for synthesis of heat exchanger networks. *Computers & Chemical Engineering*, 33(6):1169–1181, 2009.
- [69] Xiangkun MA, Pingjing Yao, Xing Luo, and Wilfried ROETZEL. Synthesis of multi-stream heat exchanger network for multi-period operation with genetic/simulated annealing algorithms. *Applied Thermal Engineering*, 28(8-9):809–823, 2008.
- [70] Thokozani Majazi. Heat integration of multipurpose batch plants using a continuous-time framework. *Applied Thermal Engineering*, 26(13):1369–1377, 2006.
- [71] C. B. Miranda, C.B.B. Costa, J. A. Caballero, and M.A.S.S. Ravagnani. Optimal synthesis of multiperiod heat exchanger networks: A sequential approach. *Applied Thermal Engineering*, 115:1187–1202, 2017.
- [72] Laia Miró, Jaume Gasia, and Luisa F. Cabeza. Thermal energy storage (tes) for industrial waste heat (iwh) recovery: A review. *Applied Energy*, 179:284–301, 2016.
- [73] Donald Olsen, Yasmina Abdelouadoud, Beat Wellig, and Pierre Krummenacher. Systematic thermal energy storage integration in industry using pinch analysis. In *ECOS 2016 - The 29th International Conference on Efficiency, Cost, Optimization, Simulation and Environmental Impact of Energy Systems*, 2016.
- [74] Soterios A. Papoulias and Ignacio E. Grossmann. A structural optimization approach in process synthesis - i: Utility systems. *Computers & Chemical Engineering*, 7(6):695 – 706, 1983.
- [75] Parikshit Shahane and Sujit Jogwar. A novel algorithm for design of mixed energy-integrated batch process networks.
- [76] F. Pettersson. Synthesis of large-scale heat exchanger networks using a sequential match reduction approach. *Computers & Chemical Engineering*, 29(5):993–1007, 2005.
- [77] Nasibeh Pouransari and Francois Maréchal. Heat recovery networks synthesis of large-scale industrial sites: Heat load distribution problem with virtual process subsystems. *Energy Conversion and Management*, 89:985–1000, 2015.
- [78] E. Rev and Z. Fonyo. Diverse pinch concept for heat exchange network synthesis: the case of different heat transfer conditions. *Chemical Engineering Science*, 46(7):1623 – 1634, 1991.

- [79] N. V. Sahinidis. *BARON 17.8.9: Global Optimization of Mixed-Integer Nonlinear Programs*, User's Manual, 2017.
- [80] Barbara Schlomann and Joachim Schleich. Adoption of low-cost energy efficiency measures in the tertiary sector—an empirical analysis based on energy survey data. *Renewable and Sustainable Energy Reviews*, 43:1127–1133, 2015.
- [81] Goran Slavković, Stevan J. Budimir, Ivan M. Rakonjac, Marko S. Jarić, and Nikola J. Budimir. Techno-economic analysis of heat exchangers with parallel helical tube coils. *Tehnički vjesnik*, (21):861–866, 2014.
- [82] Aleksander Soršak and Zdravko Kravanja. Simultaneous minlp synthesis of heat exchanger networks comprising different exchanger types. *Computers & Chemical Engineering*, 26(4-5):599–615, 2002.
- [83] S Stoltze, J Mikkelsen, B Lorentzen, PM Peterson, and B Qvale. Waste-heat recovery in batch processs using heat storage. *Journal of energy resources technology*, 117(2):142–149, 1995.
- [84] M. Tawarmalani and N. V. Sahinidis. A polyhedral branch-and-cut approach to global optimization. *Mathematical Programming*, 103:225–249, 2005.
- [85] Patrik Thollander, Patrik Rohdin, and Bahram Moshfegh. On the formation of energy policies towards 2020: Challenges in the swedish industrial and building sectors. *Energy Policy*, 42:461 – 467, 2012.
- [86] D. W. Townsend and B. Linnhoff. Surface area targets for heat exchanger networks. In *The IChemE Annual Research Meeting*, April 1984.
- [87] Francisco Trespalacios and Ignacio E. Grossmann. Improved big-m reformulation for generalized disjunctive programs. *Computers & Chemical Engineering*, 76:98 – 103, 2015.
- [88] T. Umeda, J. Itoh, and K. Shiroko. Heat exchange system synthesis. *Chemical Engineering Progress*, 74:70–76, 07 1978.
- [89] Tomio Umeda, Kazuo Niida, and Katsuo Shiroko. A thermodynamic approach to heat -integration in distillation systems. *AIChE Journal*, 25:423 – 429, 05 1979.
- [90] U.S. Energy Information Administration. *International Energy Outlook 2017*. 2017.

- [91] Timothy G. Walmsley, Michael R.W. Walmsley, Martin J. Atkins, and James R. Neale. Integration of industrial solar and gaseous waste heat into heat recovery loops using constant and variable temperature storage. *Energy*, 75:53–67, 2014.
- [92] Ernst Worrell, Lenny Bernstein, Joyashree Roy, Lynn Price, and Jochen Harnisch. Industrial energy efficiency and climate change mitigation. *Energy Efficiency*, 2(2):109–123, 2009.
- [93] Po Yang, Lin-lin Liu, Jian Du, Ji-long Li, and Qing-wei Meng. Heat exchanger network synthesis for batch processes by involving heat storages with cost targets. *Applied Thermal Engineering*, 70(2):1276–1282, 2014.
- [94] T. F. Yee and I. E. Grossmann. Simultaneous optimization models for heat integration-ii. heat exchanger network synthesis. *Computers & Chemical Engineering*, 14(10):1165–1184, 1990.
- [95] Krishna M. Yerramsetty and C.V.S. Murty. Synthesis of cost-optimal heat exchanger networks using differential evolution. *Computers & Chemical Engineering*, 32(8):1861–1876, 2008.
- [96] Hongmei Yu, Haipeng Fang, Pingjing Yao, and Yi Yuan. A combined genetic algorithm/simulated annealing algorithm for large scale system energy integration. *Computers & Chemical Engineering*, 24(8):2023–2035, 2000.
- [97] Juan M. Zamora and Ignacio E. Grossmann. A global minlp optimization algorithm for the synthesis of heat exchanger networks with no stream splits. *Computers & Chemical Engineering*, 22(3):367–384, 1998.
- [98] Christoph Zauner, Florian Hengstberger, Mark Eitzel, Daniel Lager, Rene Hofmann, and Heimo Walter. Experimental characterization and simulation of a fin-tube latent heat storage using high density polyethylene as pcm. *Applied Energy*, 179:237 – 246, 2016.
- [99] Hongliang Zhang, Guomin Cui, Yuan Xiao, and Jiaying Chen. A novel simultaneous optimization model with efficient stream arrangement for heat exchanger network synthesis. *Applied Thermal Engineering*, 110:1659–1673, 2017.
- [100] W. Verheyen N. Zhang. Design of flexible heat exchanger network for multi-period operation. *Chemical Engineering Science*, 61(23):7730–7753, 2006.

- [101] X. G. Zhao, B. K. O’neill, J. R. Roach, and R. M. Wood. Heat integration for batch processes. *Chemical Engineering Research and Design*, 76(6):700–710, 1998.
- [102] Xin X. Zhu. Automated design method for heat exchanger network using block decomposition and heuristic rules. *Computers & Chemical Engineering*, 21(10):1095–1104, 1997.

Curriculum Vitae

Last Update: 08.05.2019

Personal Information

Name:	BECK, Anton
Nationality:	Austria
Date of birth:	19.03.1989

Education and Training

Dates (from – to)	Name and type of the organisation	Principal subjects	Title awarded
2015 - 2018	Austrian Institute of Technology and Vienna University of Technology	Ph.D. (Energy Technology, Process Integration)	
2012 - 2015	Vienna University of Technology	Industrial Engineering (Energy Technology)	M.Sc.
2008 - 2012	Vienna University of Technology	Industrial Engineering	B.Sc.
1999 - 2007	Stiftsgymnasium Wilhering	General Education	

Work Experience

Dates (from – to)	Name and type of the employer	Position held	Main activities and responsibilities
2018 -	Austrian Institute of Technology	Research Engineer	Project Management, Optimization of Industrial and Residential Energy Systems
2013 - 2014	Vienna University of Technology (IFT)	Project Team Member	Development of tools for energy and capacity management
2011 - 2015	Vienna University of Technology (MEC)	Tutor	Tutoring students in the field of mechanics
2005 - 2013	Internships (RUAG Space, Silhouette International Schmied AG, Post AG...)	Intern	

Languages

Language	Reading / writing / verbal	Level (basic, good, excellent)
German		Mother tongue
English		Good

Technical skills ((software-)tools, machinery, equipment, etc.)

Technical skill	Level (basic, good, excellent)
MS Office	Excellent
Ansys Fluent	Good
Matlab	Good
IPSEpro	Basic
GAMS	Basic

Selected Publications

- Beck, A., R. Hofmann. Extensions for Multi-Period MINLP Superstructure Formulation for Integration of Thermal Energy Storages in Industrial Processes. In Proceedings of the 28th European Symposium on Computer Aided Process Engineering. A. Friedl, J. Klemes, S. Radl, P. Varbanov, T. Wallek (Hrg.); Elsevier B.V., Part A (2018), ISBN: 978-0-444-64237-0; S. 1335 - 1340.
- Beck, A., R. Hofmann. A Novel Approach for Linearization of a MINLP Stage-Wise Superstructure Formulation. *Computers & Chemical Engineering*, 112 (2018), 112; 17 - 26.
- Beck, A., R. Hofmann. How to tighten a commonly used MINLP superstructure formulation for simultaneous heat exchanger network synthesis. *Computers & Chemical Engineering*, 112 (2018), 112; 48 - 56.
- Beck, R. Hofmann. Tightening of MINLP Superstructure Relaxation for Faster Solution of Heat Exchanger Network Synthesis Problems. In Proceedings of the 12th Conference on Sustainable Development of Energy, Water and Environment Systems. (2017), ISSN: 1847-7178; Paper-Nr. FP-950, 11 S.
- Beck, A., M. Koller, H. Walter, M. Hameter. Transient Numerical Analysis of Different Finned Tube Designs for Use in Latent Heat Thermal Energy Storage Devices. In *Proceedings of the 2015 ASME Power & Energy Conversion Conference PowerEnergy2015*. June 28-July 2, 2015, San Diego, California
- Walter, H., A. Beck, M. Hameter. Transient Analysis of an Improved Finned Tube Heat Exchanger for Thermal Energy Storage System. In *Proceedings of the 2015 ASME Power & Energy Conversion Conference PowerEnergy2015*. June 28-July 2, 2015, San Diego, California